Development of Luminescence-based Oxygen and pH Optodes for Toxicity and Process Monitoring

A Thesis

submitted to

Department of Applied Biology and Chemical Technology

for

The Degree of Doctor of Philosophy

at

The Hong Kong Polytechnic University

by

Chan Chun Man

October, 2000

Declaration

I hereby declare that this thesis summarizes my own work carried out since my registration for the degree of Doctor of Philosophy in September, 1996, and that it has not been previously included in a thesis, dissertation or report presented to this or any other institution for a degree, diploma or other qualification.

Chan Chun Man

October, 2000

Acknowledgements

I wish to express my deepest gratitude to my supervisors Dr. W. H. Lo and Prof. K. Y. Wong for their valuable advice, encouragement and discussion throughout the course of my work, and their valuable comments on the draft of this thesis. Their novel ideas and devoted attitude in research have made my study a rewarding experience.

I would also like to thank all my postgraduate colleagues, Dr. P. Guo, Dr. W. H. Chung, Dr. K. W. Yeung, Mr. S. H. Lau, Mr. K. C. Cheung, Miss S. N. Poon, Mr. S. J. Hong, Dr. K. M. Leung, Dr. T. P. Chan and Mr. T. F. Cheng for their help and encouragement in my study.

I am also greatly indebted to members of my family and Miss W. M. Chiu for their support and concern in the past four years.

Finally, I would like to acknowledge the Research Committee of The Hong Kong Polytechnic University for the award of a research studentship and a tuition scholarship in 1996-1999 and for the grant supporting my conference presentation in the 215th ACS National Meeting held in Dallas in March, 1998.

Abstract of thesis entitled "Development of Luminescence-based Oxygen and pH Optodes for Toxicity and Process Monitoring"

submitted by Chan Chun Man

for the degree of Doctor of Philosophy

at The Hong Kong Polytechnic University

in October, 2000.

Abstract

Oxygen quenching of luminescence of the metal-organic dye ruthenium tris(4,7-diphenyl-1,10-phenanthroline), $[Ru(Ph_2phen)_3(ClO_4)_2]$ has been shown to be an accurate method for measuring oxygen concentration. Silicone rubber is commonly used as the matrix for fabrication of oxygen optode due to its high permeability toward oxygen and chemical inertness. However, the low solubility of the ionic ruthenium dye in silicone rubber is a detriment to the performance of the sensor because the ionic dye molecules tend to form aggregates in the hydrophobic environment which leads to inaccessibility of the dye molecules to oxygen quenching. In order to solve this 'solubility' problem, oxygen sensing films were prepared by adsorbing the tris(4,7-diphenyl-1,10-phenanthroline)ruthenium dye onto high surface area hydrophilic fumed silica and dispersing the ruthenium-loaded silica in silicone rubber support. Our results show that these sensing films possess desirable properties including higher luminescence intensity, larger response towards oxygen and more linear Stern-Volmer calibration curves than films prepared by simple mixing of the ruthenium dye with silicone rubber.

The applicability of this oxygen optode to toxicity monitoring of organic chemicals to microorganisms has been investigated. An optical scanning respirometer has been developed to measure the dissolved oxygen concentration of wastewater samples by monitoring the luminescence intensity of the immobilized ruthenium dye. The toxicity of various substituted phenols, benzenes and alkanes were evaluated by measuring their effect on the respiration rate of microorganisms which was monitored

by the oxygen optode. The IC_{50} values (concentration of a chemical that exhibits 50% respiration inhibition) of chemicals in activated sludge were found to correlate well with standard methods. The reproducibility and sensitivity of the respirometer were also evaluated and found to be comparable with existing methods. The main advantage of this respirometer is its capability of screening a large number of samples in a short period of time.

In addition, the Quantitative Structure Activity Relationship (QSAR) of the toxic chemicals on microorganisms has been worked out based on the collected toxicity data. Five different descriptors including 1-octanol/water partition coefficient (log P), aqueous solubility (log S), molecular volume (V_i), molecular connectivity index (MCI) and the combination of log P and ELUMO (energy of lowest unoccupied molecular orbital) have been used for correlating the toxicity of the organic chemicals to activated sludge. The partition coefficient and aqueous solubility were found to be suitable parameters to model substituted alkanes and benzenes. However, molecular volume, molecular connectivity and the combination of log P and ELUMO are the most desirable parameters in the QSAR model as they can cover all three classes of chemicals together. The ability of the developed models for predicting mixture toxicity has also been investigated. The accuracy of the developed MCI and log S QSAR equations are superior over other models in mixture toxicity studies.

A luminescent ruthenium complex $[Ru(bpy)_2(dhphen)]^{2+}$ (bpy = 2,2'-bipyridine, dhphen = 4,7-dihydoxy-1,10-phenanthroline) was immobilized into a Nafion film as an optical pH sensor. This pH optode displays pH-dependent

luminescent intensities and exhibits advantages over existing optical pH sensors including wide dynamic pH range, ease of fabrication, high sensitivity, good photostability and minimal interference from metal cations. The application of this optical pH sensor to pH monitoring of fermentation by *Klebsiella pneumoniae* has been investigated. The experimental results showed that interference from the culture medium can be eliminated by addition of a black microporous filter membrane on top of the sensing film. The response of this pH optode was found to show good correlation with the conventional pH electrode.

Structure of Ligands and Abbreviation

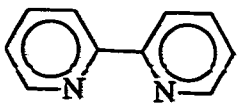

2,2'-bipyridine
(bpy)

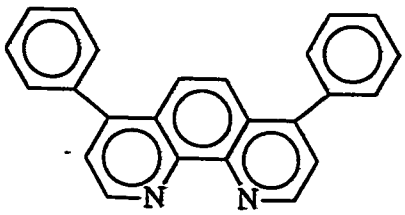

4,7-diphenyl-1,10-phenanthroline
(Ph_2phen)

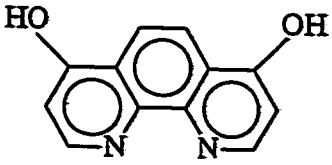

4,7-dihydroxy-1,10-phenanthroline
(dhphen)

I_{100}	Luminescence intensity at 100% oxygen
I_0	Luminescence intensity at 100% nitrogen
I_0/I_{100}	Oxygen quenching ratio
MLCT	Metal to ligand charge transfer
IC_{50}	Concentration of substance producing 50% respiration inhibition
LED	Light emitting diode
I.D.	Inside diameter
PMT	Photomultiplier tube
K_{SV}	Stern-Volmer Constant
V_o	Output voltage of PMT under pure nitrogen
V	Output voltage of PMT in the presence of oxygen
V_f	'False light' luminescence intensity
PO_2	Oxygen partial pressure
R	Respiration rate
H	Henry's constant
I%	Percentage inhibition
SD	Standard deviation
CV	Coefficient of variation
3,5-DP	3,5-Dichlorophenol
PCP	Pentachlorophenol
2-NP	2-Nitrophenol
4-NP	4-Nitrophenol
2-CP	2-Chlorophenol

2,4-DP	2,4-Dinitrophenol
2-BP	2-Bromophenol
QSAR	Quantitative Structure Activity Relationship
Log P	1-Octanol/water partition coefficient
ELUMO	Energy of lowest unoccupied molecular orbital
LSER	Linear Solvation Energy Relationship
MCI	Molecular connectivity index
MR	Molar refractivity
Log S	Aqueous solubility
V_i	Molecular van der Waals volume
s	Root mean square error
n	Number of observation
r^2	Coefficient of determination
F	Fisher statistic value

List of Figures

List of Tables

Table of Contents

Chapter 1

Introduction

1.1 Background

There has been an explosion of interest in the development of optical sensors (optodes) for various applications in the past two decade. Optodes have many advantages over conventional electrochemical sensors including high sensitivity, small size, electrical safety and possibility of remote sensing. Luminescence-based optical sensors are of particular interest because of their high sensitivity and specificity. Among the various analytes, oxygen and pH are two important parameters that needed to be monitored in clinical diagnosis, environmental analysis and process control. In this context, luminescence-based oxygen and pH sensors have received the most attention. Most oxygen optodes are based on the measurement of the decrease in luminescence intensity or excited state lifetime of a sensing dye which can be quenched by oxygen. For pH optodes, the difference in luminescence properties of the acid-base conjugate pair of a pH sensitive dye is measured. Ruthenium metal complexes with diimine ligands show great promise as sensing dyes because of their long excited state lifetime, intense visible absorption and high quantum yield.

The application of oxygen and pH sensors can be extended to measure other analytes provided there is a change in oxygen or proton concentration in the time-frame of analysis. Typical examples are the fabrication of biosensors based on the Clark-type oxygen electrode and pH electrode. Figure 1.1 shows a glucose biosensor based on the Clark oxygen electrode. The oxygen electrode has an oxygen-permeable membrane (such as PTFE) covering the electrodes. A layer of enzyme (glucose oxidase) is placed over

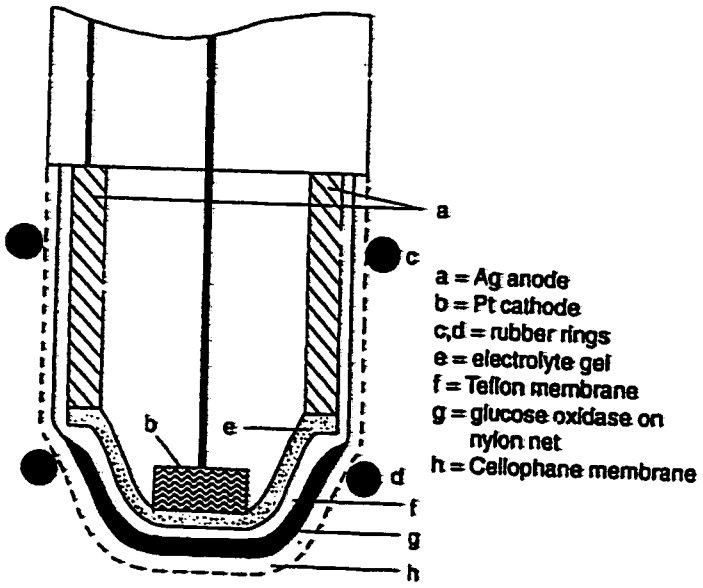

Figure 1.1 A glucose biosensor based on the Clark oxygen electrode.

this and held in place with a second membrane such as cellulose acetate. The oxidation of glucose is catalyzed by the enzyme glucose oxidase (GOD):

$$\text{glucose} + O_2 + H_2O \xrightarrow{\text{GOD}} \text{gluconic acid} + H_2O$$

At the electrode:

$$O_2 + 2e^- + 2H^+ \longrightarrow H_2O_2$$

A voltage sufficient to reduce the oxygen to hydrogen peroxide is applied between the platinum cathode and the silver anode and the cell current, which is proportional to the oxygen concentration, is measured. The concentration of glucose is then proportional to the decrease in current (oxygen concentration).

Figure 1.2 shows a urea biosensor based on a pH electrode. The enzyme urease is mixed with a gel and coated onto a nylon net membrane covering the electrode. It is held in place with a second (dialysis) membrane. Urea is hydrolysed by the enzyme to form ammonia and carbon dioxide:

$$CO(NH_2)_2 + H_2O \xrightarrow{\text{urease}} CO_2 + 2NH_3$$

The concentration of ammonia is then monitored by the glass pH electrode.

In this dissertation, the development of optical oxygen and pH sensors based on luminescent ruthenium diimine dyes is described. The oxygen optode was used as a

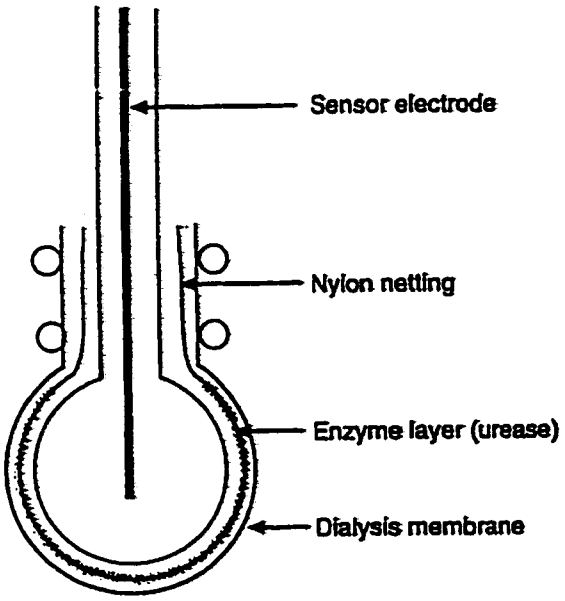

Figure 1.2 A urea sensor based on a pH electrode.

toxicity sensor to monitor the effect of toxic chemicals on microorganisms by measuring the inhibition of respiration in the presence of various chemicals. Attempts were made to develop a quantitative structure activity relationship (QSAR) model for the prediction of chemical toxicity. In addition, the pH optode was applied to pH monitoring in fermentation.

In the sections that followed, literature reviews on oxygen and pH optodes, biosensors based on optical sensing of oxygen, bacterial toxicity tests and quantitative structure activity relationship (QSAR) are given. The aims and objectives of this project are given at the end of this chapter.

1.2 Development of Luminescence Based Oxygen Sensors

Oxygen is an essential chemical species for the well-being of human life. Quantitative determination of oxygen concentration has become a routine analysis in environmental and clinical monitoring. Traditionally, the Clark electrode is used in measuring oxygen concentration (Clark, 1956). The Clark electrode is an amperometric sensor consisting of a gold or platinum cathode covered with a polypropylene membrane. Oxygen diffuses through the membrane and is reduced at the cathode, the magnitude of the diffusion-limited reduction current serves as the basis for oxygen determination. This

sensor is quite reliable, rapid in response and requires inexpensive instrumentation. However, this electrochemical-based technique has the drawbacks of electrode fouling, the need for constant supply of oxygen to the sensor surface because oxygen is consumed during measurement and diffusion-limited passage of oxygen through the membrane (Bates et al, 1975; Albery et al, 1981).

The development of optical sensor for oxygen measurement began as early as in the late sixties. The oxygen optode has the advantages of small size, nil consumption of oxygen and inertness toward sample flow rate and stirring. In conjunction with optical fibers it can be used for remote sensing of oxygen. Most oxygen optodes are based on the luminescence quenching of an indicator dye by oxygen. Quenching is the deactivation of the excited state of a luminophore by interaction with another species resulting in the decrease of luminescence lifetime and emission intensity. Measurement of these changes provides the basis for a relatively simple and inexpensive analysis method. Oxygen is an effective luminescence quencher because it has a triplet ground state and a low-lying singlet excited state. This method is also subjected to minimum interference from most common gases like N_2, CO_2, Ar, CO as they are not luminescence quencher.

A number of luminescent organic dyes have been used to detect traces of oxygen produced in photosynthesis or to measure the diffusion coefficient of oxygen in polymer matrices. These include trypaflavine, benzoflavine, rheonine 3A, rhoduline yellow, chlorophyll, safranine and hematoporphyrin (Pollak et al, 1944; Kautsky et al, 1932; Shaw, 1967). Unfortunately, these dyes have low photostability and can be easily

quenched by water. The first example of useful oxygen optode, based on polycyclic aromatic hydrocarbons (PAHs), was described by Bergman (1968). After that, a variety of PAHs such as pyrene, pyrenebutyric acid (PBA), fluoranthene, decacyclene and benzo(ghi)perylene were tested as sensing materials (Wolfbeis et al, 1985; Wolfbeis, et al, 1991). Although these organic dyes have long excited state lifetime and hence are subjected to strong quenching, they absorb light mainly in the ultra-violet region and the small Stoke's shift requires expensive light source and instrumentation for sensor fabrication. Peterson and co-workers (1984), in a search for longwave absorbing and emitting indicators, found perylene dibutyrate adsorbed on polystyrene beads to be a suitable sensing material. This dye has excitation and emission maxima at 468 and 512 nm respectively, but the whole system had limited photostability, slow response time and suffered interference from water and the anesthetic halothane.

In the past decade, the attention in searching for oxygen sensing dyes has been focused on luminescent metal-organic compounds. These materials have very desirable features such as long excited state lifetime, high quantum yield and intense visible absorption; this increases sensitivity, simplifies sensor design and extends the variety of excitation source available. They also tend to be thermally and photochemically robust. Among various metal-organic dyes, ruthenium (II) diimine complexes with the ligands 2,2'-bipyridyl (bpy), 1,10-phenanthroline (phen) and 4,7-diphenyl-1,10-phenanthroline (Ph_2phen) received the most attention. Wolfbeis and co-workers (1986; 1988) first reported the use of $[Ru(bpy)_3]^{2+}$ as a material for optical oxygen measurement. They prepared the sensing film by entrapping the dye adsorbed kieselgel particles into silicone

polymer and brought onto the distal end of an optical fiber or a glass-slide. The film has higher sensitivity and better optical characteristic (excitation maximum: 460 nm, emission maximum: 610 nm) than the PAH based sensor.

The photophysics and photochemistry of oxygen sensors based on $[Ru(bpy)_3]^{2+}$ and its analogues have been extensively studied by Demas group (Carraway et al, 1991a; Carraway et al, 1991b; Carraway et al, 1991c; Bacon and Demas, 1987; Xu et al, 1994). The oxygen sensing films were prepared by casting silicone rubber films containing the ruthenium polypyridyl complexes onto glass slides (Bacon and Demas, 1987; Carraway et al, 1991c) or by die-casting silica disks with adsorbed ruthenium dyes (Carraway et al, 1991a). Among the ruthenium dyes, $[Ru(Ph_2phen)_3]^{2+}$ is most attractive as it has the longest excited state lifetime (~5μs), highest quantum yield (0.3) and largest quenching constant. Recently, the same research group has reported the construction of a portable and solid-state oxygen sensor for the determination of gaseous and dissolved oxygen (Watkins et al, 1998). The sensor was fabricated by casting a sol-gel film containing $[Ru(Ph_2phen)_3]^{2+}$ onto the surface of a blue light emitting diode (LED). This sensor exhibits fast response and good reproducibility. The optical characteristics of $[Ru(Ph_2phen)_3]^{2+}$ in the silicone rubber have been reported by our research group (Li et al, 1993). The optical properties were found to depend on the concentration of ruthenium dye and the solvent used in the preparation of the sensing film. A luminescence-based imaging-fiber oxygen sensor for *in situ* measurement of oxygen consumption from intact mouse hearts was described by Zhao et al (1999). The imaging sensor was fabricated by photoinitiated polymerization of an oxygen-sensitive film on an imaging fiber. The

oxygen sensing film comprised of entrapped $[Ru(Ph_2phen)_3]^{2+}$ in a gas-permeable photopolymerizable siloxane matrix.

In addition, several longwave absorbing ruthenium diimine complexes, $Ru(L)_2(DMCH)$ (L = 2,2'-bipyridine or 4,7-diphenyl-1,10,-phenanthroline, DMCH = 6,7-dihydro-5,8-dimethyl-dibenzo[i,j][1,10]-phenanthroline) have been described by Klimant et al (1994). The excitation maxima (535 nm to 570 nm) strongly overlap the emission of green LEDs which have higher intensities and smaller emission bandwidths than the blue LEDs. However, the luminescence quantum yields of these complexes are much lower than the other ruthenium (II) derived probes. Recently, a new acrylate ruthenium diimine complex, tris(5-acrylamido-1,10-phenanthroline) chloride, has been used as an oxygen indicator (McNamara et al, 1998). The acrylate functional group of the complex is suitable for covalent co-polymerization with acrylamide to produce an oxygen sensing film. The film has similar oxygen response and improved stability when compared with that of $Ru(phen)_3^{2+}$.

Apart from ruthenium polypyridyl complexes, a number of platinum and palladium dyes have been described as oxygen sensing indicators. These include tetrakis(pyrophosphito) diplatinate(II) $[Pt_2(pop)_4]^{4-}$ (Li and Wong, 1992), dicyanoplatinum (II) complexes $[Pt(Ph_2phen)(CN)_2]$ and $[Pt(dtbpy)(CN)_2]$ (Lee et al, 1993a) (where pop = $P_2O_5H_2^{2-}$, dtbpy = 4,4'-di-*tert*-butyl-2,2-'-bipyridine) and platinum/palladium porphyrins. Among these, platinum and palladium porphyrins exhibit strong room temperature phosphorescence with intense visible absorption (480-580 nm),

high quantum yield and long excited state lifetime (0.1-1.0 ms) and are a very promising class of materials for oxygen sensing. Gouterman and co-workers have reported that the luminescence of Pt (II) and Pd (II) complexes of tetra(pentafluorophenyl)porphyrin (TFPP), octaethylporphyrin (OEP), tetraphenylporphyrin (TPP) and tetrabenzporphyrin (TBP) are very sensitive to oxygen quenching (Khalili et al, 1989). An oxygen-sensitive paint based on Pt(OEP) for continuous mapping of surface pressure on airplanes or other aerodynamic surfaces has also been developed (Kavandi et al, 1990).

In addition, Papkovsky and co-workers (1991; 1992; 1993) have constructed several fibre-optic oxygen sensors by immobilizing the complexes Pt(OEP), Pt(TPP), Pt(CP-TEE) (CP-TEE = coproporphyrin tetraethyl ester) and Pt(EP) (EP = ethioporphyrin) in polystyrene. However, most of the porphyrin dyes suffer from photo-oxidation when illuminated in the presence of oxygen (Khalili et al, 1989). In 1993, our research group has demonstrated that the photostability of the platinum porphyrin dyes can be improved by introducing halogenated substituents on the porphyrin ring (Lee et al, 1993b). The electron withdrawing effect of the halogen substituents raises the oxidation potential and reduces the electron density on the porphyrin ring which makes the molecule less reactive toward photooxidation. On the other hand, the quantum yield and lifetime are lower in the presence of halogen atoms. Recently, new platinum (II) and palladium (II) octaethylporphine ketone (Pt-OEPK and Pd-OEPK) dyes have been synthesized by Papkovsky et al (1995). These dyes display higher photochemical stability, longer wave spectral characteristics and better compatibility with semiconductor optoelectronics than other platinum porphyrin dyes.

In the fabrication of oxygen optode, sensor molecules are usually held in a supporting material. Silicone rubber is most commonly used as supporting materials because of its high permeability toward oxygen and high chemical and mechanical stability. Moreover, the hydrophobic nature of silicone rubber minimizes dye leaching and interference quenching by ionic species in the test samples. However, the ionic ruthenium diimine complexes have rather poor solubility in silicone rubber. Early optical oxygen sensors were made by entrapping the ruthenium adsorbed silica gel into silicone rubber (Wolfbeis et al, 1986; Moreno Bondi et al, 1990) or soaking the silicone rubber film in dichloromethane solutions of ruthenium complexes (Bacon and Demas, 1987; Carraway et al, 1991c). Recently, Kilmant and Wolfbeis (1995) have shown that luminescent ruthenium (II) diimine complexes can be made silicone-soluble by coupling the cationic dye with hydrophobic anion trimethylsilylpropansulfonate (TSPS) or dodecyl sulfate (DS). The oxygen sensing films prepared have greater stability to dye leaching and film fogging, better response time and higher luminescence intensity. Besides silicone rubber, other polymer matrices having been used to date include poly(vinyl chloride) (PVC) (Hartmann and Trettnak, 1996), polystyrene (Hartmann and Trettnak, 1996; Hartmann et al, 1995), sol-gel (Watkins et al, 1998; Costa-Fernandez et al, 1998) poly(methyl methacrylate) (PMMA) (Mills and Lepre, 1997; Mills and Thomas, 1997), cellulose acetate (CA) (Mills and Williams, 1997) and cellulose acetate butyrate (CAB) (Mills and Lepre, 1997). The PVC, PMMA, CA and CAB films are usually plasticised with bis(2-ethylexyl) adipate (Hartmann and Trettnak, 1996) or tributyl phosphate (TBP) (Mills and Lepre, 1997; Mills and Williams, 1997) to improve the permeability to oxygen

and hence the response. However, plasticizers may leach from the polymers and are potential source of contamination. In fact, the properties of the matrix material have profound effects on the sensor response time and sensitivity. Recently, oxygen quenching of $[Ru(Ph_2phen)_3]^{2+}$ has been studied in a series of poly(dimethylsiloxane) (PDMS) polymers (Xu et al, 1994) and in Gp-163 (an acrylate modified PDMS) (Kneas et al, 1997) by Demas group. The polymer composition was systematically varied in order to delineate the important structural features for satisfactory use of oxygen sensor supports. The quenching behaviour was found to be a function of polymer structure, including the amount and type of copolymer cross-linker and the amount of hydrophobic silica additive in the polymer matrix.

In a homogenous medium, the relationship between the luminescence intensity and oxygen concentration is described by the Stern-Volmer equation:

$$I_o / I = 1 + K_{sv}[O_2] \qquad (1.1)$$

$$K_{sv} = k_2 \tau_o \qquad (1.2)$$

where I_o and I are luminescence intensities in the absence and presence of oxygen respectively, K_{sv} and k_2 are the Stern-Volmer and bimolecular quenching respectively, τ_o is the luminescence lifetime in the absence of oxygen. However, in heterogeneous systems such as luminescent metal complexes immobilized in polymer films, the Stern-Volmer plots are usually nonlinear with downward curvature. Demas and co-workers attributed the non-linearity of the Stern-Volmer plots to inhomogeneous binding sites in

the polymer and thus, difference in the local oxygen quenching constants (Carraway et al, 1991b). The intensity quenching data are fitted by a proposed two-site model:

$$I_o / I = [f_{01} / (1 + K_{sv1}[O_2]) + f_{02} / (1 + K_{sv2}[O_2])]^{-1} \qquad (1.3)$$

where f_{01} and f_{02} are the fraction of each of the two sites, K_{sv1} and K_{sv2} are the quenching constant for each site. Recently, the same group attempted to collect evidence for the existence of multiple sites in polymer by a detailed study of oxygen quenching for a series of luminescent $ReL(CO)_3CNR^+$ complexes with different degree of bulkiness(L = α-diimine such as 2,2'-bipyridine or 1,10-phenanthroline and R = alkyl group such as tert-butyl) (Sacksteder et al, 1993). Their study suggested that the complex can bind in sites that are readily or poorly quenched by oxygen. Good quenching occurs when the complexes do not bind to the protective sites and are exposed to oxygen quenching.

On the other hand, Li and Wong (1992) have proposed the Nonlinear Solubility Model based on the nonlinear solubility of oxygen in the polymer and kinetics of oxygen quenching. It is proposed that the dissolution of gas obeys Henry's Law only at low concentration of gas. At high concentration of gas, the dissolution of gas shows a negative deviation from Henry's Law due to adsorption of gas in the microvoids of the polymer. In this way, the solubility of oxygen in polymer does not follow a proportional increase for a increase in partial pressure of oxygen outside the polymer. The Nonlinear Solubility Model is given by:

$$I_o/I = 1 + A[O_2] + B[O_2] / (1 + b[O_2]) \qquad (1.4)$$

where A, B and b are constants related to the parameters in the kinetic and solubility equations. A comparison of the two models (Demas et al, 1995) indicated that both models are mathematically equivalent for data fitting in spite of the difference in the underlying physical bases. However, it is possible that both models can not reveal the real situation in the system. Indeed, the oxygen quenching mechanism and kinetics inside polymer matrices are probably much more complicated than the underlying assumptions in the above two models.

More recently, research efforts on oxygen optodes have been extended to chromophores with other metal centers such as osmium (II) (Xu et al, 1996), iridium (III) (Marco et al, 1998), gold (I) (Mills et al, 1997) and copper (I) (Miller and Karpishin, 1999). However, the response of these complexes to oxygen quenching is much lower than ruthenium complexes. In addition, Wolfbeis and co-workers have prepared an oxygen sensor by immobilizing the $[Ru(bpy)_3]^{2+}$ complex inside zeolite cage before incorporation into silicone (Meier et al, 1995). This material possesses advantageous features including fast response and stability towards high temperature. Ruffolo et al (2000) have examined the use of thionylphosphazene-based block copolymers as matrixes for oxygen sensor. The films of poly(methylaminothionylphosphazene)-*b*-poly(tetrahydrofuran) ($PBATP_y$-$PTHF_x$) containing $[Ru(Ph_2phen)_3]^{2+}$ were found to exhibit linear Stern-Volmer plots, as well as better photostability and higher sensitivity to oxygen quenching than simple mixtures of the analogous homopolymers. These provide

attractive alternative to existing oxygen sensors. Two reviews on optical oxygen sensors have recently appeared (Mills, 1997; Demas et al, 1999).

1.3 Development of Biosensors Based on Optical Sensing of Oxygen

The development of biosensors based on optical sensing of oxygen has great potential for exploitation. Wolfbeis and co-workers have reported the use of oxygen optode, based on incorporating $[Ru(phen)_3]^{2+}$-adsorbed silica gel into silicone matrix, for the determination of glucose concentration (Moreno-Bondi et al, 1990). The enzyme glucose oxidase is used to catalyze the oxidation of glucose. The decrease in oxygen concentration during glucose oxidation provides the basis for measurement. In this biosensor, the enzyme was immobilized on the surface of oxygen optode. A layer of carbon black is used to prevent interference from ambient light and sample fluorescence. However, the sensor suffers from long response time (6 minutes). Later, Li and Walt (1995) have developed a dual-analyte fiber-optic sensor for simultaneous determination of glucose and oxygen measurements. The oxygen sensor consists of a hydrophobic gas-permeable siloxane polymer containing $[Ru(Ph_2phen)_3]^{2+}$ on top of which is a poly(hydroxyethyl methacrylate) (polyHEMA) polymer. The glucose sensor is another oxygen sensor with immobilized glucose oxidase on polyHEMA membrane. This sensor

has a fast response time (<30 s) and is relatively stable. More recently, an optical biosensor for the continuous determination of glucose in beverages has been described by Wu and co-workers (2000). Glucose oxidase was entrapped with a glass matrix by a sol-gel method. The matrix was then ground to a powder form and packed into a flow cell together with an oxygen-sensitive membrane fabricated with the $[Ru(Ph_2phen)_3]^{2+}$ complex. Common interferents such as fructose, galactose, lactose and raffinose in beverage samples have no effect on the sensor response.

Apart from glucose sensors, optical sensors for the determination of biochemical oxygen demand (BOD) have also been developed. Wolfbeis and co-workers reported a fiber-optic microbial sensor for determination of BOD in 1994 (Preininger et al, 1994). The yeast *Trichosporon cutaneum* immobilized in poly(vinyl alcohol) was covered with a porous polycarbonate membrane to retain the yeast cells. This microbial layer was then placed on top of an oxygen sensing membrane which was prepared by dispersing the luminescent $[Ru(Ph_2phen)_3]^{2+}$ complex in plasticized poly(vinyl chloride). The BOD values estimated by this new biosensor correlated well with those determined by the conventional BOD_5 method. A scanning optical BOD sensor has also been developed by our research group (Li et al, 1994). The sensing element is a silicone rubber film with embedded $[Ru(Ph_2phen)_3]^{2+}$ complex. A scanner with an excitation light source and optic fiber connected to a light detector are used to collect the signal from the sensing film placed inside the BOD bottle. The main advantage of this sensor is its capability of measuring a large number of BOD samples in a short period of time.

The application of oxygen optode in the determination of other biochemical analytes such as bilirubin (Li et al, 1996; Li and Rosenzweig, 1997), alcohol (Wolfbeis and Posch, 1988; Lau et al, 1999), choline (Marazuela and Moreno-Bondi, 1998) and cholesterol (Trettnak and Wolfbeis, 1990; Marazuela et al, 1997) have been described in the literature. For example. Li and Rosenzweig (1997) have developed a miniaturized fiber optic sensor for the analysis of bilirubin in serum. The fabrication of the sensor is based on immobilizing the complex $[Ru(Ph_2phen)_3]^{2+}$ and the enzyme bilirubin oxidase in an acrylamide polymer that is attached covalently to the distal end of a optical fiber via controlled photopolymerization. Bilirubin is oxidized to biliverdin by bilirubin oxidase, and its concentration is determined by measuring the luminescence intensity change caused by the oxygen consumption in the enzymatic reaction. Lau and co-workers (1999) have reported the use of the $[Ru(Ph_2phen)_3]^{2+}$ complex immobilized in plasticized carboxylated poly(vinyl chloride) as oxygen transducer for monitoring of alcohol concentration. Alcohol oxidase was covalently entrapped in the same membrane by condensation with 1-ethyl-3-(3-dimethylaminopropyl) carbodiimide. The sensor has fairly rapid response time (<1min) and good storage stability. More recently, an optical immunosensor based on glucose oxidase (GOx) as label was described by Papkovsky and co-workers (1999). The immunoaffinity membrane was formed by immobilizing the protein antigen on polystyrene-based oxygen sensitive coating containing platinum (II)octaethylporphine ketone (Pt-OEPK). The concentration of antibodies conjugated with GOx was determined from the change in luminescence lifetime of the immunoaffinity membrane in the presence of glucose. The sensitivity of this sensor is

comparable to that of the standard ELISA method for the detection of human lactate dehydrogenase isoenzymes.

1.4 Bacterial Toxicity Tests

Activated sludge process is one of the most commonly used process for treatment of both domestic and industrial waste waters. The activated sludge can degrade the organic waste into simple and harmless form. However, the process will be disturbed if the influent contains toxic contaminants such as heavy metals and chlorinated hydrocarbons. The toxic contaminants may inhibit the removal of waste organic, reduce the efficiency of solids separation and modify the sludge compacting properties. These problems affect adversely the operation of the plant resulting in degradation of effluent water quality (Koopman and Bitton, 1986). Five mg/L Hg^{2+} in the influent could cause 45% repression in removal of chemical oxygen demand, 50% reduction in oxygen uptake rate and 75% reduction of suspended solids growth in a batch activated sludge system (Gosh and Zugger, 1973). To monitor the environmental impact of toxic materials in both natural and engineered aquatic systems, toxicity testing on the toxic materials should be carried out.

Recently, research efforts have been directed towards the development of short-term bioassay tests for microorganisms. Microbial tests are simple, rapid and inexpensive. Microtox test was the first commercial toxicity test to assess the impact of toxicants introduced by Bulich in 1979 (Bulich, 1979). A specialised strain of luminescent bacterium *Photobacterium phosphoreum* was employed as the bioassay microorganism. A low-level of toxicant can alter the metabolism of this bacterium and affect its luminescence intensity which serves as a parameter to monitor the toxicity of chemicals. Since Microtox test uses only one species of microorganisms in the test, the result from a single-species test may not be able to represent the adverse effect of a chemical on other microorganisms such as activated sludge. Blum (1989) found that the test results obtained from Microtox were quite different from those obtained from respiration inhibition test of activated sludge. It also requires specific instrumentation and the microorganisms are not readily available in most laboratories.

Other methods have also been developed for determining the toxicity of chemicals to activated sludge. Parameters such as substrate uptake rate (Larson and Schaeffer, 1982), cell growth (Broecker and Zahn, 1977), respiration rate (Brown et al, 1981) and enzymatic activity (Anderson et al, 1988) have all been used as indicators for toxicity. For example, Larson and Schaeffer (1982) have developed a rapid method for toxicity screening based on the inhibition of [^{14}C] glucose uptake after 15 min. The glucose uptake inhibition is a nonlinear function of test chemical concentrations. IC_{50} values (concentration of a chemical that exhibits 50% inhibition) for Hg^{2+} and 3,5-dichlorophenol agree well with data reported in the literature. Among these methods,

measurement based on microbial respiration is most frequently used as it has the advantages of speed and simplicity. It is also not subjected to interference from color or turbidity of the test sample, which may invalidate measurements on optical density as those used in the growth method.

Traditionally, BOD inhibition test has been based on respirometric measurement (Montgomery, 1967). It requires a five-day test period which does not allow a quick assessment of toxicity. Later, two standard methods ISO (A) and ISO (B), were proposed by International Standards Organisation (ISO) (ISO, 1986). The sludge concentrations used in the methods are about 100-200 mg/L and 1500 mg/L for ISO (A) and ISO (B), respectively. In these tests, samples of activated sludge are incubated with nutrients and different concentrations of toxicant. The concentration of dissolved oxygen of well-aerated sample of sludge is measured by an oxygen electrode at regular time intervals for three hours. The linear portion of the plot of oxygen consumption versus time is used to calculate oxygen uptake rate and the IC_{50} value is determined. In 1986, King and Painter (1986) studied the variability and reproducibility of the ISO methods. They used nine different sources of sludges. The coefficient of variation (CV) of IC_{50} values within batches of sludge was approximately 9%. However, between batch and between source variations were poor and ranged from 29-76% depending on the test chemical. They explained that the variations may be due to the adsorption to different inert materials, acclimation in sludge previously exposed to industrial wastes and difference in bacterial species. Kilroy and Gary (1992) have done similar work to evaluate the ISO (B) method using ethylene glycol, methanol, isopropanol and acetone as test chemicals. They also

found that between batch and between source variations were larger than within batch variation.

In 1984, the Organization for Economic Cooperation and Development (OECD) published a procedure to test the effect of chemicals on the respiration rate of activated sludge (OECD, 1984). The main difference between the OECD and the ISO methods is the use of synthetic sewage for feeding the sludge. The synthetic sewage stock solution was composed of fixed amount of Bacto-Peptone, Bacto-Beef extract, urea, K_2HPO_4, $MgSO_4$, $CaCl_2$, NaCl and H_3PO_4. The OECD activated sludge respiration inhibition test was evaluated by Klecka and Landi (1985). The bottle to bottle variation in the respiration rates was 5-6% while the variability in IC_{50} values for the three reference compounds 3,5-dichlorophenol, mercuric chloride and phenol was in the range of 12 to 22%. Yoshioka and co-workers (1986) investigated the effect of test conditions such as aeration time, aeration rate, temperature, mixed liquor suspended solids (MLSS) concentration and acclimation on OECD method. They found that moderate deviation from the test conditions defined by the test guideline did not affect the determination of IC_{50} values. Tang et al (1990) compared the serum bottle (SB) toxicity test with OECD method. They showed that these two procedures gave comparable results for nonvolatile chemicals. However, the SB procedure was more reliable for determining the toxicity of volatile chemicals because OECD procedures involved the aeration in open vessel which stripped out the chemical of interest.

Many researchers have carried out studies to compare the performance of different microbial toxicity tests. Dutka and co-workers (1983) compared four short-term toxicity tests: Microtox, the *Spirillum volutans* motility test, ISO (B) and inhibition of activated sludge TTC-dehydrogenase activity. They studied seven test chemicals representing a wide range of toxicity. The results indicate that each method has its own sensitivity pattern, with great variability between IC_{50} values. Most importantly, their study demonstrates that it is unwise to try and assess the presence of toxicants in waters or effluents by a single species or single biochemical test. A battery of several tests is required. Reteuna et al (1989) studied the performance of three bacterial assays in toxicity assessment. The three assays were Microtox, ISO (A) and glucose U-^{14}C mineralization (the rate of release of $^{14}CO_2$ by *Escherichia coli*). The coefficient of variations (CV) of IC_{50} values for 3,5-dichlorophenol and copper sulphate were between 5 and 32%. They concluded that there was no one single ideal assay. The choice of a bacterial assay in toxicity assessment is dependent on the objectives of the work. For example, the Microtox test appears to be well adapted to the detection of aquatic environmental pollution, and to the toxicity screening of complex solid waste effluents. The ISO (A) assay is more suitable to measure the impact of sewage on activated sludge in biological treatment plants.

Due to the variable nature of activated sludge and difficulties in running toxicity assays on activated sludge, researchers and plant operators have been seeking surrogate tests with standardized cultures to assess toxicity. Blum (1989) employed Microtox as a surrogate test. However, the correlation between Microtox and inhibition of respiration

rates of activated sludge was found to be 'fair' for 34 chemicals with $r^2 = 0.69$ and standard error, SE = 0.48. Sun and co-workers have determined the IC_{50} values of 50 organic chemicals based on inhibition of respiration rates of activated sludge and Polytox (Sun et al, 1994; Nirmalakhandan et al, 1996). The Polytox is a commercial blend culture contains 12 strains of microorganisms isolated from activated sludge. The correlation between the IC_{50} values for the two cultures was found to be highly significant. Therefore, the toxicity of chemicals to activated sludge can be estimated with good accuracy by Polytox culture.

Recently, many researchers have developed various biosensors for toxicity monitoring. Kong and co-workers (1993) have developed RODTOX (Rapid Oxygen Demand and TOXicity tester) respirographic biosensor for on-line measurement of microbial respiration in an activated sludge. The principle of toxicity detection is based on the comparison of calibration respirograms before and after receiving a potential toxicant. The RODTOX biosensor provides a fast and accurate method for IC_{50} estimation. Its performance is comparable to that of Microtox test. Evans and co-workers (1998) described the use of redox-mediated amperometric biosensor for toxicity determination in wastewaters. This redox-mediated biosensor employed immobilized activated sludge on electrode to monitor continuously the cellular redox events. The toxic effect was detected by a change in the amplitude of the biosensor signal (current). The results obtained from this biosensor were well correlated with the respiration inhibition test. These two biosensors are both based on amperometric measurement. However, owing to the inherent disadvantages of amperometric method, there is a growing trend

towards the development of biosensor based on optical sensing scheme as described in the previous section. Our research group has developed a luminescence-based scanning respirometer for heavy metal toxicity monitoring (Wong et al, 1997). Instead of using amperometric dissolved oxygen electrode, the measurement of oxygen concentration in the respirometer is based on the quenching of luminescent dyes by oxygen. The inhibition effect of heavy metals on the respiration rate of microorganisms can be evaluated by monitoring the luminescence of the sensing film. The repeatability and sensitivity of this respirometer are comparable to those existing methods. This respirometer has the advantages of speed and low cost, and can measure a large number of samples simultaneously.

1.5 Quantitative Structure Activity Relationship (QSAR)

Worldwatch Institute reports that there are 70,000 synthetic chemicals in use. But no information on the toxic effects of 80% of these chemicals is available. Determination of chemical toxicity is time consuming and expensive. For example, acute toxicity tests cost $2000-$3000 for each test. Hence, tremendous research efforts have been devoted to develop Quantitative Structure Activity Relationships (QSAR) for prediction of toxicity in recent years. QSARs are developed by first testing a set of chemicals for the biological property of interests, in this case toxicity. Chemical and physical descriptors of these

chemicals are then identified and correlated to toxicity. A mathematical relationship between chemical toxicity and its physico-chemical or structural properties is developed by the means of statistical methods such as multiple linear regression. QSAR models are used increasingly to predict quantitatively and screen rapidly the toxicity of chemicals that have not been tested experimentally and also provide a better understanding of the mechanisms involved.

In the past, QSAR methodology was used most extensively in the areas of drug and pesticide by Hammett (1930s), Taft (1950s) and Hansch (1960s). In the late 1970s, QSAR began to be applied to the area of environmental microbiology for analyzing the biocentration, biodegradability (Deardon and Nicholson, 1986), toxic effects to fish (Könemann, 1981b) and inhibition of bacterial activity (Liu et al, 1982). However, there are very few studies on employing QSARs for predicting the toxicity of chemicals on activated sludge. In the present study, different QSARs' approaches were evaluated for their predictive ability of chemical toxicity to activated sludge.

It is important to differentiate between different toxicity mechanisms when developing QSAR. The QSAR developed to describe one mode of toxicity cannot be expected to predict the toxicity of chemical acting by a different mechanism. Acute toxicity mechanism can be complied into two general types: specific toxicity (or reactive) non-specific toxicity (or narcosis). Reactive toxicity results from specific chemical reactions at the toxic site such as a chemical reaction with an enzyme or inhibition of metabolic pathway. Non-specific toxicity (narcosis) is simply the retardation of

cytoplasmic activity due to the partitioning of the chemical onto biological membranes and is considered as baseline narcosis toxicity. It is not associated with a specific mechanism and is related directly to the quantity of toxicant acting upon the cell.

Different QSAR approaches have been developed for predicting the chemical toxicity. They are based on different kinds of descriptors including hydrophobic (octanol-water partition coefficient, log P; aqueous solubility, log S), electronic (energy of lowest unoccupied molecular orbital, ELUMO) and topological (molecular connectivity index, MCI) descriptors. Some of these descriptors have also been combined for developing QSAR. In the following paragraphs, literature reviews on these approaches are given.

The octanol-water partition coefficient (log P) is the most common used parameter in the toxicity QSARs. It describes the relative partitioning between the aqueous phase and the more nonpolar lipid-like biophase. The toxicity of the chemicals increases with log P values. Most organic chemicals exhibit narcosis mode of toxic action and are well modeled by the log P. Schultz and Riggin (1985) studied the relationships between toxicity (log BR), monitored as cell growth, and log P for a series of 20 alkylated and halogenated phenols on *Tetrahymena pyriformis*. The equation log BR = 0.9455 log P - 1.919 has been found to be an excellent model for these compounds. It explained 93.8% of the variability in toxicity. They also noted that phenols substituted with alkyl groups (with electron-releasing effects) were slightly less toxic than halogenated substituted (with electron-withdrawing effects). Later, Schultz and co-

workers have focused on the development of QSARs for the prediction of the acute toxicity of phenols (Schultz et al, 1986; Schultz and Cajina-Quezada, 1987; Schultz, 1987; Schultz et al, 1989; Cajina-Quezada and Schultz, 1990). Schultz and co-workers (1986) investigated the relative toxic response of 27 selected phenols to fathead minnow and *Tetrahymena pyriformis*. They showed that phenol itself and some alkyl and/or halogenated substituted phenols exhibited polar narcosis. These chemicals were more toxic than the baseline toxicity of nonionic narcotic chemicals. Pentahalogenated and selected nitro-substituted phenols may exhibit reactive toxicity as weak acid uncouplers. Hence, two separate log P dependent QSARs were formulated, one for polar narcosis and the other for uncoupling of oxidative phosphorylation. In 1987, Schultz (1987) demonstrated that pK_a values were useful for predicting the mechanism of toxic action of a given phenol. Polar narcotic chemicals have pK_a values > 8.0, while uncoupling agents have pK_a values < 6.5. They also showed that combining log P and pK_a in a single model provides excellent predictability of toxicity of phenols (polar narcosis and uncoupling of oxidative phosphorylation). Their findings are consistent with those of Saarikoski and Viluksela (1982). The predictability of fish toxicity was improved when ΔpK_a (pK_a of phenol - pK_a value of substituted phenol) was added to log P as a second descriptor. Veith et al (1985) suggested that the predictive ability of polar narcosis model may be improved by the addition of an orthogonal electronic parameter.

Apart from Schultz, development of QSAR is of continuing interest for numerous toxicologists. Koch (1982) used first and second order valence connectivity indices to correlate toxicological data for a variety of species. Better correlations were found for

homologous series of chemical rather than more diverse sets. The concept of molecular connectivity indices (MCIs) was first proposed by Randic and had been extensively developed by Kier and Hall (1976; 1981; 1986). MCI is a nonempirical numerical descriptor of molecular structure. It is based solely on bonding and branching patterns rather than physical or chemical characteristics. It encodes structural and atomic information of a molecule. For example, first order valence index carries information relating to both volume and electronic character. Moreover, it has been demonstrated to correlate well with a wide range of physio-chemical properties such as heat of atomization and formation, molar fraction, boiling point and liquid density (Kier and Hall, 1976; 1986). Leegwater (1989) studied the acute toxicity of industrial pollutants to the guppy. He found that QSARs based on second order valence index or a combination of simple and valence first order indices with a dummy variable for the presence of a benzene ring were equivalent to and sometimes even superior to those based on log P values. Nirmalakhandan et al (1994a) and Sun et al (1994) studied toxicity of 50 organic chemicals to activated sludge and commercial culture Polytox. They developed a set of separate QSARs for different classes of chemicals (simple and halogenated alkanes, aromatics, esters, ketones, amines) using molecular connectivity indices (MCIs). They found that the toxicity of each chemical class could be correlated with either zero or first order valence indices. Moreover, satisfactory agreement was found between values predicted by QSAR and data reported in the literature ($r^2 = 0.798$ at $p = 0.0001$).

Some researchers have tried to use combined descriptors for predicting the toxicity of chemicals. Blum and Speece (1991b) employed LSER models for predicting

non-reactive toxicity of large set of organic chemicals (including chlorinated and other substituted benzenes, phenols, and aliphatic hydrocarbons) to activated sludge, methanogens, *Nitrosomonas* and *Photobacterium phosphoreum*. They found that LSER approach produced the most accurate QSARs and covered the widest range of chemicals. LSER approach is based on a combination of four different molecular characteristics called solvatochromic descriptors: V_i, the molecular van der Waals volume; π^*, measure of polarity or polarizability; and α_m and β_m, measure of the ability to participate in hydrogen bonding as a hydrogen donor and acceptor respectively. However, the solvatochromic parameters of LESR are only available for a finite number of chemicals. Recently, a set of ground rules has been proposed by Hickey and Passino-Reader (1991) for the estimation of these parameters. The rules are far from rigid and consistent. Their application to new chemicals requires considerable insight, intuition and judgement; and several optional corrections, modification and adjustments have to be made by the user themselves (Hickey and Passino-Reader, 1991). Tang and co-workers (1992) determined the toxicity of total 43 phenols, benzene and aliphatic chemicals to *Nitrobacter* and compared the log P, LSER and MCI approaches.

Akers and co-workers (1999) investigated the QSARs of 39 halogenated alkanes, alkanols and cyanoalkanes in a population growth impairment assay using *Tetrahymena pyriformis*. The toxicity of halogenated alkane and alcohol derivatives was found to depend mostly on the hydrophobicity (log P) of the toxicants. Nitrile derivatives exhibited toxicity that depended more on the ELUMO, but this parameter did not perfectly explain their toxicity. Log P and ELUMO could model the toxicity for all three substituent

classes when some statistical outliers were rejected. These two parameters offer mechanistic understanding of toxicity by modeling transport and electrophilicity, respectively. This concept of a hydrophobic- and electrophilic- dependent model was discussed in more details by Veith and Mekenyan (1993). They demonstrated that generalized parameters can be used to develop QSAR even where reaction mechanisms were multiple or unknown. Similar work has been done for 200 substituted benzenes by Schultz (1999). Again, a two-parameter model (log P and maximum superdelocalizability, (S_{max}) can be developed regardless the toxicity mechanisms of the chemicals.

In addition to the above approaches, other descriptors such as molecular (molar refractivity, MR), quantum chemical (Theoretical Linear Solvation Energy Relationship parameters, TLSER; dipole moment, Dip; etc.) and electronic (nucleophilic susceptibility, NS; partial atomic charge, PAC; etc.) parameters have also been used by researchers in the development of QSAR. Hermens et al (1985) discussed QSAR models for 22 nonreactive aliphatic and aromatic compounds. They found linear relationships between log P and toxicity. The models were improved by addition of MR descriptor. Sixt and co-workers (1995) investigated the acute toxicity of 80 chlorinated aliphatic and aromatic compounds to *Photobacterium phosphoreum* using TLSER parameters. Molecular volume appeared to be the most important TLSER descriptor. For the complete data set and for phenols the TLSER descriptor is superior to log P alone. Bláha et al (1998) developed QSAR for halogenated alkane and alkene using 23 different molecular and electronic parameters. They found that the size of molecules (MV, MR) was the most

significant parameters for haloalkane. This characteristic can be related to accumulation of the haloalkane in biological membrane or binding to biomacromolecules. The molar refractivity and electronic energy were able to describe the toxicity of both haloalkane and haloalkene. Recently, Okey and Martis (1999) have identified twenty steric and electronic descriptors (number of pi electrons, zero and first order valence indices, ELUMO, EHUMO, bond distortion energy, etc.) that related to chemical toxicity. Warne and co-workers (1999) have correlated the toxicity of 138 halogenated benzene with 86 semi-empirical molecular-orbital descriptors such as nucleophilic susceptibility, dipole moment, partial atomic charge and so on. They found that molar refractivity was the most important parameter, followed by solvent accessible surface area of the compound. More recently, Trevizo and Nirmalakhandan (1999) have shown that aqueous solubility (log S) of a compound was a good predictor for microbial toxicity. Three reviews on QSAR have been given by Nirmalakhandan and Speece, (1988), Blum and Speece (1990) and Cronin and Dearden (1995).

1.6 Development of Optical pH Sensors

The measurement and control of pH are important in analytical, biomedical and environmental chemistry. The conventional pH electrode is reliable over a large pH range and easy to operate which make it suitable for most kinds of application. In recent

years, however, considerable efforts have been directed toward the development of optical pH sensors. This is because the optical pH sensors offer several advantages over the potentiometric pH electrode such as electrical safety, amenable to miniaturization, immune to electrical interference, no need for a reference electrode and possibility of remote sensing which allow the measurement of pH under circumstances that may not be convenient for a pH electrode.

Optical pH sensors are based on the pH-dependent change of the optical properties of a pH indicator. These indicators are weak acid whose dissociated and undissociated forms have different absorption or luminescent properties in the pH range of interest. The first fiber optic pH sensor was developed by Peterson et al (1980). The principle of the pH optode was based on the absorbance changes of an indicator phenol red (phenolsulfonphthalein). The indicator was covalently bound to polyacrylamide packed in a dialysis tubing at the end of an optical fiber. However, the system has limited pH range (7.0-7.4). Kirkbright et al (1984) constructed another pH optode based on absorption changes. The sensitive layer consists of bromothymol blue immobilized on polymer XAD-2 which are retained in position by a porous polytetrafluoroethylene membrane. It showed good response to pH in the range between 8 and 10.5. The response time of the sensor was rather long, being about 5 minute for 99% of total signal change. Later, Jones and Porter (1988) have fabricated an optical pH sensor by immobilizing Congo red (3,3'-[(1,1'-biphenyl)-4,4'-diylbis(azo)]bis[4-amino-1-naphthalenesulfonic acid) on a base-hydrolyzed cellulose acetate film. The sensor has fast response (<1.3 s) and large dynamic range (> 4 pH units). They claimed that the

rapid response is due to the porous structure of the polymeric support which minimizes barriers to mass transport between the analyte and immobilized indicator. Sensors using cresol red (Moreno et al, 1986; 1990), neutral red (Kostov and Tzonkov, 1993), bromophenol blue (Boisdè et al, 1988), azo dyes (Mohr and Wolfbeis, 1994) and thiazole yellow (Safavi and Abdollahi, 1998) as absorbance indicators have also been reported. For example, Moreno and co-workers used cresol red immobilized on the anion-exchange resin Dowex 1-X10 as pH sensor to test with milk sample (Moreno et al, 1986) and monitor acid-base titration (Moreno et al, 1990). Safavi and Abdollahi (1998) have developed a pH optode by convalently immobilizing thiazole yellow on triacetylcellulose membrane for measurement of high pH values (12.0-13.5), where glass electrodes show an alkaline error.

Apart from absorbance indicators, a large number of fluorescent indicators have been used in the construction of pH optodes. The first fluorescence-based pH sensor has been reported by Saari and Seitz (1982). It was based on fluoresceinamine immobilized on cellulose or controlled porous glass, which were attached to the end of a bifurcated fibre optic. Unfortunately, the large background signal and low emission intensity limited the precision of the optode. A similar approach was taken by Munkholm et al (1986). They have prepared optical sensor by incorporating fluoresceinamine into acrylamide-methlenebis(acrylamide) copolymer attached covalently to a surface-modified glass fiber via thermal photomerization. The polymer serves to increase the surface area for allowing multiple sites attachment of the indicator which results in enhanced fluorescence signal. The response is fast as no membrane is required. However, the sensor still suffers

the problem of photobleaching. Hydroxypyrenetrisulfonic acid is another class of dye commonly used for pH sensing. Its major advantages include high fluorescence quantum yield, visible excitation and emission, and a large Stokes' shift. Zhujun and Seitz (1984) have developed an pH optode by electrostatic immobilization of 8-hydroxyl-1,3,6-pyrene trisulfonic acid (HOPSA) on anion-exchange membrane. The ratio of fluorescence intensities resulting from excitation at 405 and 470 nm was used to quantify pH in physiological range (6.5 - 8.5). The dual excitation ratiometric method was said to be insensitive to light source fluctuations, changes in temperature and ionic strength. With respect to practical application, the ratiometric method requires more complex instrumentation to isolate two excitation wavelengths from one light source and differentiate the signals in the detection system. An optical sensor based on immobilization of 1-hydroxpyrene-3,6,8-trisulphonate (HPTS) on porous glass support has been reported by Wolfbeis group (Offenbacher et al, 1986). The effect of ionic strength was eliminated by chemical treatment of the glass surface with an aminosilane reagent which renders the indicator's environment highly charged. As a result, the effects introduced by electrolytes from the sample are minimized. Similar to HOPSA-based sensor, however, photostability of the HSTP-based sensor was not very good.

The spectral and photophysical of series of fluorescent, long-wavelength benzo[c]-xanthene dyes have been studied in detail by Whitaker and co-workers (1991). The general classes of these indicators are semi-naphthofluoresceins (SNAFLs) and seminaphthorhodafluors (SNARFs). They showed that these dyes have desirable characteristics as pH indicators including distinct emission from the protonated and

deprotonated forms, absoption maxima at above 500 nm and pK_a values within the physiological pH range. Later, Parker et al (1993) have prepared a fiber-optic sensor for pH measurement using the SNARF dyes immobilized on poly(hydroxyethyl methacrylate) (PHEMA). The excitation source of the sensor was inexpensive green LEDs and the ratio of emission intensities from the acid and base tautomers was used to measure the physiological pH range (6.8–7.8).

pH optodes based on near-infrared dyes, carboxylated cyanine (Zen and Patonay, 1991) and acidochrome (Lehmann et al, 1995) have also been reported. Since the absorption maxima of the dyes are in the near-IR region, more intense and cheap laser diodes can be used as light source. Moreover, the sensor has lower interference on studying the biological sample in the near-IR region.

Carey and Jorgensen (1991) have developed a pH optode for monitoring acid concentration from 0.1 to 10 M by using fluorescent polymers. The fluorescent polymers are poly(phenylquinoline), poly(biphenylquinoline) and poly(phenylquinoxaline), which can be protonated under highly acidic conditions. The optode is based on the change in fluorescent emission as a function of acid concentration. Recently, optical sensors based on polypyrrole (Marcos and Wolfbeis, 1996), polyaniline (Ge et al, 1993; Pringsheim et al, 1997; Grummt et al, 1997) and substituted polyaniline (Pringsheim et al, 1997; Sotomayor et al, 1997) have been described. For example, polypyrrole films obtained by chemical oxidation of pyrrole showed pH-dependent absorbance changes between pH 6 and 12 with an apparent pK_a around 8.6. It provides an interesting alternative to

indicator-based pH sensor because it simplifies the indicator immobilization chemistry on the transducer. However, the sensor's practicability on pH measurement is limited by the presence of hysteresis effect which requires reconditioning of the sensor (Macros and Wolfbeis, 1996; Grummt et al, 1997).

Apart from intensity-based pH optodes, new systems based on the measurement of fluorescent lifetime (Szmacinski and Lakowicz, 1993; Draxler and Lippitsch, 1993; Draxler and Lippitsch, 1995) and energy transfer (Jordan et al, 1987; Lakowicz et al, 1993; Gabor et al, 1995; Kosch et al, 1998; Kosch et al, 1999) have also been described. A fiber-optic pH sensor based on energy transfer was first developed by Jordan et al (1987). A pH-insensitive fluorophore, eosin (the donor) and a pH-sensitive absorber, phenol red (the absorber) were co-immobilized on the distal end of a fiber. The emission spectrum of eosin overlaps with the absorption spectrum of the base form of phenol red. As the pH increases, the concentration of the base form of phenol red increases, resulting in an increased energy transfer from eosin to phenol red and in a diminished emission intensity of eosin. Later, Walt and co-workers studied the energy transfer between two pH-sensitive fluorophores having similar pK_a values and pH dependence (Gabor et al, 1995). The donor is 7-hydroxy-4-methylcoumarin-3-acetic acid (HCA) while the acceptors are fluorescein or 5-(and 6-) carboxy-4',5'-dimethyl fluorescein (CDF). Since the emission of the HCA itself is pH dependent, excitation of the acceptor through energy transfer has a multiplicative effect on its emission. As a result, the pH sensitivity of acceptor dyes, fluorescein and CDF are enhanced when excite via energy transfer. More recently, Wolfbeis and co-workers have developed a pH optode with luminescence decay

times in the microsecond time regime (Kosch et al, 1998). The optode is based on radiationless energy transfer from a luminescent complex, ruthenium (II) tris-4,4'-diphenyl-2,2'-bipyridyl (the donor) to colorimetric pH indicators, bromothymol blue or reactive azo dye (the acceptors) which are co-immobilized into hydrogel matrix. The optode shows pH response in the range of 7 to 9 and allows lifetime measurement with rather inexpensive optoelectronic components such as blue LED as light source. However, photostability of the optode is poor and the response is affected by oxygen.

In addition to organic dyes, a number of luminescent transition metal complexes with ligands containing non-coordinated proton transfer sites show pH-dependent luminescent characteristics. Several pH-sensitive luminescent complexes based on photoinduced electron transfer (PET) have been reported by Grigg and co-workers. The luminescent complexes were aminomethyltetraphenylporphyrin-tin(IV) derivatives (Grigg et al, 1992b), di(2,2'-bipyridyl)(5,5'-diaminomethyl-2,2'-bipyridyl)- ruthenium (II) complexes (Grigg et al, 1992a) and *p-tert*-butylcalix[4]arene-linked ruthenium (II) tris(bipyridyl) complexes (Grigg et al, 1994). Recently, the searching of pH-sensitive complexes has mainly focused on $[Ru(bpy)_2L]^{2+}$ derivatives (L = (i) 2,2':4',4"-terpyridine, (ii) 4(4-pyridyl)-2,2':4',4"-terpyridine, (iii) 4-(4-hydroxyphenyl)-2,2'-bipyridine, (iv) 4-(3-hydroxyphenyl)-2,2'-bipyridine (Cargill Thompson et al, 1997), (v) imidazo[f]-1,10-phenanthrolines (Jing et al, 1999), (vi) 4,4'-diethylaminomethyl-2,2'-bipyridine (Murtaza et al, 1997)). For instance, the last complex $[Ru(deabpy)(bpy)_2]^{2+}$ was found to display pH-dependent intensities, emission spectra, and decay time, with the changes centered near the physiological pH value of 7.5. However, all the complexes

described above have not been incorporated into polymer supports as pH sensors. The first fiber-optic pH sensor based on metal complex has been described by Blair and co-workers (1993). Cobalt(II) tetrakis(p-hydroxyphenyl)porphyrin was polymerized electrochemically on indium(tin) oxide glass slides. The sensor is highly selective to pH, presenting minimal interferences from anions and has a linear response from pH 8 to 12. More recently, Demas and co-workers have prepared a pH sensor by incorporating the $[Ru(phen)_2(phen(OH)_2)]^{2+}$ or $[Ru(Ph_2phen)_2(phen(OH)_2)]^{2+}$ (phen = 1,10-phenanthroline, Ph_2phen = 4,7-diphenyl-1,10-phenanthroline, $phen(OH)_2$ = 4,7-dihydroxy-1,10-phenanthroline) into a network polymer containing cyclic methyl siloxane ring and poly(ethylene oxide) cross-linkers (Price et al, 1998). The useful range of these pH sensors is 2-6, and most importantly the feasibility of using this new system in constructing a pH sensor is demonstrated.

Numerous substrates and fabrication schemes for indicator immobilization have been evaluated. The substrates having been used included sintered and controlled-porosity glass (Sarri and Seritz, 1982; Offenbacher et al, 1986; Bacci et al, 1991), anion-exchange resin (Kirkbright et al, 1984; Zhujun and Seitz, 1984; Moreno et al, 1990), cellulose (Jones and Porter, 1988; Kostov and Tzonkov, 1993; Cardwell et al, 1995; Cardwell et al, 1993; Ensafi and Kazemzadeh, 1999), polyacrylamide (Peterson et al, 1980; Munkholm et al, 1986) and cross-linked poly(vinyl alcohol) (Zhujun et al, 1989). Most researchers have either used covalent chemical linking or physical encapsulation techniques to immobilize dye molecules. Physical entrapment is the technically simpler technique, but the response is relatively long and the dye can leach out from the matrix.

For covalent linking of the dye molecules surface modification of the optical fiber or substrate is required. Films proposed by covalent immobilization do not leach in general. However, this method is often more difficult to implement and may lead to loss of dye sensitivity or results in poor absorption and fluorescence properties. Recently, sol-gel glasses (Rottman et al, 1992; Lee and Saavedra, 1994; Badini et al, 1995; Grant and Glass, 1997; Gupta and Sharma, 1998) have gained particular interest as matrices because of their optical transparency, chemical durability, mechanical stability and better protectability of the trapped molecules. Rottman and co-workers (1992) have immobilized a series of pH indicators including methyl orange, methyl red, thymol blue, bromothymol blue, phenol red and cresol red in sol-gel porous glass. A fiber optic sensor based upon sol-gel encapsulation of seminaphthorhodamine-1 carboxylate (SNARF-1C) for blood pH measurement has been developed by Grant and Glass (1997). The sensor was shown to have low leachability and reproducible response in the pH range of 6.8 – 8.0.

1.7 Aims and Objectives of this Project

Among various oxygen sensing dyes, ruthenium (II) tris(4,7-diphenyl-phenanthroline), [$Ru(Ph_2phen)_3^{2+}$] have received the most attention as it has the longest excited lifetime, highest quantum yield and largest quenching constant. Silicone rubber was found to be a suitable matrix for fabrication of oxygen sensor. However, low solubility of ionic complex in silicone rubber is a detriment to the performance of the sensor as ionic dyes tend to form aggregates in the hydrophobic polymer matrix. In this project, an oxygen sensing film is prepared by adsorbing the [$Ru(Ph_2phen)_3^{2+}$] onto high surface area hydrophilic fumed silica and dispersing the ruthenium-loaded silica in silicone rubber support. The performance of the sensing film will be compared with the film without fumed silica.

We are also interested in evaluating the applicability of oxygen optodes for determination of the toxicity of chemical substrates to microorganisms. An optical scanning respirometer based on the oxygen optode has been developed. The IC_{50} values (concentration of a chemical that exhibits 50% respiration inhibition) of various organic chemicals were determined and compared with other methods to investigate the reproducibility and sensitivity of the respirometer. In addition, QSARs were developed to determine the relationships between the toxicity and physio-chemical or structural properties of the chemical substances. The ability of the developed QSAR models for predicting the toxicity of chemical mixtures was also investigated in this project.

Besides oxygen optode, there has been much research effort devoted to the development of optical pH sensors. However, pH optode based on incorporation of luminescent transition metal complex in polymer support is rare. Thus an optical pH sensor based on immobilized luminescent ruthenium complex $[Ru(bpy)_2(dhphen)]^{2+}$ (bpy = 2,2'-bipyridine, dhphen = 4,7-dihydroxy-1,10-phenanthroline) in Nafion film has been studied and the pH optode was applied to pH monitoring of fermentation by *Klebsiella pneumoniae* fermentation.

Chapter 2

The Performance of Oxygen Sensing Films with Ruthenium-Adsorbed Fumed Silica Dispersed in Silicone Rubber

2.1 Introduction

Quantitative determination of oxygen concentration is important in chemical analysis related to environmental, clinical and industrial applications (Surgi, 1989; Gottlieb et al, 1991). In recent years, much effort has been devoted to the development of optical oxygen sensors based on luminescence quenching of transition metal dyes because of their high sensitivity and desirable optical properties (Demas and DeGraff, 1991). Among the different metal complexes being investigated, ruthenium tris(4,7-diphenyl-1,10-phenanthroline), $[Ru(Ph_2phen)_3^{2+}]$ (Bacon and Demas, 1987; Li et al, 1993; Hartmann et al, 1995; Klimant and Wolfbeis, 1995) and platinum/palladium porphyrins (Lee et al, 1993b; Papkovsky et al, 1995; Mills and Lepre, 1997) are the two classes of luminescent metal dyes that have received most attention. In the fabrication of an oxygen sensing film, the luminescent dye has to be immobilized in a polymer support which provides the mechanical strength and protects the dye from potential interferents in the measuring environment. Although the hydrophobic metalloporphyrins encounter relatively little 'solubility' problem in most polymer matrix, the ionic ruthenium dyes are immiscible with hydrophobic polymers such as silicone rubber. Uneven distribution of the ruthenium dye within the polymer matrix would result in the formation of aggregated ion pairs (Klimant and Wolfbeis, 1995), leading to a large portion of the dye molecules not quenched by oxygen. Previous attempts to solve this 'solubility' problem include entrapping an aqueous emulsion of the ruthenium complex in silicone rubber (Wolfbeis et al, 1986), adding polar co-polymer cross-linkers to the nonpolar polymer (Xu et al, 1994) and employing a ruthenium dye with a surfactant anion such as dodecyl sulfate (Klimant and Wolfbeis, 1995). During our investigations on optical oxygen sensors, we found

that a convenient way to prepare oxygen sensing films is to adsorb the ionic ruthenium dye onto high surface area fumed silica followed by dispersing the silica particles in silicone rubber. A comparison of the performance of oxygen sensing films with and without fumed silica is presented in this chapter.

2.2 Experimental Section

2.2.1 Materials

Potassium aquapentachlororuthenate (III) was obtained from Johnson Matthey. The ligand Ph_2phen was purchased from Aldrich. The RTV silicone rubber purchased from Nice Top Quality Ltd. is a one-part clear polymer containing no silica filler. The fumed silica employed in this study were Cab-O-Sil fumed silica LM-130, HS-5 and EH-5 obtained from Cabot Corporation. The surface of these fumed silica contains hydroxyl groups (about 3.5-4.5 hydroxyl groups per square nanometers of silica surface) (Cabot Corporation) and is therefore hydrophilic. These fumed silica particles are three-dimensional branched chain aggregates with a length of approximately 0.2 to 0.3 microns. The difference in the different grades of fumed silica lies in their surface areas which are 130, 325 and 380 $m^2 g^{-1}$ for LM-130, HS-5 and EH-5 fumed silica, respectively (Cabot Corporation). Other chemicals were analytical-grade reagents and were used without further purification. Oxygen and nitrogen gases (99.9%) were purchased from Hong Kong Oxygen Co.

2.2.2 Synthesis

$[Ru(Ph_2phen)_3](ClO_4)_2$ was synthesized and purified according to a published method (Lin et al, 1976). Potassium aquapentachlororuthenate (III) (0.5 g, 1.33 mmol) was dissolved in 50 ml of hot water containing one drop of 6M hydrochloric acid. The ligand Ph_2phen (1.6 g, 4.8 mmol) was dissolved in 30 ml of N,N-dimethylformamide (DMF), added slowly to the above aqueous ruthenium solution. The mixture was boiled 10-20 min until deep green solution was observed and was then filtered. Hypophosphorous acid (1.2 ml of 30% solution) neutralized with sodium hydroxide (3.5 ml of 2 M solution) was added to the filtrate and the mixture was refluxed 15-30 min until the color had changed to deep orange red. Then excess aqueous solution of $LiClO_4$ was added with stirring to the mixture. The precipitated complex was isolated by filtration and washed with deionized water.

2.2.3 Physical Measurements

Ultraviolet/visible absorption spectra were recorded on a Hewlett Packard 8452A Diode Array Spectrophotometer. Luminescence intensity measurements were performed using a Perkin-Elmer LS50B Luminescence Spectrometer with a 20 kW xenon discharge lamp as light source. The excitation and emission wavelengths used in this work were 467 nm and 598 nm respectively. Two gas flowmeters calibrated by volumetric method individually were used to monitor the flow rates of oxygen and nitrogen. The oxygen and nitrogen gases were mixed in a one meter long tygon tubing

and then fed into a flow cell in which the sensing films was exposed to the mixed gas stream, and the glass slide was facing the excitation light source in the spectrometer. The oxygen concentration (% v/v) was calculated by dividing the oxygen flow rate with the sum of the oxygen flow rate and the nitrogen flow rate. All measurements were conducted at room temperature (25 ± 2°C) and atmosphere pressure.

2.2.4 Preparation of the Oxygen Sensing Films

A 0.18 mM stock solution of $[Ru(Ph_2phen)_3](ClO_4)_2$ in ethanol was prepared. An aliquot of the stock solution (0.1-1 ml depending on the required loading of ruthenium on silica) was transferred into a test tube containing 0.05 g fumed silica. The mixture was allowed to stand at room temperature for 24 h, after which most of ruthenium complexes had adsorbed onto the silica and the ethanol solution became colorless or very pale in color. The silica was then separated from the liquid by centrifuge and dried under vacuum overnight. The amount of ruthenium adsorbed on the silica surface was estimated from the difference in ruthenium content of the ethanol solutions before and after treatment with silica by measuring its absorbance at 467 nm. The ruthenium-loaded silica was then mixed thoroughly with 0.5 g of uncured silicone rubber and 3 ml toluene in an ultrasonic bath. A 0.3 ml portion of the slurry mixture was transferred to a glass slide of 11 mm diameter. For comparison purpose, films containing ruthenium complex but no silica were prepared by mixing appropriate aliquot of the ruthenium complex solutions in tetrahydrofuran with silicone rubber and toluene under sonication and transferring the mixture to the glass

slide. The films were left undisturbed for 24 h to allow complete curing. The films prepared in this way have a thickness of about 0.2 mm. Variation of film thickness can be achieved by pipetting different amount of the slurry mixture to the glass slide. The concentration of ruthenium complex in the film was calculated as the number of moles of complex added divided by the volume of the sensing film. The volume of the sensing film was calculated from the weight of the film and its density which was measured separately using a block of the same polymer.

2.3 Results and Discussion

2.3.1 Adsorption of Ruthenium Complex on Fumed Silica

Cab-O-Sil LM-130, HS-5 and EH-5 are high surface area hydrophilic fumed silica with acidic hydroxyl groups on the silica surface (Cabot Corporation). The loading of ruthenium on fumed silica was calculated from the difference in ruthenium content of the ethanol solutions before and after treatment with silica. A plot of adsorbed ruthenium complex against concentration of complex in solution for different fumed silica is shown in Figure 2.1. It shows that the maximum loading of $[Ru(Ph_2phen)_3]^{2+}$ on these silica surfaces is approximately 3.0 and 3.5 μmole ruthenium complex per gram of silica for LM-130 and HS-5/EH-5 respectively. It appears that the maximum loading does not depend much on the surface area of the fumed silica used. If one takes the radius of $[Ru(Ph_2phen)_3]^{2+}$ as 15 Å (Carraway et al, 1991a), the amount of adsorbed ruthenium complex only represents a 4-10% coverage of the surface area of the silica. However, it should be noted that Cab-O-Sil fumed silica are silica aggregates (Cabot Corporation) and its clustered nature may make it difficult for large molecules such as $[Ru(Ph_2phen)_3]^{2+}$ to gain access to all surfaces which can be reached by the gas molecules in the surface area measuring procedure. Moreover, the cationic ruthenium complex may interact more favorably with the hydrophilic hydroxyl groups on the silica surface. Hence it is not unreasonable that the maximum loading does not represent a complete coverage of the silica surface.

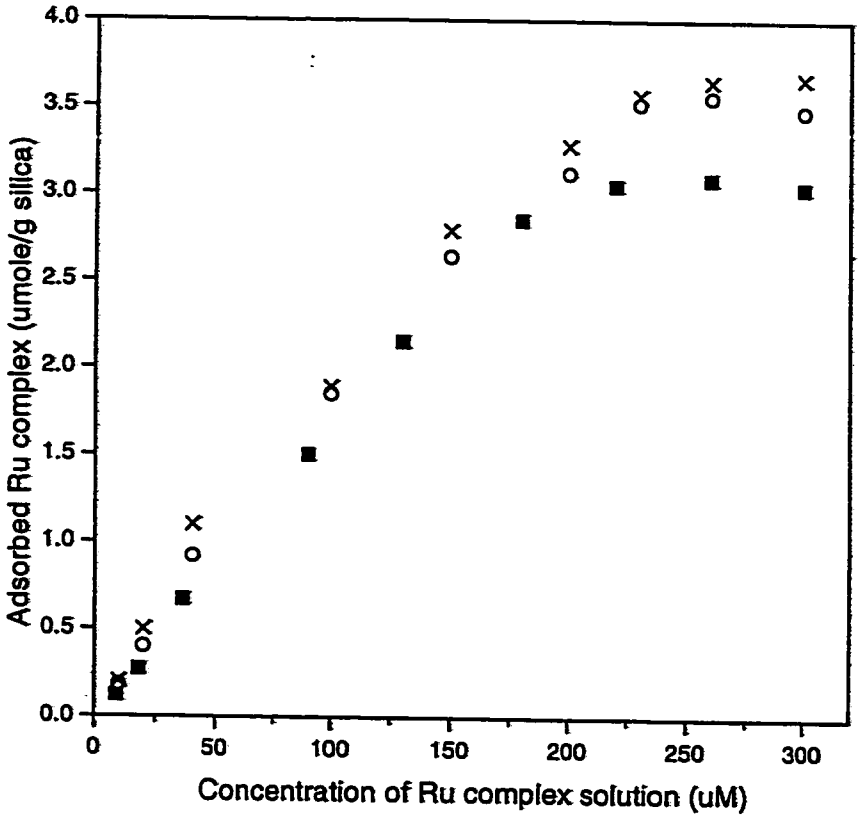

Figure 2.1 Plots of adsorbed $[Ru(Ph_2phen)_3](ClO_4)_2$ complex against concentration of complex in solution for different fumed silica. (■) LM-130, (o) EH-5, (×) HS-5.

2.3.2 Characteristics of Oxygen Sensing Films

The luminescence of the $[Ru(Ph_2phen)_3](ClO_4)_2$ arises from metal-to-ligand charge-transfer (MLCT) excited state which is derived from a configuration involving promoting a metal d e^- to a ligand π^* antibonding orbital. The emission spectra of $[Ru(Ph_2phen)_3](ClO_4)_2$ in silicone rubber with and without fumed silica are shown in Figure 2.2. The emission wavelength of the ruthenium complex remains essentially unchanged in the presence of fumed silica. The optimum concentration of the ruthenium dye (which corresponds to a particular loading of ruthenium on silica) in the sensing film was determined from the luminescence intensity under 100% nitrogen atmosphere (I_0) with different concentrations of the immobilized dye. The plots of luminescence intensity versus concentration of $[Ru(Ph_2phen)_3](ClO_4)_2$ in different polymer supports are shown in Figures 2.3-2.6. The plots show an initial upward curve indicating an increase in luminescence intensity with the ruthenium concentration followed by a downward curve as the dye concentration further increases. The decrease in luminescence intensity at high ruthenium concentration may be attributed to self-quenching of the complexes on the silica surface. It was also noticed that the quenching ratio I_0/I_{100} (I_{100} corresponds to the intensity under 100% oxygen) does not change much with the dye concentration. The optimum concentrations of the ruthenium dye with its quenching ratio and maximum luminescence intensity in different polymer supports are summarized in Table 2.1. These films with optimum ruthenium concentration were used in subsequent studies to evaluate the performance of the sensor.

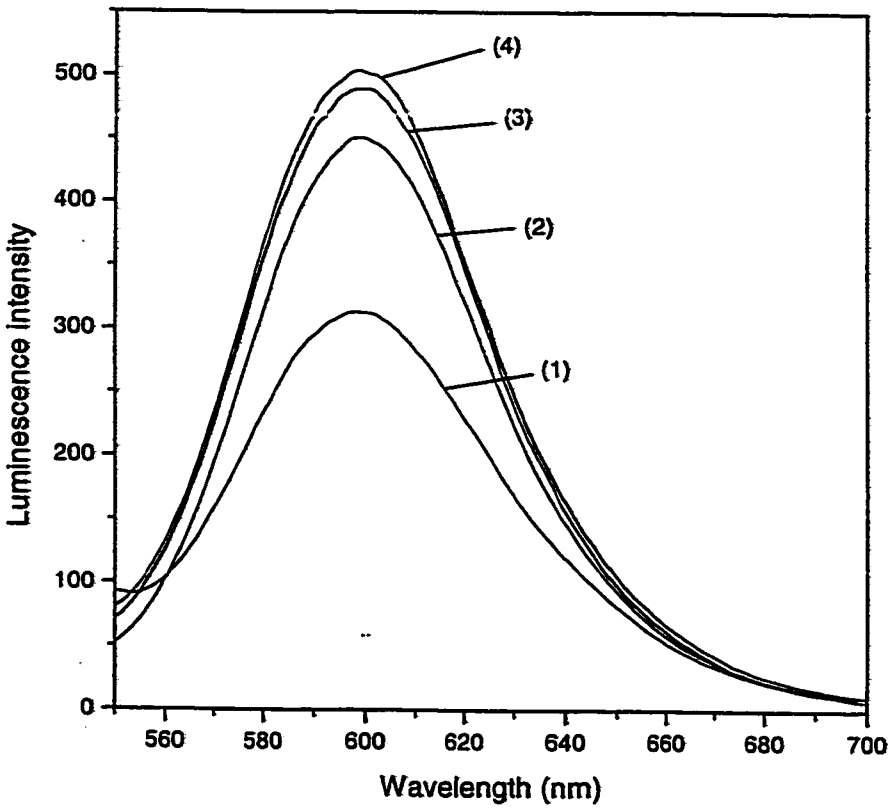

Figure 2.2 Emission spectra of $[Ru(Ph_2phen)_3](ClO_4)_2$ in different supports. (1) silicone rubber, (2) silica(HS-5)-silicone, (3) silica(LM-130)-silicone and (4) silica(EH-5)-silicone.

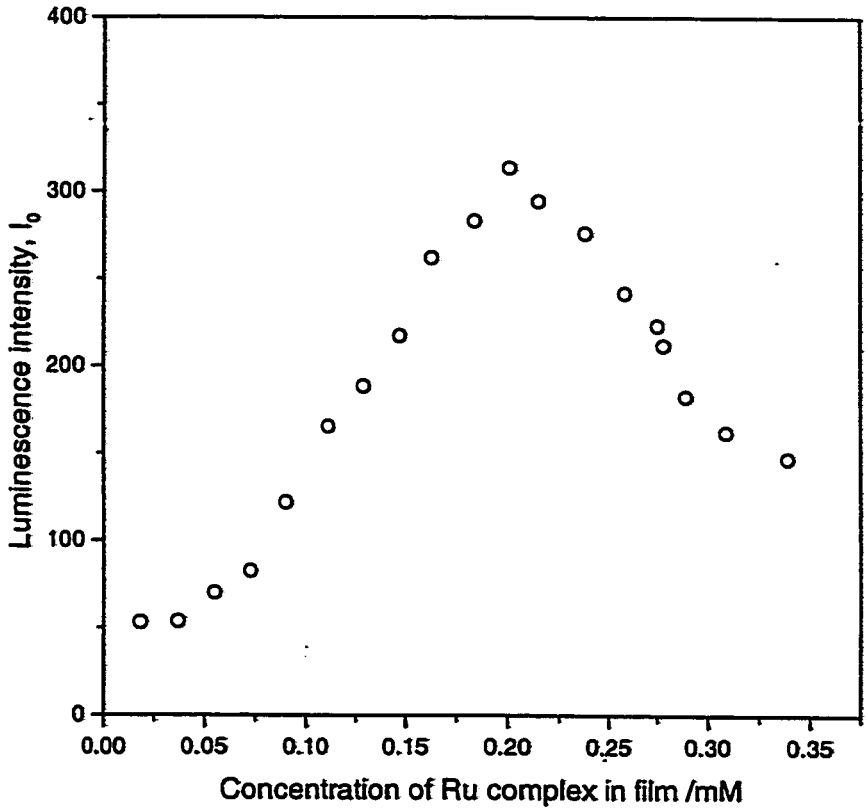

Figure 2.3 Plot of luminescence intensity (I_0) versus concentration of $[Ru(Ph_2phen)_3](ClO_4)_2$ in silicone rubber support.

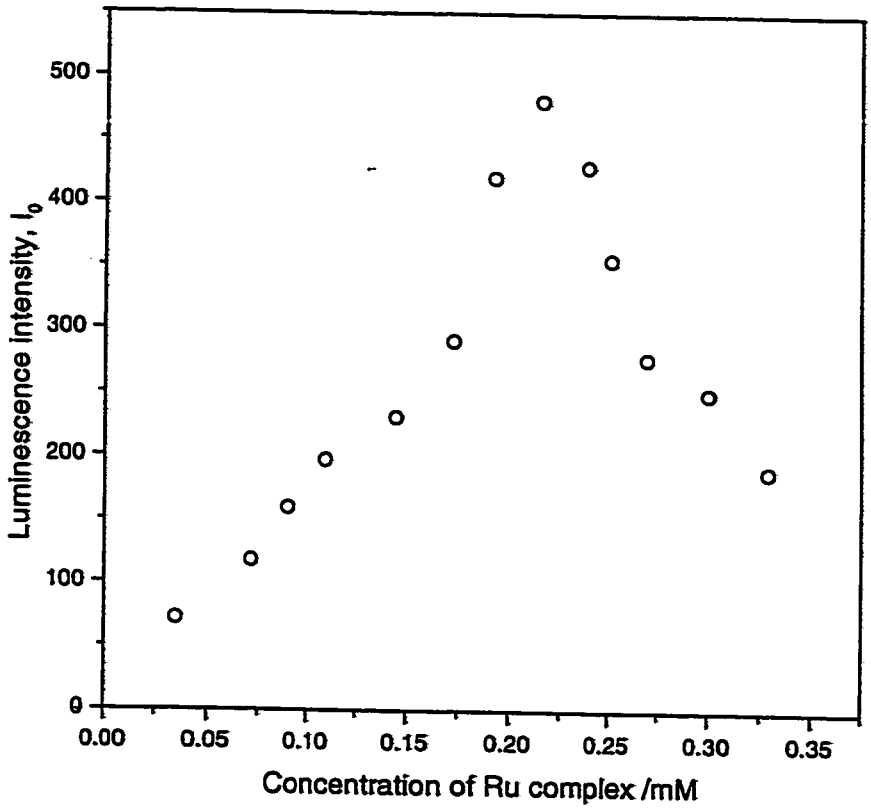

Figure 2.4 Plot of luminescence intensity (I_0) versus concentration of $[Ru(Ph_2phen)_3](ClO_4)_2$ in silica(LM-130)-silicone support.

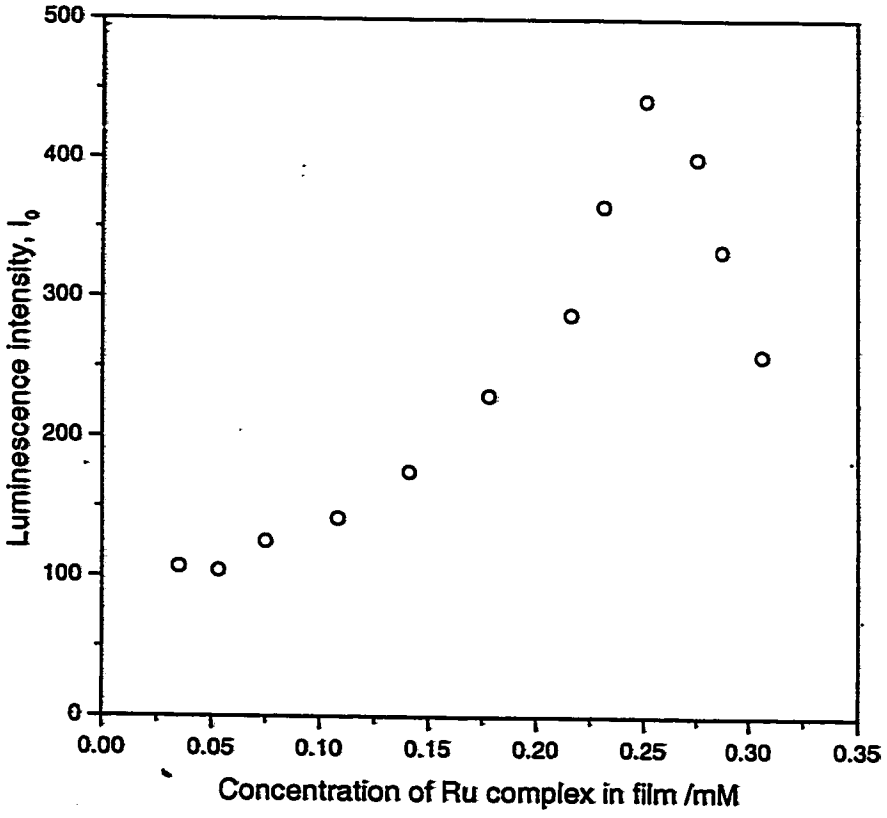

Figure 2.5 Plot of luminescence intensity (I_0) versus concentration of $[Ru(Ph_2phen)_3](ClO_4)_2$ in silica(HS-5)-silicone support.

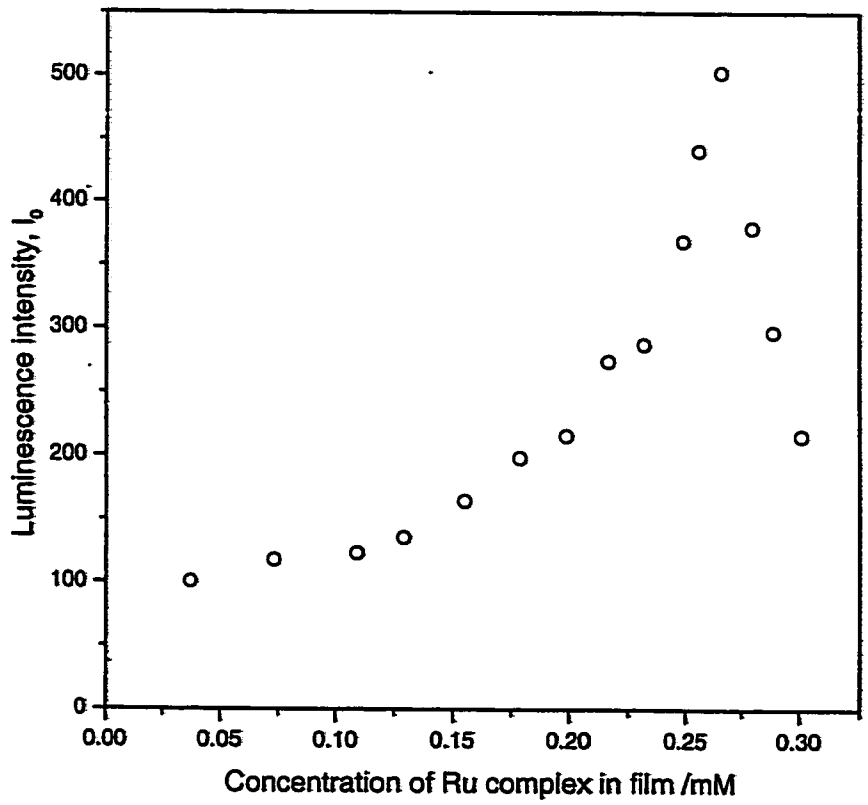

Figure 2.6 Plot of luminescence intensity (I_0) versus concentration of $[Ru(Ph_2phen)_3](ClO_4)_2$ in silica(EH-5)-silicone support.

Table 2.1 Optimum concentration of $[Ru(Ph_2phen)_3](ClO_4)_2$ in different supports with its quenching ratio (I_0/I_{100}) and maximum luminescence intensity (I_0).

Support	Maximum I_0	I_0/I_{100}	Optimum Ru concentration /mM
Silicone rubber	318	6.31 ± 0.6	0.20
Silicone rubber with silica (LM-130)	481	13.7 ±1.0	0.22
Silicone rubber with silica (HS-5)	440	14.6 ± 1.2	0.25
Silicone rubber with silica (EH-5)	500	14.4 ± 1.1	0.27

Table 2.1 indicates that the luminescence intensities of films with ruthenium-loaded fumed silica are higher than those films without silica. The increase in intensity is about the same magnitude for using different fumed silica. Immobilization of the luminescent ruthenium complex into a rigid medium such as fumed silica is known to lower the rate of non-radiative relaxation and will result in higher luminescence intensity (Carraway et al, 1991a). The higher luminescence intensity may also be a result of the more even distribution of the ruthenium complex in the polymer matrix which minimizes the formation of aggregates and hence decreases the self quenching effect.

2.3.3 Oxygen Sensitivity

The Stern-Volmer plots of $[Ru(Ph_2phen)_3]^{2+}$ in different supports are shown in Figure 2.7. Similar to other luminophores in heterogeneous systems (Lee et al, 1993b; Xu et al,1994), the quenching curves are not linear. However, in silica-containing polymer systems, the Stern-Volmer plots are obviously more linear and the quenching ratio is higher. Good quenching occurs when the complexes are easily accessible to oxygen. The silica causes a more even distribution of the complexes in the polymer (an improvement in homogeneity) and the amount of unquenchable complexes is greatly reduced. On the other hand, the presence of silica particles may favor the adsorption of oxygen molecules which would enhance the effective collision between the ruthenium dye and the oxygen quencher. Therefore, higher sensitivity and more linear plots are obtained.

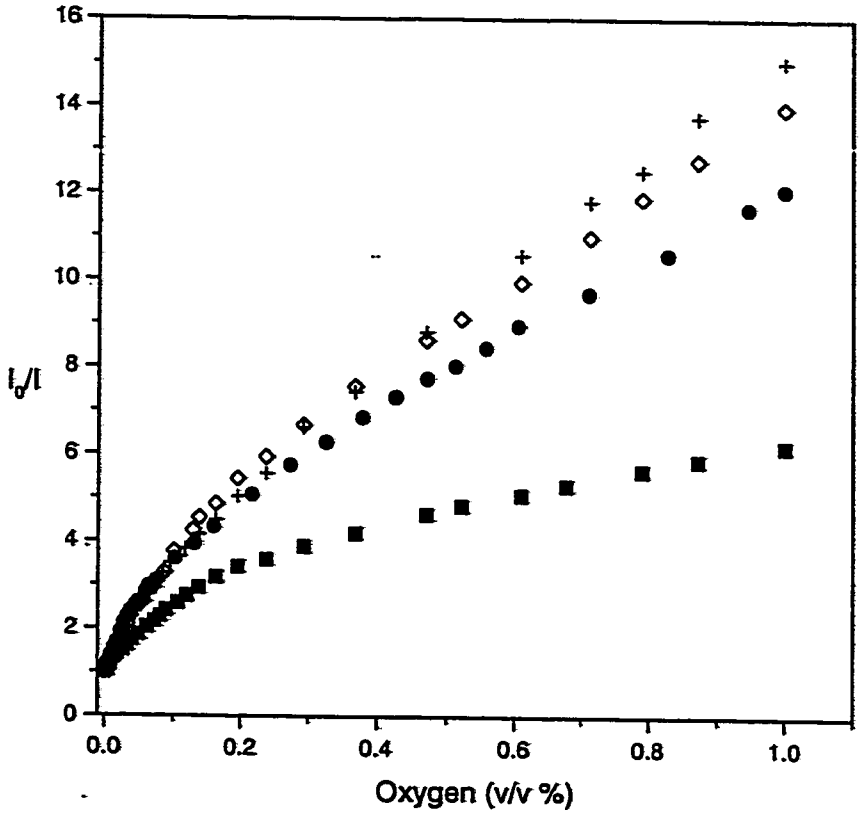

Figure 2.7 Stern-Volmer plots of $[Ru(Ph_2phen)_3](ClO_4)_2$ in different supports. (■) silicone rubber, (•) silica(LM-130)-silicone, (◊) silica(EH-5)-silica and (+) silica(HS-5)-silicone.

2.3.4 Response Time

Apart from sensitivity, fast response is another important requirement for oxygen sensors. The effect of fumed silica on the response time of the sensor was also investigated in this study. The response times of the sensor in different polymer supports were measured by exposing the film to pure oxygen and pure nitrogen environment alternatively. The response curves of $[Ru(Ph_2phen)_3]^{2+}$ in different supports are shown in Figures 2.8-2.11. The response of the complex in these supports is completely reversible and highly reproducible. The quenching time (N_2 to O_2 cycle) and recovery time (O_2 to N_2 cycle) taken as 95% of the full signal are given in Table 2.2. Our results show that while there is not much change in the quenching time, the recovery time is significantly lengthened in the presence of silica. When the amount of incorporated silica is decreased by 40%, a shortening of the recovery time from 64 s to 43 s was observed for the LM-130 films. Small molecules such as oxygen are well known to adsorb strongly on silica surface and the longer recovery time can be attributed to slow desorption of oxygen from the silica surface in the support. Figure 2.12 shows the effect of film thickness on the response time for silicone rubber and silica(LM-130)-silicone rubber sensing films. As expected, the response time of the film increases with its thickness. However, a thinner film would have lower emission intensity compared with thicker film of the same complex concentration. Hence the selection of film thickness for a specific application should be compromise between the emission intensity and the response time.

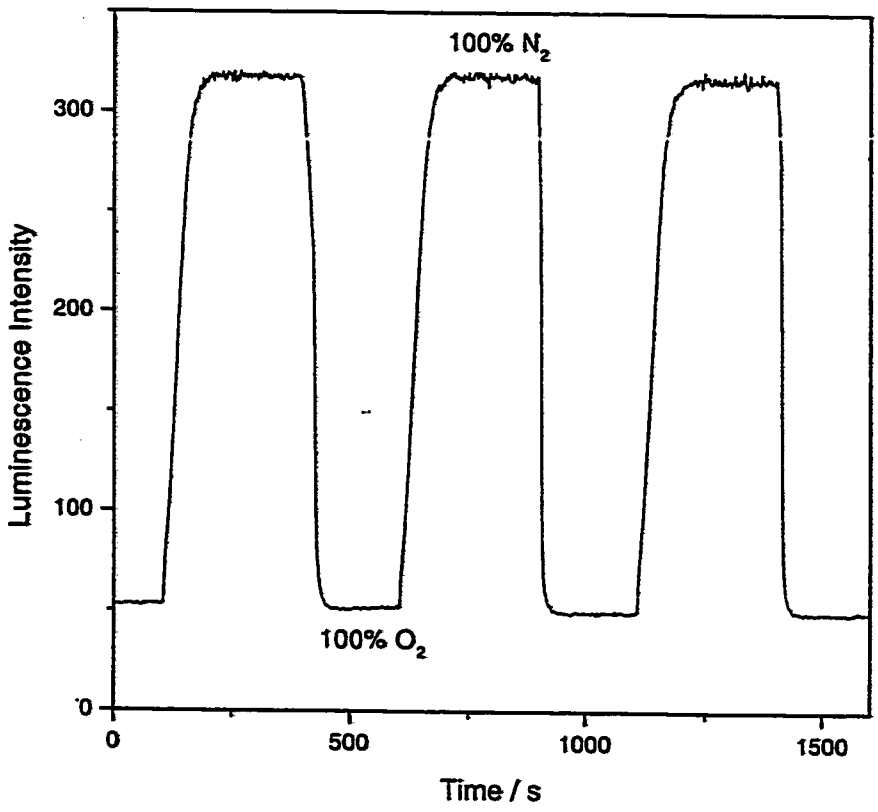

Figure 2.8 Response curve of $[Ru(Ph_2phen)_3](ClO_4)_2$ in silicone rubber support when subjected to step changes in oxygen concentration.

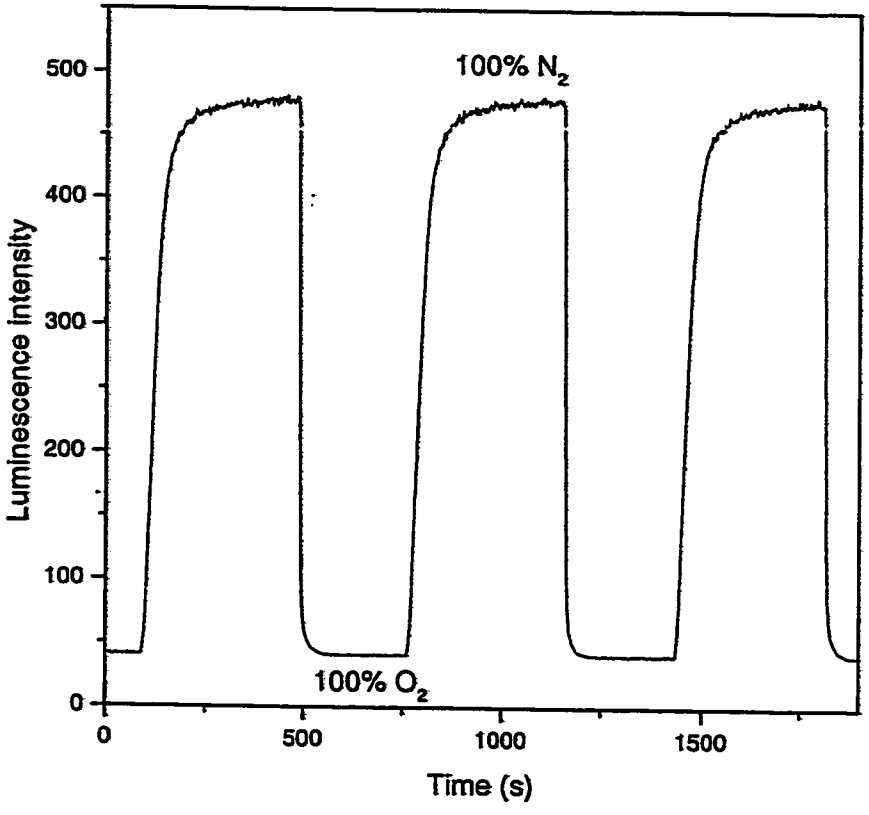

Figure 2.9 Response curve of $[Ru(Ph_2phen)_3](ClO_4)_2$ in LM-130 silica-silicone support when subjected to step changes in oxygen concentration.

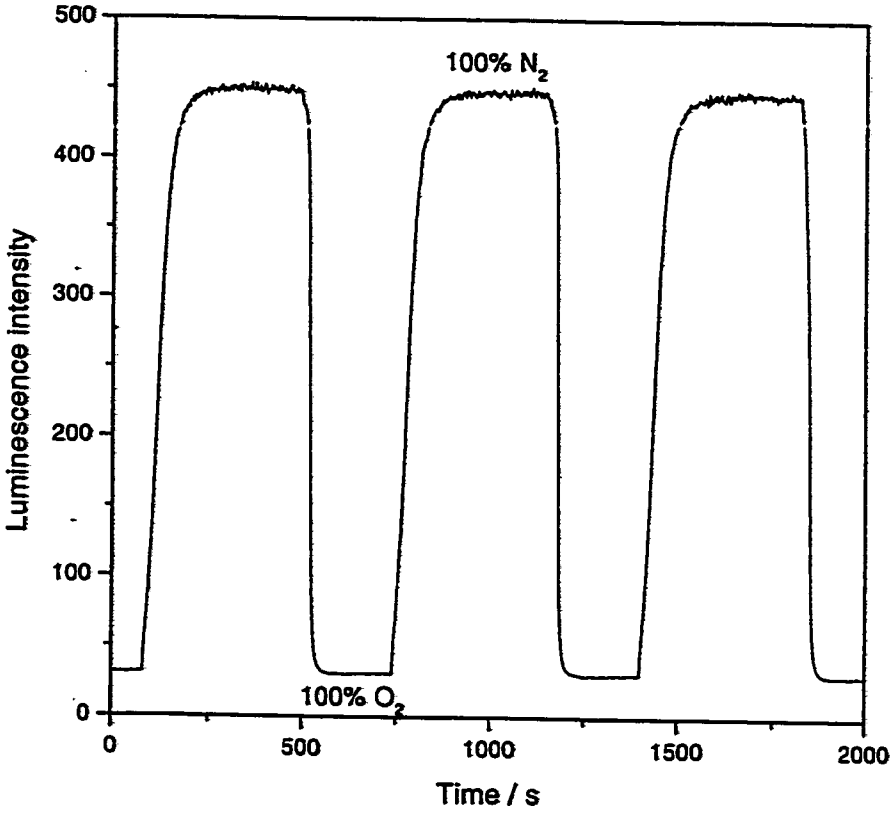

Figure 2.10 Response curve of $[Ru(Ph_2phen)_3](ClO_4)_2$ in HS-5 silica-silicone support when subjected to step changes in oxygen concentration.

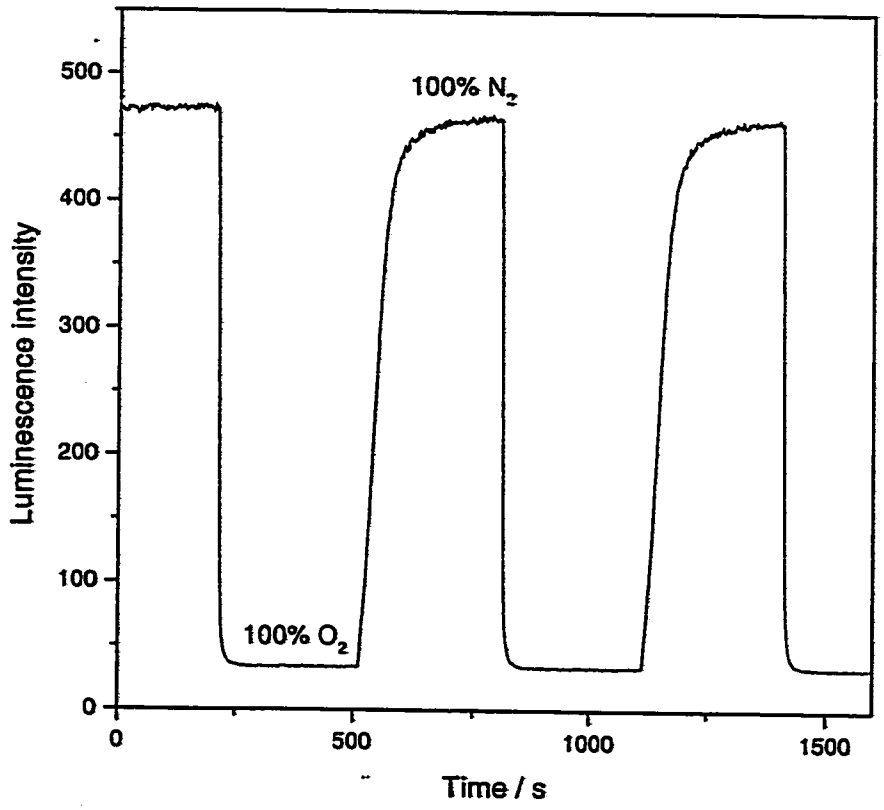

Figure 2.11 Response curve of $[Ru(Ph_2phen)_3](ClO_4)_2$ in EH-5 silica-silicone support when subjected to step changes in oxygen concentration.

Table 2.2 Response time for $[Ru(Ph_2phen)_3](ClO_4)_2$ in different supports.

Support	Quenching time[a] / s	Recovery time[b] /s
silicone rubber	25 ± 6	48 ± 6
silicone rubber with silica (LM-130)	27 ± 7	64 ± 8
silicone rubber with silica (HS-5)	30 ± 5	74 ± 10
silicone rubber with silica (EH-5)	24 ± 4	72 ± 8

[a] The time required for the luminescent intensity of the sensing film to reach 95% of its final value for nitrogen to oxygen transition

[b] The time required for the luminescent intensity of the sensing film to reach 95% of its final value for oxygen to nitrogen transition

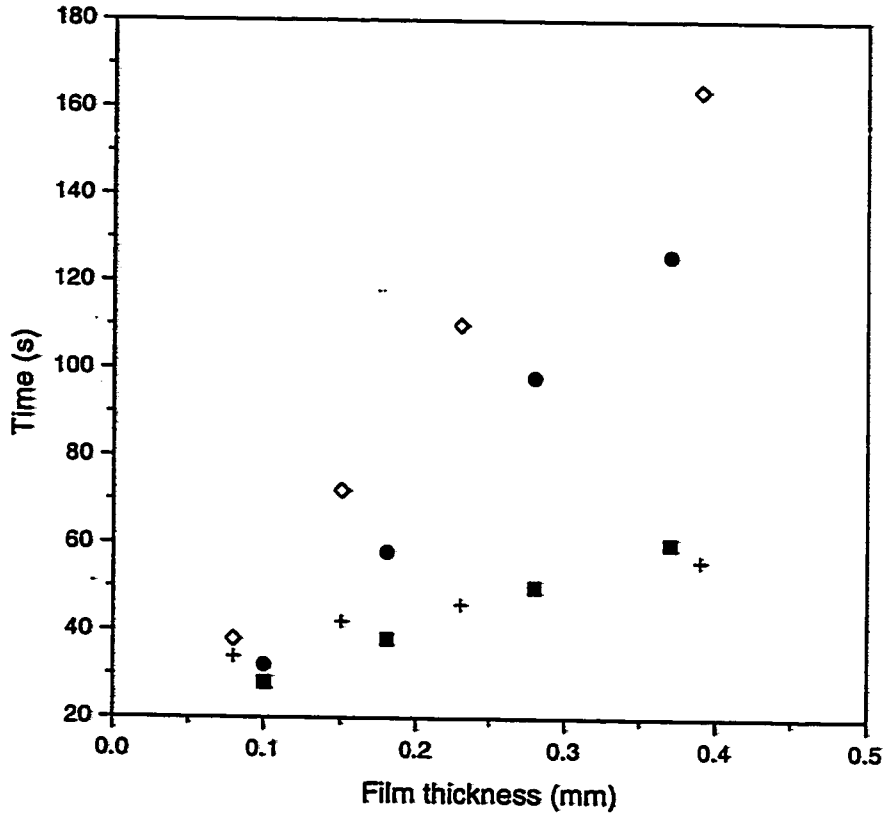

Figure 2.12 Effect of film thickness on the response time of $[Ru(Ph_2phen)_3](ClO_4)_2$ in silicone rubber: (■) N_2 to O_2 transition, (•) O_2 to N_2 transition; and in silica(LM-130)-silicone: (+) N_2 to O_2 transition, (◊) O_2 to N_2 transition.

2.3.5 Stability

$[Ru(Ph_2phen)_3](ClO_4)_2$ is known to be a relatively stable dye towards photochemical degradation (Bacon and Demas, 1987). Under our experimental conditions with a 20 kW xenon lamp as light source and the excitation wavelength and bandwidth set at 467 nm and 15 nm respectively, no photo bleaching of the ruthenium dye was observed under several hours of illumination. A small decrease in luminescence intensity (less than 5%) could be observed, however, if the films were exposed under extensive illumination for 2-3 days. This indicates that the photostability of the ruthenium dye is superior over the platinum porphyrins which show a photo bleaching effect under several hours of illumination (Lee et al, 1993b). The stability of the sensing film was investigated by measuring its response to oxygen after evacuating the film under vacuum for certain time. Figure 2.13 shows that there is no significant change in luminescence quenching behaviour of silica(LM130)-silicone film for different pumping days.

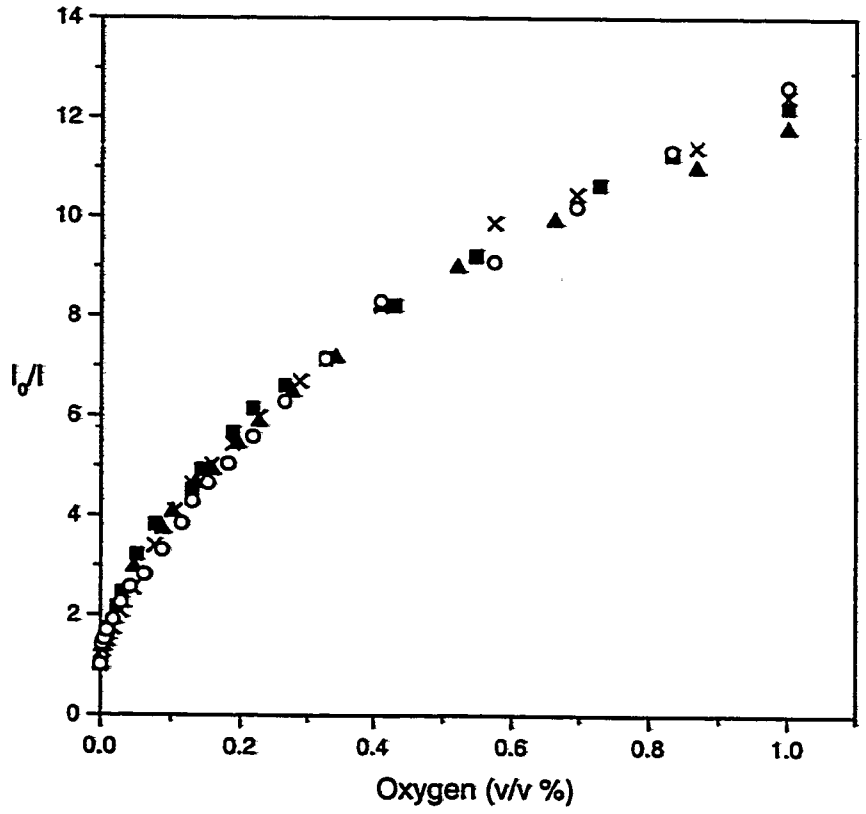

Figure 2.13 Stern-Volmer plots of $[Ru(Ph_2phen)_3](ClO_4)_2$ in LM-130 silica-silicone support with different pumping days : (o) Day 1, (■) Day 2, (×) Day 5 and (▲) Day 13.

2.4 Concluding Remarks

It is well known that silicone rubber is a suitable matrix for fabrication of oxygen sensors due to its high permeability toward oxygen and chemical inertness. However, the solubility of ionic dye such as $[Ru(Ph_2phen)_3](ClO_4)_2$ in silicone rubber is poor which is a detriment to the performance of the sensor. We have presented here a convenient method to incorporate ruthenium dye in silicone rubber by dispersing dye-containing fumed silica particles in the polymer matrix. The luminescence intensity and quenching ratio of the new sensing films are much improved. However, these improvements are obtained as a sacrifice of the response time in the recovery cycle. Hence these silica-containing sensing films are best utilized in the continuous monitoring of oxygen concentration such as the prototype oxygen sensor that we will report in the next chapter in which no switching between high and low oxygen environment is required.

Chapter 3

Monitoring the Toxicity of Organic Chemicals to Activated Sludge Using a Novel Optical Scanning Respirometer

3.1 Introduction

With the increased world-wide industrialization and the concomitant higher demand for chemicals, it becomes increasingly important to assess the environmental impact of toxic substances discharged to the environment. Toxicity testing is an essential tool for monitoring the environmental impact of many low concentration toxicants in both natural and engineered aquatic systems. Research efforts have been directed towards the development of short-term bioassay tests for rapid and sensitive assessment of the toxicant levels in water or effluents. Among the various biological toxicity methods developed, toxicity tests based on microorganisms are necessary since prokaryotes play an important role in ecological systems. Microbial tests are also simple, rapid and inexpensive (Bitton and Dutka, 1986). Various such toxicity tests have been developed (Anderson et al, 1988; Broecker and Zahn, 1977; Larson and Schaeffer, 1982; Kong et al, 1993; OECD, 1984). In most of these tests, respiration rate, ATP contents, enzymatic activity, bacterial luminescence and substrate uptake rate have served as the indicating parameters of toxicity. Among these methods, measurement based on microbial respiration is the most frequently used as it has the advantage of speed and simplicity (OECD, 1984; ISO, 1986; King and Dutka, 1986; King and Painter, 1986).

In most existing respirometers, oxygen concentration is measured by electrochemical oxygen sensors such as Clark electrode (Clark, 1956), which is based on reduction of oxygen at the cathode. Despite its inexpensive instrumentation and relatively rapid response, this method has several drawbacks including the need for a

reference cell, the requirement for a steady supply of oxygen to the electrode surface, the easiness of electrode fouling and difficulty of miniaturization. Recently, luminescence-based optical sensing of oxygen has been developed as one of the new and superior techniques for oxygen detection (Bacon and Demas, 1987; Mills, 1997; Wolfbeis, 1991). Our research group has been developing novel oxygen optode based on the quenching of oxygen of the luminescent ruthenium (II) diimine complexes and platinum porphyrins (Lee et al, 1993b; Li and Wong, 1992; Li et al, 1993). This oxygen optode works on the principle that the dynamic quenching of oxygen on the fluorescence and phosphorescence of the luminescent chemicals reduces their emission intensities or luminescence lifetimes. The emission intensities of the luminescent chemicals can be related quantitatively to the concentration of oxygen. The advantages of optical sensor include small dimension, fast response time, high sensitivity and nil consumption of oxygen. The development of such sensors for applications in various fields such as medicine, biotechnology, environmental studies, process control and chemical analysis has, therefore, grown rapidly.

The oxygen optode described in Chapter 2 possesses many promising properties for the construction of biosensor. Thus, because of the importance of toxicity testing, an optical scanning respirometer based on this oxygen optode will be developed for determining the toxicity of organic chemicals. The sensing film is irradiated with an excitation light source and the resulting light emission is then sensed and transmitted by an optical fiber connected to a photomultipler tube. The light intensities sensed at a specific wavelength can be related to the dissolved oxygen concentrations in the samples. Both the excitation light source and the optical fiber are

carried on a scanner, which can be used to measure the dissolved oxygen concentrations of a large number of samples in a short period of time. The toxicity assessment is based on the inhibition of microbial respiration. IC_{50} value (concentration of a substance producing 50% respiration inhibition) is measured for comparing the toxicity of different organic chemicals to activated sludge, which is the most important and widely used biological wastewater treatment process in the world. The chemicals tested are important environmental pollutants including halogenated phenols, benzenes and alkanes. Most chemicals have been categorized as priority pollutants by the U.S. Environmental Protection Agency (Davis and Crowell, 1991). Additionally, these selected chemicals are often found in industrial and sewage effluents as they are heavily used in various industries. For example, phenol is a common constituent of effluents from polymeric resin production plants, oil refining factories, paper as well as pulp processing and coal liquefaction industries. Halogenated aliphatic hydrocarbons are used as solvent or reactants for chemical synthesis in ink and dye, oil, as well as in drug industries. The performance of this respirometer is evaluated and compared with other toxicity methods, and the results are reported in this chapter.

3.2 Experimental Section

3.2.1 Materials

$[Ru(Ph_2phen)_3](ClO_4)_2$ (Ph_2phen = 4,7-diphenyl-1,10-phenanthroline) was synthesized and purified according to the method previously published (presented in chapter 2) (Lin et al, 1976). Amorphous fumed silica (LM-130) was obtained from Cabot Corporation. Silicone rubber and black silicone rubber were purchased from Nice Top Quality Ltd. Oxygen and nitrogen gases (99.7 %) were purchased from Hong Kong Oxygen Company. 2-nitrophenol (2-NP), 4-nitrophenol (4-NP) and 2,4-dinitrophenol (2,4-DNP) were purchased from BDH Ltd. Hydroquinone and 2-chlorophenol (2-CP) were bought from Ridel-De Haen. Phenol was obtained from Peking Chemical Works and recrystallized from petroleum ether before use. Nitrobenzene and p-cresol were purchase from Acros Ltd. 1,2-Dichloroethane, dichloromethane and choroform were obtained from Lab-Scan Co. All the other test chemicals were of analytical-reagent grade obtained from Aldrich Chemical Co.

3.2.2 Preparation of Oxygen Sensing Films

The oxygen sensing films with optimum ruthenium concentration were prepared as described in Chapter 2, but the films were instead coated onto the bottom of Wheaton sample vials. To minimize light scattering from the excitation light source (LED), a layer of black silicone rubber was placed on top of the film surface. This

coating was prepared by transferring 0.3 ml of toluene solution containing 0.2 g dissolved black silicone rubber onto the film surface. A schematic diagram of the oxygen sensing film which spreads on the bottom of transparent glass vial with LED light sources and optic-fiber underneath is shown in Figure 3.1.

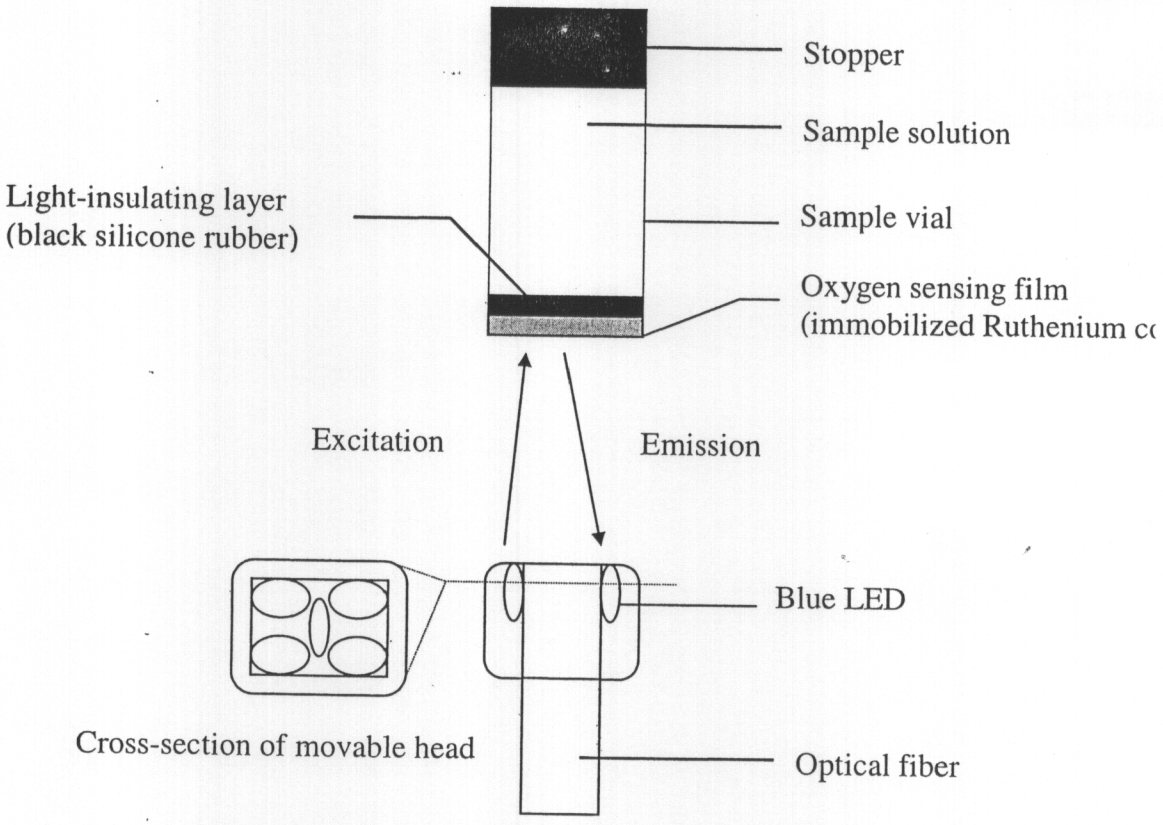

Figure 3.1 A schematic diagram showing the oxygen sensing part of the respirometer.

3.2.3 Instrumentation

A schematic diagram of the integrated respirometer is shown in Figure 3.2. Oxygen optode is one of the main components in the respirometer for measuring dissolved oxygen concentration in the sample culture. Oxygen sensing film with immobilized ruthenium (II) complex was first coated on the inside surface of the bottom of each transparent glass sample vial, as described in the previous section. The vials were held in a rack to ensure a right location for fixing a scanner with a movable head underneath. The movable head was equipped with an optic-fiber in the center (1 mm I.D.) surrounded by four blue LEDs (Figure 3.1). When the ruthenium complex was irradiated by the blue LEDs at 460 nm peak emission wavelength, it emitted strongly at 610 nm. The emission light was then sensed and transmitted by the optical fiber to photomultipler tube (PMT). The movement of the movable head was controlled by a scanning controller made of a modified XY plotter. This complete equipment set-up was placed in a light-tight compartment to prevent background radiation affecting the signal received.

To eliminate interference of emission light (610 nm) from irradiation (460 nm), the signal was transmitted through a long-pass filter (> 505 nm) before reaching the PMT. The current produced was converted into voltage and further amplified by a preamplifier. The output signal was fed into a personal computer via A/D converter. The personal computer was used for the control of optode scanning and data acquisition.

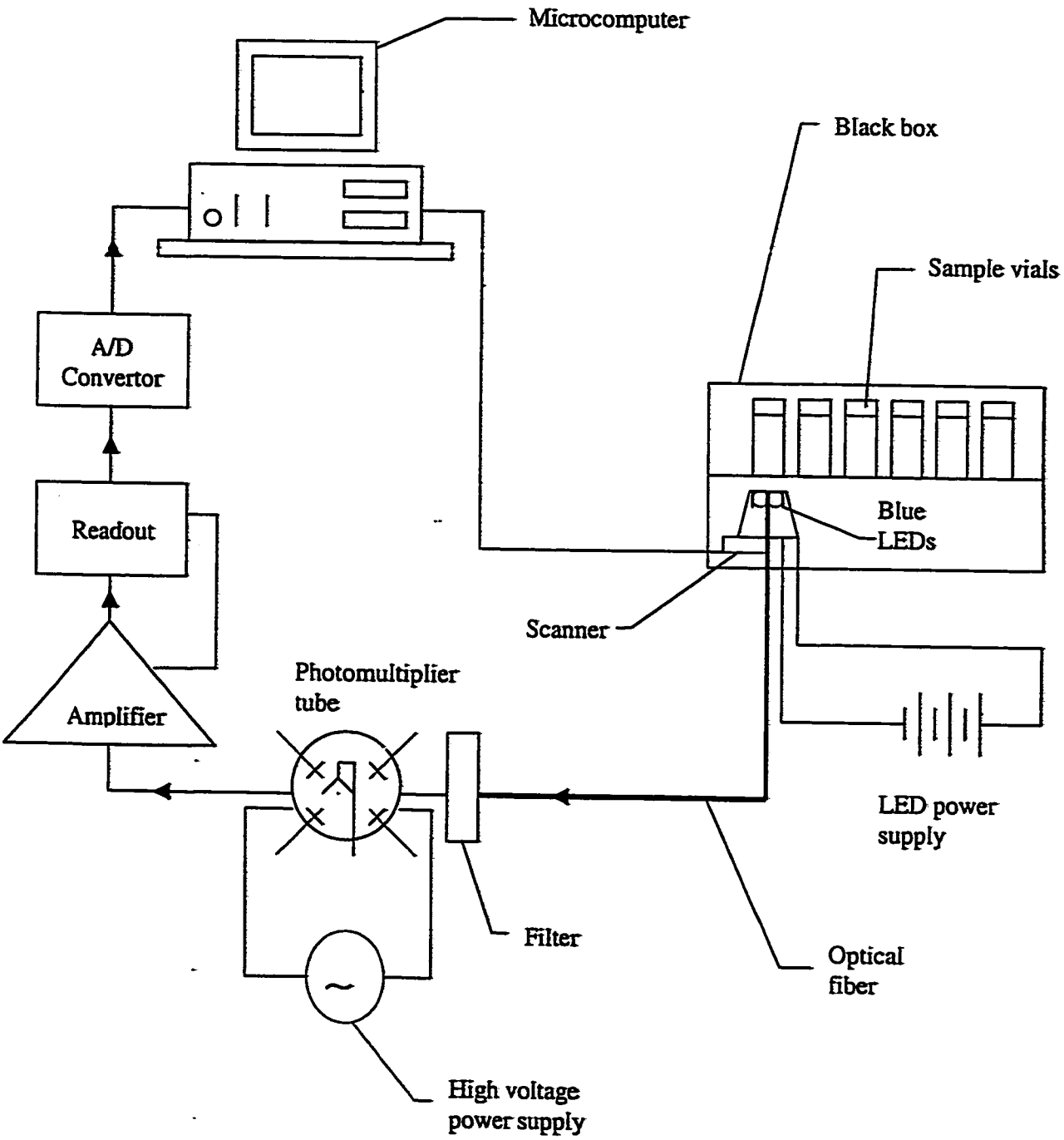

Figure 3.2 A schematic diagram of the integrated respirometer.

3.2.4 Toxicity Assays

Activated sludge obtained from Shatin Sewage Treatment Works in Hong Kong SAR was used as the source of wastewater microorganisms for toxicity studies. The plant treats predominantly domestic sewage. On return to the laboratory, the sludge was allowed to settle and the waste liquor was discarded so as to concentrate the activated sludge sample to one tenth of its original value. If the sludge was not used on the day of collection, the concentrated sample was stored at 4°C and aerated occasionally. In each run of experiment, 1 ml of concentrated sample was mixed with 100 ml deionized water and 2 ml of sodium acetate (10 % w/w), which was used as exogenous substance to ensure that the microorganisms were respiring, growing and dividing rapidly when exposed to the potential inhibitor. The resulting sample solution was then aerated for about 2 hours at 20°C before conducting the toxicity tests. The concentration of suspended solid in resulting sample solution was about 300 mg/L.

Before conducting the toxicity assays using the integrated respirometer, each sample vial was calibrated individually by measuring the PMT voltage of the sensing film under air, pure oxygen and pure nitrogen respectively. The data obtained were fitted into a modified Stern-Volmer equation that will be discussed in the following section, for obtaining the calibration curves.

Stock solutions of phenolic chemicals were prepared in deionized water. For solubility purpose, 0.066 g/L and 0.4 g/L of sodium carbonate were added into stock solutions of pentachlorophenol (PCP) and 2,4-dinitrophenol (2,4-NP) respectively.

However, because of their low solubility in water, various substituted benzenes and alkanes were prepared in ethanol. A series of reaction mixture were prepared by adding 0.5 ml test chemical solution with different concentrations and 7 ml air-saturated microbial sample into each of the five different vials. One vial was left containing only 7 ml air-saturated microbial sample and 0.5 ml deionized water (for phenolic chemicals) or ethanol (for benzenes and alkanes) as control. Stoppers were used to seal all the six vials. The change of PMT voltage with time was monitored by the respirometer, until the dissolved oxygen in the control sample was completely consumed. All toxicity assays were conducted at pH 7.0±0.1 and 20±1°C to minimize their effects on respiration of microorganisms in activated sludge. Duplicate or triplicate measurements were done for each run of the experiment.

3.3 Results and Discussion

3.3.1 Dissolved Oxygen Measurement

Each sample vial containing oxygen-sensing film has to be calibrated before determination of dissolved oxygen concentration in sample culture. Owing to the presence of ambient stray light and immobilization of the luminescent indicator in polymer matrix, a linear relationship between luminescence intensity and oxygen concentration cannot be obtained. Since the output voltage of the PMT is proportional to the luminescence intensity, a modified Stern-Volmer equation (Wong et al, 1997; Trettnak et al, 1988) can be used to correlate the data:

$$\frac{V_o - V_f}{V - V_f} = 1 + K_{sv}[O_2] \tag{3.1}$$

where V_o and V denote the output voltage of PMT in the absence and presence of oxygen, respectively; V_f and K_{SV} are the output voltage produced by 'false' light which cannot be quenched by oxygen and the Stern-Volmer constant respectively. In each run of experiment, the three output voltages of PMT under pure nitrogen, pure oxygen and atmospheric air environments, respectively, were measured to determine the values of V_f and K_{SV} for each sample vial. Moreover, the concentration of dissolved oxygen $[O_2]$ can be correlated with the oxygen partial pressure, Po_2, by Henry's Law as shown below:

$$[O_2] = H \cdot P_{O_2} \quad (3.2)$$

where H is the Henry's constant.

After calibration of the respirometer, the change in dissolved oxygen concentration with time can be measured by monitoring the output voltage for each sample vial in the presence of different amount of toxicants added. As the luminescence intensity of the ruthenium complex can be quenched by oxygen, lesser amount of dissolved oxygen in a given time will result in a larger output voltage sensed by the optical fiber. Upon addition of a toxicant to the sample culture, microorganisms will be subsequently subjected to a toxic stress. This can be reflected by the decrease in respiration rate of the microbial population. The degree of inhibition on respiration rate is greater with higher concentration of toxicants as shown in the plots of dissolved oxygen versus incubation time in the presence of toxicants in Figures 3.3-3.6 for phenols, Figures 3.7-3.11 for alkanes and Figures 3.11-3.14 for benzenes. The respiration rate of each mixture can be determined from the slope of the linear part of the plots.

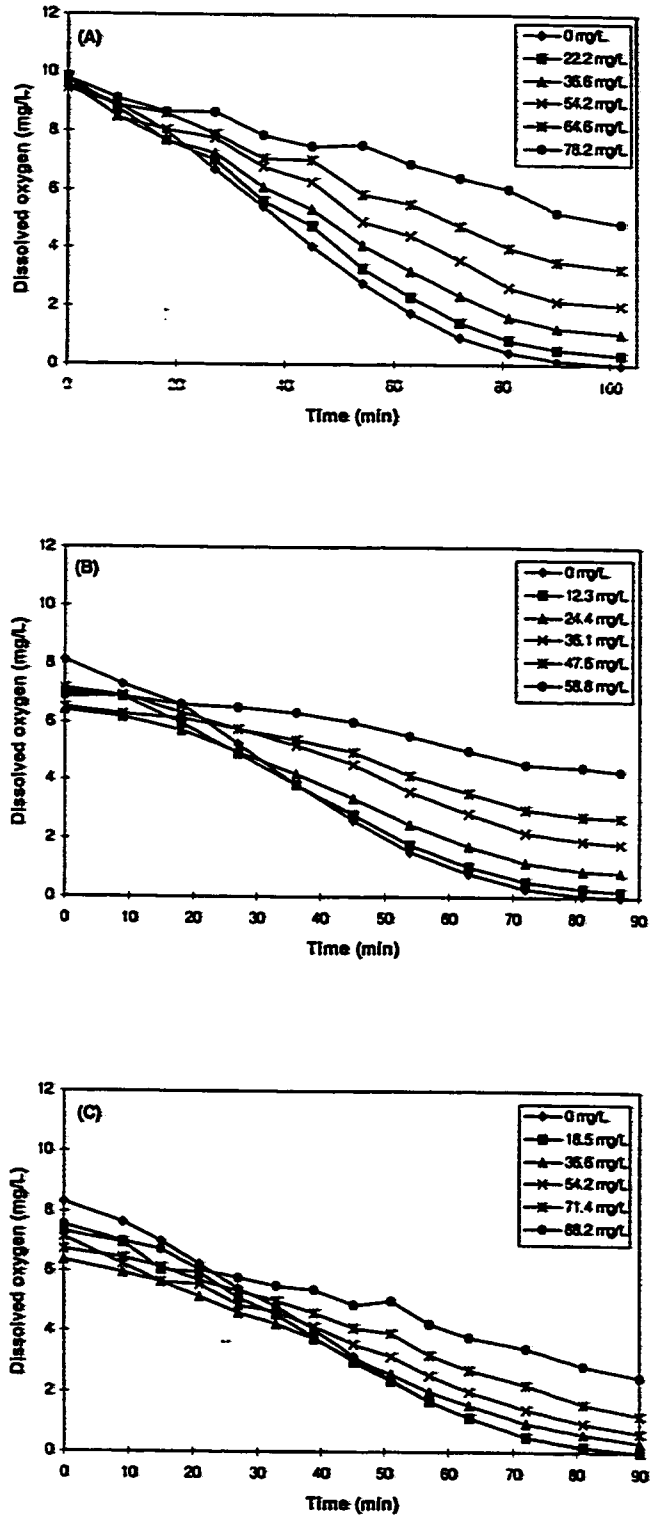

Figure 3.3 - Plot of dissolved oxygen concentration versus incubation time in the presence of (A) 3,5-dichlorophenol, (B) pentachlorophenol and (C) hydroquinone.

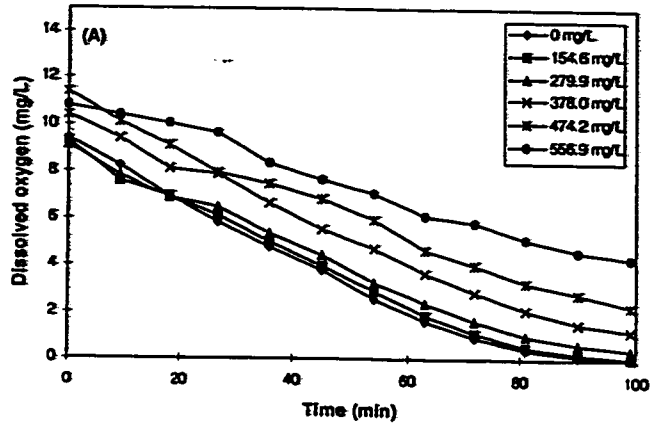

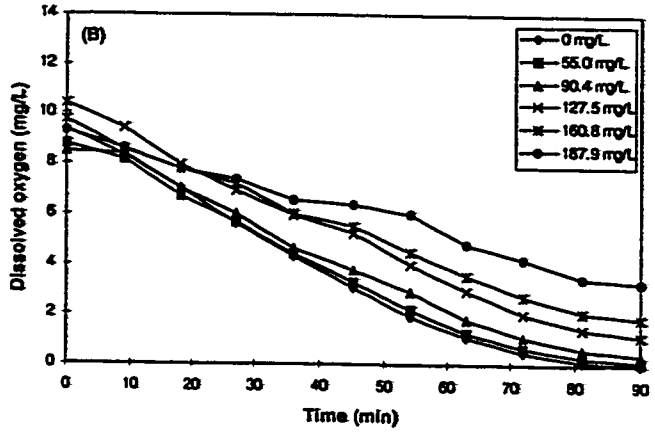

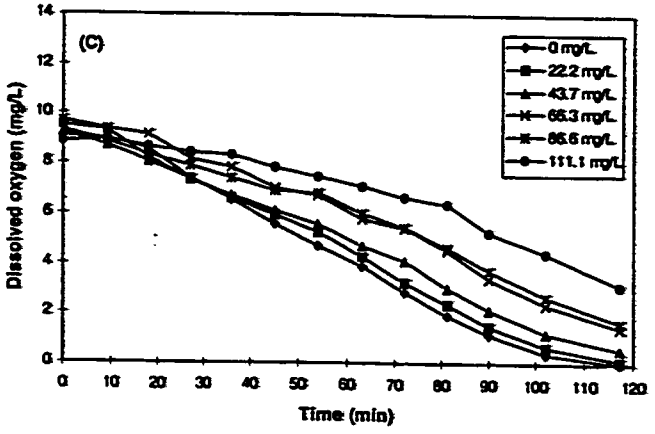

Figure 3.4 Plot of dissolved oxygen concentration versus incubation time in the presence of (A) phenol, (B) 2-nitrophenol and (C) 4-nitrophenol.

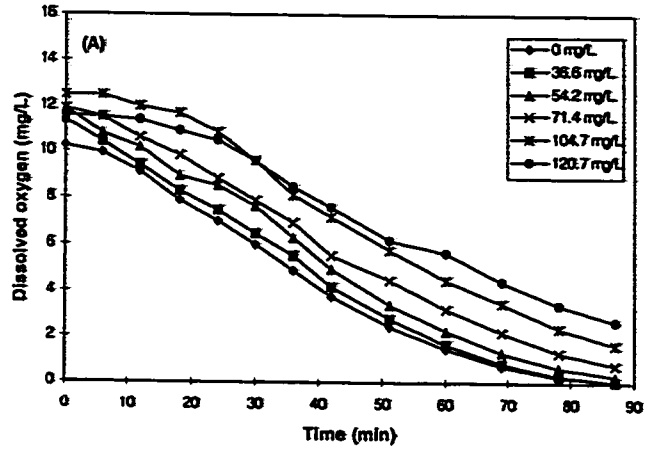

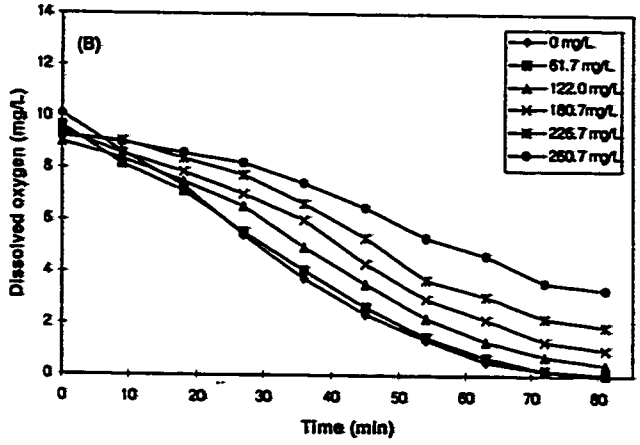

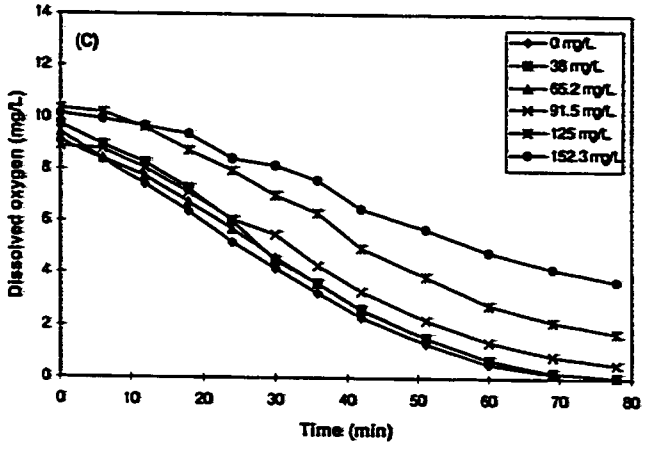

Figure 3.5 . Plot of dissolved oxygen concentration versus incubation time in the presence of (A) 2-chlorophenol, (B) 2-bromophenol and (C) 2,4-dinitrophenol.

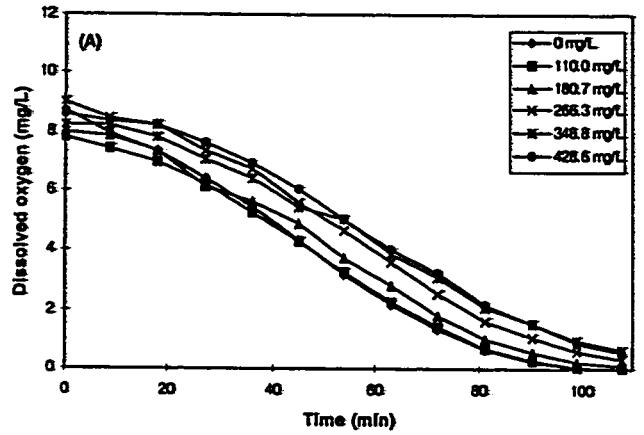

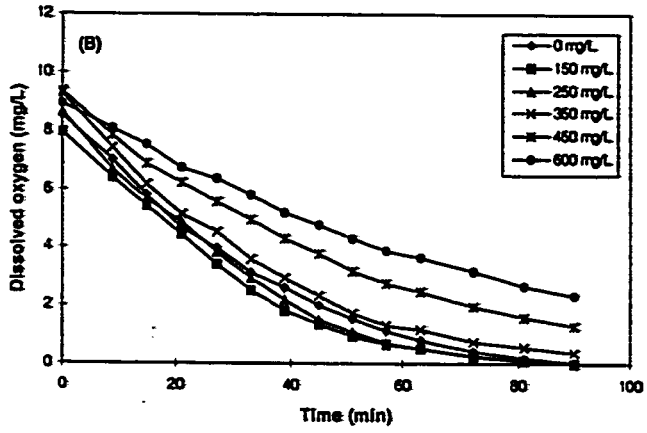

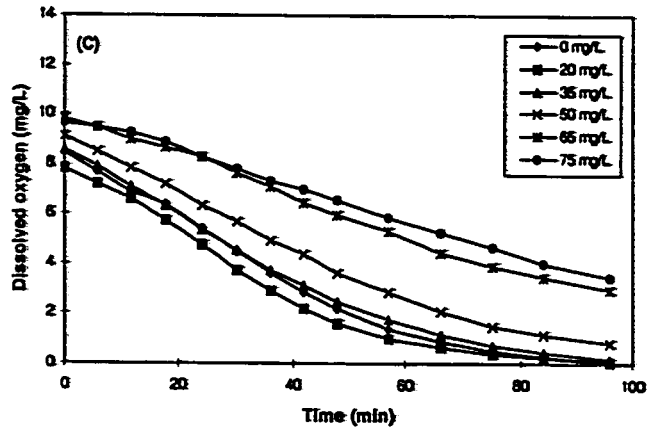

Figure 3.6 Plot of dissolved oxygen concentration versus incubation time in the presence of (A) p-cresol, (B) 2,4-dimethylphenol and (C) 2,4,6-trichlorophenol.

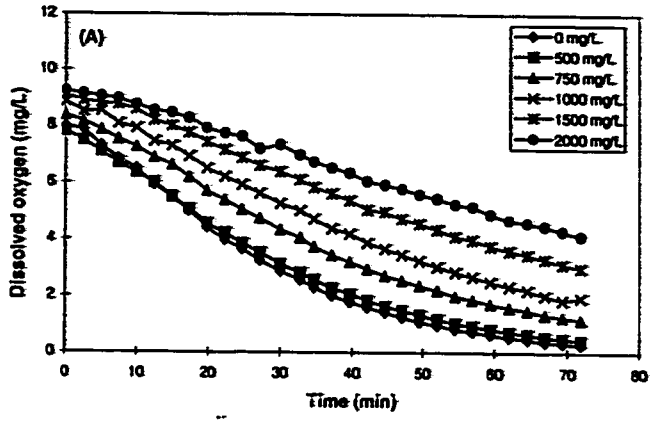

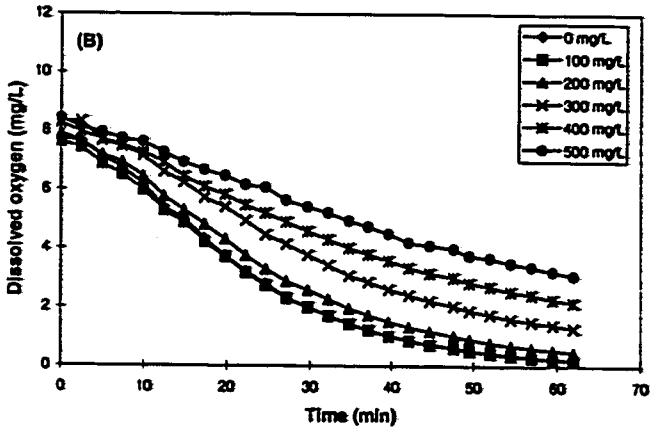

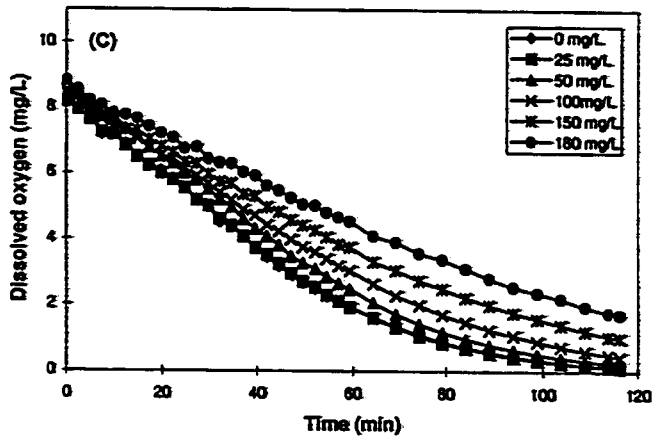

Figure 3.7 Plot of dissolved oxygen concentration versus incubation time in the presence of (A) benzene, (B) chlorobenzene and (C) 1,3-dichlorobenzene.

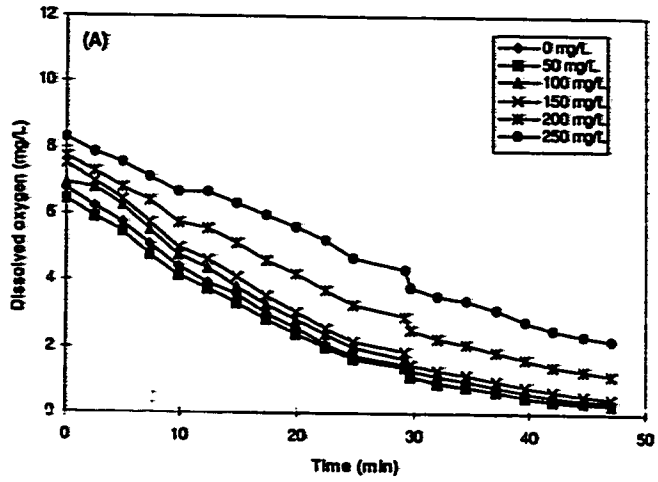

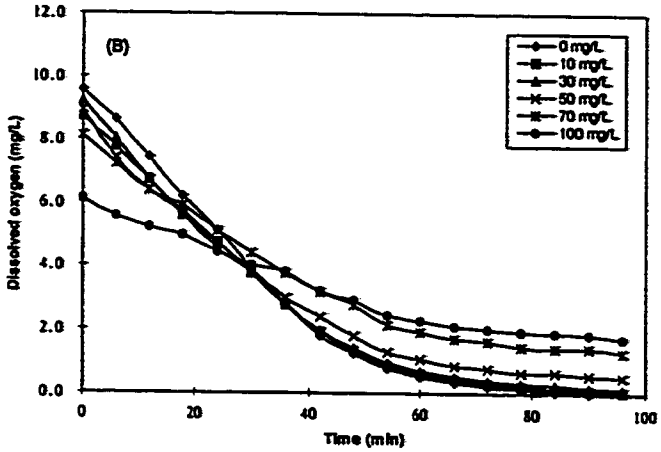

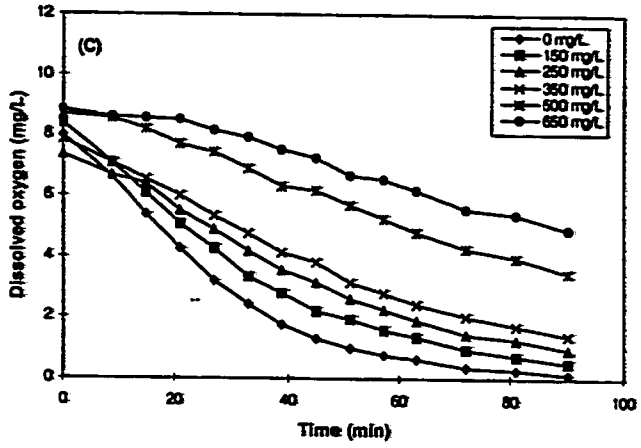

Figure 3.8 Plot of dissolved oxygen concentration versus incubation time in the presence of (A) ethylbenzene, (B) 1,2,4-trichlorobenzene and (C) nitrobenzene.

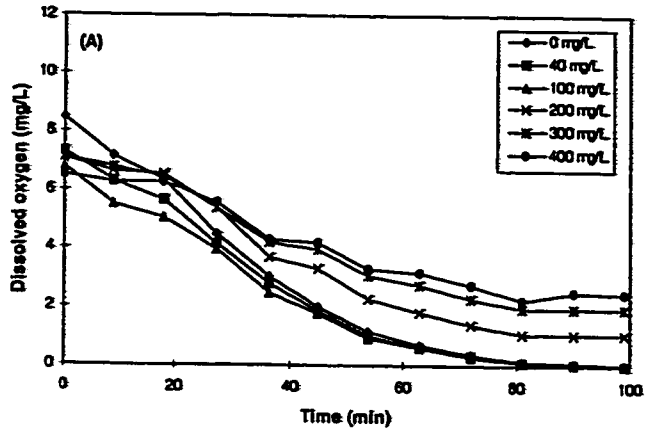

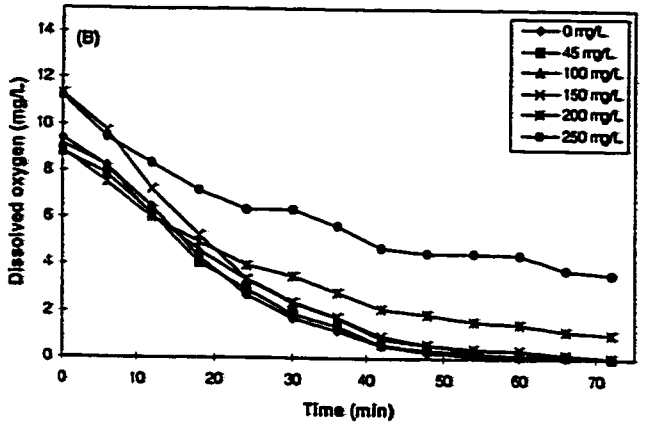

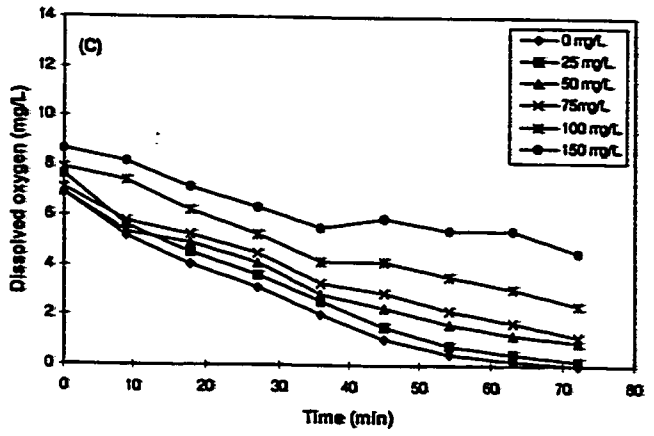

Figure 3.9 Plot of dissolved oxygen concentration versus incubation time in the presence of (A) 1,2-dichlorobenzene, (B) 1,4-dichlorobenzene and (C) naphthalene.

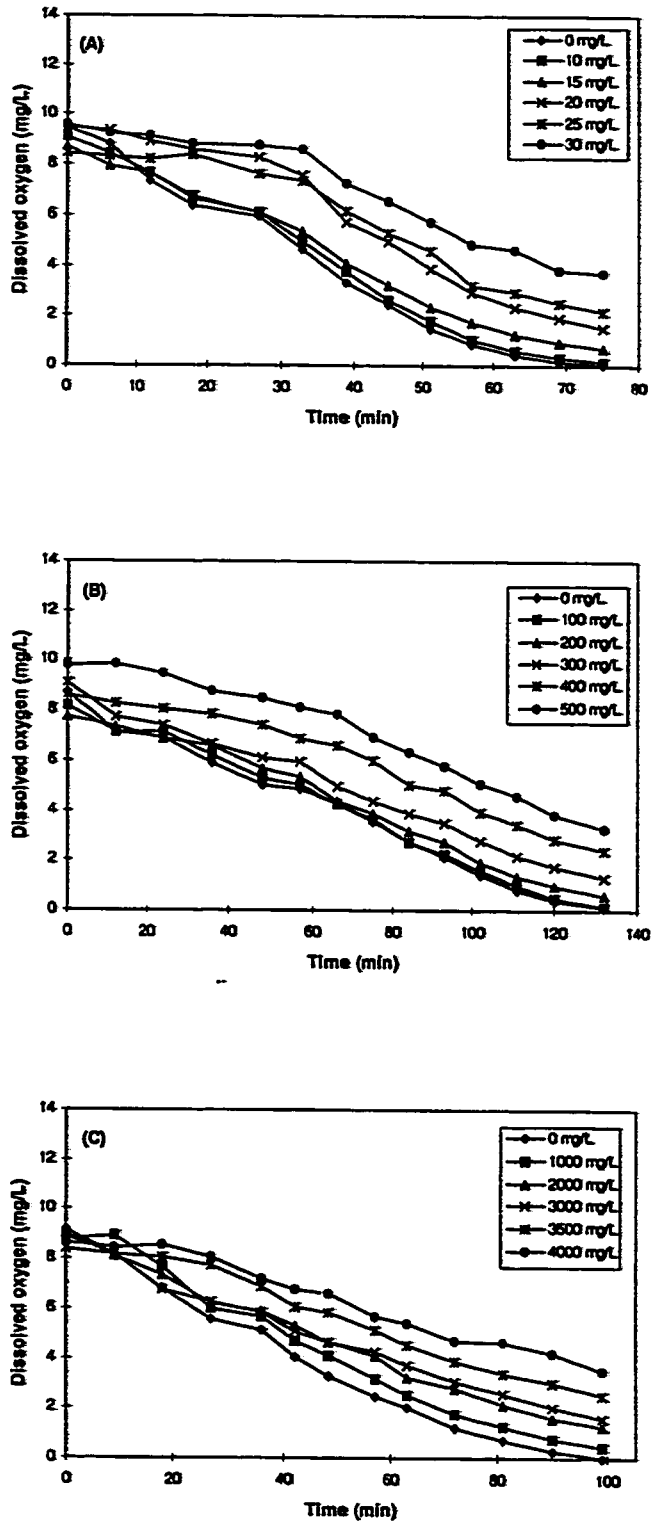

Figure 3.10 Plot of dissolved oxygen concentration versus incubation time in the presence of (A) hexachlorobenzene, (B) benzonitrile and (C) aniline.

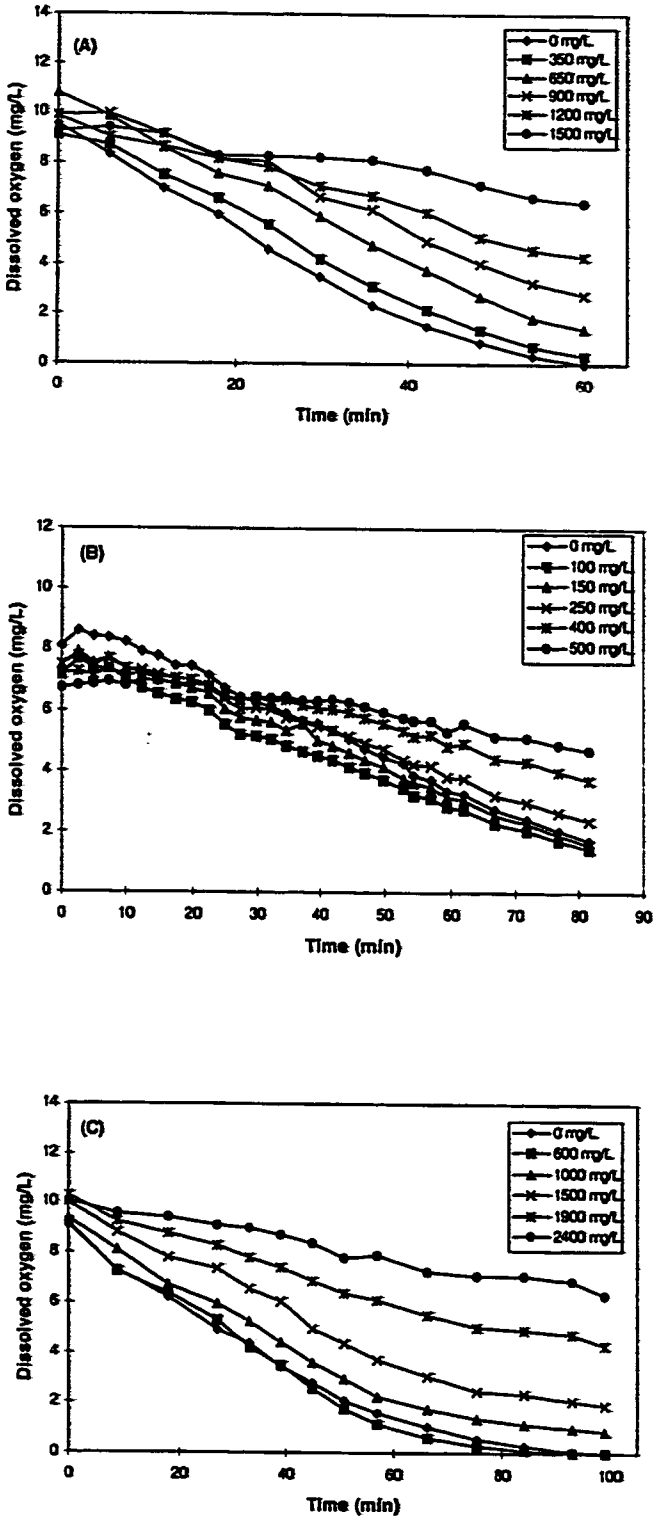

Figure 3.11 Plot of dissolved oxygen concentration versus incubation time in the presence of (A) bromobenzene, (B) tetrachloromethane and (C) 1,1,2-trichloroethane.

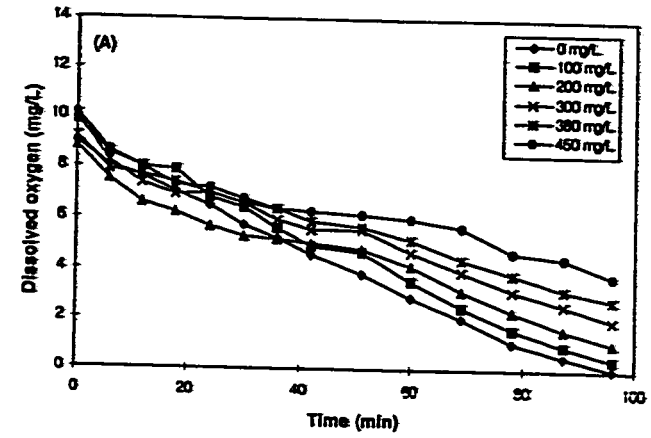

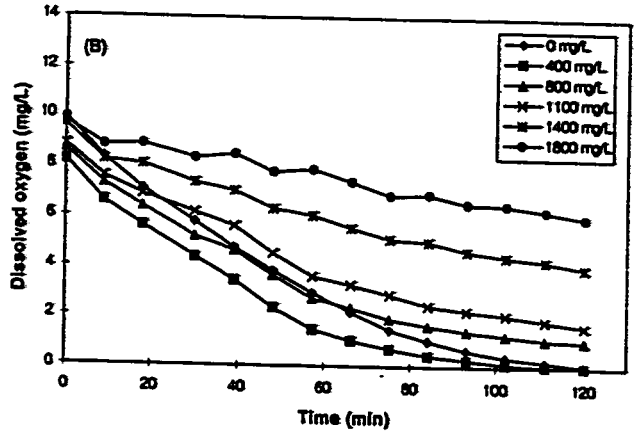

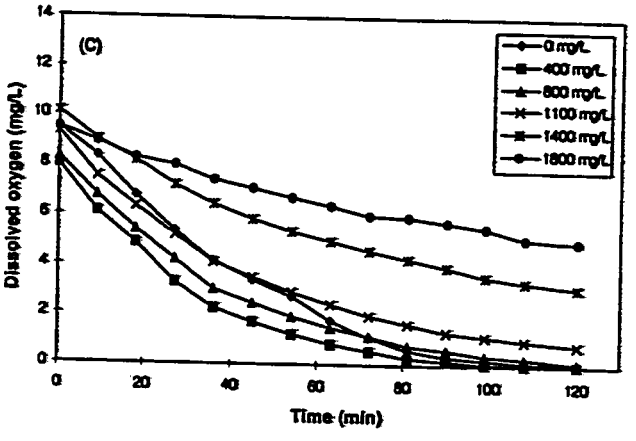

Figure 3.12 Plot of dissolved oxygen concentration versus incubation time in the presence of (A) hexachloroethane, (B) 1,1,2,2-tetrachloroethane and (C) 1,2-dichloropropane.

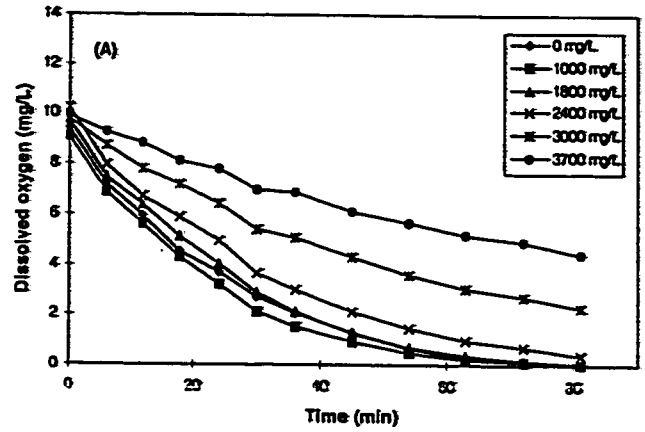

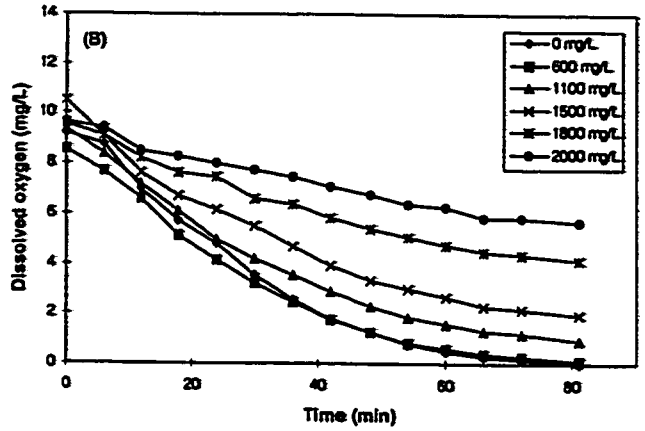

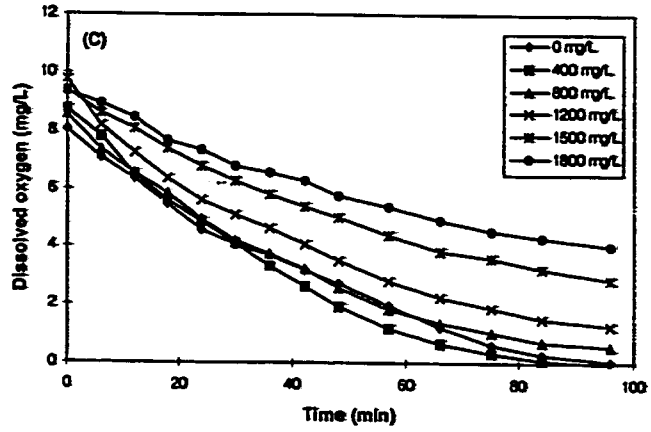

Figure 3.13 Plot of dissolved oxygen concentration versus incubation time in the presence of (A) 1-chloropropane, (B) chlorodibromomethane and (C) chloroform.

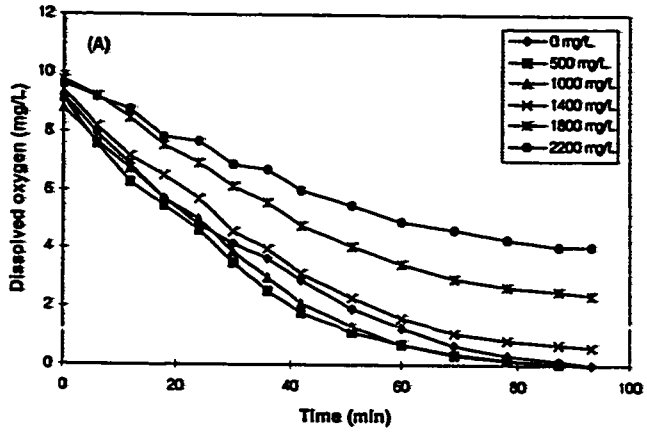

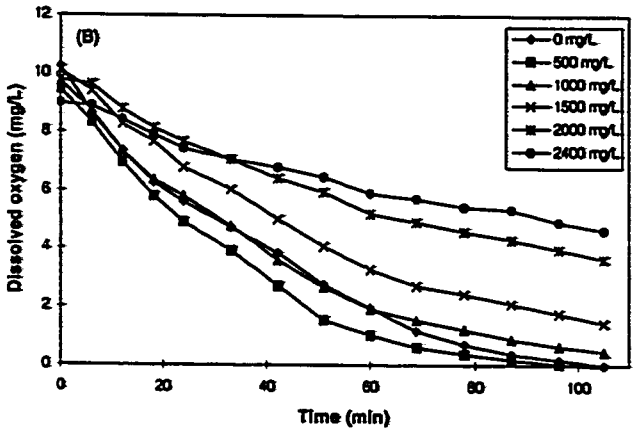

Figure 3.14 Plot of dissolved oxygen concentration versus incubation time in the presence of (A) 1,2-dichloroethane, (B) dichloromethane.

3.3.2 Determination of IC_{50} Values

The percentage inhibition (I %) at each concentration of test chemical can be calculated as follows:

$$I\% = \frac{R_c - R}{R_c} x100\% \tag{3.3}$$

where R and R_c are the respiration rate of testing sample and control sample respectively. The concentration that exhibits 50% respiration inhibition (IC_{50}) can be derived from plotting the percentage inhibition against concentration and using nonlinear regression to correlate the data:

$$I\% = K_1[C] + K_2[C]^2 \tag{3.4}$$

where K_1 and K_2 are the regression parameters and [C] denotes the concentration of the testing chemical. The plots of I % versus concentration of toxicants are shown in Figures 3.15-3.18 for phenols, Figures 3.19-3.23 for benzenes and Figures 3.23-3.26 for alkanes and the black solid lines represent the nonlinear regression curves.

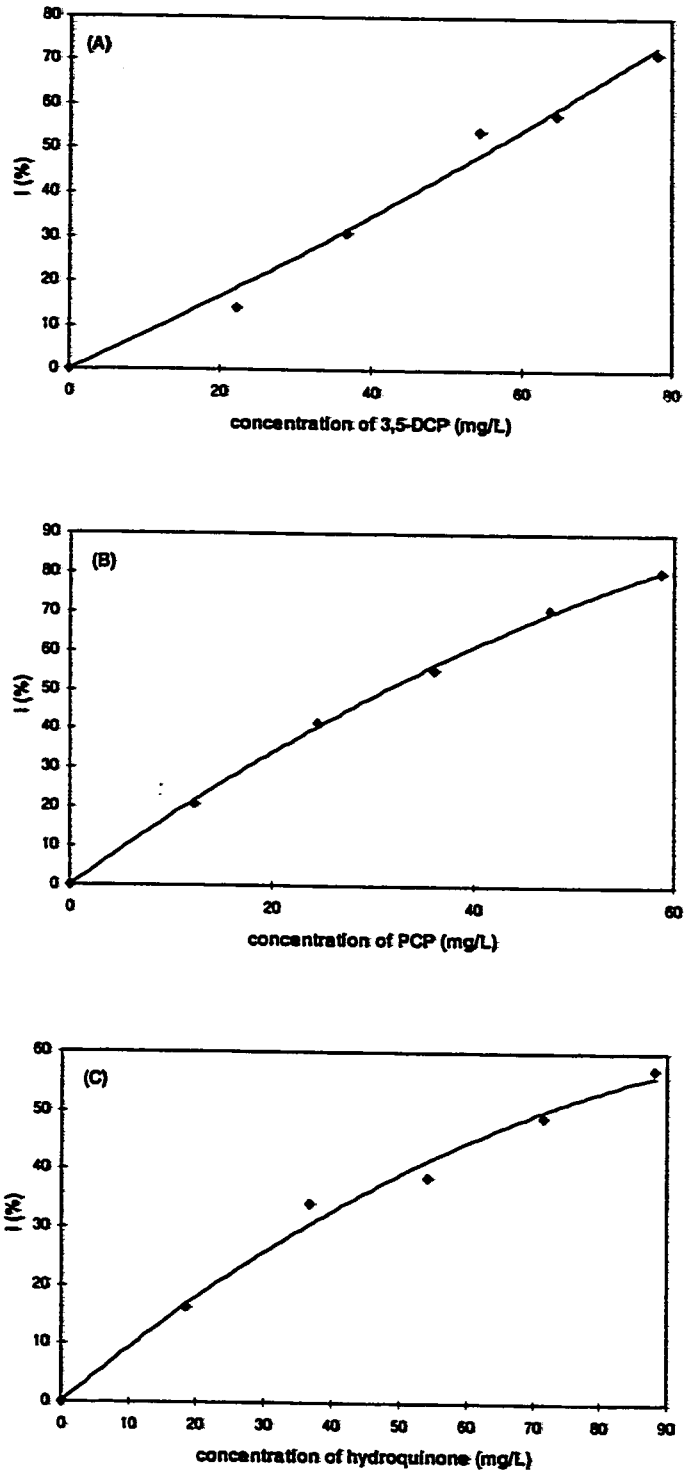

Figure 3.15 Plot of percentage inhibition (I%) versus concentration of (A) 3,5-dichlorophenol, (B) pentachlorophenol and (C) hydroquinone.

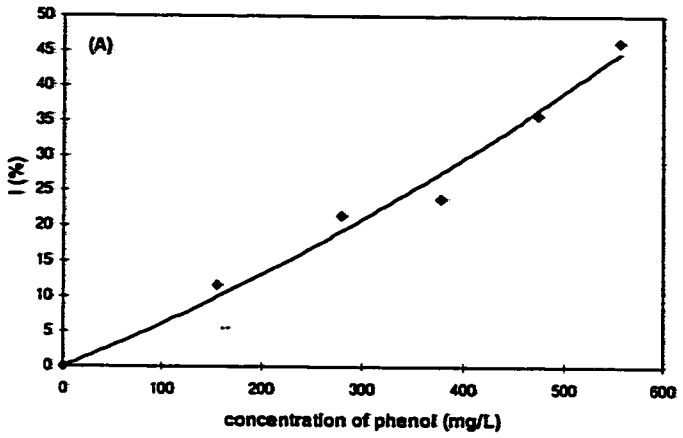

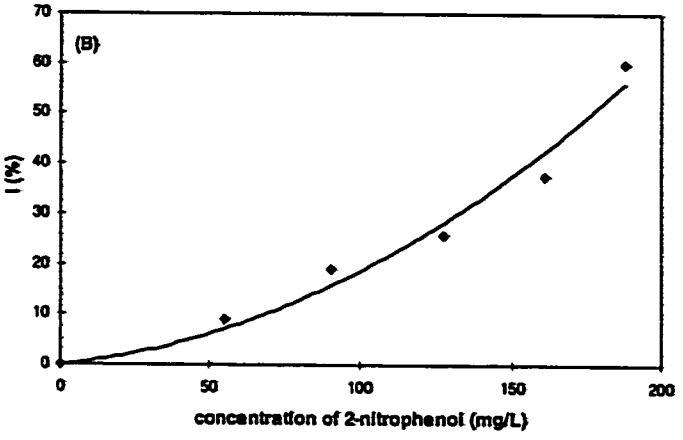

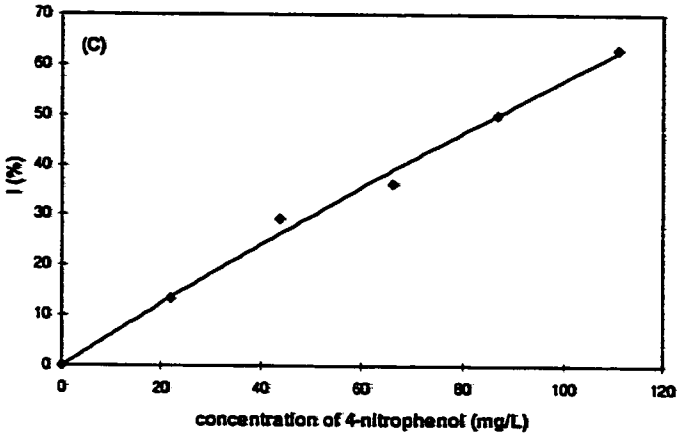

Figure 3.16 Plot of percentage inhibition (I%) versus concentration of (A) phenol, (B) 2-nitrophenol and (C) 4-nitrophenol.

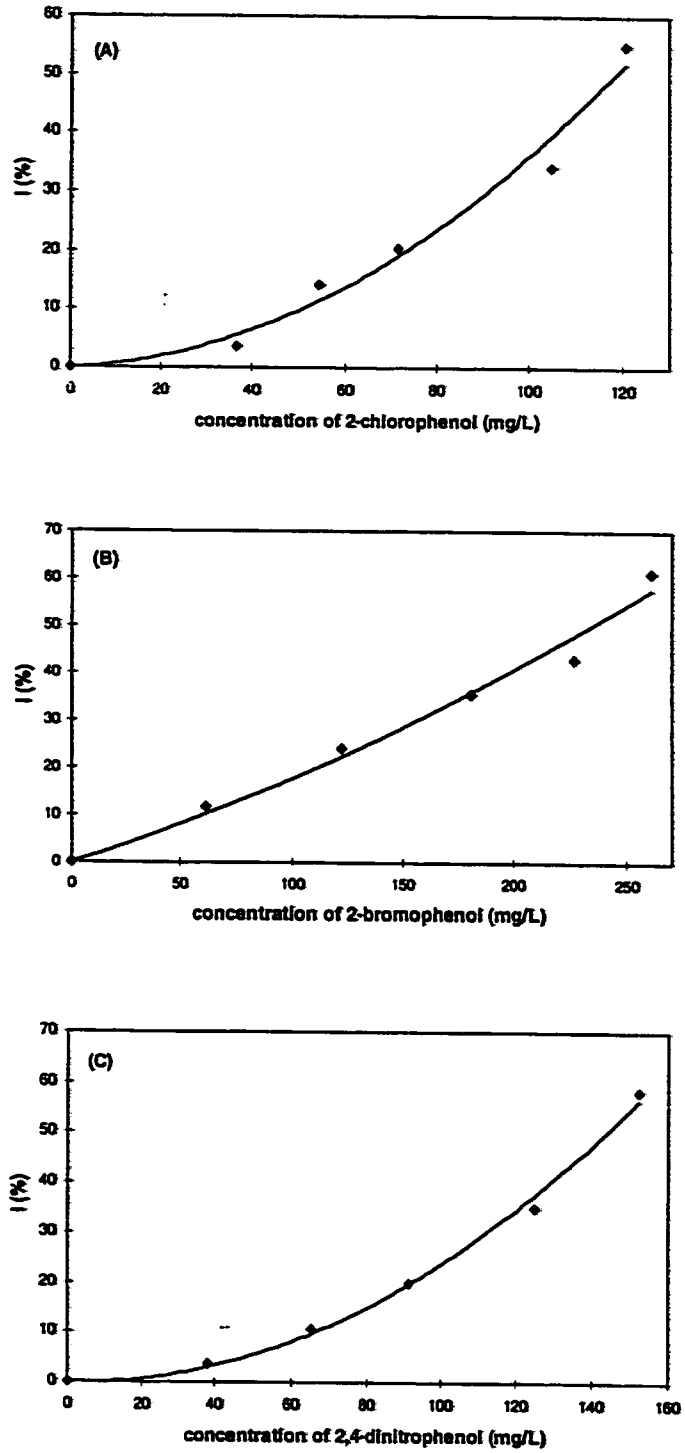

Figure 3.17 Plot of percentage inhibition (I%) versus concentration of (A) 2-chlorophenol, (B) 2-bromophenol and (C) 2,4-dinitrophenol.

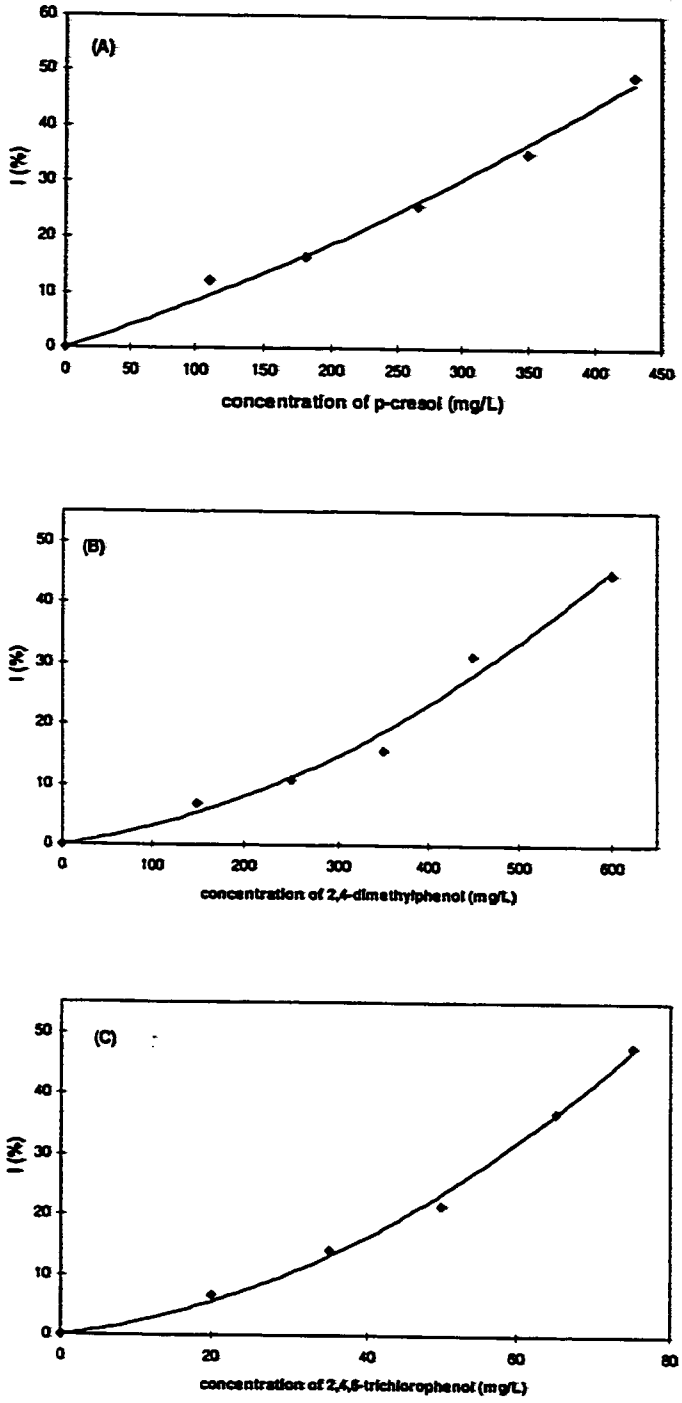

Figure 3.18 Plot of percentage inhibition (I%) versus concentration of (A) p-cresol, (B) 2,4-dimethylphenol and (C) 2,4,6-trichlorophenol.

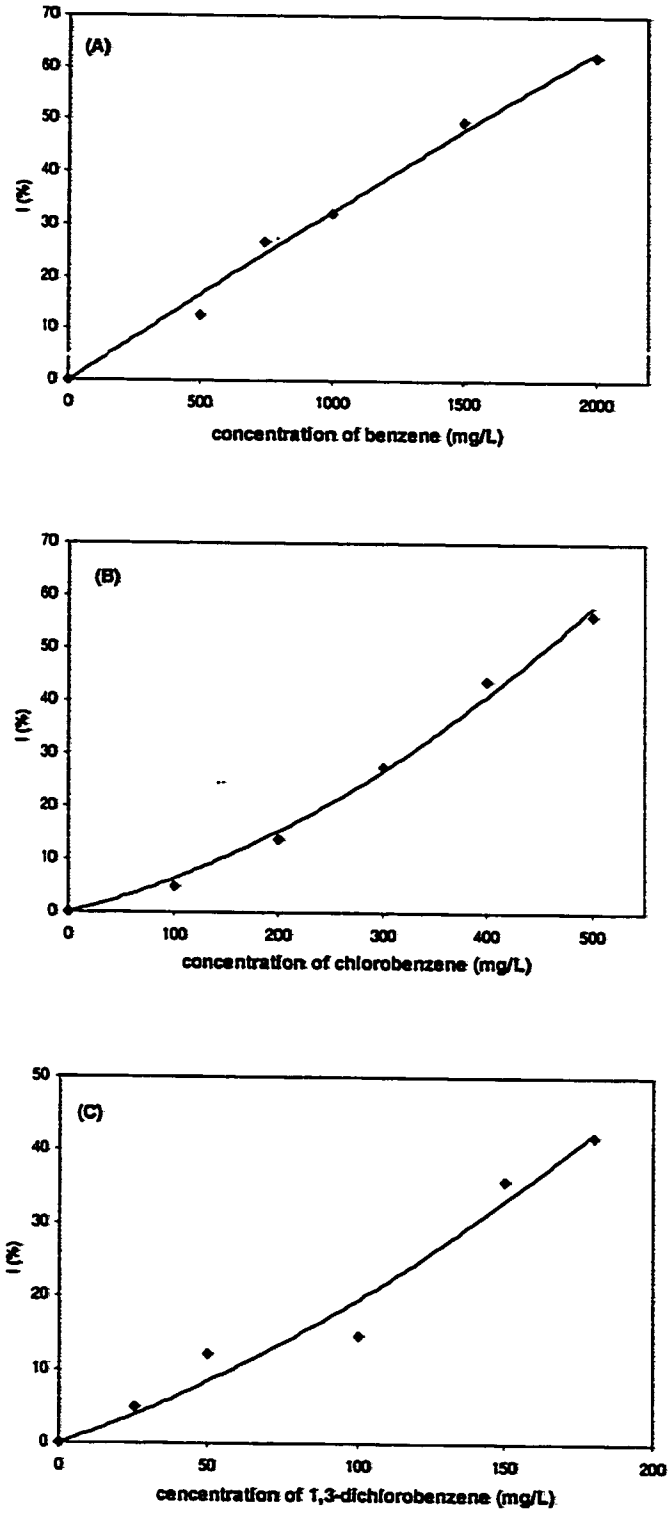

Figure 3.19 Plot of percentage inhibition (I %) versus concentration of (A) benzene, (B) chlorobenzene and (C) 1,3-dichlorobenzene.

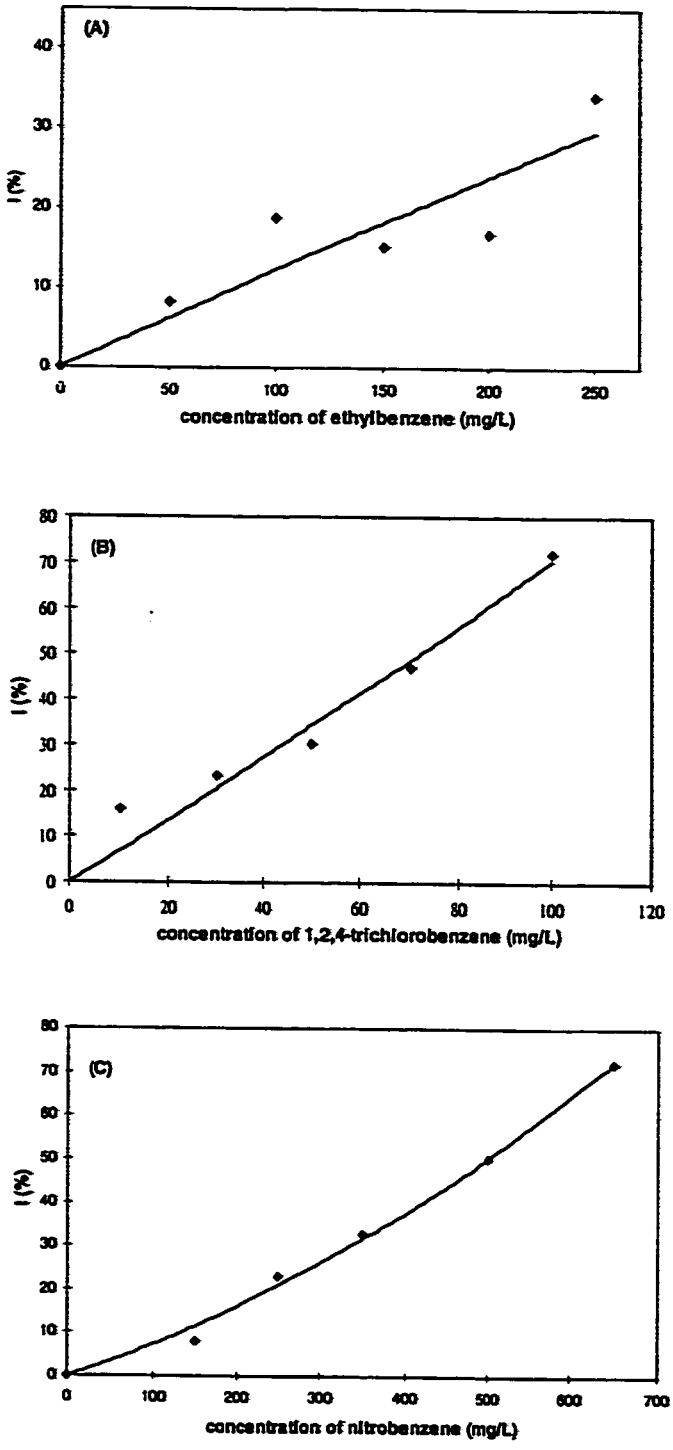

Figure 3.20 Plot of percentage inhibition (I %) versus concentration of (A) ethylbenzene, (B) 1,2,4-trichlorobenzene and (C) nitrobenzene.

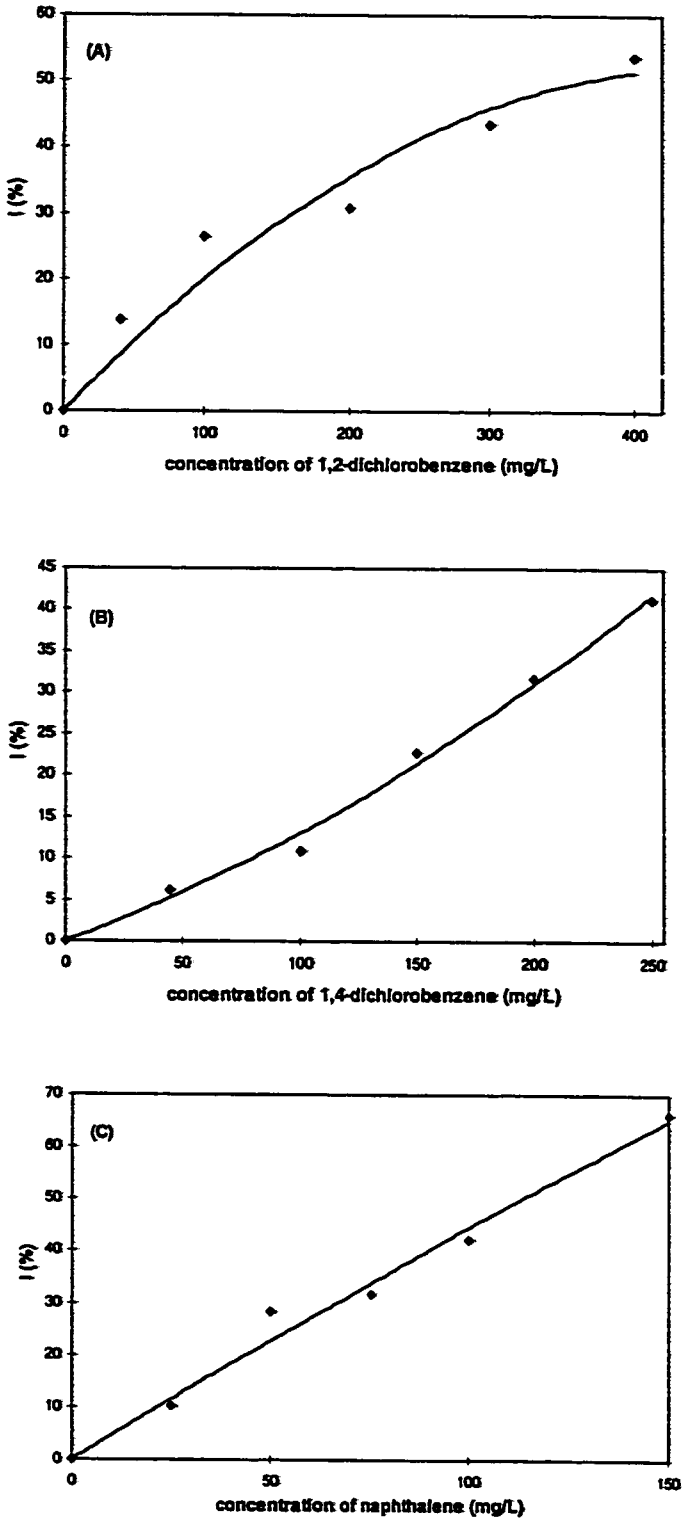

Figure 3.21 Plot of percentage inhibition (I %) versus concentration of (A) 1,2-dichlorobenzene, (B) 1,4-dichlorobenzene and (C) naphthalene.

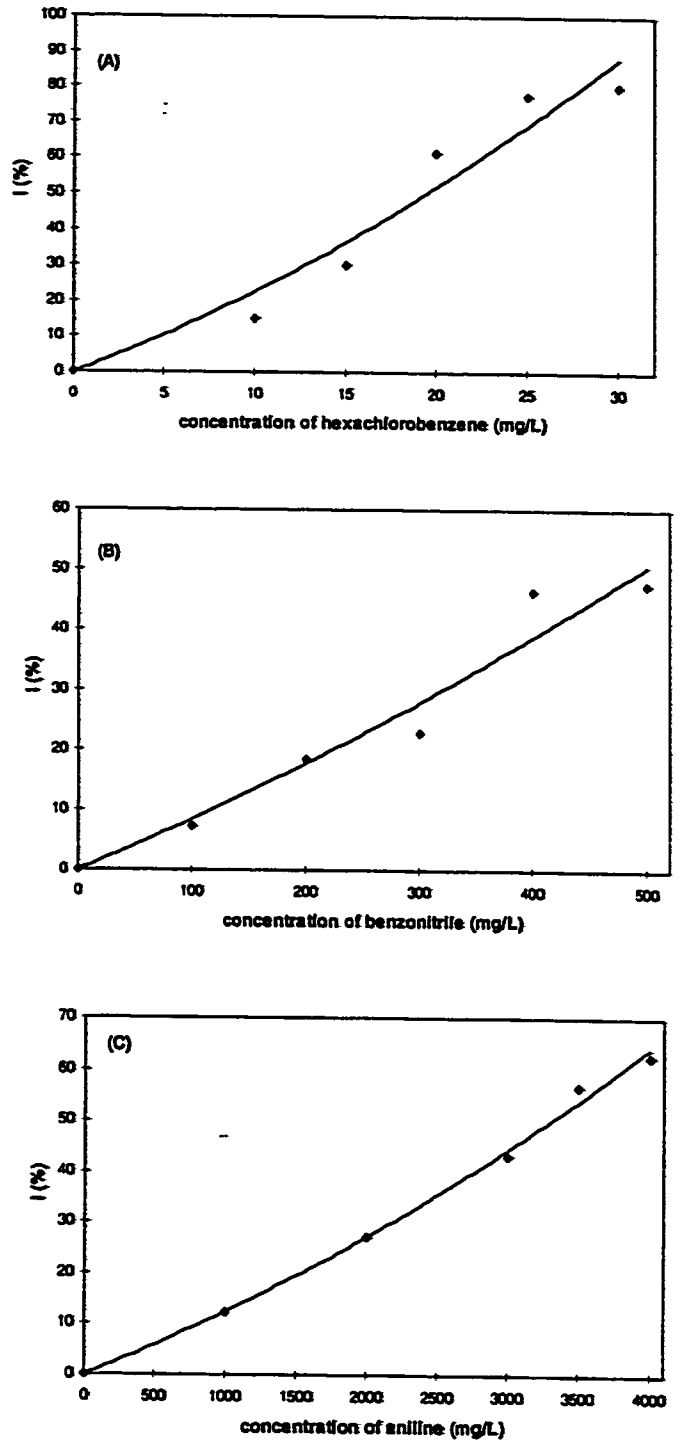

Figure 3.22 Plot of percentage inhibition (I %) versus concentration of (A) hexachlorobenzene, (B) benzonitrile and (C) aniline.

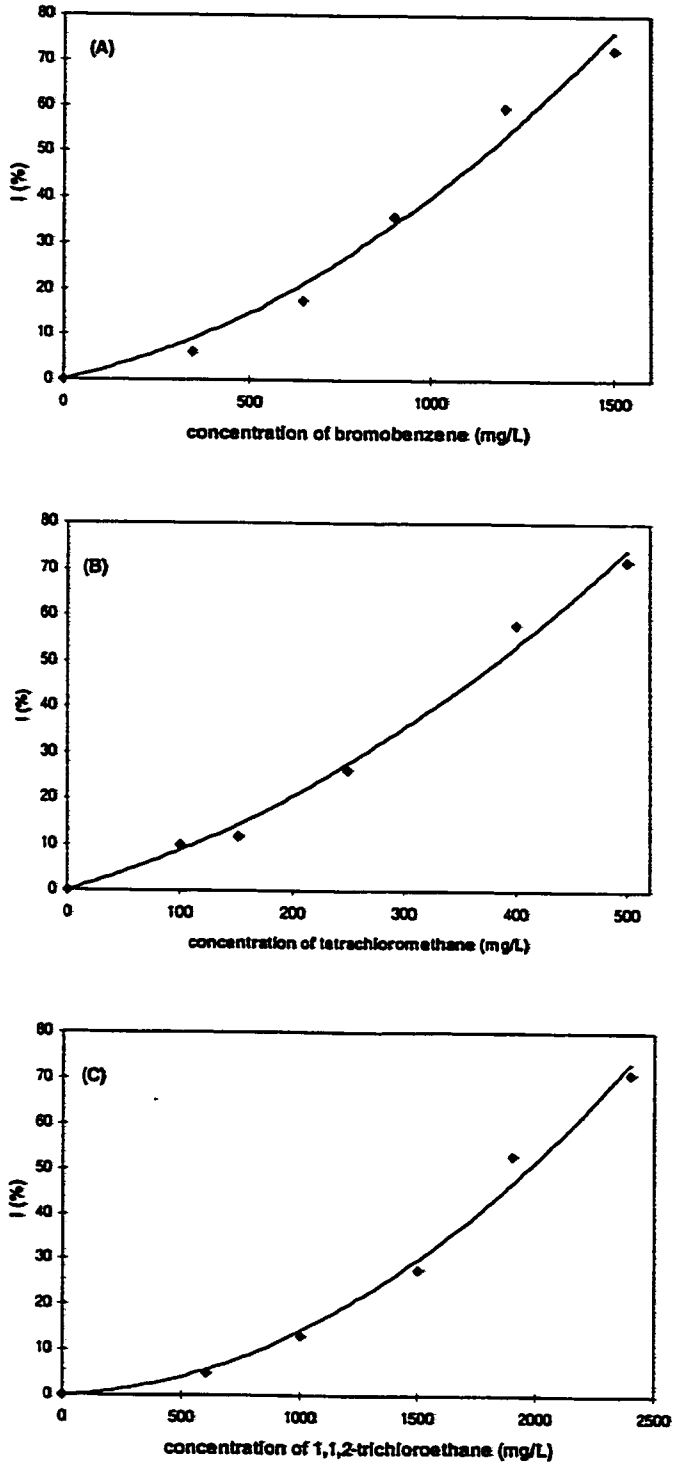

Figure 3.23 Plot of percentage inhibition (I %) versus concentration of (A) bromobenzene, (B) tetrachloromethane and (C) 1,1,2-trichloroethane.

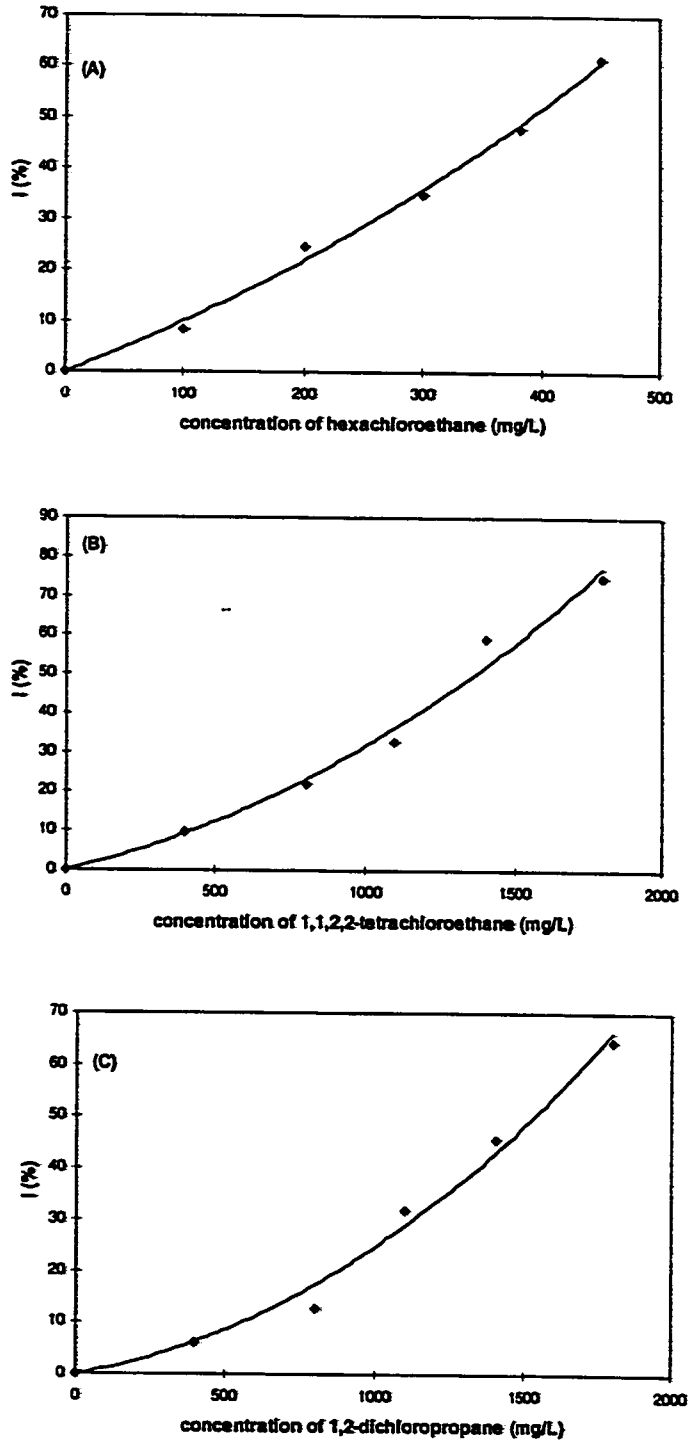

Figure 3.24 Plot of percentage inhibition (I %) versus concentration of (A) hexachloroethane, (B) 1,1,2,2-tetrachloroethane and (C) 1,2-dichloropropane.

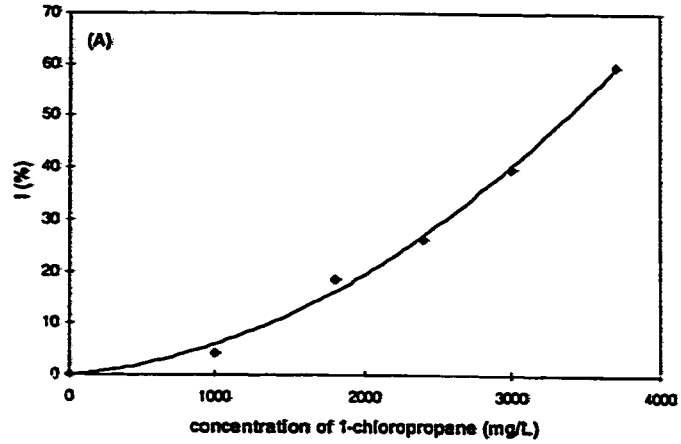

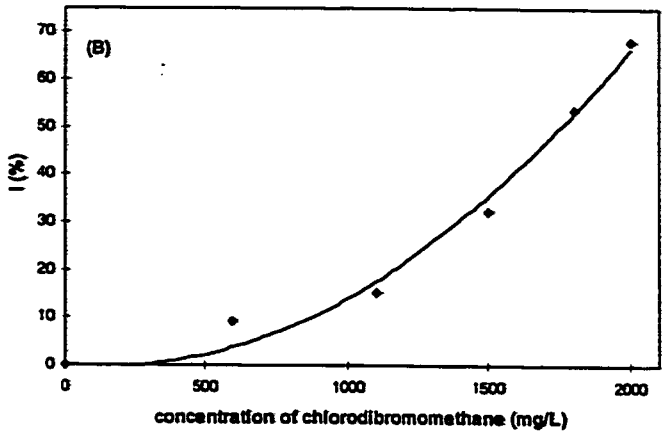

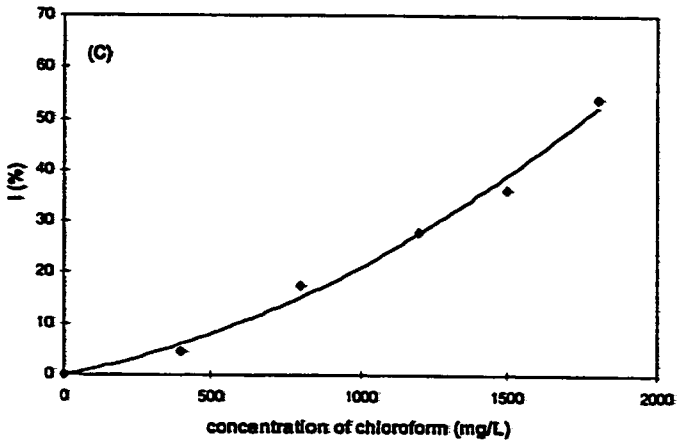

Figure 3.25 Plot of percentage inhibition (I %) versus concentration of (A) 1-chloropropane, (B) chlorodibromomethane and (C) chloroform.

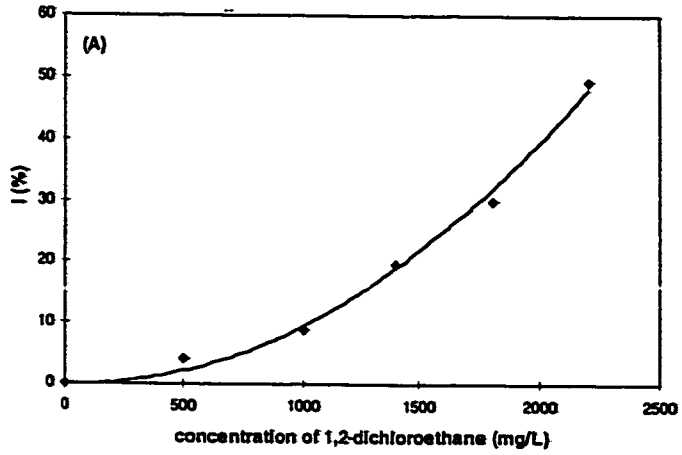

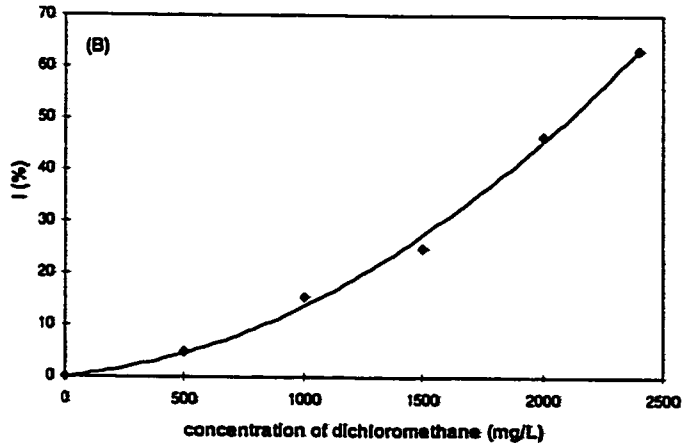

Figure 3.26 Plot of percentage inhibition (I %) versus concentration of (A) 1,2-dichloroethane and (B) dichloromethane.

3.3.3 Toxicity of Chemicals

The IC_{50} values, mean, standard deviation and coefficient of variation obtained from the same batch of sludge for various substituted phenols, benzenes and alkanes are summarized in Tables 3.1-3.3 respectively. The IC_{50} data show that each chemical exerts different degree of toxic effect on activated sludge. Since some chemicals can be metabolized at low concentrations but become toxic only at high concentrations, toxicants action is concentration dependent (Bitton and Dutka, 1986). The smallest value of IC_{50} indicates that the chemical is the most toxic one. According to the IC_{50} values, the toxicity ranking of each class of chemicals on activated sludge is also listed in Tables 3.1-3.3. Table 3.1 indicates that the toxicity of phenols with chlorine, bromine and nitro substitution is higher than that without substitution. Phenol with bromine and methyl substitution is less toxic than phenol with nitro and chlorine substitution. Moreover, the inhibitory effects of the chlorinated phenols increase with the degree of chlorination. Our results are consistent with the results reported in the literature (Klecka et al, 1985). Comparison of the toxicity of 4-nitrophenol and 2-nitrophenol suggests that the position of nitro substitution on the phenol could be one of the major factors determining its toxicity (Megharaj et al, 1991).

Table 3.2 shows that benzene is less toxic than chloro, nitro, ethyl or cyano substituted benzene. The results of dichlorobenzenes indicate that toxicity is dependent on the positions of chlorine on the benzene. Moreover, benzene with amine and bromine substitution is less toxic than benzene with chlorine and nitro substitution. Similar to phenol, the toxic effect increases with the degree of chlorine substitution.

Table 3.1 A summary of IC_{50} values, mean, standard deviation, coefficient of variation and ranking of toxicity for various substituted phenols.

Test chemical	IC_{50} (mg/L)	Mean ± (SD)[a]	Coefficient of Variation[b] (%)	Ranking[c]
3,5-Dichlorophenol (3,5-DP)	55.7, 42.1	48.9 ± (9.6)	19.7	2
Pentachlorophenol (PCP)	31.2, 34.6	32.9 ± (2.4)	7.3	1
Hydroquinone	71.0, 87.3	79.2 ± (11.5)	14.6	4
Phenol	608.1, 638.9	623.5 ± (21.8)	3.5	11
2-Nitrophenol (2-NP)	174.3, 168.2	171.3 ± (4.3)	2.5	8
4-Nitrophenol (4-NP)	87.0, 90.2	88.6 ± (2.3)	2.6	5
2-Chlorophenol (2-CP)	118.2, 120.1	119.2 ± (1.3)	1.1	6
2-Bromophenol (2-BP)	229.0, 221	225 ± (5.7)	2.5	9
2,4-Dinitrophenol (2,4-DNP)	135.3, 130.7	133 ± (3.3)	2.4	7
p-Cresol	439.5, 431	444.9 ± (7.6)	1.7	10
2,4-Dimethylphenol	630, 690	660 ± (42.4)	6.4	12
2,4,6-Trichlorophenol	77.7, 78.4	78.1 ± (0.5)	0.6	3

[a] SD = standard deviation

[b] coefficient of variation = (SD / mean) × 100%

[c] 1 represents the most toxic and 12 represents the least toxic

Table 3.2 A summary of IC_{50} values, mean, standard deviation, coefficient of variation and ranking of toxicity for various substituted benzenes.

Test chemical	IC_{50} (mg/L)	Mean ± (SD)[a]	Coefficient of Variation[b] (%)	Ranking[c]
Benzene	1000, 1250, 1500	1250 ± (250.0)	20	11
Chlorobenzene	360, 450, 450	420 ± (52.0)	12.4	8
1,3-Dichlorobenzene	300, 200, 250	250 ± (50.0)	20	4
Ethylbenzene	275, 500, 420	398.3 ± (114.1)	28.6	7
1,2,4-Trichlorobenzene	55,70	62.5 ± (10.6)	17	2
Nitrobenzene	493, 448	470.5 ± (31.8)	6.8	10
1,2-Dichlorobenzene	302.2, 325.3	313.8 ± (6.8)	5.2	6
1,4-Dichlorobenzene	260.5, 299.8	280.2 ± (27.8)	9.9	5
Naphthalene	112.3, 120.4	116.4 ± (5.7)	4.9	3
Hexachlorobenzene	19.4, 21.5	20.5 ± (1.5)	7.3	1
Benzonitrile	438.7, 496.7	467.7 ± (41.0)	8.8	9
Aniline	3420, 2790	3105 ± (445.4)	14.3	13
Bromobenzene	1340, 1190	1265 ± (106.1)	8.4	12

[a] SD = standard deviation

[b] coefficient of variation = (SD / mean) × 100%

[c] 1 represents the most toxic and 13 represents the least toxic

Table 3.3 A summary of IC_{50} values, mean, standard deviation, coefficient of variation and ranking of toxicity for various substituted alkanes.

Test chemical	IC_{50} (mg/L)	Mean ± (SD)[a]	Coefficient of Variation[b] (%)	Ranking[c]
Tetrachloromethane	390, 500	445 ± (77.8)	17.5	2
1,1,2-Trichloroethane	2240, 2120	2180 ± (84.9)	3.9	7
Hexachloroethane	330, 388	359 ± (41.0)	11.4	1
1,1,2,2-Tetrachloroethane	1510, 1520	1515 ± (7.1)	0.5	4
1,2-Dichloropropane	1360, 1490	1425 ± (91.9)	6.5	3
1-Chloropropane	3360, 3260	3310 ± (70.7)	2.1	10
Chlorodibromomethane	1700, 1710	1705 ± (7.1)	0.4	6
Chloroform	1750, 1590	1670 ± (113.1)	6.8	5
1,2-Dichloroethane	2160, 2280	2220 ± (84.9)	3.8	9
Dichloromethane	2110,2260	2185 ± (106.1)	4.9	8

[a] SD = standard deviation

[b] coefficient of variation = (SD / mean) × 100%

[c] 1 represents the most toxic and 10 represents the least toxic

Among the six chlorobenzenes tested, hexachlorobenzene is the most toxic and chlorobenzene is the least toxic. Similar trend is observed for class of alkane chemicals. For chlorinated ethane, methane and propane, shown in Table 3.3, the inhibitory effects of chlorinated aliphatic compounds increase with the degree of chlorination. Comparison of tetrachloromethane with tetrachloroethane or trichloroethane with chloroform reveals that chlorinated methane is more toxic than chlorinated ethane.

Our results show that phenolic compounds are generally more toxic than substituted benzenes and alkanes. This is consistent with the works of other researchers (Schultz et al, 1986; Veith and Broderius, 1987). Benzene and alkane are considered to have baseline toxicity elicited by membrane perturbation or narcosis mode of action (Schultz et al, 1989). Narcosis, as the reversible state of arrested cytoplasmic activity, is simply the result of toxicant partitioning into the microorganism. However, many polar aromatic compounds such as phenol are found to be more toxic than predicted by baseline toxicity. They are called to exhibit polar narcosis. The increased toxicity can be attributed to stronger electronic interactions with cellular nucleophiles in microorganism (Veith and Mekenyan, 1993).

3.3.4 Reproducibility of the Results

The reproducibility of our method for toxicity testing was evaluated by determining the coefficient of variation (CV). Tables 3.1-3.3 show that the coefficients of variation within batch of sludge for each class of chemicals ranged from 0.4 to 28.6% with the mean value of 8.1%. It is comparable to the works of Blum who found that the mean CV value was 6% for 45 toxicants on activated sludge (Blum, 1989). Table 3.4 shows the coefficients of variation between batches of sludge for ten selected phenolic chemicals collected in January and April 1997, which ranged from 0.6 to 13.6%.

The reproducibility of this method for particular chemicals was also compared with ISO (B) and OECD methods. Table 3.5 compares the coefficient variations of IC_{50} values estimated by this method with those by the ISO (B) (King and Painter, 1986) and OECD (Klecka et al, 1985) methods. The results indicate that the reproducibility of our method is comparable with ISO (B) method and better than OECD method. Hence, the reproducibility of applying the luminescence-based respirometer for toxicity assessment is quite satisfactory.

Table 3.4 Between-batch variation of IC_{50} values for ten selected phenolic chemicals.

Test Chemical	IC_{50} (mg/L)	mean ± (SD)[b]	Coefficient of Variation[c](%)
3,5-DCP	48.5[a] 48.9[a]	48.7 ± (0.3)	0.6
PCP	33.9[a] 32.9[a]	33.4 ± (0.7)	2.1
Hydroquinone	75.4[a] 79.2[a]	77.3 ± (2.7)	3.5
Phenol	514.3[a] 623.5[a]	568.9 ± (77.2)	13.6
2-NP	183.1 171.3[a]	177.2 ± (8.3)	4.7
4-NP	97.5 88.6[a]	93.1 ± (6.3)	6.8
2-CP	115.2 119.2[a]	117.2 ± (2.8)	2.4
2-BP	220.3 225[a]	222.7 ± (3.3)	1.5
2,4-DNP	121.8 133[a]	127.4 ± (7.9)	6.2
p-Cresol	424.0 444.9[a]	434.5 ± (14.8)	3.4

[a] average value

[b] SD = standard deviation

[c] coefficient of variation = (SD / mean) × 100%

Table 3.5 Comparison of reproducibility of this method with ISO (B) and OECD methods.

Test Chemical	PCP		Phenol	
	This method	ISO (B)[a]	This method	OECD
mean $IC_{50} \pm$ (SD)	33.9 ± (2.9)	55 ± (7.5)[1] 29 ± (5.1)[2] 35 ± (2.0)[3]	514.3 ± (15.9)	798.9 ± (97.1)
CV (%)	8.6	14[1] 17[2] 6[3]	3.1	12

[a] measured at different locations, [1] Rye Meads , [2] Luton , [3] Stevenage

3.3.5 Comparison with Other Test Methods

IC_{50} values of some selected chemicals determined by different methods are compared in Tables 3.6-3.8. The ISO (B), OECD, Serum bottle test, Comput-OX respirometer and our luminescence-based respirometer tests can be compared as all these methods use respiration inhibition of a mixed culture derived from domestic sewage as the measuring parameter. Other toxicity tests, such as those based on growth inhibition and light production, tend to use very few species of bacteria and often pure cultures, so that inter-method comparison is not strictly valid. Among these testing methods, from Table 3.6, OECD and Comput-OX respirometer resulted in almost identical toxicity ranking with our method. These data suggest that the sensitivity pattern of our method is similar to these methods for phenolic chemicals. Comparison of IC_{50} values of 3,5-DCP and PCP obtained from the methods listed in Table 3.6 shows that our method gives larger values than other methods. However, IC_{50} values of phenol, 4-NP, 2-NP and 2-CP are relatively small in our method. These data suggest that the sensitivity of our method is dependent on the chemicals being tested. Similar phenomenon can also be observed in 4-NP and p-cresol with Serum bottle test and Comput-OX respirometer or PCP and 4-NP with ISO (B) and OECD methods.

Tables 3.7 and Table 3.8 show that the toxicity ranking of our method is comparable with Comput-OX respirometer for benzene and alkane chemicals. However, no correlation can be observed between our test and Serum bottle test for benzene and alkane chemicals. Indeed, the data of Serum bottle test was found to

Table 3.6 Comparison of IC_{50} (mg/L) results of different microbial toxicity tests for substituted phenols.

Chemicals	Microtox[a] 5 min EC_{50}	ISO (B)[b,c]	OECD[d,e]	Serum bottle test[a]	Comput-OX respirometer[f]	This method
3,5-DCP	7.3	6	20	-	-	48.9
PCP	-	32	25	-	-	32.9
Phenol	34	-	800	1100	-	623.5
4-NP	6.4	98	126.0	160	125	88.6
2-NP	21	-	400.0	11	318	171.3
2-CP	18	-	380	360	-	119.2
p-Cresol	-	-	-	260	522	444.9
2,4-DNP	-	-	-	-	169	133
2,4-Dimethylphenol	-	-	-	-	224	660

[a] Blum and Speece, 1991a

[b] Bitton and Dutka, 1986

[c] King and Painter, 1986

[d] Yoshioka et al, 1986

[e] Klecka et al, 1985

[f] Xu and Nirmalakhandan, 1998

Table 3.7 Comparison of IC_{50} (mg/L) results of different microbial toxicity tests for various substituted benzenes.

Chemicals	Microtox[a] 5 min EC_{50}	OECD[b]	Serum bottle test[c]	Comput-OX respirometer[d]	This method
Benzene	75	-	520	993	1250
Ethylbenzene	-	-	130	222	398.3
Chlorobenzene	9.4	-	310	155	420
1,2-Dichlorobenzene	2.7	100	910	49	313.8
1,3-Dichlorobenzene	3.1	-	720	63	250
1,4-Dichlorobenzene	4.3	-	330	14	280.2
1,2,4-Trichlorobenzene	2.3	-	7700	35	62.5
Hexachlorobenzene	-	-	350	-	20.5
Nitrobenzene	-	100	370	-	470.5
Benzonitrile	-	-	470	-	467.7
Naphthalene	-	-	670	-	116.4

[a] Kaiser and Ribo, 1987

[b] Yoshioka et al, 1986

[c] Blum and Speece, 1991a

[d] Xu and Nirmalakhandan, 1998

Table 3.8 Comparison of IC_{50} (mg/L) results of different microbial toxicity tests for various substituted alkanes.

Chemicals	Microtox[a] 5 min EC_{50}	Serum bottle test[a]	Comput-OX respirometer[b]	This method
Tetrachloromethane	-	130	432	445
1,2-Dichlorethane	-	470	1385	2220
Chloroform	-	640	-	1670
Dichoromethane	-	320	1994	2185
Hexachloroethane	0.45	-	-	359
1,1,2-Trichloroethane	110	240	-	2180
1,1,2,2-Tetrachloroethane	5.4	130	197	1515
1-Choropropane	830	700	-	3310
1,2-Dichloropropane	59	-	861	1425
Chlorodibromomethane	-	-	206	1705

[a] Blum and Speece, 1991a

[b] Xu and Nirmalakhandan, 1998

contradict with the results reported in the literatures (Klecka et al, 1985; Kaiser and Ribo, 1987). The toxicity of chemical usually increases with the degree of chlorination. However, their results show that 1,2,4-trichlorobenzene was less toxic than benzene and three other dichlorobenzenes. We have also correlated our data with the Comput-OX respirometer and the Serum bottle tests for all three different classes of chemicals. The log IC_{50} values obtained from our method and the Comput-OX respirometer are compared in Figure 3.27. The correlation between our method and the Comput-OX respirometer was fair with $r^2 = 0.569$ and root mean square error (s) = 0.439.

Many studies have reported that Microtox method, which measures the inhibition of natural luminescence of a photobacterial strain (*Photobacterium phosphoreum*), is the most sensitive method (Klecka and Landi, 1985; Dutka et al, 1983). Tables 3.6-3.8 show that the IC_{50} values of various phenols, alkanes and benzenes determined by Microtox method are much smaller than those determined by other methods. However, Microtox method is based on the use of a single bacterial strain. Therefore, it may not be well suited for toxicity assessment for activated sludge. Each microbial toxicity test has its own sensitivity pattern that cannot be readily correlated with other procedures. The common use of IC_{50} values to indicate the sensitivity of a specific method may not be consistently reliable. Thus, multiple tests should be carried out in order to assess the toxicity of chemicals. The IC_{50} values obtained with activated sludge depend also very much on its source, wastewater composition and operating conditions of the treatment plants, etc. Often, sludge from

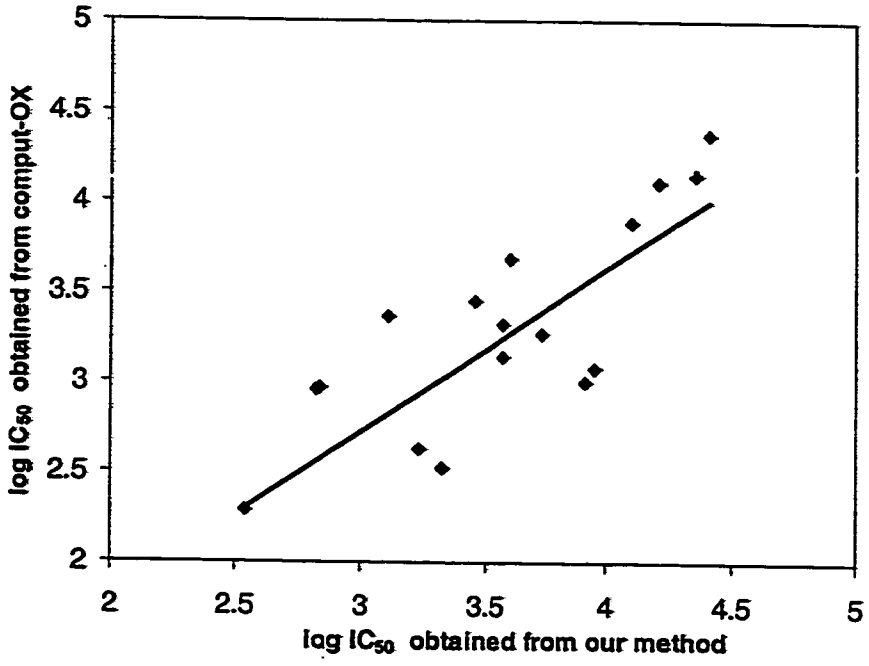

Figure 3.27 A plot of log IC_{50} (μmol/L) obtained from Comput-OX respirometer versus log IC_{50} (μmol/L) obtained from our method.

different sources may give different responses to inhibitors depending on the types and the relative number of microorganisms present. As a matter of fact, the application of biochemical test results for regulators of wastewater treatment plants is only reliable when the sludge is obtained from the plant(s) to which the chemical is expected to be discharged.

3.4 Concluding Remarks

This chapter demonstrates that the optical scanning respirometer developed, using the oxygen optode described in Chapter 2, can be used to detect the potential toxicity of various substituted phenols, benzenes and alkanes on activated sludge. The reproducibility of this respirometer is comparable with ISO (B) method and superior to OECD method. The sensitivity of this method is dependent on the chemicals tested and is comparable with that of the OECD method and Comput-OX respirometer for phenolic chemicals. For alkanes and benzenes, the sensitivity pattern of our method is comparable with Comput-OX respirometer and different from that of Serum bottle test. For general purposes, the respirometer is expected to be an effective tool for toxicity screening.

Chapter 4

Quantitative Structure Activity Relationships for Substituted Alkanes, Benzenes and Phenols to Activated Sludge

4.1 Introduction

Toxicity testing is essential to assess the environmental risk of chemicals. However, due to the large number of chemicals being released into the environment, it is costly and time consuming to obtain toxicity data. For this reason, quantitative structure activity relationship (QSAR) becomes increasingly important for predicting the toxicity of untested chemicals. The principle of QSAR is based on the existence of correlation between the chemical toxicity and its physicochemical or structure properties. QSAR has been used most extensively in the areas of drug and pesticide in the past. Recently, research efforts have been devoted to applying QSAR in toxicology studies.

Three common QSAR approaches used in toxicity studies are hydrophobic approach (e.g., log P), linear solvation energy relationship (LSER) and topological approach (e.g., MCI). Octanol-water partition coefficient (log P) is the key parameter for toxic behaviour since it describes the tendency of a chemical to accumulate in the nonpolar lipid-like biophase and was shown to be quite successful at correlating the toxicity of most organic chemicals. Schultz and Riggin (1985) found that toxicity of 20 alkylated and halogenated phenols on *Tetrahymena pyriformis* correlated well with log P of the compounds. The use of linear solvation energy relationship (LSER) was pioneered by Kamlet and co-workers (1986). LSER is based on four solvatochromic parameters: the intrinsic molecular volume, V_i ; polarity/polarizability, π^* ; and hydrogen bond donor acidity, α_m ; and basicity, β_m. Blum and Speece (1991b) found that LSER approach could be used to predict the toxicity of the widest range of

chemicals. However, LSER suffers from the limitation of insufficient solvatochromic parameters for all different groups of chemicals. Molecular connectivity index (MCI) is a method of describing molecular structure in terms of molecular topology and does not relate to any specific physicochemical properties of the chemicals. Nirmalakhandan et al (1994a) and Sun et al (1994) found that molecular connectivity approach has better QSAR correlation for homogeneous class of chemicals than diverse set of chemicals. Different types of descriptors can also be combined to give better QSAR correlations.

In this study, IC_{50} values of 35 substituted alkanes, benzenes and phenols in activated sludge, obtained from optical scanning respirometer, were used to develop QSAR models. Apart from commonly used descriptors (log P and MCI), other approaches such as molecular volume, log S or combination of log P and ELUMO were used to model toxicity on each chemical class and all 35 tested chemicals. The predictive abilities of the developed QSARs for analyzing mixture toxicity were then evaluated.

4.2 Experimental Section

4.2.1 Determination of IC_{50} Data

The toxicity data of 35 chemicals on activated sludge were determined using the optical scanning respirometer developed by us. Details of the toxicity assessment have been presented in chapter 3. The IC_{50} values were originally expressed in mg/L. To account for the effect of molecular weight, they were converted to μM/L. For statistical reasons, log units have been used for IC_{50} values to reduce many orders of magnitude. Table 4.1 summarizes the data used in the development of QSAR equations.

4.2.2 Molecular Descriptors

The log P (Hansch, et al, 1995), aqueous solubility (mg/L) and pK_a values (phenolic chemicals) at 25°C (Howard and Meylan, 1997) for each toxicant were obtained from reference handbooks (Table 4.2). The aqueous solubility values were converted to log μM/L and abbreviated as log S. The solute molecular van der Waals volume values (V_i/100), shown in Table 4.2, were obtained from literature sources (Blum and Speece, 1991b; Luehers et al, 1996). For determination of ELUMO, the molecular specification parameters were described as Z-matrix, which was calculated by using Chem3D Pro. (Cambridgesoft Corp.). The optimized ELUMO (Table 4.2) were determined by inputting the Z-matrix to Gaussian 98W Rev. A7 programs (Gaussian, Inc.) and using the AM1 hamiltonian theory (Dewar et al, 1985) on a 586

Table 4.1 A summary of toxicity data.

Chemical Class	Toxicant	Average IC_{50} (mg/L)	Molecular Weight (g)	Log IC_{50} (μmol/L)
Alkanes	Tetrachloromethane	445	153.82	3.461
	1,2-Dichloroethane	2220	98.96	4.351
	Chloroform	1670	119.39	4.146
	Dichloromethane	2185	84.94	4.410
	Hexachloroethane	359	236.74	3.181
	1,1,2-Trichloroethane	2180	133.42	4.213
	1,1,2,2-Tetrachloroethane	1515	167.86	3.955
	1,2-Dichloropropane	1425	112.99	4.101
	1-Chloropropane	3310	78.54	4.625
	Chlorodibromomethane	1705	208.29	3.913
Phenols	Pentachlorophenol	33.0	266.34	2.093
	3,5-Dichlorophenol	48.7	163.00	2.475
	Hydroquinone	73.9	110.11	2.827
	4-Nitrophenol	92.3	139.11	2.822
	2-Chlorophenol	116.7	128.56	2.958
	2,4-Dinitrophenol	128.6	184.11	2.844
	2-Nitrophenol	178.7	139.11	3.109
	2-Bromophenol	224.7	173.01	3.113
	p-Cresol	431.8	108.14	3.601
	Phenol	568.9	94.11	3.781
	2,4-Dimethylphenol	660	122.17	3.733
	2,4,6-Trichlorophenol	78.1	197.45	2.597

Table 4.1 (cont'd) A summary of toxicity data.

Chemical Class	Toxicant	Average IC_{50} (mg/L)	Molecular Weight (g)	Log IC_{50} (μmol/L)
Benzenes	Benzene	1250	78.11	4.204
	Ethylbenzene	398	106.18	3.574
	Chlorobenzene	420	112.56	3.572
	1,3-Dichlorbenzene	250	147	3.231
	1,2,4-Trichlorobenzene	62.5	181.45	2.537
	Nitrobenzene	470.5	123.11	3.582
	1,4-Dichlorobenzene	280.2	147.00	3.280
	1,2-Dichlorobenzene	313.8	147.00	3.329
	Hexachlorobenzene	20.5	284.8	1.856
	Naphthalene	116.4	128.16	2.958
	Benzonitrile	467.7	103.12	3.657
	Aniline	3105	93.13	4.523
	Bromobenzene	1265	157.02	3.906

Table 4.2 A summary of log P, log S, $V_i/100$, ELUMO and pK_a for all chemicals.

Chemical	Log P	Log S (μmol/L)	$V_i/100$ (cm^3/mol)	ELUMO (eV)	pK_a
Tetrachloromethane	2.83	3.68	0.514	-1.116	/
1,2-Dichloroethane	1.48	4.94	0.442	0.683	/
Chloroform	1.97	4.82	0.427	-0.306	/
Dichloromethane	1.25	5.18	0.336	0.595	/
Hexachloroethane	4.14	1.53	0.790	-0.968	/
1,1,2-Trichloroethane	1.89	4.52	0.519	0.170	/
1,1,2,2-Tetrachloroethane	2.39	4.25	0.617	-0.007	/
1,2-Dichloropropane	1.99	4.39	0.541	1.051	/
1-Chloropropane	2.04	4.54	0.450	1.519	/
Chlorodibromomethane	2.16	4.11	0.520	-0.728	/
Pentachlorophenol	5.12	3.86	0.986	-0.977	4.70
3,5-Dichlorophenol	3.62	4.66	0.716	-0.285	8.18
Hydroquinone	0.59	5.82	0.581	0.233	10.85
4-Nitrophenol	1.91	4.92	0.676	-1.065	7.15
2-Chlorophenol	2.15	4.95	0.626	0.067	8.56
2,4-Dinitrophenol	1.67	4.18	0.810	-1.887	4.09
2-Nitrophenol	1.79	4.20	0.676	-1.185	7.23
2-Bromophenol	2.35	4.11	0.669	-0.014	8.45
p-Cresol	1.94	5.30	0.634	0.435	10.26
Phenol	1.46	5.94	0.536	0.398	9.99
2,4-Dimethylphenol	2.30	4.81	0.734	0.404	10.61
2,4,6-Trichlorophenol	3.69	3.61	0.806	-0.502	5.99

Table 4.2 (cont'd) A summary of log P, log S, $V_i/100$, ELUMO and pK_a for all chemicals.

Chemical	Log P	Log S (μmol/L)	$V_i/100$ (cm^3/mol)	ELUMO (eV)
Benzene	2.13	4.36	0.491	0.555
Ethylbenzene	3.15	3.20	0.687	0.538
Chlorobenzene	2.89	3.65	0.581	0.155
1,3-Dichlorbenzene	3.53	2.93	0.671	-0.158
1,2,4-Trichlorobenzene	4.02	2.43	0.761	-0.469
Nitrobenzene	1.85	4.23	0.631	-1.068
1,4-Dichlorobenzene	3.44	2.71	0.671	-0.216
1,2-Dichlorobenzene	3.43	3.03	0.671	-0.142
Hexachlorobenzene	5.73	-1.66	1.031	-1.041
Naphthalene	3.30	2.38	0.753	-0.265
Benzonitrile	1.56	4.29	0.590	-0.294
Aniline	0.90	5.59	0.562	0.640
Bromobenzene	2.99	3.42	0.624	0.059

personal computer. Simple and valence connectivity indices up to third order path levels were calculated as described by Kier and Hall (1976; 1986), with 0.78 and 0.26 as the delta valence values for chlorine and bromine respectively (Table 4.3). A simple calculation illustrating this algorithm is shown in Appendix.

4.2.3 Statistical Analysis

QSAR equations were developed using the linear regression procedure of SPSS statistical package version 9 on a 586 personal computer. For each regression equation, the following information is provided:

(n) = number of observations used in the analysis;

(r^2) = coefficient of determination; this measures the goodness of fit of a model;

(s) = root mean square error; a measure of the variability in the data due to experimental error and any other factors not included in the equation;

(F) = Fisher statistic value; a check of significance of the model at 95% level.

The residual values, the difference between the observed value and predicted value, were calculated to identify the outlier or influential data. The data with residue value substantial larger than others is considered to be the outlier. The outlier was eliminated one at a time and multiple regression analysis was repeated to assess its influence on the correlation. The collinearity (strong linear correlation between the descriptors) was diagnosed using methods described by Belsley et al (1980), based on eigenvalues of the variance-covariance matrix. A condition index

Table 4.3 A summary of molecular connectivity indices for all chemicals.

Chemicals	^0X	$^0X^v$	^1X	$^1X^v$	^2X	$^2X^v$	^3X_p	$^3X_p{}^v$
Tetrachloromethane	4.50	5.03	2.00	2.26	3.00	3.85	0.00	0.00
1,2-Dichloroethane	3.41	3.68	1.91	2.10	1.00	1.13	0.50	0.64
Chloroform	3.58	3.97	1.73	1.96	1.73	2.22	0.00	0.00
Dichloromethane	2.71	2.97	1.41	1.60	0.71	0.91	0.00	0.00
Hexachloroethane	7.00	7.79	3.25	3.65	4.50	5.55	2.25	2.89
1,1,2-Trichloroethane	4.28	4.68	2.27	2.52	1.80	2.13	0.82	1.04
1,1,2,2-Tetrachloroethane	5.15	5.68	2.64	2.94	2.49	3.00	1.33	1.71
1,2-Dichloropropane	4.28	4.55	2.27	2.44	1.80	1.98	0.82	0.99
1-Chloropropane	3.41	3.55	1.91	2.01	1.00	1.07	0.50	0.57
Chlorodibromomethane	3.58	5.63	1.73	2.92	1.73	4.78	0.00	0.00
Pentachlorophenol	9.46	9.11	5.46	4.55	5.15	3.80	4.98	3.44
3,5-Dichlorophenol	6.85	5.94	4.18	3.08	4.02	2.50	2.41	1.28
Hydroquinone	5.98	4.20	3.79	2.26	3.37	1.52	2.30	0.85
4-Nitrophenol	7.56	5.02	4.70	2.63	4.26	1.77	3.00	1.06
2-Chlorophenol	5.98	4.89	3.80	2.61	3.24	1.85	2.54	1.17
2,4-Dinitrophenol	10.01	6.21	6.02	3.14	5.70	2.19	4.10	1.32
2-Nitrophenol	6.98	5.02	4.72	2.64	4.17	1.75	3.03	1.08
2-Bromophenol	5.98	5.72	3.80	3.03	3.24	2.30	2.54	1.52
p-Cresol	5.98	4.75	3.79	2.54	3.37	1.83	2.30	1.03
Phenol	5.11	3.83	3.39	2.13	2.74	1.33	1.89	0.76
2,4-Dimethylphenol	6.85	5.67	4.20	2.96	3.87	2.28	2.86	1.35
2,4,6-Trichlorophenol	7.72	7.00	4.98	3.57	4.39	2.96	3.34	1.77

Table 4.3 (cont'd) A summary of molecular connectivity indices for all chemicals.

Chemical	^{0}X	$^{0}X^{v}$	^{1}X	$^{1}X^{v}$	^{2}X	$^{2}X^{v}$	$^{3}X_{p}$	$^{3}X_{p}^{v}$
Benzene	4.24	3.46	3.00	2.00	2.12	1.15	1.50	0.67
Ethylbenzene	5.82	5.09	3.93	2.97	2.91	1.83	2.30	1.25
Chlorobenzene	5.11	4.52	3.39	2.47	2.74	1.73	1.89	0.99
1,3-Dichlorbenzene	5.98	5.57	3.79	2.95	3.38	2.31	2.20	1.26
1,2,4-Trichlorobenzene	6.85	6.63	4.20	3.44	3.87	2.81	2.86	1.85
Nitrobenzene	6.69	4.65	4.30	2.50	3.64	1.59	2.59	0.97
1,4-Dichlorobenzene	5.98	5.57	3.79	2.95	3.37	2.31	2.30	1.30
1,2-Dichlorobenzene	5.98	5.57	3.80	2.96	3.24	2.23	2.54	1.58
Hexachlorobenzene	9.46	9.79	5.46	4.90	5.15	4.15	4.98	4.00
Naphthalene	6.81	5.62	4.97	3.40	4.09	2.35	3.47	1.66
Benzonitrile	5.82	4.33	3.93	2.38	2.91	1.48	2.30	0.90
Aniline	5.11	3.96	3.39	2.20	2.74	1.41	1.89	0.80
Bromobenzene	5.11	5.35	3.39	2.89	2.74	2.21	1.89	1.26

(the square roots of the ratios of the largest eigenvalue to each individual eigenvalue) greater than 15 indicates the existence of collinearity problem. Highly correlated descriptors were eliminated. Finally, QSAR equations were validated by removing about 20% data points randomly from the entire data set. The new correlation equations were generated using the remaining data points and were then used to calculate the predicted IC_{50} values of the omitted toxicants. The predicted values were checked to confirm that they fell within 95% confidence interval of the original correlation equations.

4.3 Results and Discussion

4.3.1 Octanol-Water Partition Coefficient (log P)

The correlation results of using log P as descriptor for each individual chemical class, and for all 35 chemicals combined are shown as follows:

Substituted alkanes:

$$\log IC_{50} = 5.10 - 0.48 \log P \qquad (4.1)$$

$n = 10, r^2 = 0.783, s = 0.2157, F = 28.912$

Substituted benzenes:

$$\log IC_{50} = 4.92 - 0.51 \log P \qquad (4.2)$$

$n = 13, r^2 = 0.804, s = 0.3188, F = 45.028$

Substituted phenols:

$$\log IC_{50} = 3.63 - 0.26 \log P \qquad (4.3)$$

$n = 12, r^2 = 0.39, s = 0.4192, F = 6.398$

All chemicals:

$$\log IC_{50} = 4.46 - 0.40 \log P \qquad (4.4)$$

$n = 35, r^2 = 0.428, s = 0.5305, F = 24.651$

The plots of observed log IC_{50} versus predicted log IC_{50} are shown in Figures 4.1-4.4. As the chemicals with larger P (increased partitioning into the lipid phase) can accumulate more easily in the lipid phase of the cellular membrane, they should be more toxic. Our results show that log P can be used to describe fair well the toxicity of substituted alkanes and benzenes. As expected, toxicity of the chemical (smaller log IC_{50} value) increased with log P. Examination of Figure 4.1 and residual value revealed that 1-chloropropane was a statistical outlier. It was less toxic than predicted by eqn. (4.1). Sixt and co-workers (1995) also found that 1-monochloroalkanes were considerably less toxic than would be expected based on log P or V_{mc}. Excluding 1-chloropropane from the regression improved significantly the precision of the model (Figure 4.5):

Substituted alkanes except 1-chloropropane:

$$\log IC_{50} = 5.01 - 0.46 \log P \qquad (4.5)$$

$n = 9, r^2 = 0.935, s = 0.1109, F = 101.161$

No statistically significant correlations were found for phenolic chemicals (eqn. 4.3) and all 35 chemicals (eqn. 4.4). Elimination of two statistical outliers (hydroquinone and 2,4-dimethylphenol) from the regression for phenolic chemicals improved the precision of the model ($r^2 = 0.675$, $s = 0.3042$, $F = 16.615$). Schultz's

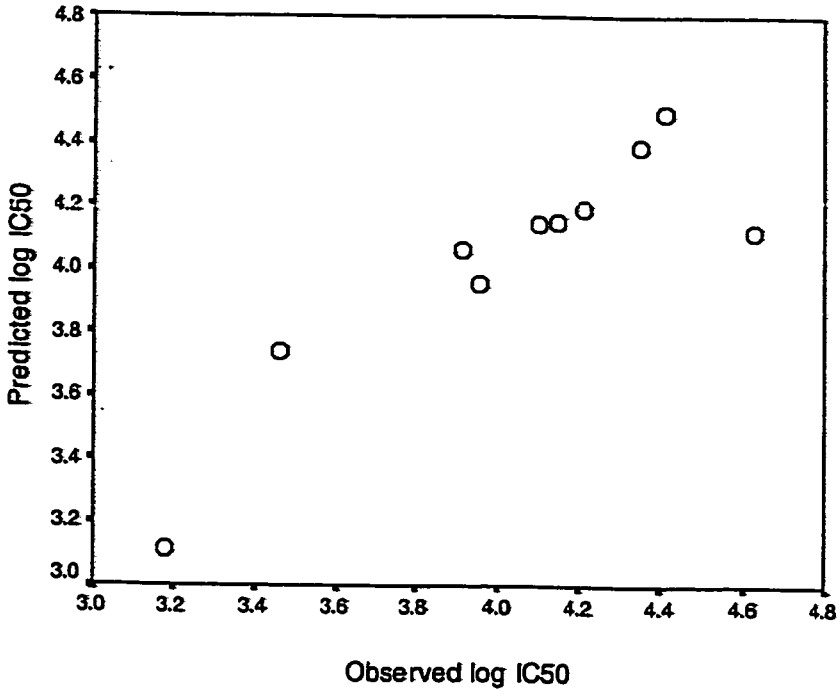

Figure 4.1 A plot of predicted log IC_{50} (μmol/L) versus observed log IC_{50} (μmol/L) using log P as descriptor for substituted alkanes.

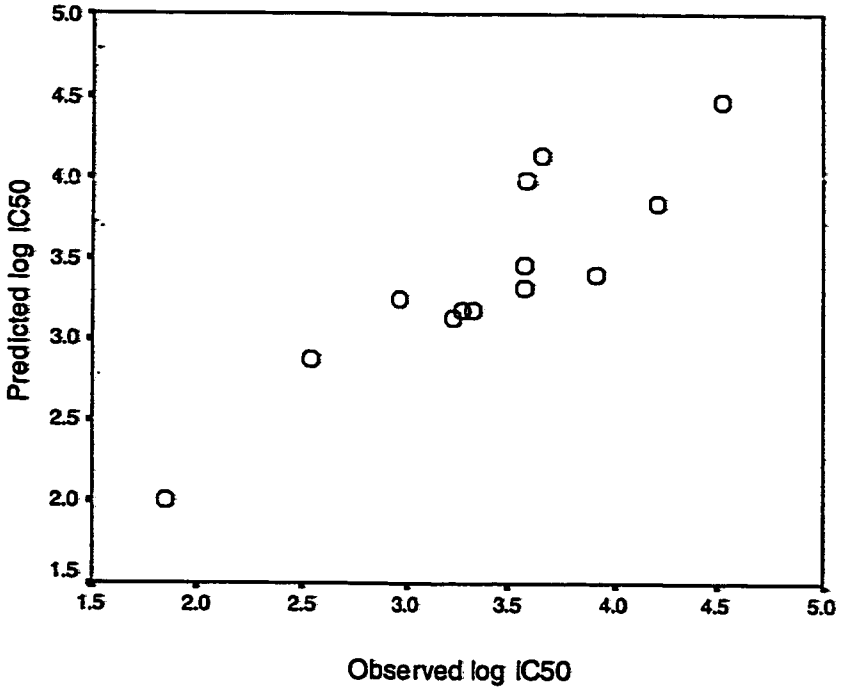

Figure 4.2 A plot of predicted log IC_{50} (μmol/L) versus observed log IC_{50} (μmol/L) using log P as descriptor for substituted benzenes.

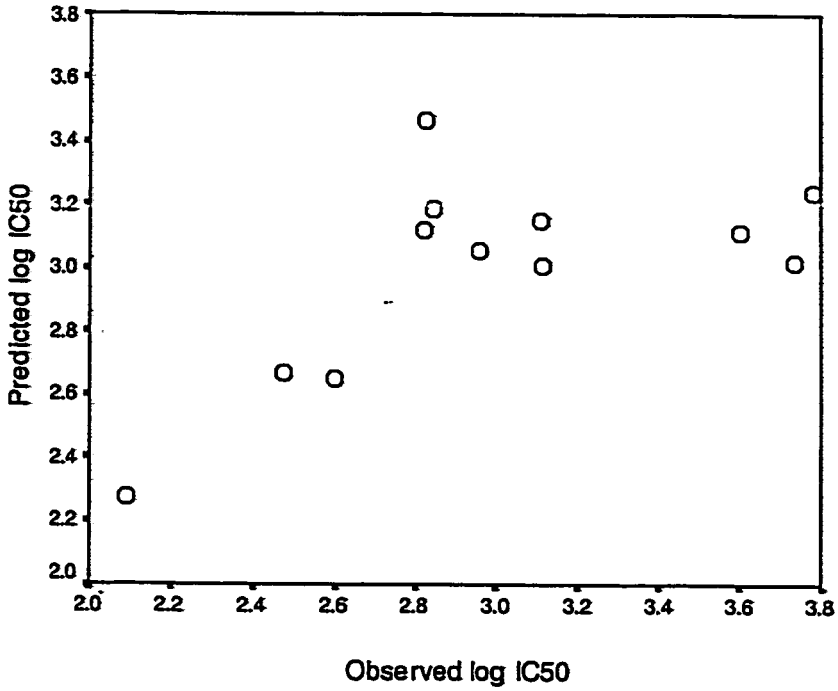

Figure 4.3 A plot of predicted log IC_{50} (μmol/L) versus observed log IC_{50} (μmol/L) using log P as descriptor for substituted phenols.

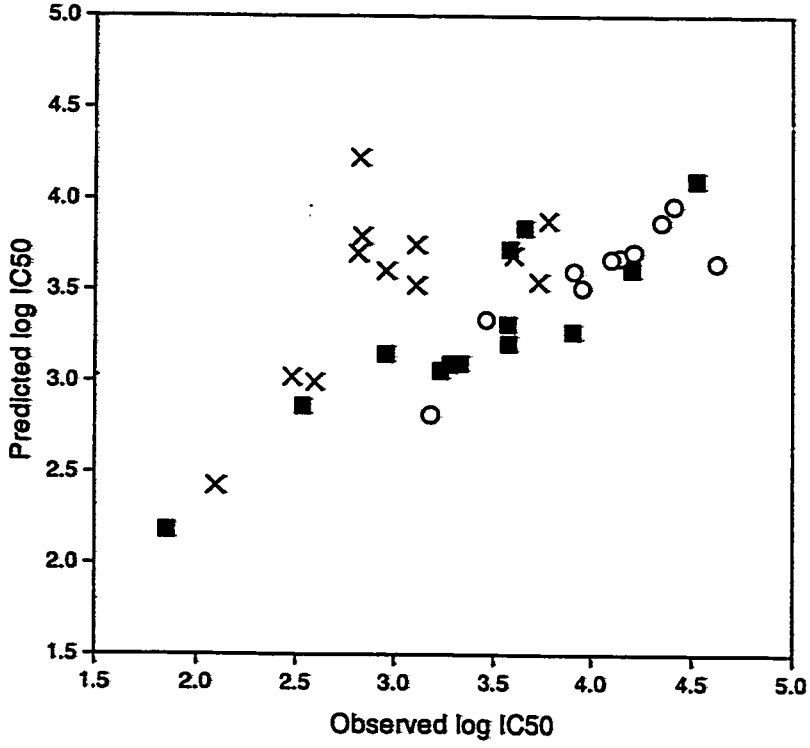

Figure 4.4 A plot of predicted log IC_{50} (μmol/L) versus observed log IC_{50} (μmol/L) using log P as descriptor for all chemicals: (O) alkanes, (■) benzenes and (×) phenols.

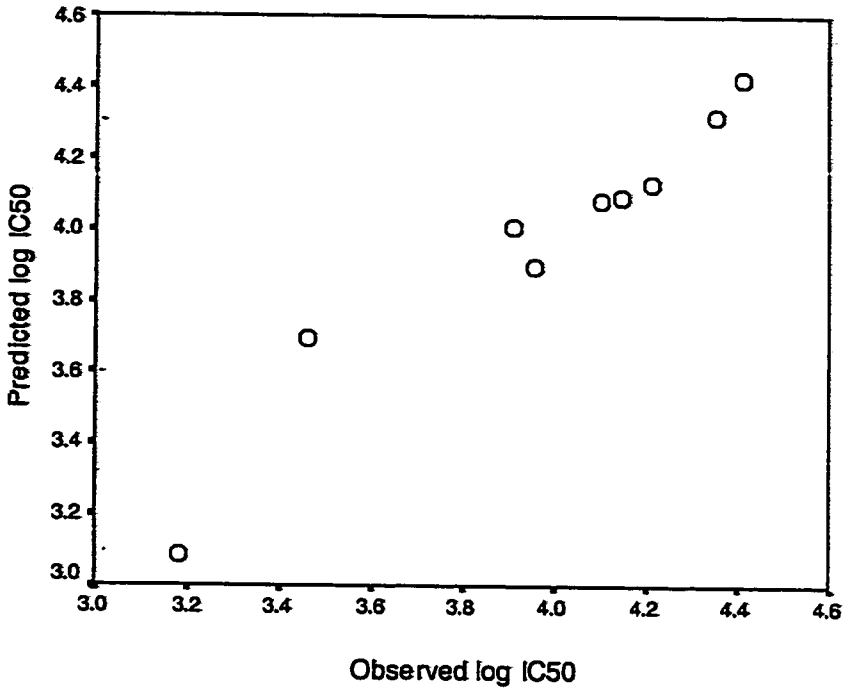

Figure 4.5 A plot of predicted log IC_{50} (μmol/L) versus observed log IC_{50} (μmol/L) using log P as descriptor for substituted alkanes except 1-chloropropane.

works (1986) showed that phenols can exhibit different toxic mechanisms which cannot be correlated with log P in simple model. Other parameters may have to be included with log P in developing QSAR equation. Phenols are generally more toxic than nonionic chemicals (benzenes and alkanes) and designated as polar narcotics. Tang and co-workers (1992) studied the toxicity of 43 phenols, benzenes and aliphatic chemicals to *Nitrobacter*. They found that the phenolic chemicals should be separated from other chemicals in QSAR development when log P and log S were used as descriptors. The overall equation accuracy was increased markedly after excluding all the phenolic chemicals in the correlation (Figure 4.6):

All chemicals except substituted phenols:

$$\log IC_{50} = 5.11 - 0.54 \log P \qquad (4.6)$$

$$n = 23,\ r^2 = 0.815,\ s = 0.2919,\ F = 92.715$$

For chemicals that have high values of log P, they may exhibit lower toxicity than expected since their aqueous solubility is low. Therefore, a second order term $(\log P)^2$ was added to log P to check whether there was improvement on the correlation. The correlation did not improve significantly when compared with correlating with log P alone. Schultz (1987) demonstrated that combination of log P and pK_a could be used to predict the toxicity of phenols. In our work, combined log P and pK_a as descriptors can correlate very well the IC_{50} values of substituted phenols excluding statistical outlier hydroquinone (Figure 4.7):

Substituted phenols except hydroquinone:

$$\log IC_{50} = 2.54 - 0.25 \log P + 0.14\ pK_a \qquad (4.7)$$

$$n = 11,\ r^2 = 0.855,\ s = 0.2270,\ F = 23.650$$

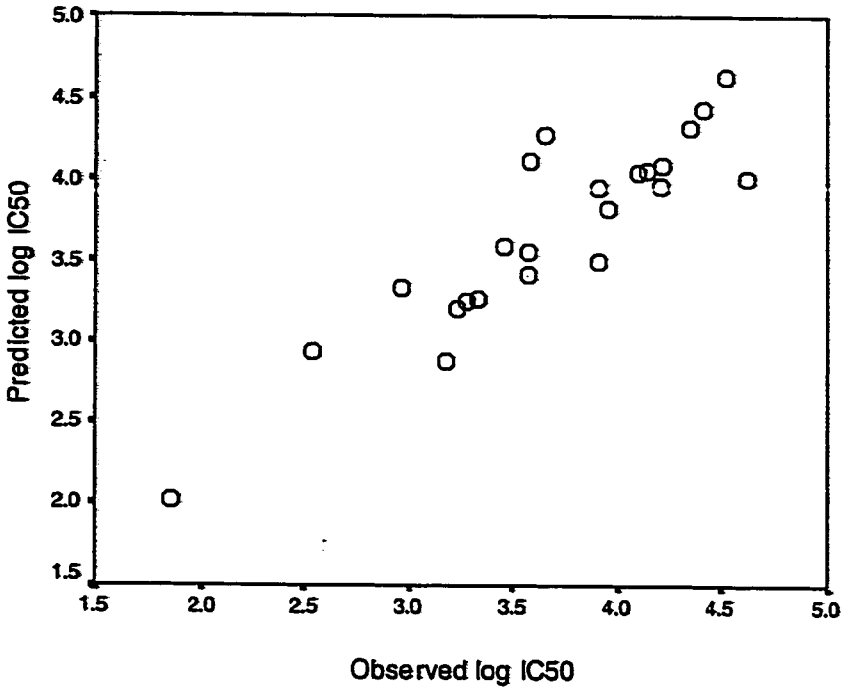

Figure 4.6 A plot of predicted log IC_{50} (μmol/L) versus observed log IC_{50} (μmol/L) using log P as descriptor for nonphenolic chemicals.

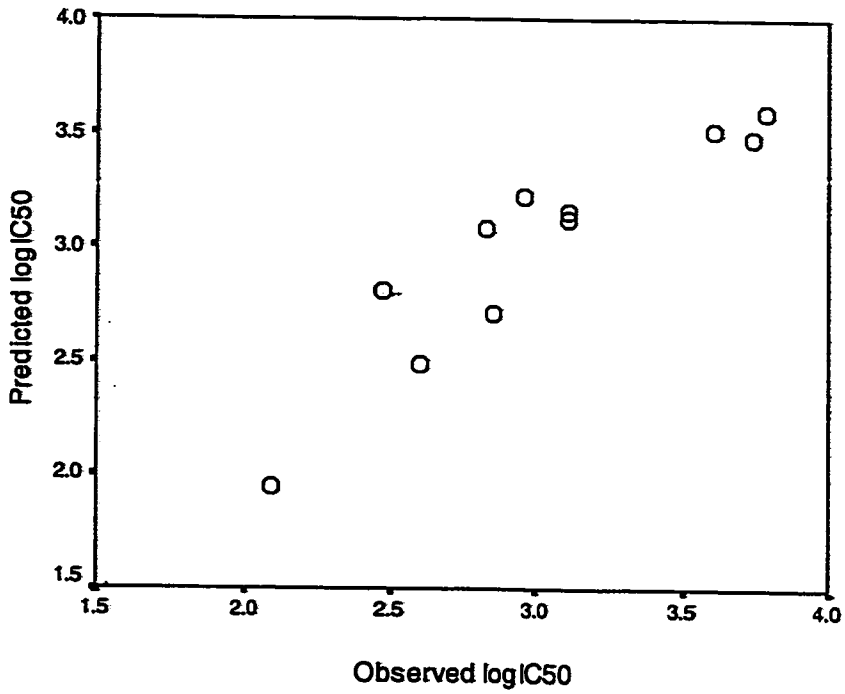

Figure 4.7 A plot of predicted log IC_{50} (μmol/L) versus observed log IC_{50} (μmol/L) using combination of log P and pK_a as descriptors for phenolic chemicals except hydroquinone.

4.3.2 Aqueous Solubility (log S)

The correlation results of using log S as descriptor are shown as follows:

Substituted alkanes:

$$\log IC_{50} = 2.49 + 0.37 \log S \quad (4.8)$$

$n = 10$, $r^2 = 0.758$, $s = 0.2281$, $F = 25.014$

Substituted benzenes:

$$\log IC_{50} = 2.24 + 0.37 \log S \quad (4.9)$$

$n = 13$, $r^2 = 0.845$, $s = 0.2834$, $F = 59.894$

Substituted phenols:

$$\log IC_{50} = 1.17 + 0.39 \log S \quad (4.10)$$

$n = 12$, $r^2 = 0.317$, $s = 0.4436$, $F = 4.639$

All chemicals:

$$\log IC_{50} = 2.45 + 0.25 \log S \quad (4.11)$$

$n = 35$, $r^2 = 0.258$, $s = 0.6038$, $F = 11.504$

The plots of predicted log IC_{50} versus observed log IC_{50} are shown in Figures 4.8-4.11. The toxicity of the chemicals decreased with log S. Fairly well QSAR equations were obtained for substituted alkanes ($r^2 = 0.758$) and benzenes ($r^2 = 0.845$). Elimination of statistical outlier 1-chloropropane yielded a better correlation equation for substituted alkanes (Figure 4.12).

Substituted alkanes except 1-chloropropane:

$$\log IC_{50} = 2.51 + 0.35 \log S \quad (4.12)$$

$n = 9$, $r^2 = 0.868$, $s = 0.1582$, $F = 46.209$

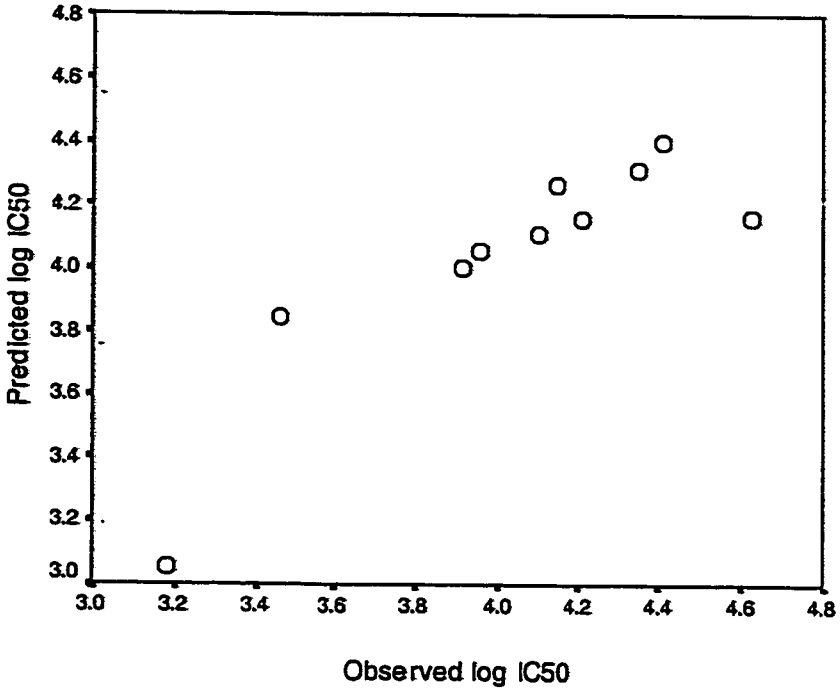

Figure 4.8 A plot of predicted log IC_{50} (μmol/L) versus observed log IC_{50} (μmol/L) using log S as descriptor for substituted alkanes.

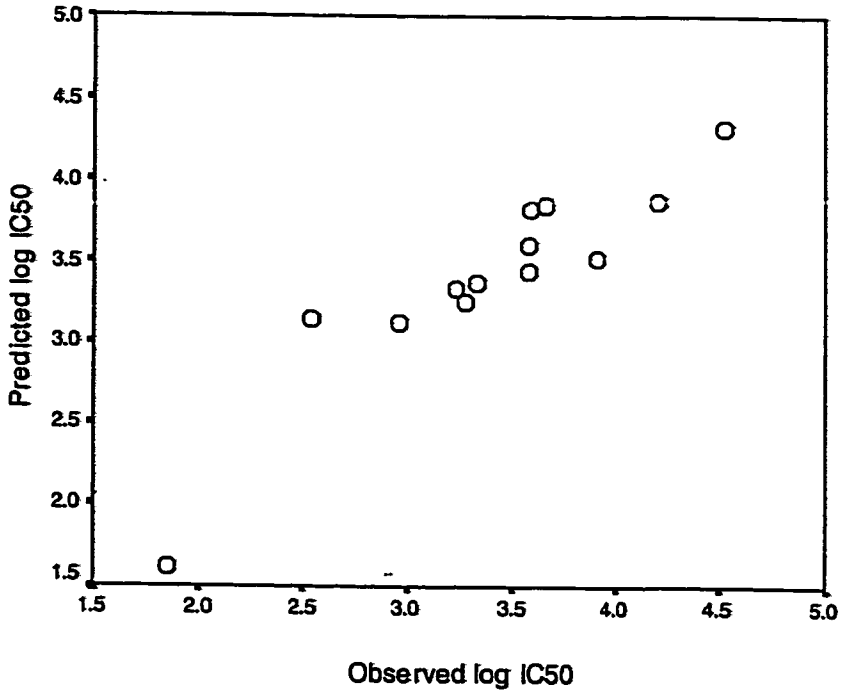

Figure 4.9 A plot of predicted log IC_{50} (μmol/L) versus observed log IC_{50} (μmol/L) using log S as descriptor for substituted benzenes.

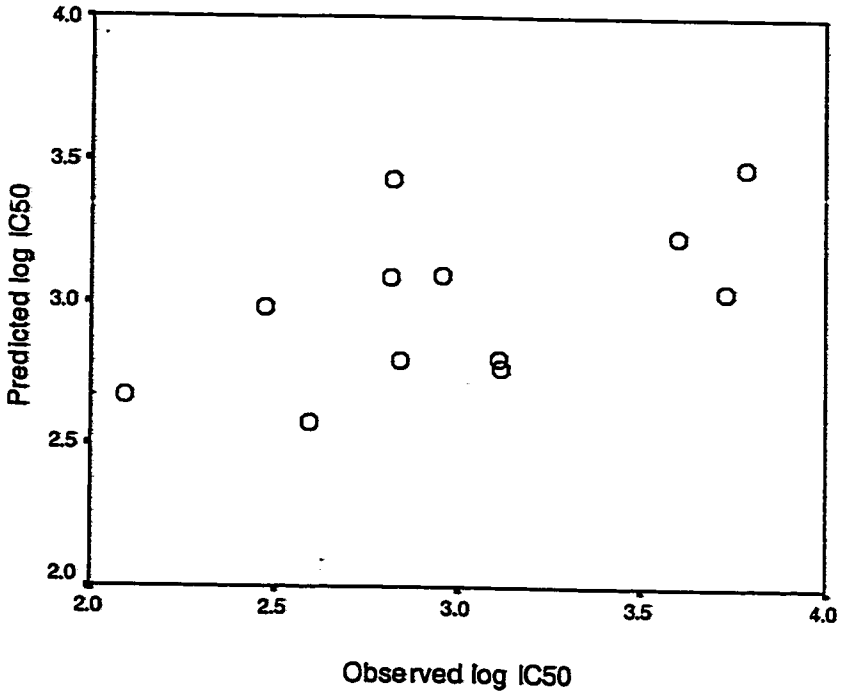

Figure 4.10 A plot of predicted log IC_{50} (μmol/L) versus observed log IC_{50} (μmol/L) using log S as descriptor for substituted phenols.

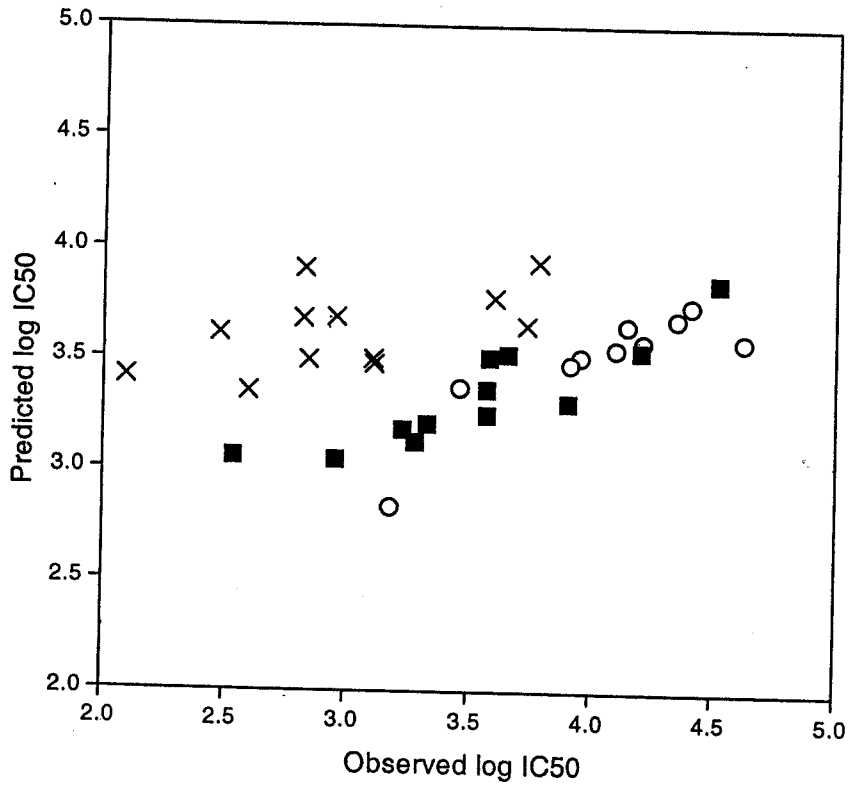

Figure 4.11 A plot of predicted log IC_{50} (μmol/L) versus observed log IC_{50} (μmol/L) using log S as descriptor for all chemicals: (○) alkanes, (■) benzenes and (×) phenols.

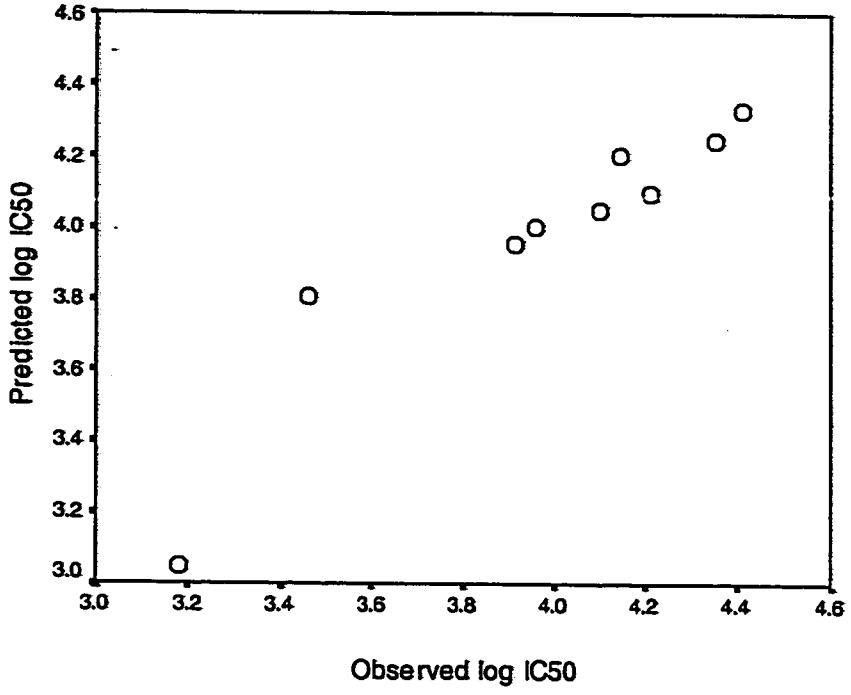

Figure 4.12 A plot of predicted log IC_{50} (μmol/L) versus observed log IC_{50} (μmol/L) using log S as descriptor for substituted alkanes except 1-chloropropane.

However, attempts to correlate the entire data set (r^2 = 0.258) and phenolic compounds (r^2=0.317) did not result in accurate equations. Strong correlation was observed between the aqueous solubility and nonphenolic chemicals (Figure 4.13).

All chemicals except substituted phenols:

$$\log IC_{50} = 2.24 + 0.4 \log S \qquad (4.13)$$

$n = 23, r^2 = 0.838, s = 0.2736, F = 108.466$

The use of log S as descriptor to predict toxicity was similar to that of log P. They constitute the measure of hydrophobicity which reflects the tendency of a toxicant to accumulate in the lipid phase of biomembranes. Our results show that they are suitable to describe the non-specific toxicity (narcosis) which is related directly to the quantity of toxicant acting on the cells and is not associated with specific mechanism. The choice of these two QSAR methods depends on the availability of the parameters for a given toxicant.

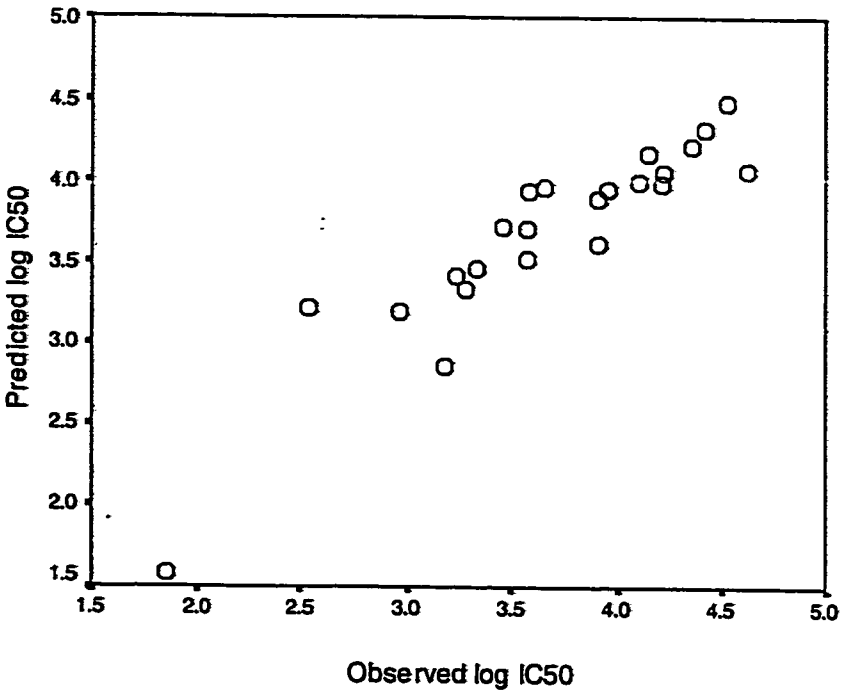

Figure 4.13 A plot of predicted log IC_{50} (μmol/L) versus observed log IC_{50} (μmol/L) using log S as descriptor for nonphenolic chemicals.

4.3.3 Molecular van der Waals Volume (molecular volume/V_i)

The linear solvation energy relationship (LSER) is a general approach to describe solvation and partitioning in different media. This approach contains four solvatochromic parameters: molecular van der Waals volume of solute molecule (V_i), polarity/polarizability (π^*), hydrogen bond donor acidity (α_m) and hydrogen bond donor basicity (β_m). Traditionally, the values of V_i are divided by 100 so that all the parameters have similar scales. $V_i/100$ can be computed theoretically based on molecular structure or determined experimentally. For this study, $V_i/100$ values were obtained from the values listed in the literatures (Blum and Speece, 1991b; Luehers et al, 1996). Among the four parameters, only consistent and reliable V_i values can be obtained in the literature. The other parameters are measured by different spectroscopic methods and are afflicted uncertainty and experimental errors. Therefore, only V_i was chosen as a descriptor in deriving QSAR equation. The correlation results are shown as follows:

Substituted alkanes:

$$\log IC_{50} = 5.47 - 2.79\ V_i/100 \qquad (4.14)$$

$n = 10,\ r^2 = 0.615,\ s = 0.2876,\ F = 12.754$

Substituted benzenes:

$$\log IC_{50} = 6.64 - 4.83\ V_i/100 \qquad (4.15)$$

$n = 13,\ r^2 = 0.849,\ s = 0.2796,\ F = 61.861$

Substituted phenols:

$$\log IC_{50} = 4.98 - 2.82\ V_i/100 \qquad (4.16)$$

$n = 12,\ r^2 = 0.438,\ s = 0.4024,\ F = 7.796$

All chemicals:

$$\log IC_{50} = 6.04 - 4.07\ V_i/100 \qquad (4.17)$$

$n = 35,\ r^2 = 0.734,\ s = 0.3618,\ F = 91.102$

The plots of predicted log IC_{50} versus observed log IC_{50} are shown in Figures 4.14-4.17. Chemical with larger molecular volume has lower aqueous solubility and hence toxicity increased, as suggested by the correlations. The correlation results are fair for alkanes ($r^2 = 0.615$) and good for benzenes ($r^2 = 0.849$). As with log P and log S methods, neither significant correlation was observed for phenolic chemicals ($r^2 = 0.438$). However, the use of molecular volume as descriptor for all 35 chemical is much better than that of log P and log S. The equation accuracy was improved slightly after eliminating all the phenolic chemicals from the entire data set (Figure 4.18).

All chemicals except substituted phenols:

$$\log IC_{50} = 6.11 - 4.04\ V_i/100 \qquad (4.18)$$

$n = 23,\ r^2 = 0.808,\ s = 0.298,\ F = 88.106$

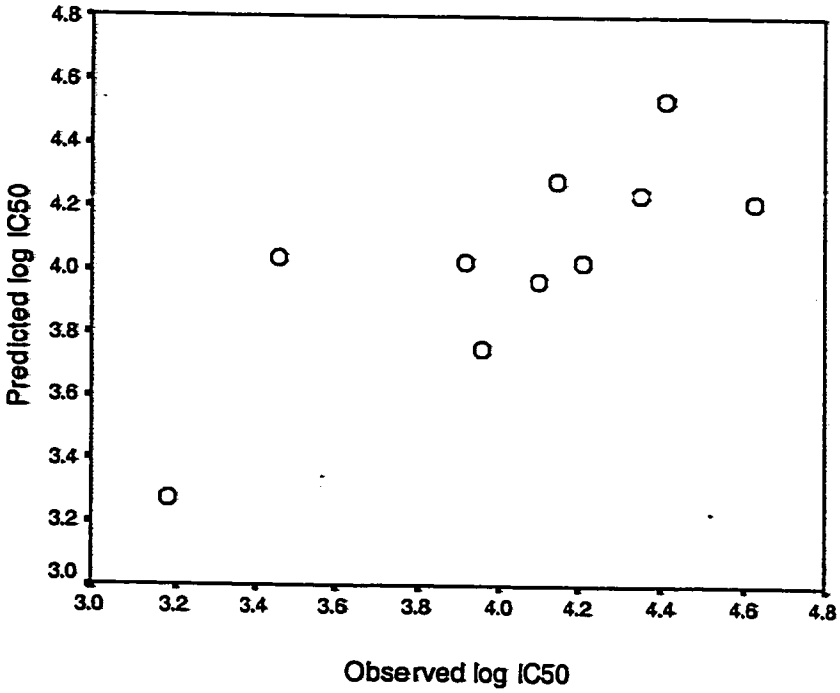

Figure 4.14 A plot of predicted log IC_{50} (μmol/L) versus observed log IC_{50} (μmol/L) using $V_i/100$ as descriptor for substituted alkanes.

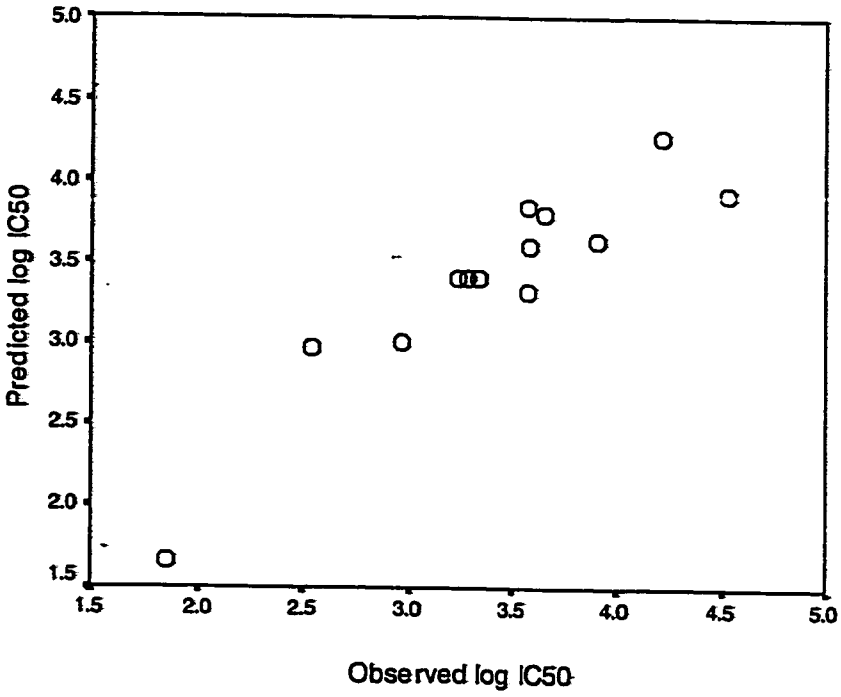

Figure 4.15 A plot of predicted log IC_{50} (μmol/L) versus observed log IC_{50} (μmol/L) using $V_i/100$ as descriptor for substituted benzenes.

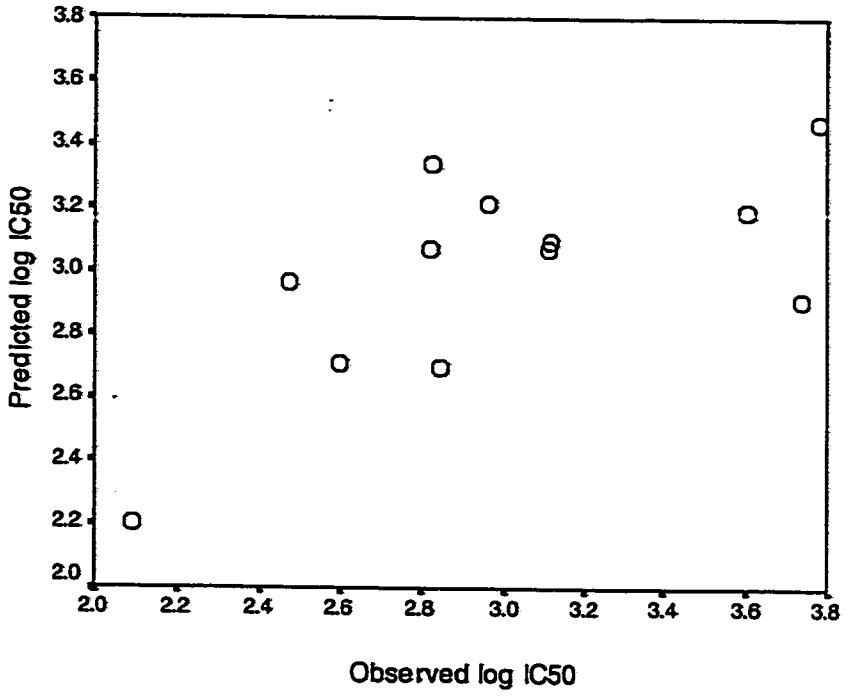

Figure 4.16 A plot of predicted log IC_{50} (μmol/L) versus observed log IC_{50} (μmol/L) using $V_i/100$ as descriptor for substituted phenols.

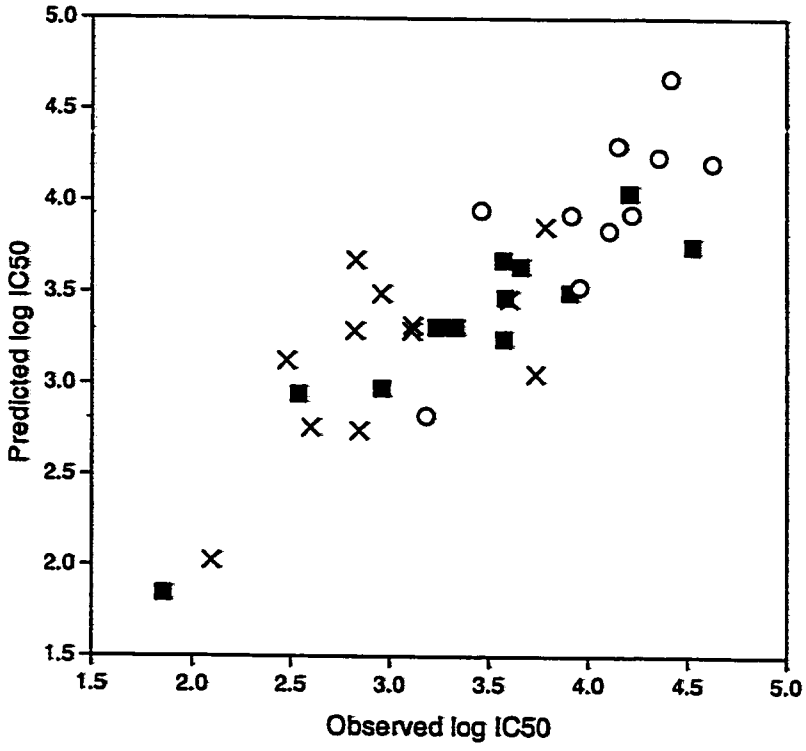

Figure 4.17 A plot of predicted log IC_{50} (μmol/L) versus observed log IC_{50} (μmol/L) using $V_i/100$ as descriptor for all chemicals: (O) alkanes, (■) benzenes and (×) phenols.

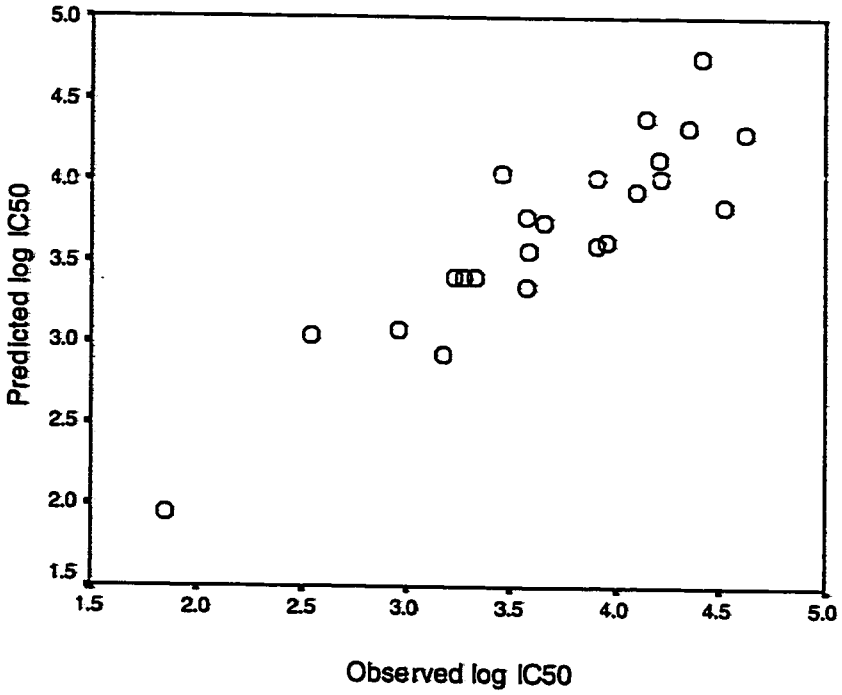

Figure 4.18 A plot of predicted log IC_{50} (μmol/L) versus observed log IC_{50} (μmol/L) using $V_i/100$ as descriptor for nonphenolic chemicals.

4.3.4 Molecular Connectivity Index (MCI)

The stepwise procedure provided by SPSS was used to select the best variable(s) among various simple, valence and difference of simple and valence indices (zero to third order). The SPSS software was also used to diagnose collinearity. A condition index (the square roots of the ratios of the largest eigenvalue) greater than 15 indicates the existence of collinearity problem. Highly correlated molecular indices were eliminated. The developed QSAR equations are shown as follows:

Substituted alkanes:

$$\log IC_{50} = 4.76 - 0.39\ {}^{2}X \qquad (4.19)$$

$n = 10,\ r^2 = 0.896,\ s = 0.1492,\ F = 69.081$

Substituted benzenes:

$$\log IC_{50} = 5.92 - 0.86\ {}^{1}X^{v} \qquad (4.20)$$

$n = 13,\ r^2 = 0.845,\ s = 0.2832,\ F = 59.988$

Substituted phenols:

$$\log IC_{50} = 4.42 - 0.25\ {}^{0}X^{v} \qquad (4.21)$$

$n = 12,\ r^2 = 0.489,\ s = 0.3839,\ F = 9.555$

All chemicals:

$$\log IC_{50} = 5.48 - 0.36\ {}^{2}X - 0.32\ {}^{1}X^{v} \qquad (4.22)$$

$n = 35,\ r^2 = 0.792,\ s = 0.3245,\ F = 61.064$

The plots of predicted log IC_{50} versus observed log IC_{50} are shown in Figures 4.19-4.22. The molecular connectivity index was a good parameter in correlating toxicity for substituted alkanes (eqn. 4.19) and substituted benzenes (eqn. 4.20) and all

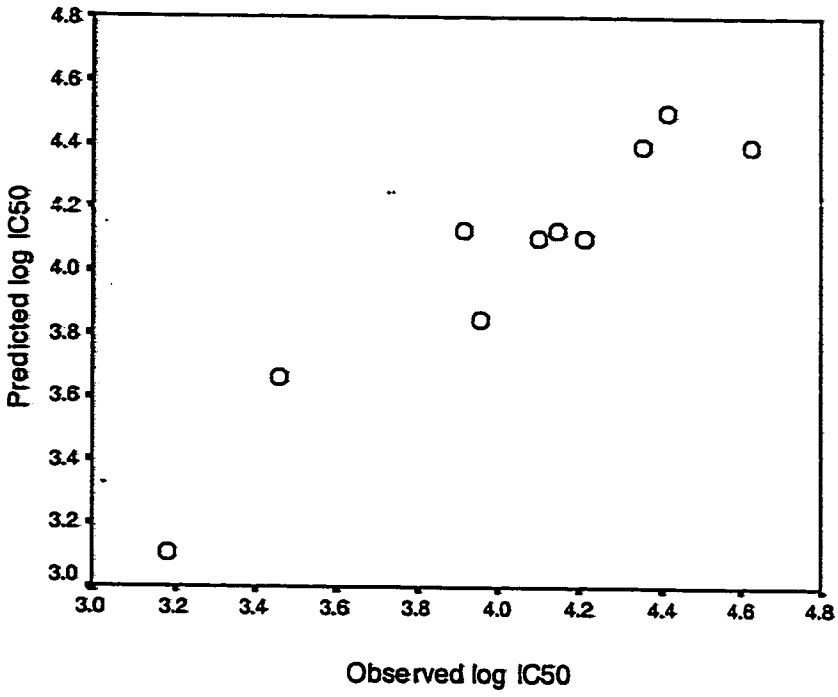

Figure 4.19 A plot of predicted log IC_{50} (μmol/L) versus observed log IC_{50} (μmol/L) using molecular connectivity index as descriptor for substituted alkanes.

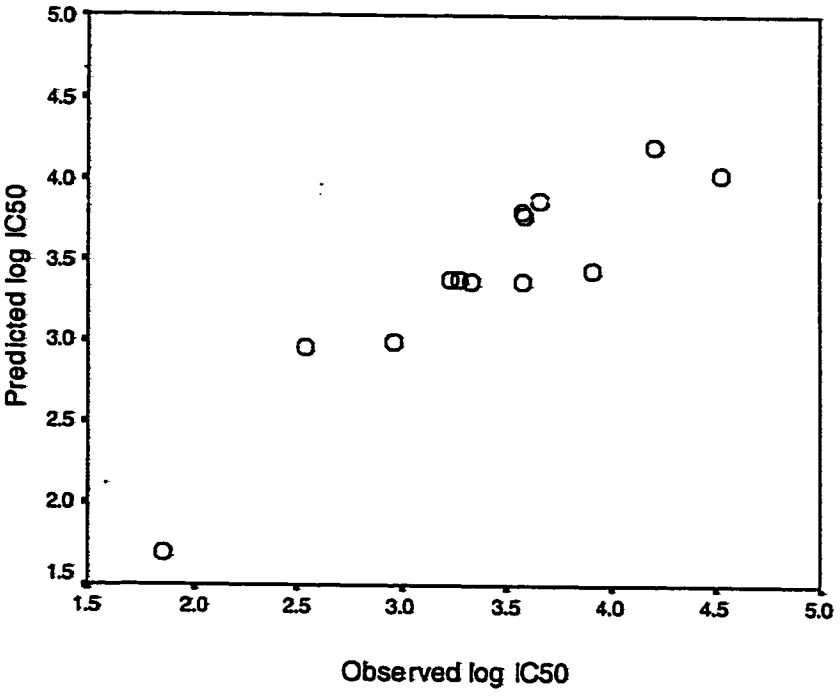

Figure 4.20 A plot of predicted log IC_{50} (μmol/L) versus observed log IC_{50} (μmol/L) using molecular connectivity index as descriptor for substituted benzenes.

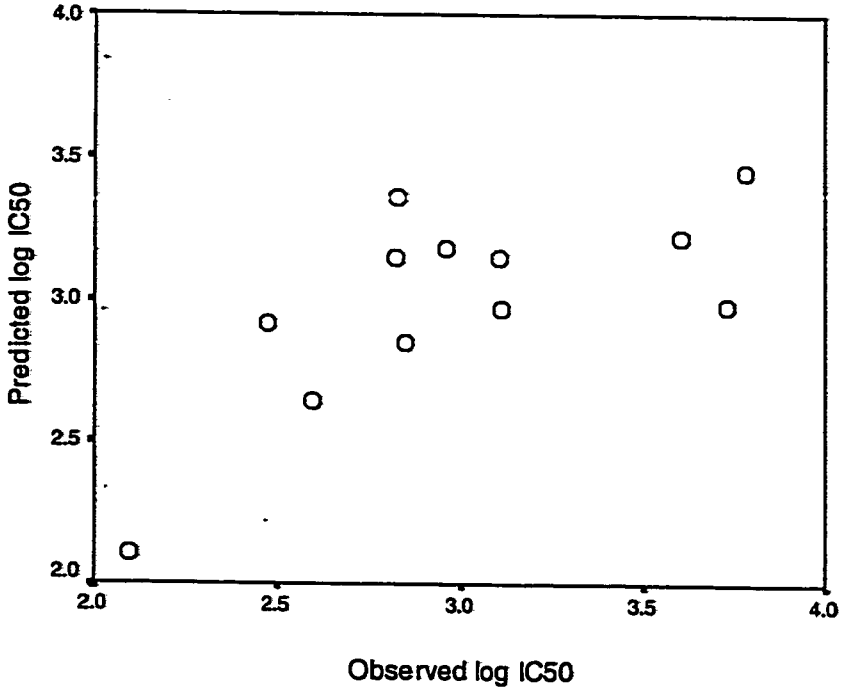

Figure 4.21 A plot of predicted log IC_{50} (μmol/L) versus observed log IC_{50} (μmol/L) using molecular connectivity index as descriptor for substituted phenols.

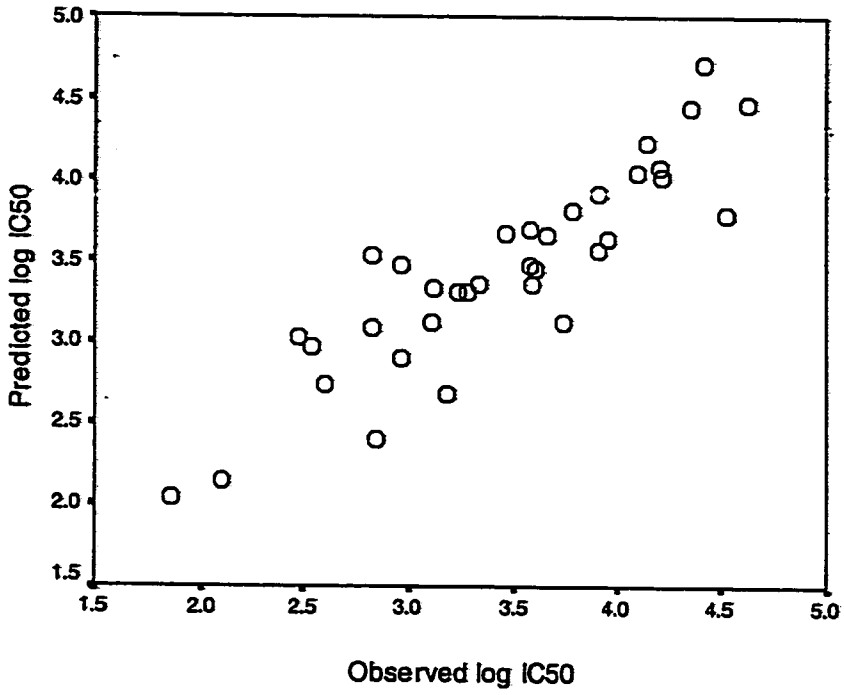

Figure 4.22 A plot of predicted log IC_{50} (μmol/L) versus observed log IC_{50} (μmol/L) using molecular connectivity index as descriptor for all chemicals.

three groups of toxicant together (eqn. 4.22). However, the correlation obtained for phenolic chemicals was insignificant (eqn. 4.21).

Much better correlation ($r^2 = 0.739$, $s = 0.2728$, $F = 22.605$) can be obtained by excluding the statistical outliers (hydroquinone and 2,4-dimethylphenol) from eqn. 4.21. Our results showed that chemical toxicity increased with connectivity index. It has been shown that the first and zero order indices encode information about the molecular volume of the compound (Kier and Hall, 1986). Compound with larger molecular volume has lower aqueous solubility and hence toxicity increases. The index used for various alkanes is ^2X which not only relates to molecular volume, but also skeletal branching of the compounds (Kier and Hall, 1986). This may be the reason why molecular index gives better accuracy than log P (eqn. 4.1), log S (eqn. 4.8) and $V_i/100$ (eqn. 4.14). Moreover, the MCI method (combination of ^2X and $^1X^v$) is superior to other methods for describing the toxicity of all 35 chemicals. Elimination of phenolic chemicals from the regression did not improve the r^2 of the equation (Figure 4.23).

<u>All chemicals except substituted phenols</u>:

$$\log IC_{50} = 5.69 - 0.38\ {}^0X \qquad (4.23)$$

$n = 23$, $r^2 = 0.791$, $s = 0.3107$, $F = 79.377$

Although it is difficult to assign the actual physical meaning of the molecular connectivity index, the use of the QSAR equations for predicting chemical toxicity is very straightforward. The indices can all be calculated quickly and accurately from the chemical structure.

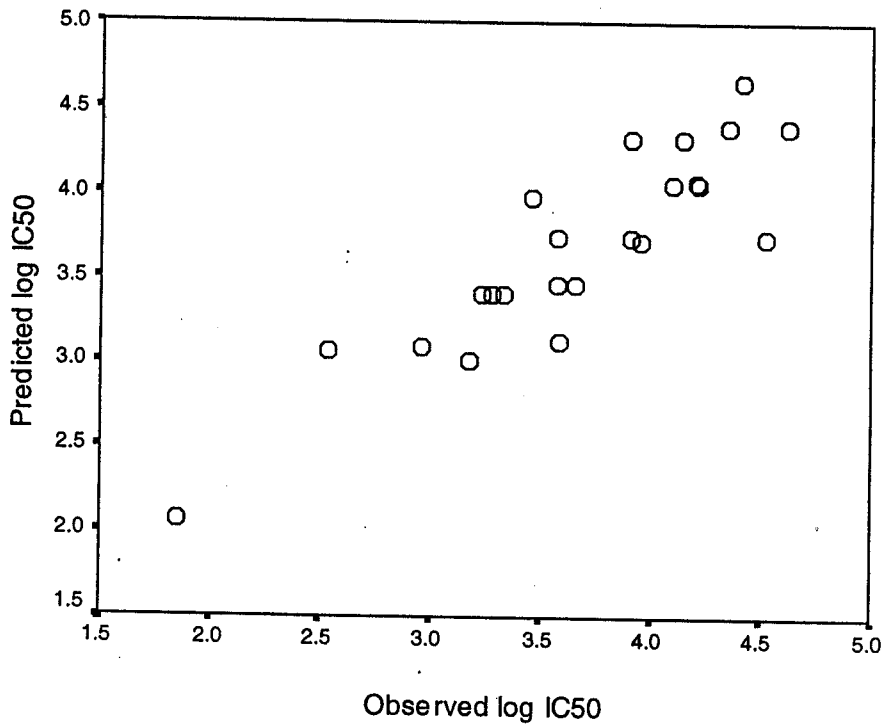

Figure 4.23 A plot of predicted log IC_{50} (μmol/L) versus observed log IC_{50} (μmol/L) using molecular connectivity index as descriptor for nonphenolic chemicals.

4.3.5 Combination of log P and ELUMO

It is clear from the correlation results described in sections 4.3.1 to 4.3.4 that log P, log S, V_i or MCI alone is not sufficient to model the toxicity of phenolic compounds to activated sludge. A suitable methodology is to combine molecular descriptors, e.g. log P, with electric, steric or MCI to simulate significantly the toxicity of the complete chemical set, especially phenolic compounds. The following section reports such an effort of using a combination of hydrophobicity descriptor (log P) and electronic properties (ELUMO) for simulating the toxicity of substituted alkanes, benzenes and phenols. The correlation results of using log P and ELUMO as descriptors are shown as follows:

Substituted alkanes:

$$\log IC_{50} = 4.70 - 0.31 \log P + 0.24 \, ELUMO \qquad (4.24)$$

$n = 10, r^2 = 0.925, s = 0.136, F = 42.92$

Substituted benzenes:

$$\log IC_{50} = 4.69 - 0.41 \log P + 0.49 \, ELUMO \qquad (4.25)$$

$n = 13, r^2 = 0.922, s = 0.2101, F = 59.485$

Substituted phenols:

$$\log IC_{50} = 3.64 - 0.22 \log P + 0.30 \, ELUMO \qquad (4.26)$$

$n = 12, r^2 = 0.582, s = 0.366, F = 6.253$

All chemicals:

$$\log IC_{50} = 4.26 - 0.29 \log P + 0.46 \, ELUMO \qquad (4.27)$$

$n = 35, r^2 = 0.628, s = 0.4346, F = 26.96$

The plots of predicted log IC_{50} against observed log IC_{50} are shown in Figures 4.24-4.27. Figure 4.26 and the calculated residual value show that hydroquinone was a strong statistical outlier among the other phenolic compounds. The accuracy of the model was significantly improved after the elimination of hydroquinone (Figure 4.28).

Substituted phenols except hydroquinone:

$$\log IC_{50} = 4.02 - 0.34 \log P + 0.37 \text{ ELUMO} \qquad (4.28)$$

$n = 11, r^2 = 0.860, s = 0.223, F = 24.647$

Hydroquinone was more toxic than predicted by this method. Better correlation result was also obtained for all chemicals in the absence of hydroquinone (Figure 4.29).

All chemicals except hydroquinone:

$$\log IC_{50} = 4.49 - 0.36 \log P + 0.45 \text{ ELUMO} \qquad (4.29)$$

$n = 34, r^2 = 0.752, s = 0.3556, F = 47.118$

Hydroquinone can be converted to quinone by peroxidase enzyme or oxygen inside a cell (Bolton et al, 2000). Quinone can cause cellular damage through binding to cellular proteins or DNA. Also, quinone is a highly redox-active molecule leading to formation of reactive oxygen species which can oxidize cellular macromolecules. These may explain why hydroquinone was more toxic than predicted.

Once again, equation accuracy was improved after exclusion of phenolic chemicals from the regression (Figure 4.30):

All chemicals except substituted phenols:

$$\log IC_{50} = 4.88 - 0.45 \log P + 0.29 \text{ ELUMO} \qquad (4.30)$$

$n = 23, r^2 = 0.883, s = 0.2382, F = 75.418$

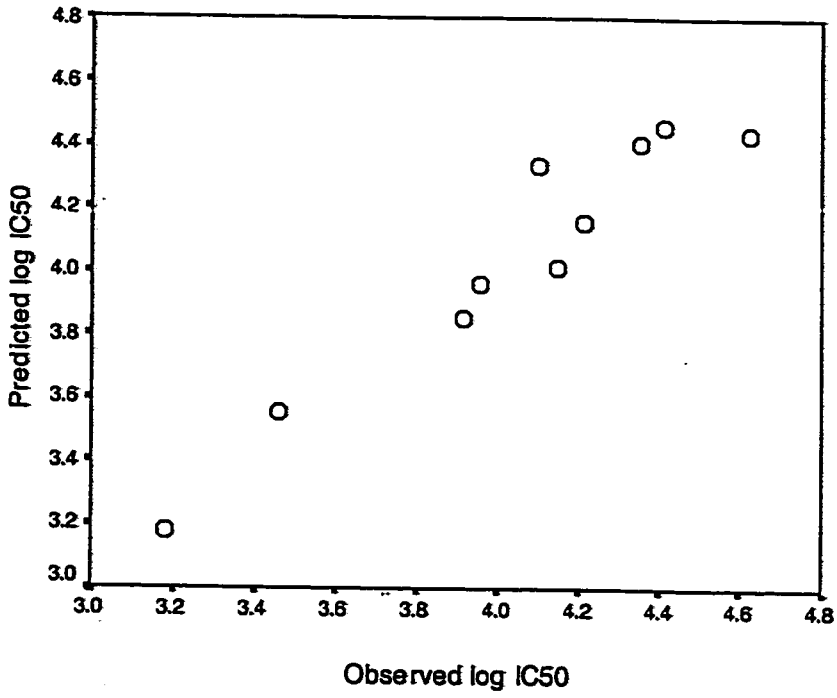

Figure 4.24 A plot of predicted log IC_{50} (μmol/L) versus observed log IC_{50} (μmol/L) using log P and ELUMO together as descriptors for substituted alkanes.

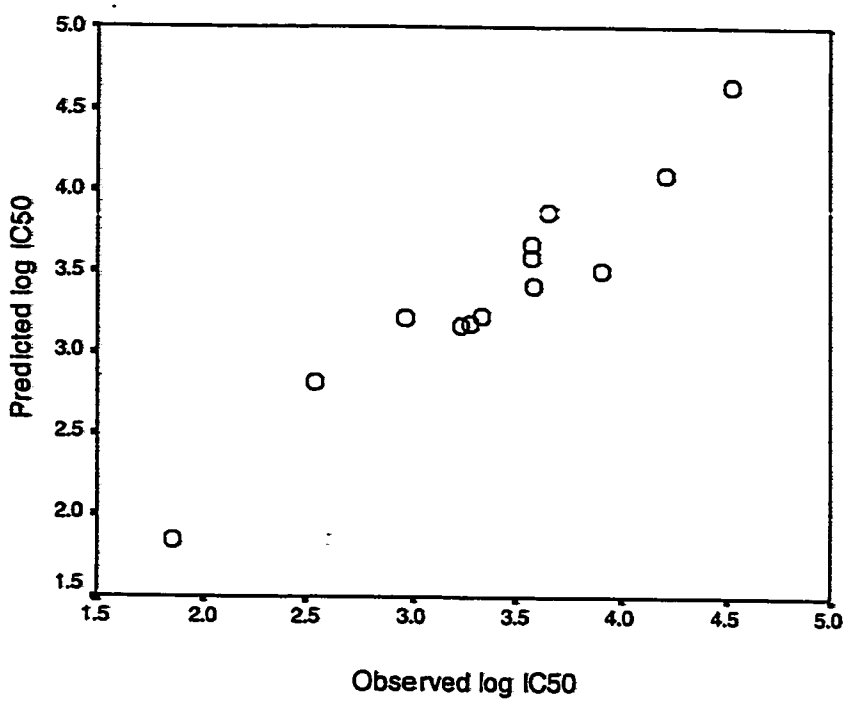

Figure 4.25 A plot of predicted log IC_{50} (μmol/L) versus observed log IC_{50} (μmol/L) using log P and ELUMO together as descriptors for substituted benzenes.

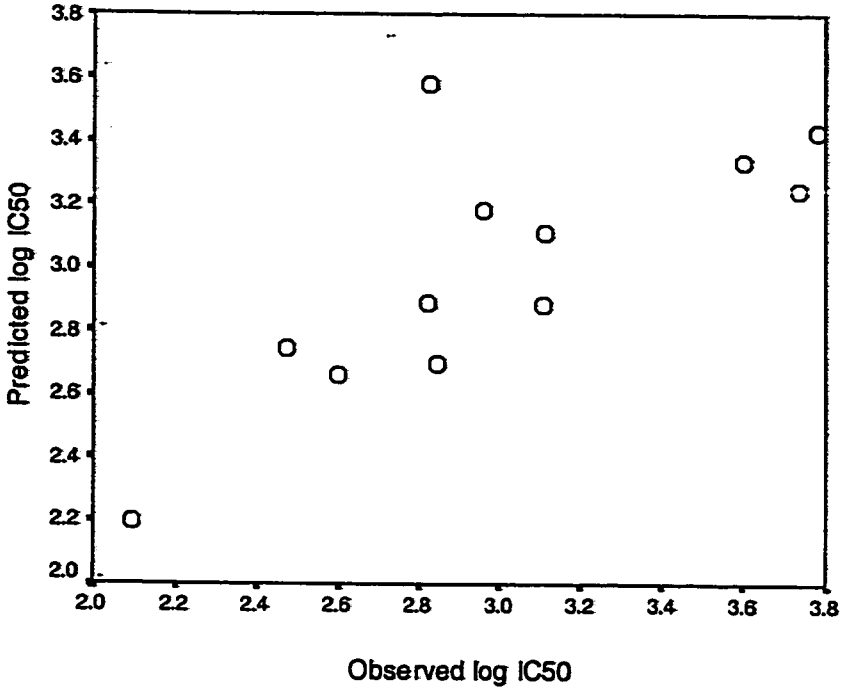

Figure 4.26 A plot of predicted log IC_{50} (μmol/L) versus observed log IC_{50} (μmol/L) using log P and ELUMO together as descriptors for substituted phenols.

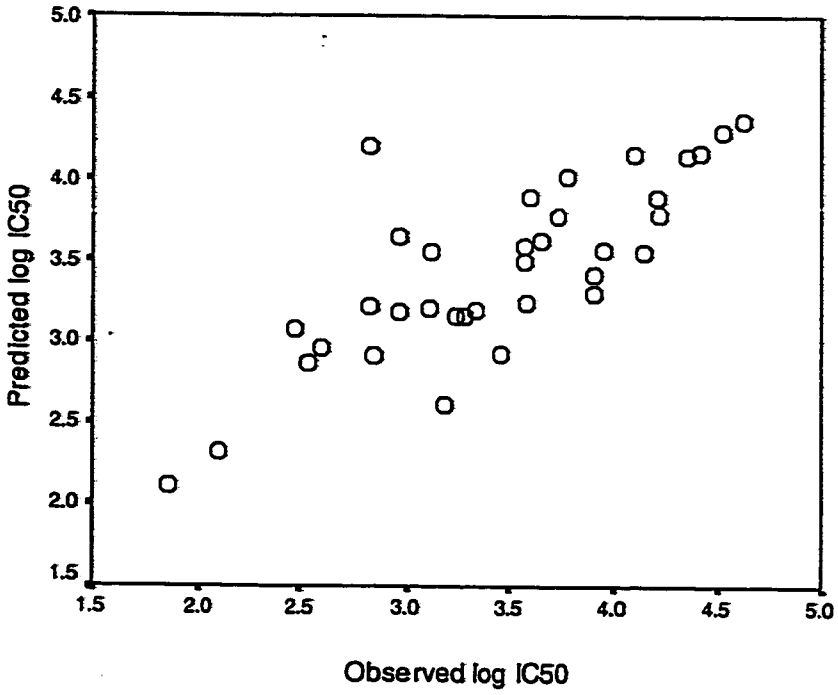

Figure 4.27 A plot of predicted log IC_{50} (μmol/L) versus observed log IC_{50} (μmol/L) using log P and ELUMO together as descriptors for all chemicals.

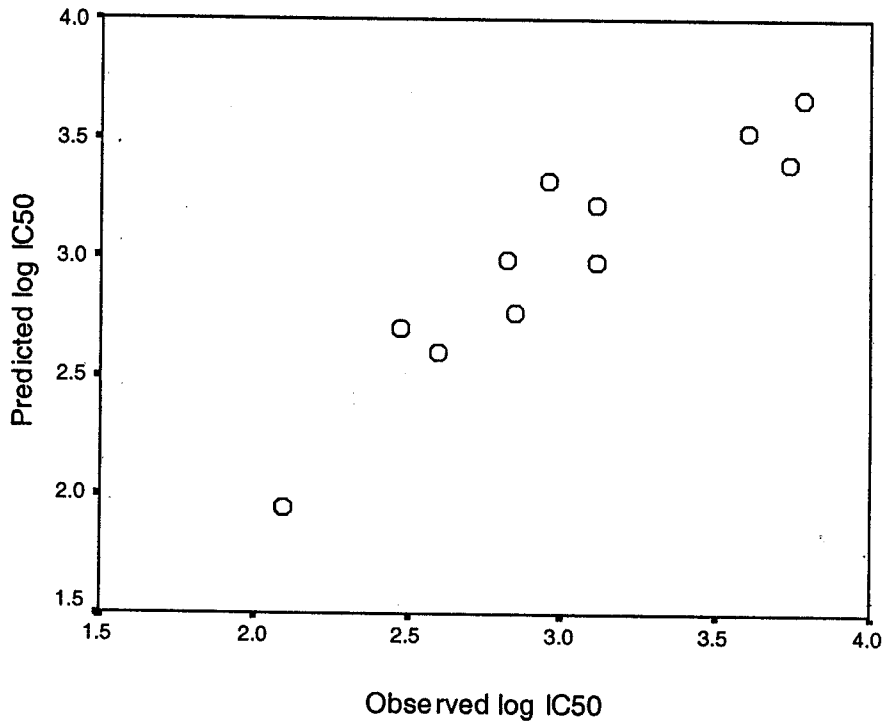

Figure 4.28 A plot of predicted log IC_{50} (μmol/L) versus observed log IC_{50} (μmol/L) using log P and ELUMO together as descriptors for all phenolic chemicals except hydroquinone.

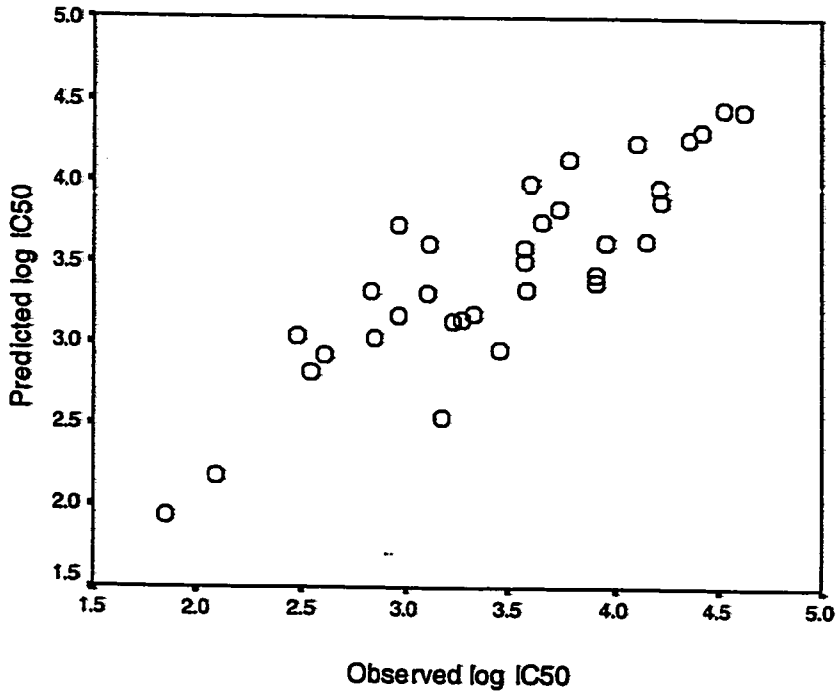

Figure 4.29 A plot of predicted log IC_{50} (μmol/L) versus observed log IC_{50} (μmol/L) using log P and ELUMO together as descriptors for all chemicals except hydroquinone.

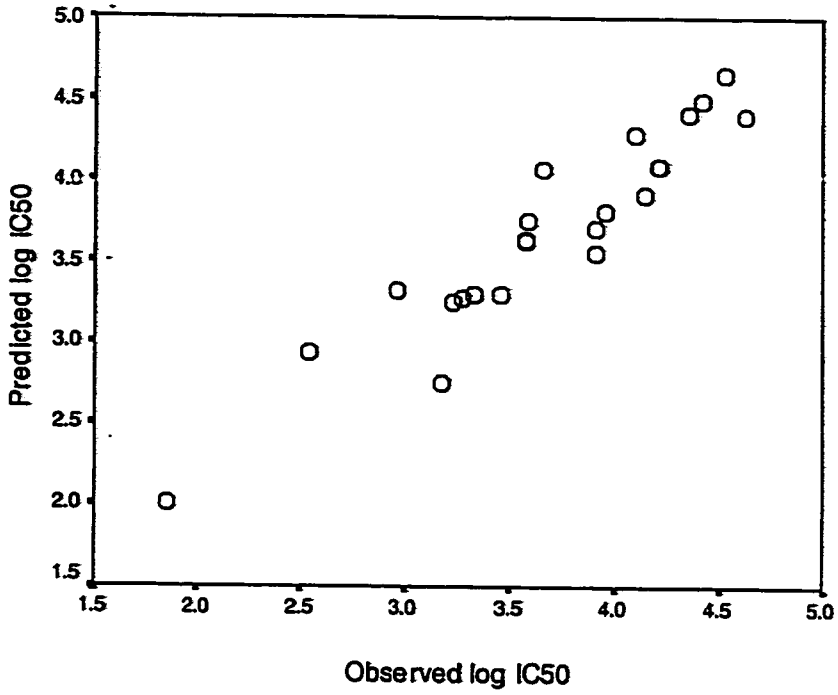

Figure 4.30 A plot of predicted log IC_{50} (μmol/L) versus observed log IC_{50} (μmol/L) using log P and ELUMO together as descriptors for nonphenolic chemicals.

Non-specific toxicity (narcosis) is often defined in QSAR by the correlation with log P. This type of toxicity is considered as baseline narcosis toxicity. The mechanism is based on the transport of the compound from the solution to the site of action of the organism. This involves the accumulation of the compound in the lipid phase of biomembranes, or the binding to the hydrophobic portion of the membrane protein. This diffusion is often simulated by hydrophobicity descriptors, e.g., log P or by models relating to solvation interactions and partitioning in different media, e.g., LSER.

Our simulation results showed that the hydrophobicity descriptors could model the toxicity of substituted alkanes and benzenes reasonably well since most of these compounds exhibited non-specific toxicity. However, the use of these descriptors for simulating the toxicity of substituted phenols was not very successful. The toxicity of most phenolic compounds was actually under-estimated by these descriptors. The combination of log P and ELUMO can simulate the toxicity of phenols excluding hydroquinone much better than the other descriptors. The ELUMO is commonly used to describe the tendency of toxicants to undergo interaction (electro(nucleo)philicity) with cellular biomolecules. Chemicals with low ELUMO are more reactive and hence higher toxicity. The phenols in our data set, in particular the halogenated substituted phenols, do not appear to fit with the general narcosis behavior. One important mode of toxic action is the uncoupling of oxidative phosphorylation. Some organic acids are known to increase proton transfer across membranes and thus to destroy the proton gradient across the cellular membranes, where oxidative phosphorylation is taking place. Ravanel et al (1989) showed that all 13 chlorophenols in their test set exhibited this type of toxicity. 2,4-Dinitrophenol and pentachlorophenol are reported to induce

uncoupling of oxidative phosphorylation (Sixt et al, 1995). Some of the other halogenated phenols in our data set may also exhibit respiratory uncoupling. The combination of log P and ELUMO appeared to model well the toxicity of phenolic compounds to activated sludge, which may exhibit a combination of non-specific toxicity and respiratory uncoupling.

A total of 16 physicochemical descriptors were used to correlate the toxicity of all three classes of chemicals. A full list of these descriptors is presented in Table 4.4. The results of stepwise regression analysis revealed that the following correlation could explain 80% of the variance:

$$\log IC_{50} = 5.18 - 0.17 \log P - 0.41\ {}^{2}X \qquad (4.31)$$

$$n = 35,\ r^2 = 0.802,\ s = 0.3171,\ F = 64.702$$

A plot of log IC_{50} values predicted from the above equation against observed log IC_{50} values is shown in Figure 4.31. The condition index of the correlation was 6.96. An index value less than 15 shows that the intercorrelation between descriptors log P and ${}^{2}X$ is low. The results of regression analysis when using log P, ELUMO, ${}^{2}X$ and ${}^{1}X^{v}$ as descriptors are summarized in Table 4.5. The relative contribution of each of the four descriptors was determined by multiplying the coefficient of each descriptor value for each chemical. The percent contribution to the toxicity was calculated as a percent of the total contribution. The average of the percent contribution is as follows: ${}^{2}X$ (37.14%); log P (10.61%); ${}^{1}X^{v}$ (8.58%) and ELUMO (1.06%). Results listed in Table 4.5 and the average percent contribution indicate that addition of ${}^{1}X^{v}$ and ELUMO to equation 4.31 did not improve the correlation significantly.

Table 4.4 The 16 physicochemical descriptors used in the analysis.

Descriptors			
Log P	Log S	V_i	ELUMO
^{0}X	$^{0}X^{v}$	^{1}X	$^{1}X^{v}$
^{2}X	$^{2}X^{v}$	^{3}X	$^{3}X^{v}$
$^{0}X - {}^{0}X^{v}$	$^{1}X - {}^{1}X^{v}$	$^{2}X - {}^{2}X^{v}$	$^{3}X - {}^{3}X^{v}$

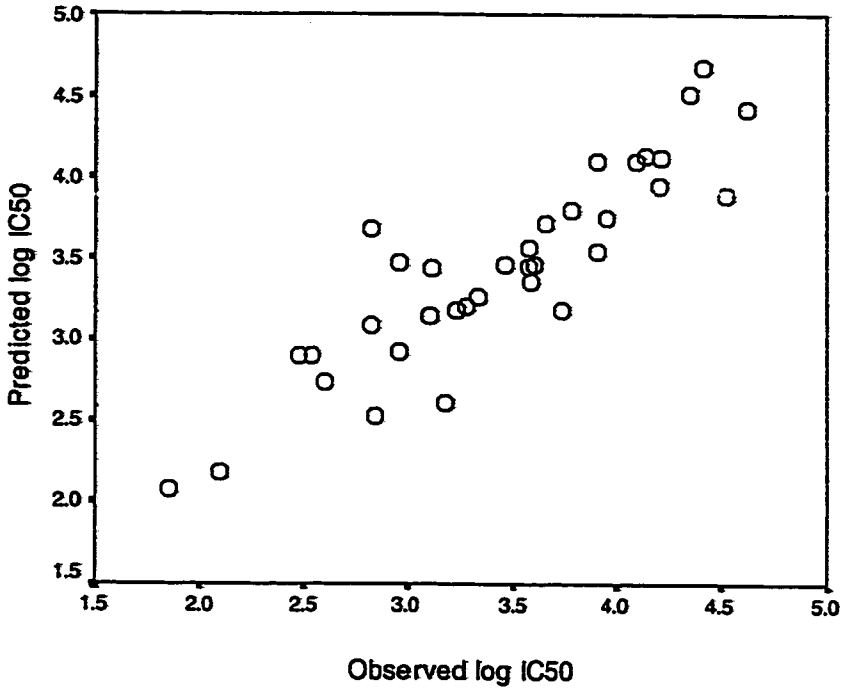

Figure 4.31 A plot of predicted log IC_{50} (μmol/L) versus observed log IC_{50} (μmol/L) using log $\bar{P}$ and ^{2}X together as descriptors for all chemicals.

Table 4.5 A summary of regression analysis for the toxicity of all three classes of chemicals when using $^{1}X^{v}$, ^{2}X, log P and ELUMO as descriptors.

Descriptors			Coefficients of regression descriptors				
	r^2	s	^{2}X	log P	$^{1}X^{v}$	ELUMO	Intercept
^{2}X	0.748	0.3518	-0.50	/	/	/	5.02
^{2}X + log P	0.802	0.3171	-0.42	-0.17	/	/	5.18
^{2}X + log P + $^{1}X^{v}$	0.803	0.3212	-0.40	-0.13	-0.10	/	5.28
^{2}X + log P + $^{1}X^{v}$ + ELUMO	0.805	0.3250	-0.37	-0.13	-0.10	0.06	5.21
^{2}X + $^{1}X^{v}$	0.792	0.3245	-0.36	/	-0.32	/	5.48
^{2}X + ELUMO	0.749	0.3566	-0.48	/	/	0.04	4.97
log P + ELUMO	0.628	0.4346	/	-0.29	/	0.46	4.26
log P + $^{1}X^{v}$	0.626	0.4355	/	0.06	-0.88	/	5.74
$^{1}X^{v}$ + ELUMO	0.702	0.3886	/	/	-0.62	0.31	5.23
^{2}X + log P + ELUMO	0.803	0.3208	-0.39	-0.17	/	0.06	5.11
^{2}X + $^{1}X^{v}$ + ELUMO	0.794	0.3281	-0.33	/	-0.33	0.06	5.41
$^{1}X^{v}$ + log P + ELUMO	0.702	0.3948	/	-0.01	-0.61	0.31	5.21

r^2 is the coefficient of determination of the model

s is the root mean square error of the model

4.3.6 Model Validation

Statistical validation studies should be carried out to ensure that the models are not specific to the data set on which they were developed. Based on the correlation results for different approaches, statistical validations were performed on QSAR equations derived for nonphenolic chemicals (eqn. 4.6 & 4.13), substituted phenols (eqn. 4.28) and all chemicals combined (eqn. 4.17, 4.22 & 4.29). The validation equations were generated after randomly removing 20% of the data points and the results are summarized in Table 4.6. It shows that the parameters of the validation equations are similar to those of the original equations for each method. The correlation coefficient (r^2) and root mean square error (s) are comparable to original equations. Table 4.7 shows that all the predicted values from the validation equation fell within 95% confidence interval of the original equations. Hence, random groups of data could be excluded without changing the QSAR equations or their accuracy for predicting the excluded points.

Table 4.6 Validation equations for different methods.

Original equation	Validation equation	n	s	r^2	F
$\log IC_{50} = 5.11 - 0.54 \log P$ (eqn. 4.6)		23	0.2919	0.815	92.715
(Substituted alkanes and benzenes)	$\log IC_{50} = 5.12 - 0.54 \log P$ (eqn. A)	19	0.2555	0.871	114.921
	$\log IC_{50} = 5.08 - 0.53 \log P$ (eqn. B)	19	0.3086	0.817	76.110
$\log IC_{50} = 2.24 + 0.4 \log S$ (eqn. 4.13)		23	0.2736	0.838	108.466
(Substituted alkanes and benzenes)	$\log IC_{50} = 2.25 + 0.39 \log S$ (eqn. C)	19	0.2872	0.838	87.743
	$\log IC_{50} = 2.17 + 0.41 \log S$ (eqn. D)	19	0.2911	0.833	85.081
$\log IC_{50} = 4.02 - 0.34 \log P + 0.37$ ELUMO (eqn. 4.28)		11	0.2230	0.860	24.647
(Substituted phenols)	$\log IC_{50} = 3.95 - 0.30 \log P + 0.40$ ELUMO (eqn. E)	9	0.2288	0.876	21.179
	$\text{Log } IC_{50} = 3.88 - 0.32 \log P + 0.27$ ELUMO (eqn. F)	9	0.1891	0.88	22.030
$\log IC_{50} = 6.04 - 4.07\ V_i/100$ (eqn. 4.17)		35	0.3618	0.734	91.102
(All chemicals)	$\log IC_{50} = 5.92 - 3.98\ V_i/100$ (eqn. G)	29	0.3475	0.721	69.851
	$\log IC_{50} = 6.25 - 4.35\ V_i/100$ (eqn. H)	29	0.3412	0.766	88.535
$\log IC_{50} = 5.48 - 0.36\ {}^2X - 0.32\ {}^1X^v$ (eqn. 4.22)		35	0.3245	0.792	61.064
(All chemicals)	$\log IC_{50} = 5.49 - 0.39\ {}^2X - 0.32\ {}^1X^v$ (eqn. I)	28	0.3211	0.759	48.353
	$\log IC_{50} = 5.48 - 0.36\ {}^2X - 0.32\ {}^1X^v$ (eqn. J)	28	0.3620	0.776	43.376
$\log IC_{50} = 4.49 - 0.36 \log P + 0.45$ ELUMO (eqn. 4.29)		34	0.3556	0.752	47.118
(All chemicals)	$\log IC_{50} = 4.54 - 0.38 \log P + 0.43$ ELUMO (eqn. K)	27	0.3860	0.727	31.974
	$\log IC_{50} = 4.50 - 0.38 \log P + 0.48$ ELUMO (eqn. L)	27	0.3064	0.830	58.620

Table 4.7 Validation results of QSAR equations.

Method	Removed toxicant	Lower 95% confidence interval of original eqn.	Upper 95% confidence interval of original eqn.	Predicted value from new eqn.	Within confidence interval
Log P (eqn. 4.6)		Validation equation (A)			
	Tetrachloromethane	3.45	3.71	3.57	Yes
	1-Chloropropane	3.86	4.15	4.01	Yes
	Nitrobenzene	3.95	4.27	4.11	Yes
	1,2-Dichlorobenzene	3.10	3.41	3.25	Yes
		Validation equation (B)			
	Chloroform	3.90	4.20	4.04	Yes
	1,1,2,2-Tetrachloromethae	3.69	3.95	3.82	Yes
	Naphthalene	3.18	3.48	3.34	Yes
	Chlorobenzene	3.42	3.68	3.56	Yes
Log S (eqn. 4.13)		Validation equation (C)			
	1,2-Dichloroethane	4.06	4.38	4.20	Yes
	1,2-Dichloropropane	3.86	4.13	3.98	Yes
	Benzene	3.85	4.12	3.97	Yes
	Benzonitrile	3.83	4.09	3.94	Yes
		Validation equation (D)			
	Hexachloroethane	2.65	3.06	2.80	Yes
	Chlorodibromomethane	3.76	4.01	3.87	Yes
	Ethylbenzene	3.40	3.64	3.49	Yes
	Aniline	4.28	4.68	4.48	Yes
Log P and ELUMO (eqn. 4.28)		Validation equation (E)			
	3,5-Dichlorophenol	2.48	2.93	2.75	Yes
	2-Nitrophenol	2.73	3.24	2.94	Yes
		Validation equation (F)			
	p-Cresol	3.28	3.77	3.39	Yes
	2,4-Dimethylphenol	3.16	3.63	3.24	Yes
V_i/100 (eqn. 4.17)		Validation equation (G)			
	Hexachloroethane	2.64	3.01	2.77	Yes
	1-Chloropropane	4.00	4.41	4.13	Yes
	Pentachlorophenol	1.70	2.35	1.99	Yes
	p-Cresol	3.34	3.58	3.40	Yes
	Nitrobenzene	3.35	3.60	3.41	Yes
	Aniline	3.61	3.89	3.68	Yes

Table 4.7 (cont'd) Validation results of QSAR equations.

Method	Removed toxicant	Lower 95% confidence interval of original eqn.	Upper 95% confidence interval of original eqn.	Predicted value from new eqn.	Within confidence interval
$V_i/100$ (eqn. 4.17)		Validation equation (H)			
	Dichloromethane	4.38	4.96	4.78	Yes
	Chloroform	4.08	4.52	4.39	Yes
	Hydroquinone	3.54	3.81	3.72	Yes
	2,4,6-Trichlorophenol	2.57	2.95	2.74	Yes
	Ethylbenzene	3.11	3.38	3.26	Yes
	Bromobenzene	3.38	3.63	3.53	Yes
MCI (eqn. 4.22)		Validation equation (I)			
	Chlorodibromomethane	3.66	4.17	3.90	Yes
	Hexachloroethane	2.49	2.86	2.60	Yes
	1-Chloropropane	4.23	4.71	4.47	Yes
	Pentachlorophenol	1.84	2.47	2.06	Yes
	2,4-Dimethylphenol	2.99	3.26	3.06	Yes
	Nitrobenzene	3.18	3.53	3.29	Yes
	Benzonitrile	3.52	3.80	3.61	Yes
		Validation equation (J)			
	Phenol	3.63	3.97	3.81	Yes
	Tetrachloromethane	2.57	2.92	2.76	Yes
	Chloroform	4.04	4.40	4.23	Yes
	2-Bromophenol	3.21	3.46	3.35	Yes
	2-Nitrophenol	2.91	3.33	3.14	Yes
	1,2-Dichlorobenzene	3.24	3.47	3.37	Yes
	Ethylbenzene	3.34	3.61	3.48	Yes
Log P and ELUMO (eqn. 4.29)		Validation equation (K)			
	1,1,2-Trichloroethane	3.72	4.03	3.90	Yes
	1,2-Dichloropropane	3.99	4.48	4.23	Yes
	2,4-Dinitrophenol	2.64	3.43	3.10	Yes
	p-Cresol	3.81	4.15	3.99	Yes
	1,3-Dichlorobenzene	2.97	3.30	3.13	Yes
	Benzonitrile	3.55	3.94	3.78	Yes
	Aniline	4.20	4.69	4.47	Yes
		Validation equation (L)			
	Chloroform	3.48	3.79	3.60	Yes
	Hexachloroethane	2.32	2.78	2.45	Yes
	1-Chloropropane	4.11	4.74	4.45	Yes
	2-Chlorophenol	3.58	3.86	3.69	Yes
	2,4-Dimethylphenol	3.67	3.99	3.81	Yes
	Nitrobenzene	3.09	3.59	3.28	Yes
	Bromobenzene	3.28	3.57	3.38	Yes

Literature data were also used to test the utility value of the QSARs that we developed for activated sludge process in other parts of the world (eqn. 4.17, 4.22 & 4.29). However, there is limited amount of toxicity data of chemicals to activated sludge in the literature. Sun et al (1994) has measured the IC_{50} values of 50 organic chemicals to activated sludge using a 12-reactor, computer-interfaced Comput-OX Respirometer (N-CON Corporation, N. Y.). These IC_{50} data were compared against predictions made with the QSAR models developed based on log P and ELUMO (eqn. 4.29) (Figure 4.32). The correlation results was fairly well with $r^2 = 0.69$. However, unsatisfactory results were obtained for MCI ($r^2 = 0.49$) and V_i ($r^2 = 0.52$) equations.

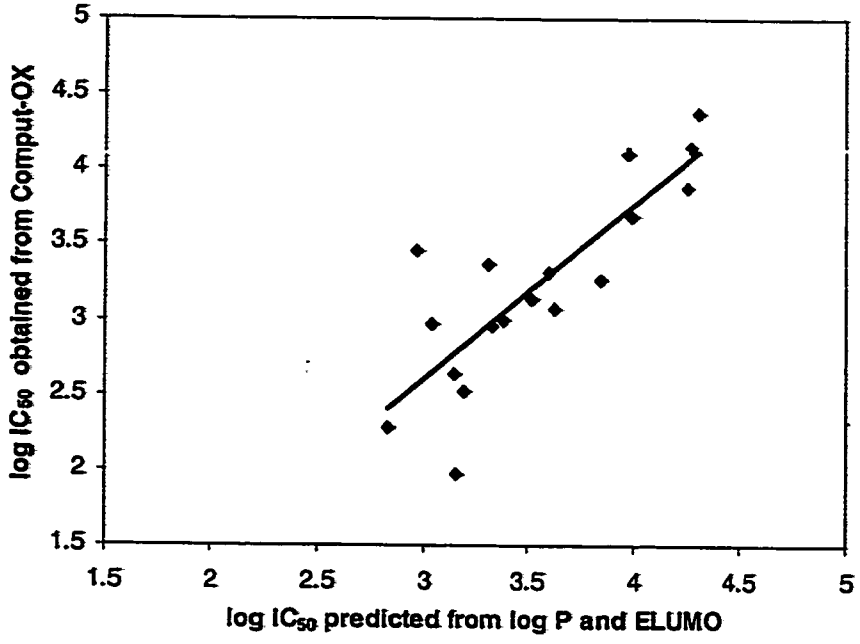

Figure 4.32 A plot of log IC_{50} (μmol/L) obtained from Comput-OX respirometer versus log IC_{50} (μmol/L) predicted from log P and ELUMO.

4.3.7 Prediction of Mixture Toxicity

Chemicals are often found in the industrial effluents and contaminated groundwaters as mixtures. Thus, an understanding and an ability to predict joint effects of mixtures of chemicals on microorganisms will be of benefit in providing very meaningful and useful inputs in managing the environmental hazards of toxic chemicals. In mixture toxicity studies, the concept of TU (Toxic Unit) proposed in the literature (Könemann, 1981a; Nirmalakhandan et al, 1994b; 1996; Hall et al, 1996) was used. It is defined as $TU_i = C_i / IC_{50i}$; where C_i is the concentration of component i in a mixture of N chemicals and IC_{50i} is the concentration of component i causing 50% inhibition when acting singly. For ideal simple additive toxicity, the sum of the toxic units of all the components ($= \Sigma TU_i$) in a mixture should be equal to 1 for 50% inhibition. Therefore, for equitoxic mixture (i.e. each component is of the same TU_i in the mixture), the toxic unit of each component is 1/N. The concentration of any component contributing 50% inhibition (by the mixture) can then be obtained as 1/N multiplying individual IC_{50i}.

Four different 5-component mixtures (mixtures 1-4) and two different 5-component of nonphenolic mixtures (mixtures 5&6) were prepared at equitoxic ratio. The toxicity of these mixtures were then determined using the optical scanning respirometer. The components in the mixture were randomly picked from each class of chemical. The percentage inhibition is plotted versus toxic unit (TU) for each mixture in Figures 4.33-4.38. The TU causing 50% inhibition was then obtained from these plots. Table 4.8 summarizes the different components of the mixtures, correlation results and experimentally determined TU values causing 50% inhibition.

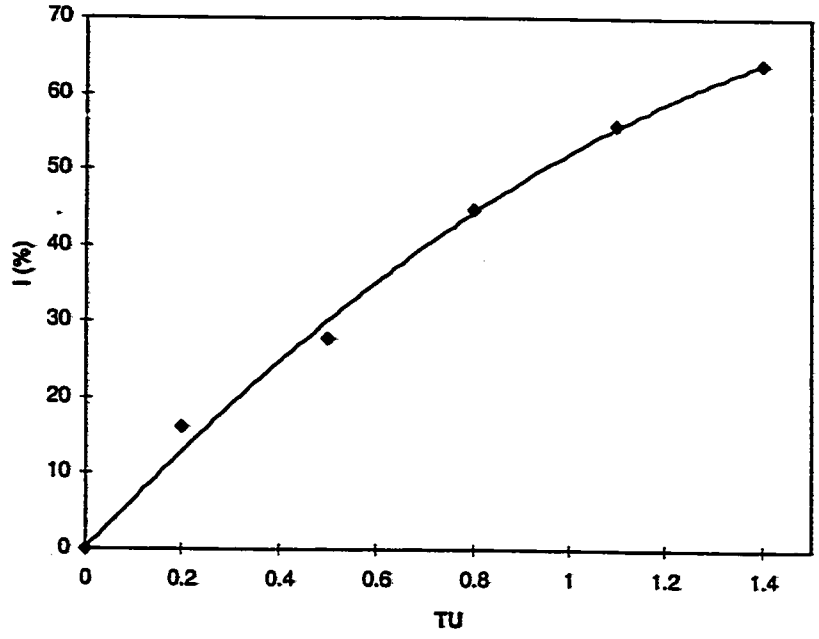

Figure 4.33 Plot of percentage inhibition (I %) versus TU unit for mixture 1.

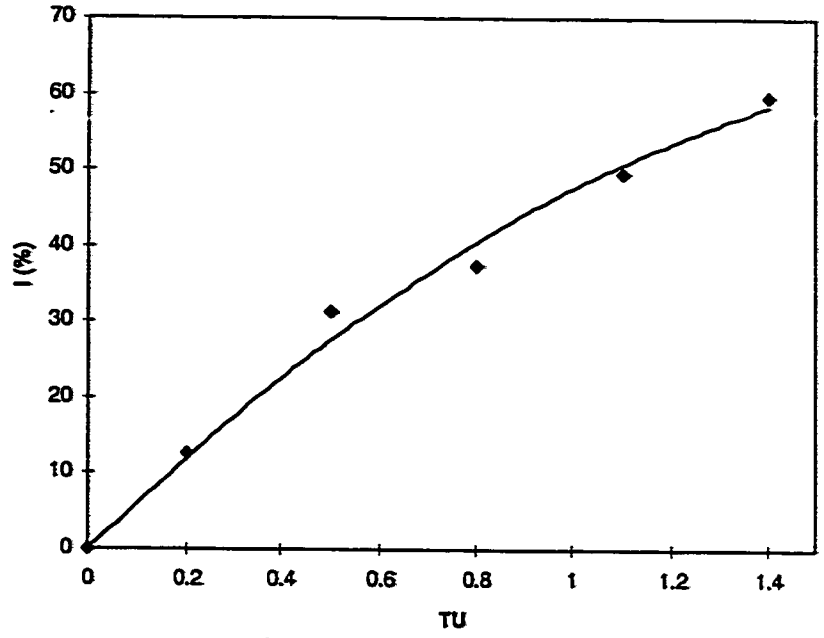

Figure 4.34 Plot of percentage inhibition (I %) versus TU unit for mixture 2.

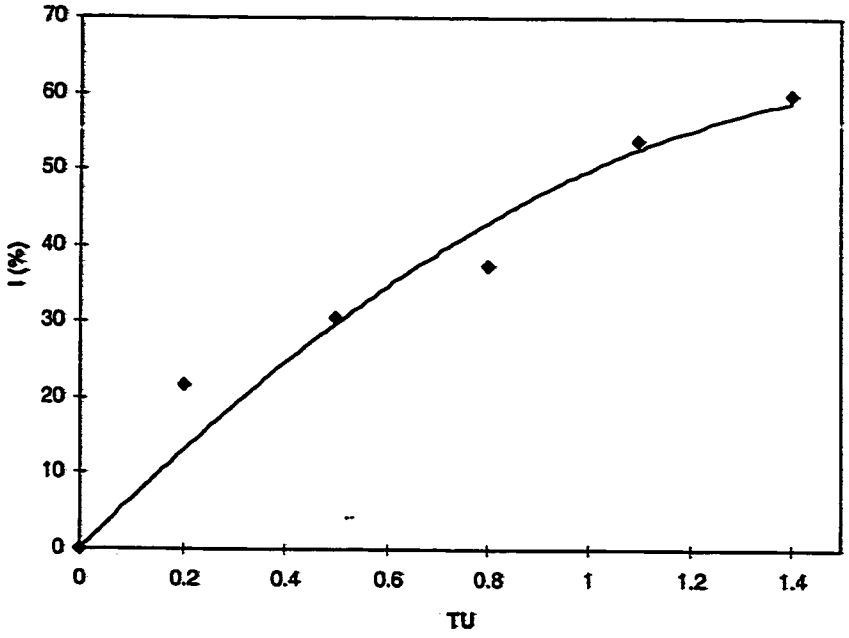

Figure 4.35 Plot of percentage inhibition (I %) versus TU unit for mixture 3.

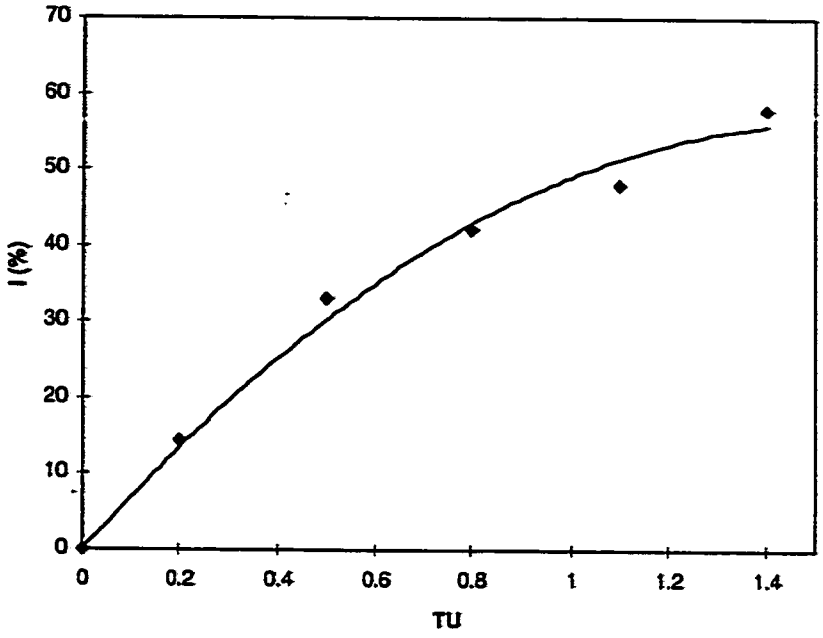

Figure 4.36 Plot of percentage inhibition (I %) versus TU unit for mixture 4.

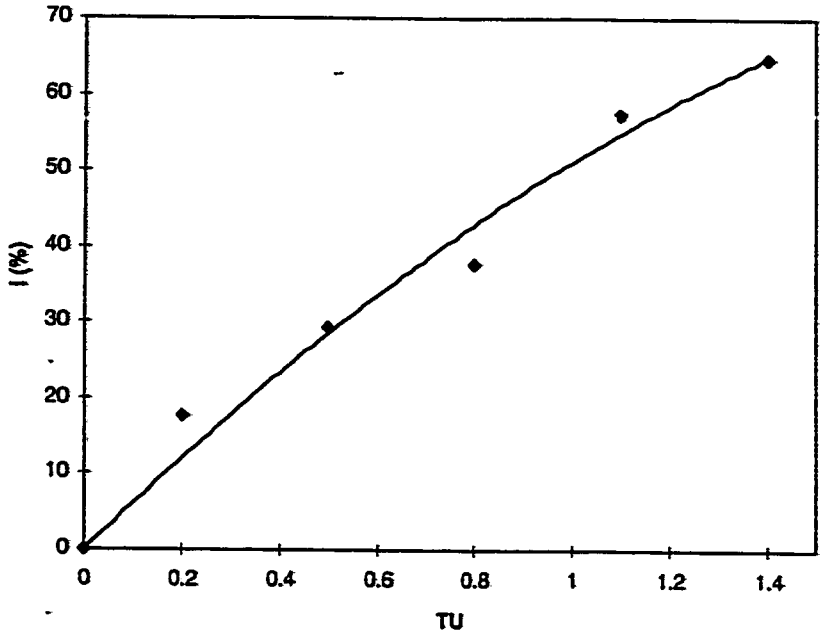

Figure 4.37 Plot of percentage inhibition (I %) versus TU unit for mixture 5.

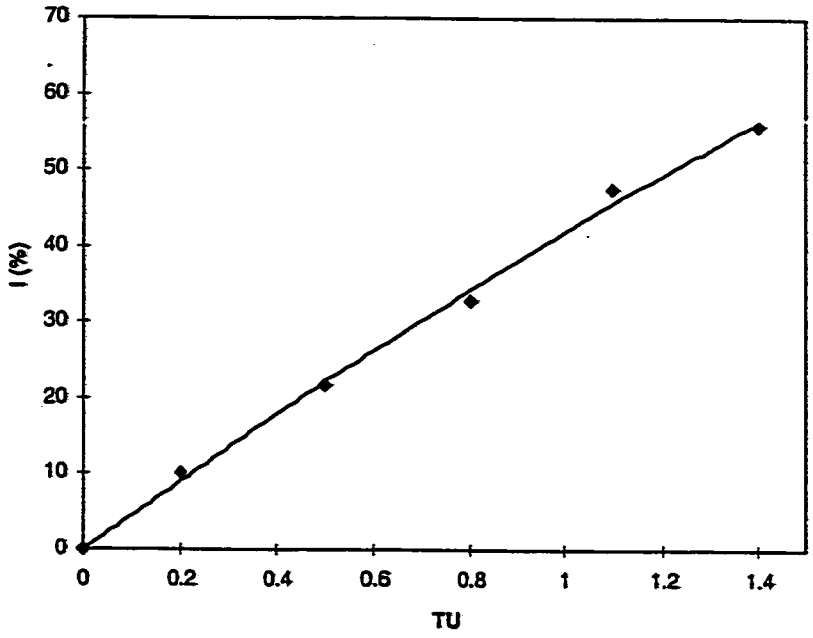

Figure 4.38 Plot of percentage inhibition (I %) versus TU unit for mixture 6.

Table 4.8 Results of mixture toxicity.

Mixture No.	Component	r^2	TU
1	1,2-Dichloropropane 1,1,2,2-Tetrachloroethane Benzonitrile Nitrobenzene 2-Chlorophenol	0.995	0.94
2	1,1,2-Trichloroethane 4-Nitrophenol 3,5-Dichlorophenol Bromobenzene Naphthalene	0.990	1.08
3	Chlorodibromomethane Dichloromethane 2,4,6-Trichlorophenol Benzene 1,2-Dichlorobenzene	0.954	1.00
4	1,2-Dichloroethane 2-Nitrophenol 2-Bromophenol Ethylbenzene 1,2,4-Trichlorobenzene	0.990	1.04
5	1,2-Dichloropropane 1,1,2-Trichloroethane Ethylbenzene Bromobenzene Benzene	0.978	0.97
6	1,1,2,2-Tetrachloroethane Chlorodibromomethane Nitrobenzene Naphthalene 1,2-Dichlorobenzene	0.997	1.22

r^2 is the coefficient of determination found in the I% versus TU plots

The Σ TU values of 6 mixtures ranged from 0.94 to 1.22 with an average value of 1.04 which is close to expected value of 1. Thus, the result indicates that the joint toxic effects of the tested chemicals in mixture were simply additive.

Different QSAR models were used to predict the concentration of each component in equitoxic mixture causing 50% inhibition of the activated sludge microorganisms. For mixtures 1-4, the approaches of using molecular volume (eqn. 4.17), molecular connectivity index (eqn. 4.22) and combination of log P and ELUMO (eqn. 4.29) as descriptors were applied successively. Since the correlations of log P (eqn. 4.6) and log S (eqn. 4.13) were only suitable for nonphenolic chemicals, they were restricted to mixtures 5 and 6. The concentrations of components predicted from developed QSAR models ($1/5 \times IC_{50i,\ predicted}$) are plotted versus the experimental determined concentrations ($TU/5 \times IC_{50i,\ measured}$) in Figures 4.39-4.43. The concentrations predicted by the different QSAR approaches are compared in Tables 4.9 and 4.10 for mixtures 1-4 and 5-6, respectively, against the observed concentration. The predictions using MCI ($r^2 = 0.805$) for all chemicals and log S ($r^2 = 0.844$) for nonphenolic compounds were reasonably good and better than other methods. The better predictive ability of MCI ad log S may be attributed to better predictive ability of their original models. Our results are comparable to the works reported in the literature (Nirmalakhandan et al, 1994a; 1994b; Hall et al, 1996). Nirmalakhandan and co-worker (1994a) showed that the concentration predicted by MCI models agreed well with experimental values with $r^2 = 0.8$.

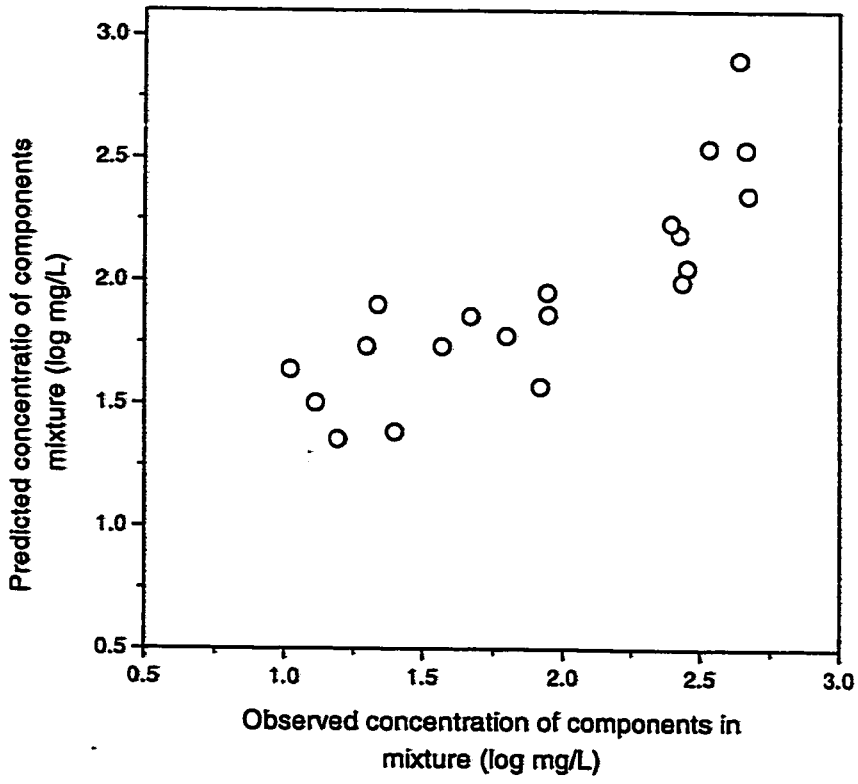

Figure 4.39 Plot of predicted concentration versus observed concentration of components using molecular volume approach.

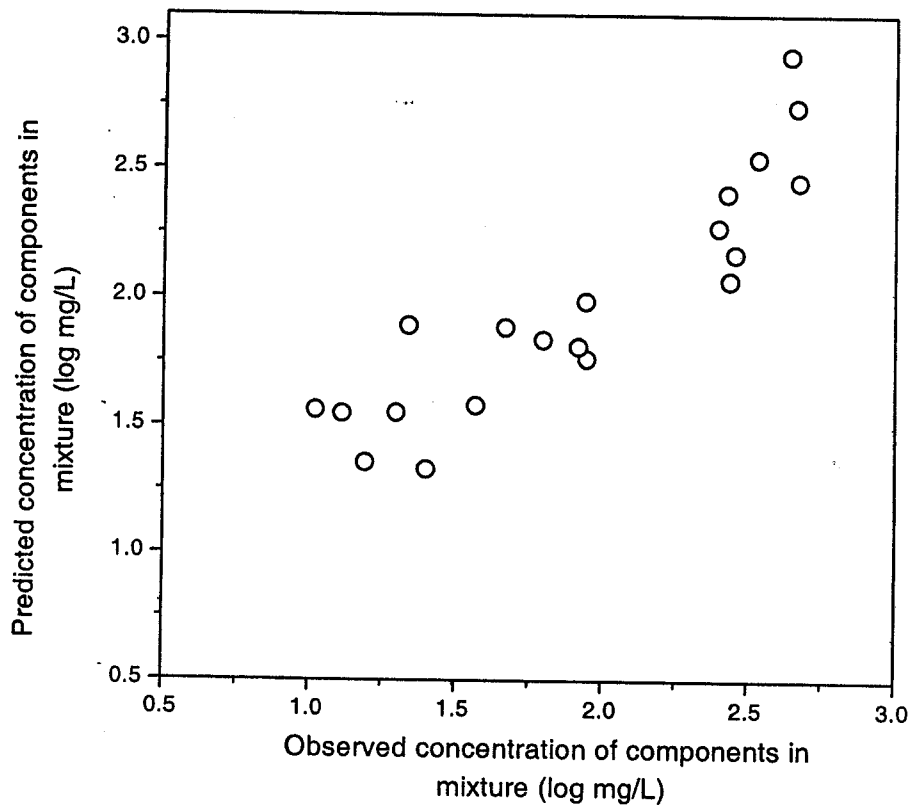

Figure 4.40 Plot of predicted concentration versus observed concentration of components using molecular connectivity index approach.

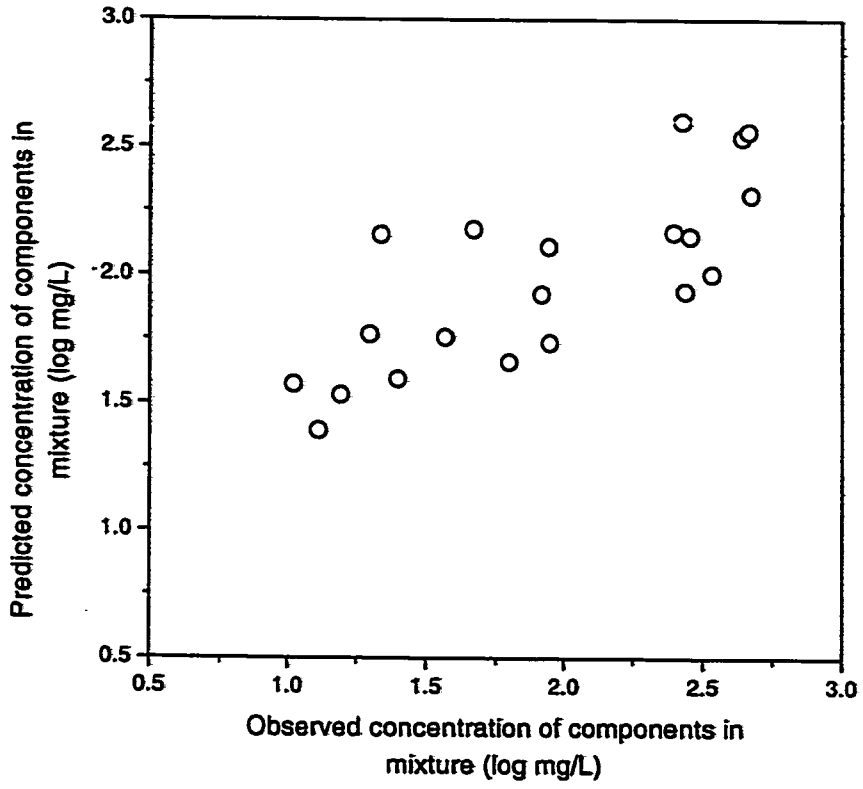

Figure 4.41 Plot of predicted concentration versus observed concentration of components using combination of log P and ELUMO approach.

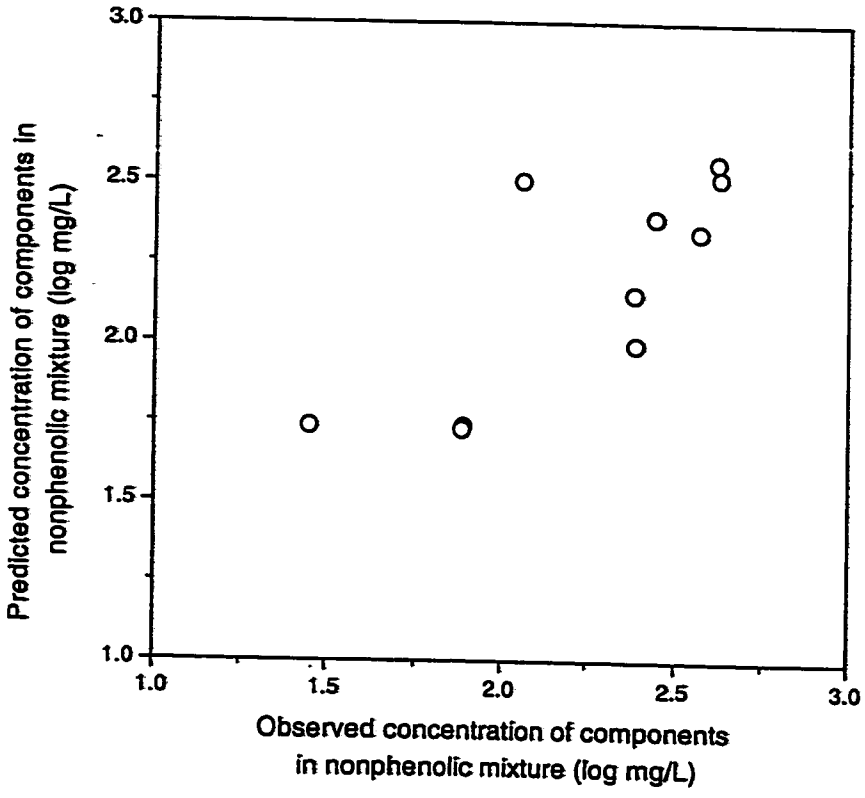

Figure 4.42 Plot of predicted concentration versus observed concentration of components using log P approach.

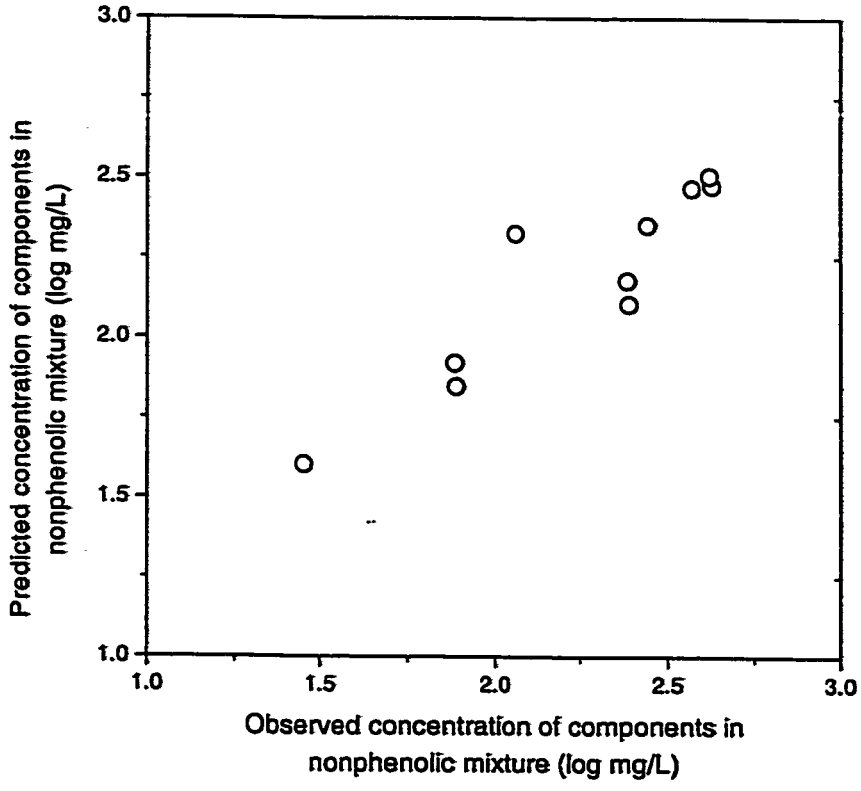

Figure 4.43 Plot of predicted concentration versus observed concentration of components using log S approach.

Table 4.9 Comparison of predicted concentration and observed concentration for mixtures 1-4.

Component	Observed (log mg/L)	Predicted by V_i/100 (log mg/L)	Predicted by MCI (log mg/L)	Predicted by log P and ELUMO (log mg/L)
1,2-Dichloropropane	2.428	2.192	2.405	2.601
1,1,2,2-Tetrachloroethane	2.455	2.055	2.169	2.152
Benzonitrile	1.944	1.953	1.985	2.11
Nitrobenzene	1.947	1.863	1.761	1.735
2-Chlorophenol	1.341	1.902	1.889	2.157
1,1,2-Trichloroethane	2.673	2.35	2.452	2.312
4-Nitrophenol	1.300	1.733	1.549	1.768
3,5-Dichlorophenol	1.022	1.639	1.56	1.572
Bromobenzene	2.437	1.997	2.066	1.937
Naphthalene	1.400	1.384	1.328	1.592
Chlorodibromomethane	2.533	2.543	2.542	2.004
Dichloromethane	2.640	2.903	2.943	2.538
2,4,6-Trichlorophenol	1.194	1.356	1.354	1.532
Benzene	2.398	2.235	2.271	2.167
1,2-Dichlorobenzene	1.798	1.777	1.835	1.66
1,2-Dichloroethane	2.664	2.538	2.744	2.561
2-Nitrophenol	1.570	1.733	1.578	1.757
2-Bromophenol	1.670	1.856	1.883	2.177
Ethylbenzene	1.918	1.571	1.809	1.925
1,2,4-Trichlorobenzene	1.114	1.503	1.546	1.392
	r^2	0.721	0.805	0.610

r^2 is the coefficient of determination between the predicted and observed values.

Table 4.10 Comparison of predicted concentration and observed concentration for nonphenolic mixtures 5 and 6.

Component	Observed (log mg/L)	Predicted by log P (log mg/L)	Predicted by log S (log mg/L)
1,2-Dichloropropane	2.442	2.389	2.35
1,1,2-Trichloroethane	2.626	2.516	2.474
Ethylbenzene	1.888	1.736	1.847
Bromobenzene	2.390	1.992	2.105
Benzene	2.385	2.15	2.178
1,1,2,2-Tetrachloroethane	2.568	2.345	2.466
Chlorodibromomethane	2.619	2.563	2.504
Nitrobenzene	2.060	2.502	2.323
Naphthalene	1.453	1.737	1.601
1,2-Dichlorobenzene	1.884	1.726	1.92
	r^2	0.605	0.844

r^2 is the coefficient of determination between the predicted and observed values.

4.4 Concluding Remarks

Five different approaches have been used for describing the toxicity of chemicals to activated sludge. Substituted alkanes and benzenes were well modeled by all the methods. For phenolic chemicals, combination of log P and ELUMO was the best method that could correlate significantly with the toxicity data. In correlating all the three classes of chemicals, no significant relationship was observed when using log P or log S as descriptors. The exclusion of phenolic chemicals from the regression improved the accuracy of QSAR equations. The molecular connectivity and the combination of log P and ELUMO were the two most accurate QSAR methods. These two approaches are able to incorporate different chemical classes. The molecular connectivity is simple to use and easy to calculate while combination of log P and ELUMO provide better explanation on toxicity mechanism. For predicting the toxicity of mixtures, MCI and log S were more accurate. The quality of prediction by these two models is comparable to the experimental uncertainty in the IC_{50} data.

Chapter 5

Evaluation of a Luminescent Ruthenium Complex as Optical pH Sensor and in pH Monitoring of Fermentation

5.1 Introduction

There have been much interest in the development of optical pH sensors (pH optodes) for biomedical applications (Wolfbeis, 1991; Peterson et al, 1980). The advantage of optodes over conventional electrochemical sensors is obvious: no electrical connection to the patients is required which makes the measurements safer for human use. In addition, the use of plastic optical fibre allows a high degree of mechanical flexibility combined with very small size and low cost. Optical pH sensors are based on pH dependent changes of the absorbance or luminescence of certain indicator molecules (Leiner and Wolfbeis, 1991). For absorbance-based sensors, the color of the dye changes with pH. For luminescence pH sensors, the difference in luminescence properties of the conjugate acid-base pair of the dye is measured. In this analytical application, luminescence method has the advantages of higher sensitivity and selectivity over the absorbance method. The major limitation of most pH optodes is the narrow pH range covered: most dyes are only sensitive to changes in pH values over 2-4 pH units. Recently, there has been considerable interest in extending the use of pH optodes in industrial and hazardous environments (Leiner and Hartmann, 1993) and the development of pH sensing dyes with greater working range in pH values is necessary.

A number of fluorescent dyes have been used as indicators for pH sensing. Fluorescein and its related compounds are widely used as pH probes and sensors (Saari and Seitz, 1982; Munkholm et al, 1986; Parker et al, 1993; Song et al, 1997). However, fluoresceins have small Stokes' shifts, overlapping pK_a values and limited

photostability. Hydroxypyrenetrisulfonic acid is another class of dye commonly used for pH sensing. Its major advantages include high fluorescence quantum yield, visible excitation and emission wavelengths, and large Stokes' shift. It has a pK_a of 7.3 which is ideal for physiological measurements (Zhujun and Seitz, 1984; Offenbacher et al, 1986). However, hydroxypyrenetrisulfonic acid is rather sensitive to changes in ionic strength due to its high charge. A near infrared fluorescence probe for pH determination has also been reported (Zen and Patonay, 1991). The sensing dye is a carboxylated cyanine incorporated into Nafion films. Instead of using fluorescent dyes that are pH sensitive, a pH optode based on co-immobilization of a pH-insensitive fluorophore, eosin and a pH-sensitive absorber, phenol red on the optical fibre has been developed (Jordan et al, 1987). The fluorescence emission spectrum of eosin overlaps significantly with the absorption spectrum of the basic form of phenol red. Thus, as pH increases, the amount of energy transfer from the fluorescent dye to the pH-sensitive indicator will increase which results in a diminution of the fluorescence intensity. In addition to organic dyes, a number of dyes based on luminescent transition metal complexes are potentially useful for pH optodes. An electropolymerized cobalt porphyrin has been reported to be optically sensitive to pH changes over the pH range 8 to 12 (Blair et al, 1993). Several luminescent pH sensors based on photoinduced electron transfer have been described by Grigg and co-workers. The luminescent complexes include tin(IV) aminoethyltetraphenylporphyrin derivatives (Grigg and Norbert, 1992b), di(2,2'-bipyridyl)(5,5'-diaminomethyl-2,2'-bipyridyl)ruthenium(II) (Grigg and Norbert, 1992a) and *p-tert*-butylcalix[4]arene-linked ruthenium(II) tris(bipyridyl) complexes (Grigg et al, 1994).

We are interested in the development of optodes based on luminescent transition metal complexes (Lee et al, 1993a; Li et al, 1993; Lee et al, 1993b). These dyes offer distinct advantages including absorption in the visible region, long excited state lifetimes, high quantum yield and photostability. In this chapter, we report our investigation on a luminescent ruthenium bipyridyl complex with the 4,7'-dihydroxy-1,10-phenanthroline ligand immobilized into Nafion film as optical pH sensor. This ruthenium complex is strongly emissive, and the protons of the hydroxy groups on the phenanthroline ligand is acidic and hence the absorption and emission spectra of the complex are dependent on the pH of the environment. It is cationic and can be easily immobilized inside the polyanionic polymer film through electrostatic binding, making it a potentially useful dye for optical pH determination. In this study, we employed Nafion as the polymer support for the pH sensing dye. Nafion is a perfluorinated polymer consisting of a tetrafluoroethylene backbone with pendent side chains of perfluorinated vinyl ethers which terminate in sulfonic acid group. The structure of Nafion is believed to consist of three regions: a hydrophobic fluorocarbon backbone, a hydrophilic sulfonate ionic clusters site and an interfacial region between the hydrophobic region and the hydrophilic region (Yeager, 1982). This inhomogeneous structure of Nafion together with its well known stability and insolubility in aqueous medium makes it a suitable polymer support for pH sensors. The hydrophilic ionic clusters region allows easy access of the analyte to the sensor molecules, whereas the relatively hydrophobic interfacial region provides a suitable environment to accommodate the hydrophobic bipyridyl ligands of the metal complex.

A limited number of reports on the application of pH optical sensor system to pH monitoring of fermentation have appeared (Junker et al, 1988; Kisaalita et al, 1991; Agayn and Walt, 1993). The major obstacle for coupling an optical pH sensor to the fermentation process is the interference from the medium broth. This is due to the content of the fermentation broth, which contains cells and other opaque components. These materials absorb and scatter light which interfere with the optical signal. Previous workers have applied a ratiometric method (Zhujun and Seitz, 1984) to overcome the broth effect by recording the ratio of two emission signals. However, the method only works under the assumption that the broth optical characteristics are the same at the two collection sites. The feasibility of using this new pH sensor to monitor the pH change in a fermentation process was investigated and included in this chapter. A black microporous filter membrane was placed on top of the pH sensing film to overcome the medium interference effect. The reliability of this sensor was compared with a conventional pH electrode.

5.2 Experimental Section

5.2.1 Materials

Ruthenium(III) chloride ($RuCl_3$) was obtained from Strem Chemical Co. 2,2'-Bipyridine (bpy), 4,7-dihydroxy-1,10-phenanthroline (dhphen) and Nafion (5 wt % solution) were purchased from Aldrich. Sodium chloride and lithium chloride

(analytical reagent) were obtained from Mallinckrodt and Merck respectively. Agar and nutrient broth were purchased from Difco. The microporous filter membrane (pore size: 0.45 μm, diameter: 60 mm) obtained from Advantec MFS was cut to a size of 0.9 cm x 3 cm and stained with black water insoluble ink from a Sanford permanent marker. All other chemicals were of analytical-reagent grade and were used without further purification. Oxygen and nitrogen gases (99.9%) were purchased from Hong Kong Oxygen. Buffer solutions prepared according to literature method (Weast, 1985), were measured by a Corning Model 7 pH meter prior to use.

5.2.2 Synthesis

cis-Dichlorobis(bipyridine)ruthenium **($Ru(bpy)_2Cl_2$)**

$Ru(bpy)_2Cl_2$ was synthesized according to a method previously published (Sullivan et al, 1978). $RuCl_3 \cdot 3H_2O$ (0.78 g), 2,2'-bipyridine (0.94 g) and LiCl (0.84 g) were heated at reflux in dimethylformamide (10 ml) for 8 hours. After the reaction mixture was cooled to room temperature, 25 ml of acetone was added and the resulting solution was cooled at 0°C overnight. The dark green-black micro-crystalline product was filtered and washed with water followed by diethyl ether.

$[Ru(bpy)_2(dhphen)](ClO_4)_2$ (dhphen = 4,7-dihydroxy-1,10-phenanthroline)

$[Ru(bpy)_2(dhphen)](ClO_4)_2$ (*caution: all perchlorate salts are potentially explosive!*) was synthesized according to a previously published method (Giordano et al, 1978) with slight modification: $Ru(bpy)_2Cl_2$ (0.5 g) and dhphen (0.25 g) were refluxed in 1:1(v/v) ethanol-1.0 M NaOH for 2 h. The dark red solution was then neutralized to pH 6 by HCl and any excess ligand was filtered off. The product was precipitated from an aqueous solution of pH2 by addition of $LiClO_4$. The crude product was purified by recrystallization from MeOH to give reddish brown crystals. The purity of the complex has been checked by elemental analysis and the C, H, N ratio of the compound synthesized is consistent with the empirical formula $C_{32}H_{24}Cl_2N_6O_{10}Ru$.

5.2.3 Preparation of pH Sensing Film

A 0.3 mM solution of the $[Ru(bpy)_2(dhphen)](ClO_4)_2$ complex was prepared in ethanol. Nafion obtained as 5 wt % solution was diluted five fold with ethanol. A complex-polymer mixture was prepared by mixing appropriate amount of the above two solutions thoroughly. A 0.4 ml aliquot of the resulting mixture was placed on the surface of a glass slide (0.9 cm x 5 cm), spin-coated and air-dried. Coatings prepared this way have an estimated thickness of about 5 μm (Shu and Anson, 1990). The

coated glass slide was then inserted into a 1 cm pathlength polystyrene cuvette containing buffer solution for spectroscopic measurements.

5.2.4 Physical Measurements

Ultraviolet-visible absorption spectra were recorded on a Milton Roy 3000 photodiode array spectrophotometer. Luminescence measurements were made either on a Spex Fluorolog-2 Spectrofluorometer or on a Perkin-Elmer LS-50B Spectrofluorometer. All luminescence measurements were performed in aerated buffer solution. The response time of the sensing film was measured by pumping different buffer solutions into and out of the cuvette with a Cole-Parmer Model 7550 peristaltic pump. Unless otherwise stated, all measurements were made at room temperature (25 ± 2 °C) and atmospheric pressure.

5.2.5 Fermentor

A schematic diagram of the setup for on-line pH monitoring is shown in Figure 5.1.

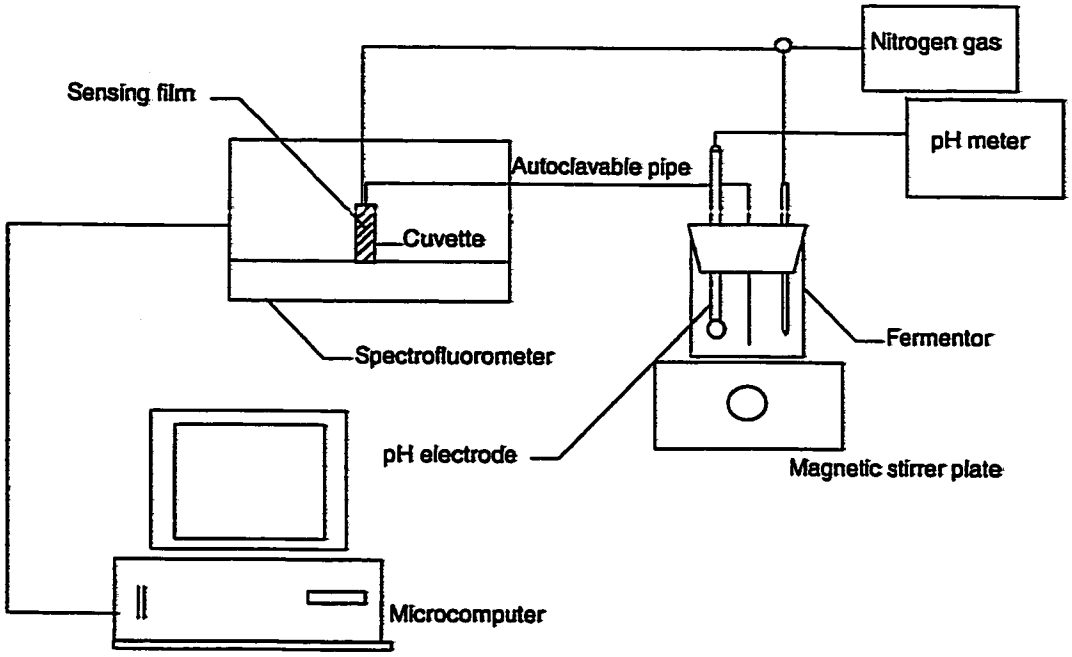

Figure 5.1 . A schematic diagram of the setup for on-line pH measurement.

The fermentor used in this study contains three outlets which can accommodate (i) a Mettler pH electrode for comparison with the optical sensor; (ii) a sterilizable nitrogen gas inlet for maintaining the anaerobic environment; and (iii) a teflon tubing for medium content transfer in and out of the fermentor. On-line pH measurement by the pH optode was achieved by pumping the medium content into a sealed quartz cuvette contained a pH sensing film (1 cm pathlength) using a Cole-Parmer Model 7521-57 peristaltic pump. The top of the sensing film was covered with a black microporous filter membrane (0.45 μm pore size) to overcome the interference from the broth. A cross-section diagram of the sensor assembly is shown in Figure 5.2. The cuvette was placed inside the sample compartment of a Perkin-Elmer LS-50B spectrofluorometer.

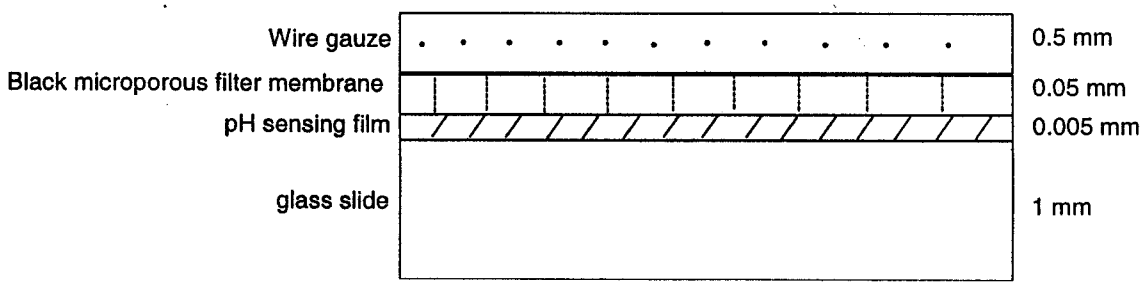

Figure 5.2 A cross-section diagram of the sensor assembly.

5.2.6 Fermentation

The microorganism used in the fermentation process was *Klebsiella pneumoniae* which is a facultative bacterium capable of growing under both aerobic and anaerobic conditions. The medium content was a nutrient broth containing Bacto beef extract (3 g/L) and peptone (5 g/L). Precultures were prepared by inoculating the bacteria on agar plate at 30°C for 24 hours. The agar plate was stored in a refrigerator at 4° C and refreshed it on a 2-week basis. A single colony of the bacteria in the agar plate was then transferred to 50 ml of nutrient broth in a 150 ml fermentor under anaerobic condition at room temperature (25 ± 1°C). The change in pH during fermentation was monitored by pumping the medium content into the cuvette which contained the calibrated sensing film. The cuvette was continuously purged with nitrogen gas. After each measurement, the solution was pumped back to the fermentor to minimize disturbance on the growth of bacteria.

5.3 Results and Discussion

5.3.1 Optical Characteristics of the pH Sensing Film

A schematic diagram showing the incorporation of the ruthenium complex in Nafion is given in Figure 5.3. The absorption spectra of $[Ru(bpy)_2(dhphen)]^{2+}$ immobilized in Nafion in different acid and base media are shown in Figure 5.4. The spectral change is a result of an acid-base equilibrium of the complex as presented in Scheme 1 (Giordano et al, 1978):

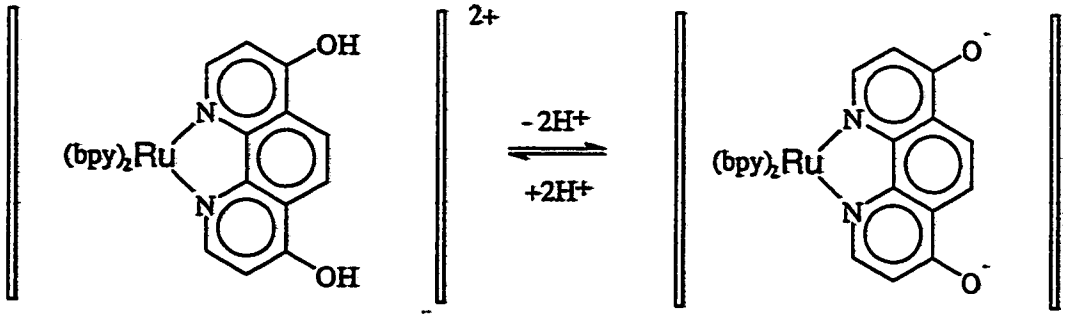

Scheme 1

The spectral changes are completely reversible with variation in pH. The absorption spectra show two isosbestic points at around 415 nm and 475 nm respectively. As the absorption spectra overlap more precisely at 415 nm, this wavelength was chosen as the excitation wavelength in subsequent luminescence measurements which will result in more accurate pH measurements. Both the protonated and the deprotonated forms

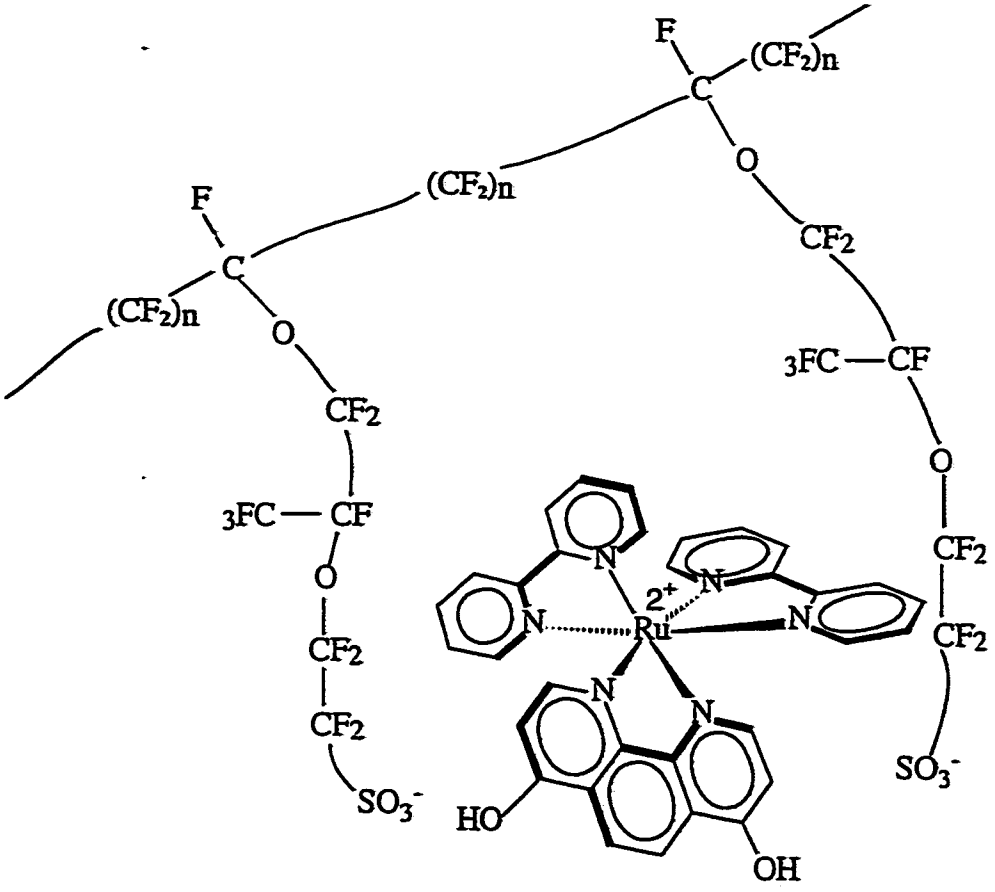

Figure 5.3 A schematic diagram showing a ruthenium complex incorporated inside Nafion.

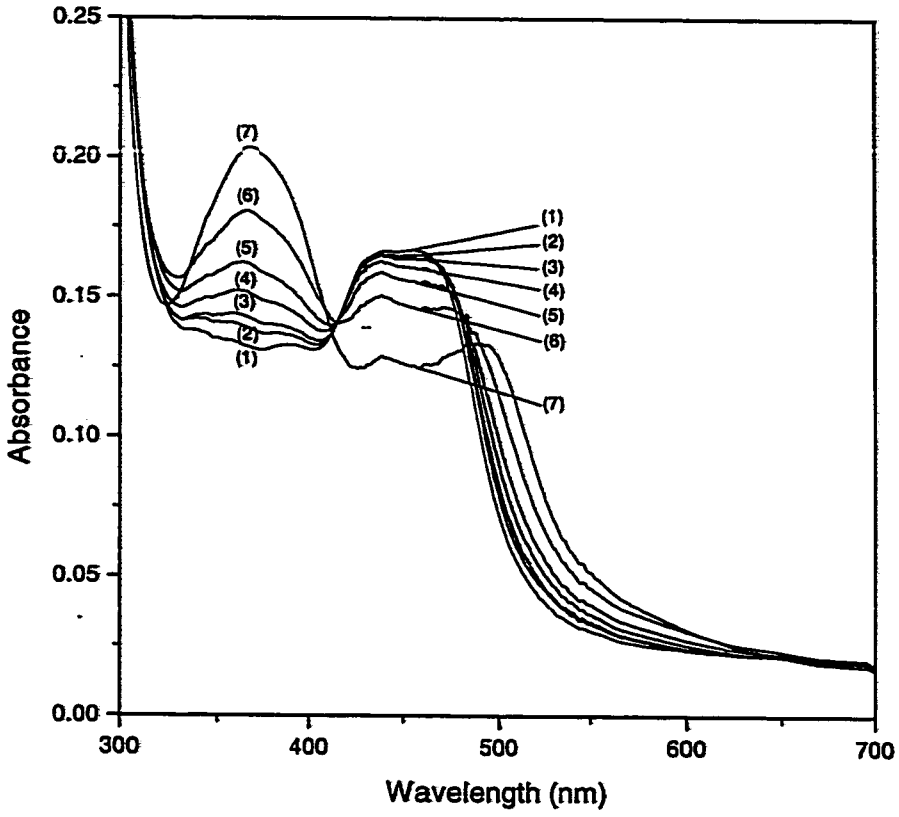

Figure 5.4 Absorption spectra of $[Ru(bpy)_2(dhphen)]^{2+}$ entrapped within Nafion film in different pH buffers. Curves 1-7 are at pH 1.12, 4.25, 5.01, 6.02, 6.89, 7.95 and 8.83 respectively.

of the complex can emit light in aerated aqueous solution, though the latter is much less emissive. Since the intensity of emission depends on the amount of light absorbed by the emitting species, the excitation has to be made at a wavelength (the isosbestic point) at which both the protonated and the deprotonated complexes absorb the same amount of light. Under such conditions, the emission intensity measured will not be affected by the difference in absorbance of the two emitting species. Excitation of the complex results in the emission spectra as shown in Figure 5.5. The emission intensity of the complex decreases with increase in pH. Plots of the emission intensity versus pH for the complex in solution and after immobilization into Nafion are shown in Figure 5.6. The emission intensity decreases gradually as the pH of the solution increases and levels off beyond pH 8. Although the complex possesses two acidic protons, previous studies indicated that the first and second acid dissociation constants, pK_{a1} and pK_{a2} , of this complex are nearly the same (Giordano et al, 1978), and hence only one inflection point is observed in the plots of change in optical density versus pH. In solution, the inflection point occurs at about pH 2.6. After incorporation inside Nafion, the inflection point was found at around pH 5.1. It is interesting to note that after immobilizing the ruthenium complex into Nafion, the apparent pK_a is higher than in solution. Increase in apparent pK_a after incorporation into Nafion films has also been observed in other metal complexes (Lai and Wong, 1993). It could be due to the polyanionic nature of the Nafion matrix which tends to stabilise the more highly charged, acidic form of the acid-base pair of the dye. The sulfonic sites (SO_3^-) of Nafion can attract protons and hinder the entrance of anionic buffers such as phosphate and acetate that make the environment inside the film more acidic than the outside

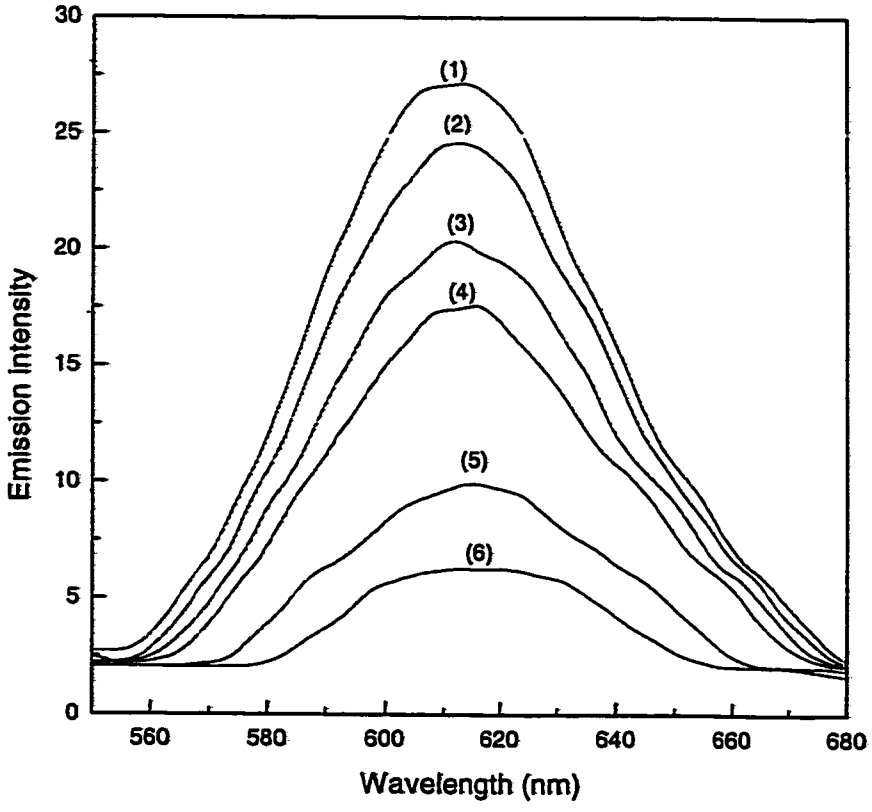

Figure 5.5 Emission spectra of $[Ru(bpy)_2(dhphen)]^{2+}$ entrapped within Nafion film in different pH buffers with excitation wavelength set at 415 nm. Curves 1-6 are at pH 2.18, 3.38, 4.49, 5.37, 6.50 and 7.11 respectively.

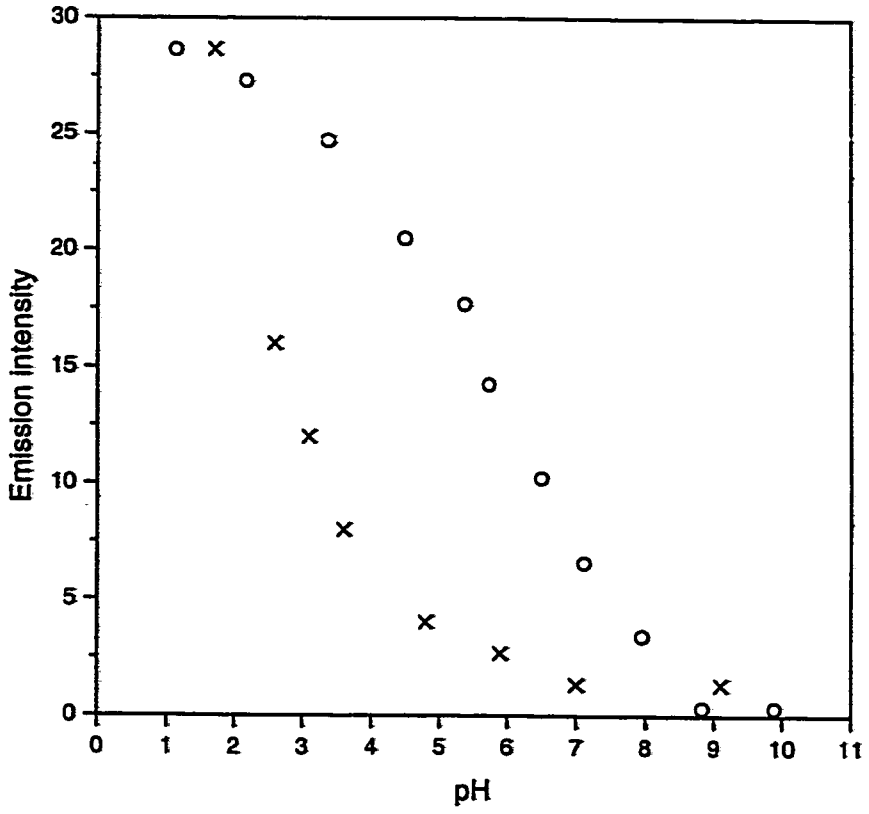

Figure 5.6 . Plots of emission intensity versus pH for the $[Ru(bpy)_2(dhphen)]^{2+}$ complex in solution (×) and after immobilisation into Nafion (o).

buffer solution. As a result, the apparent pK_a value of the complex is increased after immobilization in Nafion.

5.3.2 Response Time and Reproducibility

The response time of the sensing film was measured by replacing the buffer solutions in the cuvette rapidly with the use of a peristaltic pump. The flow rate of the peristaltic pump was set at 40 ml min^{-1} so that it takes only about 10 s to replace all the solution in the cuvette. The time taken to replace the buffer is very short compared to the response of the sensor, so the interruption did not affect the measurement of response time significantly. The change in emission intensity at 612 nm was then monitored under static condition. A typical response curve of the sensor to the change in pH is shown in Figure 5.7. The signal changes are fully reversible. The response time is taken to be the time required for 95% of the total signal change. The response time depends on the magnitude of the change in pH and is about 320 s when going from pH 2.47 to 5.37. When going from pH 3.38 to pH 1.12, the response time was 165 s. The signal levelled off after equilibrium had been reached and no drift in response was observed under the experimental conditions employed.

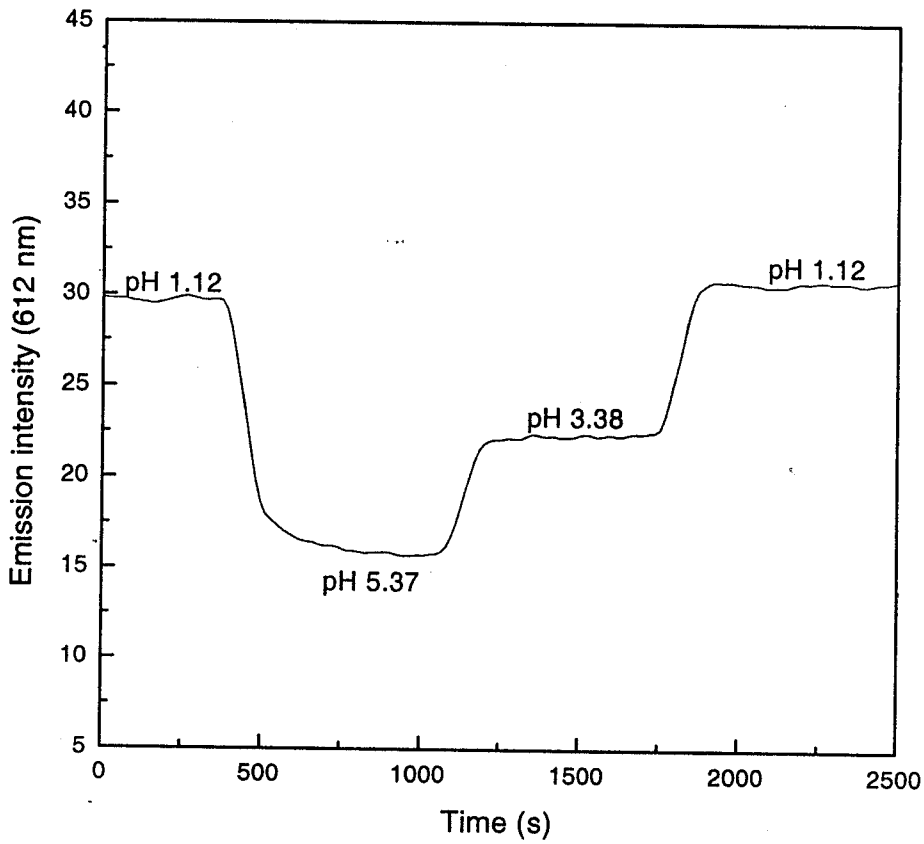

Figure 5.7 Response of the sensing film towards changes in pH. The excitation wavelength is 415 nm.

Reproducibility of the sensor was evaluated by measuring the emission intensity consecutively in pH 2.47-6.02 buffer solutions. The reproducibility for pH measurement is reasonably good with standard deviation in the range of 0.04 to 0.11 pH units. A summary of the reproducibility of the sensor under different pH conditions is given in Table 5.1.

5.3.3 Sensitivity and Interferents

The sensitivity limit of the sensing film, taken as three times the noise level, is about 0.1 pH unit. This is comparable to the conventional pH electrode. As Nafion is a polyanionic polymer, anions are excluded from the sensing film due to electrostatic repulsion whereas cations can enter the film and affect the response of the sensor. The responses of the sensing film in the presence of alkali metal and divalent transition metal ions are shown in Figure 5.8. At low concentration, the monovalent and divalent metal ions have little effect on the luminescence intensity of the sensor. When the concentration of the metal ions reaches about 1 M, a small decrease in luminescence intensity (less than 8% change) is observed. The interference effect of cations is also reflected in the change in ionic strength of the buffer solutions. As shown in Figure 5.9, there is a drop in the emission intensity as the ionic strength of the buffers increases.

Table 5.1 Reproducibility of the sensor in different pH buffers.

pH	Emission intensity[a]	± intensity (s)[b]	± pH (s)
2.47	27.24	0.27	0.11
3.38	24.29	0.22	0.06
4.49	19.51	0.21	0.04
5.37	15.53	0.25	0.05
6.02	10.91	0.25	0.04

[a] Mean (n=5), [b] s = standard deviation.

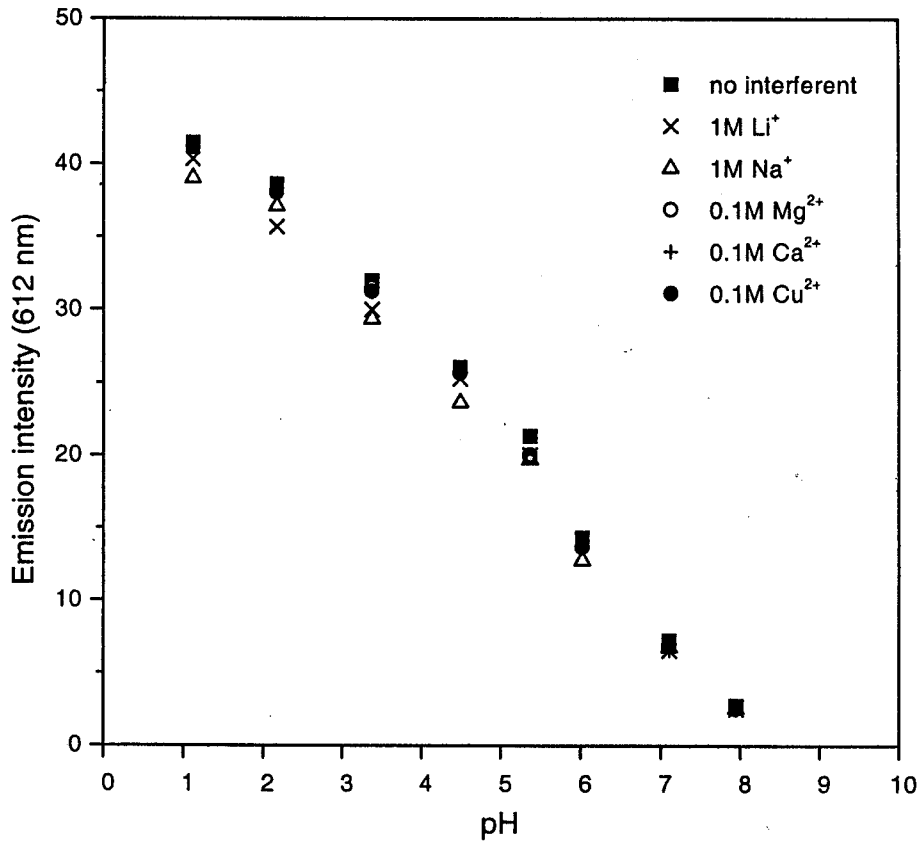

Figure 5.8 Plots of emission intensity versus pH for the sensing film in the presence of different metal cations. The excitation wavelength is 415 nm.

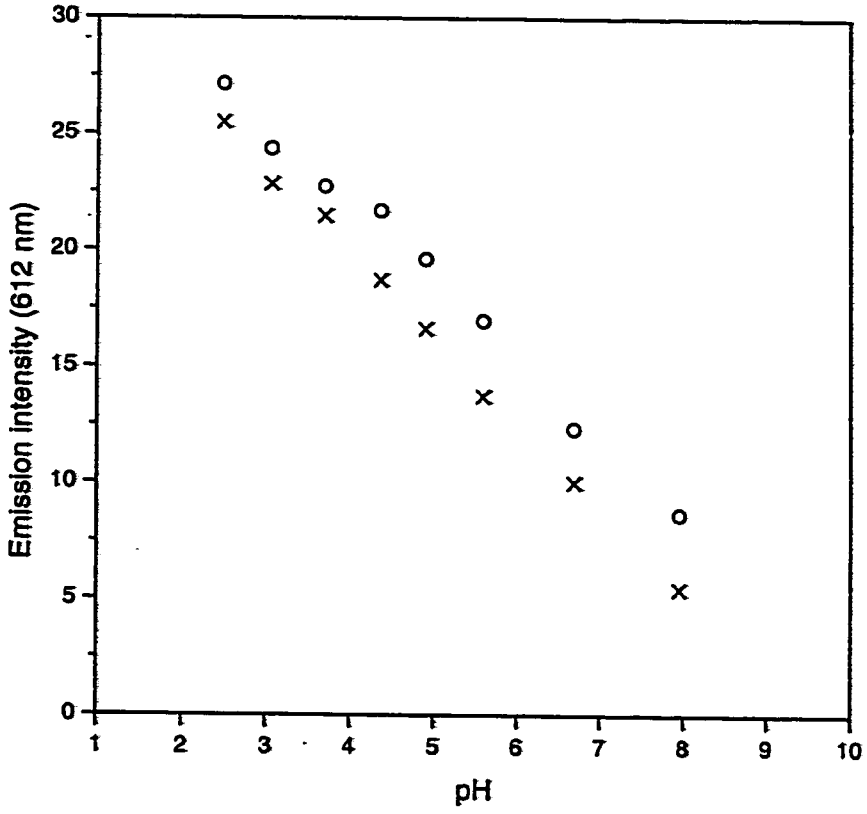

Figure 5.9 Plots of emission intensity versus pH for the sensing film in buffers of different ionic strength: (o) 0.01 M buffer, (×) 0.1 M buffer. The excitation wavelength is 415 nm.

The effect of oxygen on the response of the sensor was also studied as oxygen is a well known quencher for luminophores. Figure 5.10 shows the response of the sensing film when changing a buffer solution (pH 4.49) saturated with oxygen to a completely deaerated solution. The emission intensity decreases by 14 % from a pure nitrogen to a pure oxygen environment. The extent of oxygen quenching was found to be more or less the same in all buffer solutions. Although oxygen is an interferent, this would not cause significant error for measurements on aerated solutions in which the oxygen concentration is a constant. However, it was found that the sensor is more sensitive towards pH changes under deaerated conditions. In a nitrogen saturated environment, the average change in emission intensity is about 4.6 units per unit change in pH. When the measurement is taken under aerated conditions, the change in emission intensity unit per unit pH drops to about 4.1, representing a 11% drop in sensitivity.

5.3.4 Sensor Stability

The sensing film was usually kept in deionized water before use to prevent it from drying out. One problem with immobilised dyes is the leaching of dyes into the solution. Leaching of dye from the Nafion film was monitored by soaking the film in buffer solution continuously for two weeks and recording the emission spectrum daily. The dye was found to be stable inside the Nafion film over pH 1-9 and very little leaching of dye was observed. The emission spectrum after two weeks is

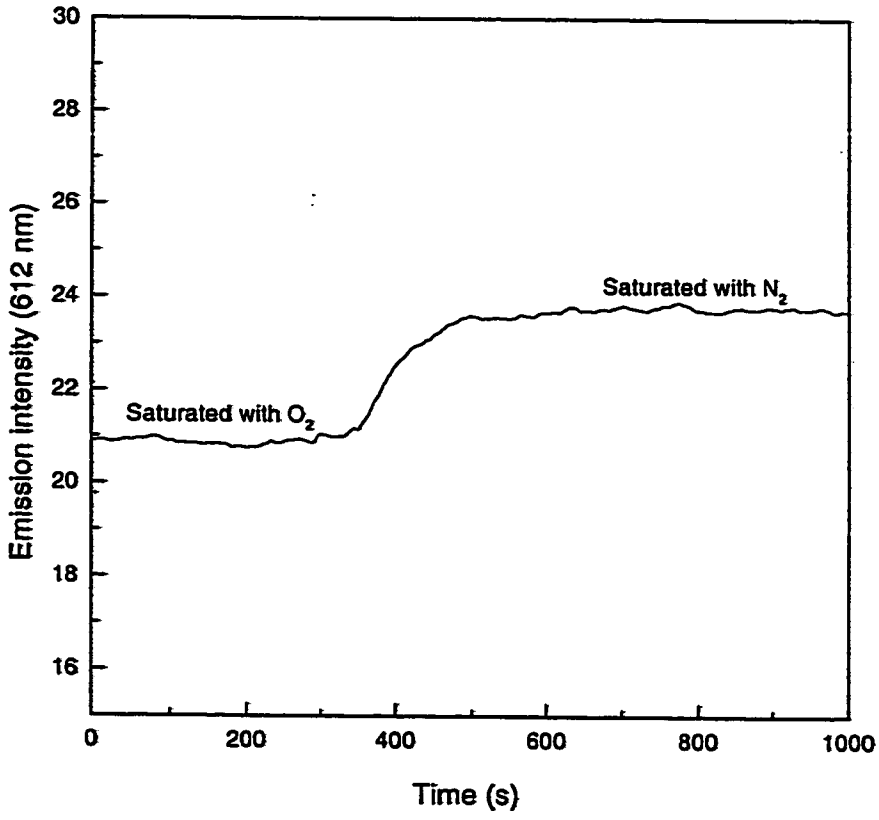

Figure 5.10 Response of the sensing film to oxygen. The solution is a pH 4.49 buffer solution. Excitation wavelength: 415 nm.

almost the same as the original spectrum recorded on the first day with little change in the emission intensity. Figure 5.11 shows the emission spectra of the sensing film recorded on the first day and after two weeks in pH 3.38 buffer solution. However, substantial leaching of dye was observed in basic medium with pH > 10. This is due to the loss of electrostatic interaction between the dye and the Nafion matrix as the immobilized complex is fully deprotonated and becomes neutral in basic media. As a result, the use of this sensor for pH measurement is limited to pH < 9.

The photostability of the sensor was also examined by illuminating the film continuously in the Perkin-Elmer LS-50B spectrofluorometer with a 20 kW (8 μs duration) xenon discharge lamp for 2 h with the excitation bandwidth set to 15 nm. Figure 5.12 shows the plots of change in emission intensity of the sensing film when irradiating under pH 2.47 buffer solution. No diminution in emission intensity was observed after the experiment indicating that the photostability of the sensor is reasonably good.

The luminescence intensity of the sensor decreases with increase in the temperature of the sample solution. The luminescence intensity of the sensor decreases by about 11% when the temperature of a pH 3.38 buffer solution is raised from 21 to 34 °C. This is consistent with an increase in radiationless decay with the temperature.

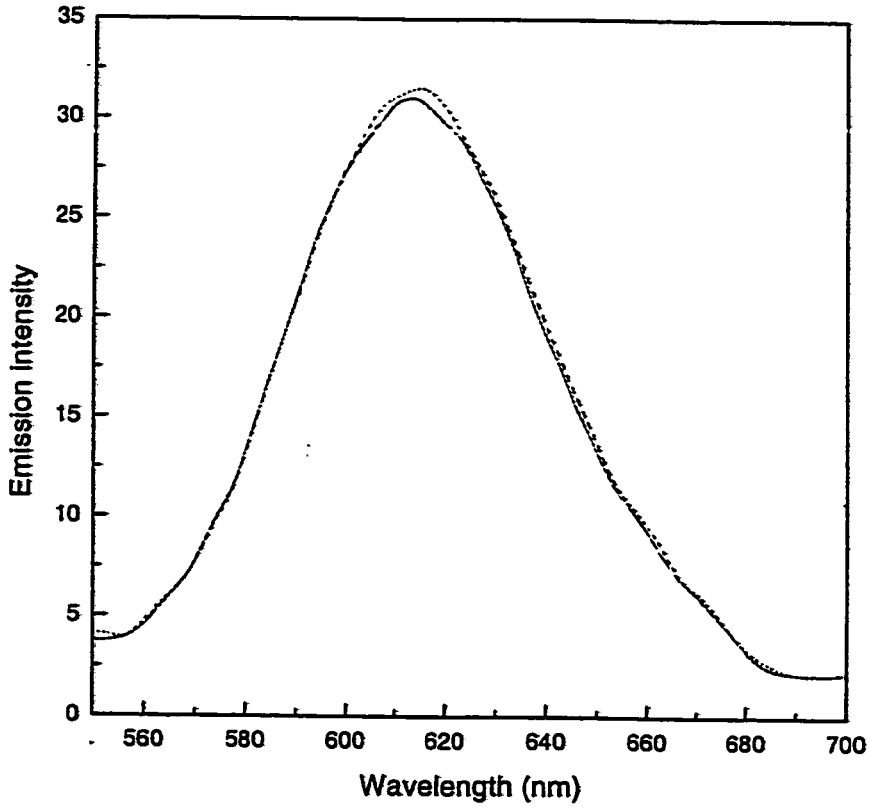

Figure 5.11 Emission spectra of the sensing film recorded on the first day (—) and after two weeks (—) in pH 3.38 buffer solution. Excitation wavelength: 415 nm.

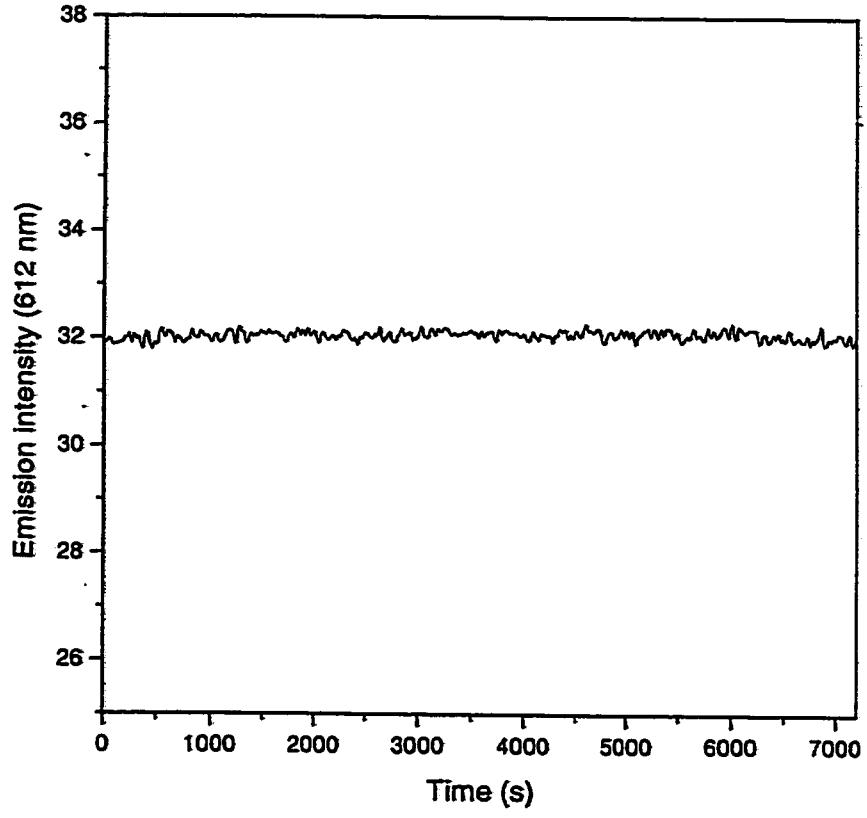

Figure 5.12 Change in emission intensity of sensing film when irradiating under pH 2.47 buffer solution. The excitation wavelength is 415 nm.

5.3.5 pH Monitoring of Fermentation

From the above results, it shows that the pH optode have many desirable features including high sensitivity, wide dynamic range (pH 1-8), good stability and minimal interference from metal cations and common anions. These features suggest that the sensor is potentially useful for pH monitoring of biological processes such as fermentation. In practice, the sensor response may be affected by the complex medium content which is usually colored and contains finely suspended particulates. Moreover, the growth in cell concentration during the fermentation process is another parameter that might interfere with the pH measurement (Junker et al, 1988; Kisaalita et al, 1991)

Figure 5.13 compares the calibration curves of the sensor taken in colorless buffer with that from a culture medium. It was noted that higher emission intensities are always obtained with the culture medium which can be attributed to background emission. The effect of cell concentration on the response was also investigated. The maximum cell density achieved in the fermentation was estimated to be about 0.8 g dry weight/L. The cells were separated from the culture by centrifuge, washed several times with deionized water to remove the broth residues and resuspended in deionized water. Different quantities of the washed cells were added to pH 4.4 and 6.7 buffer solutions and the emission intensities of the pH sensing film were measured. The results are shown in Figure 5.14. The emission intensity was found to increase with the cell concentration. This is probably due to light scattering which gives a high background emission.

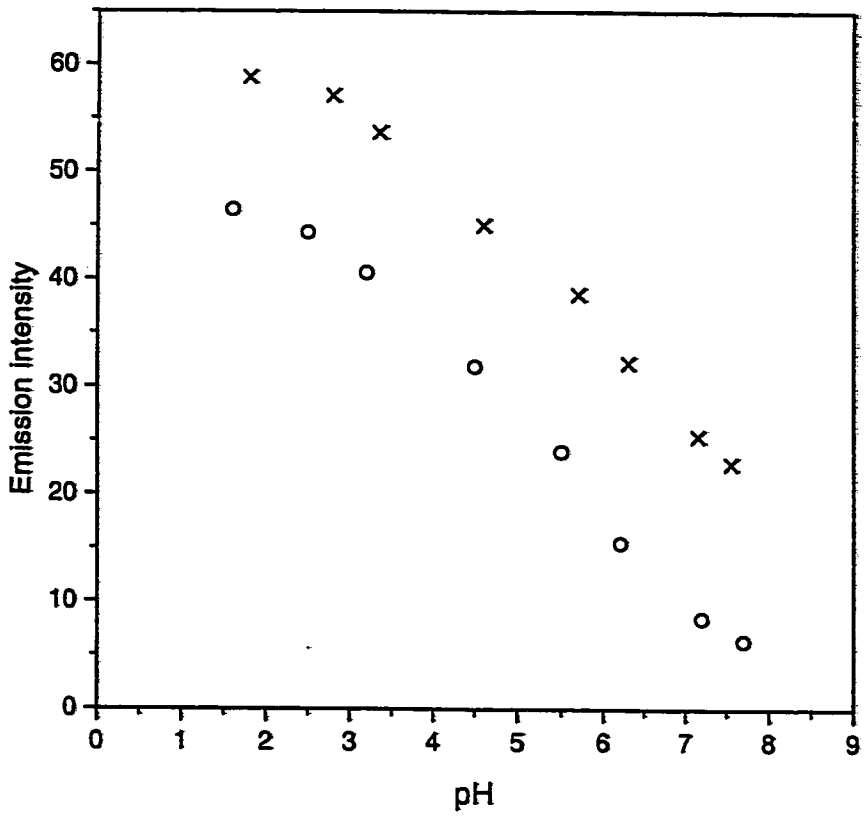

Figure 5.13 A comparison of the sensor responses in colorless buffer (o) and in fermentation medium (×). Excitation wavelength: 415 nm; the emission was monitored at 612 nm.

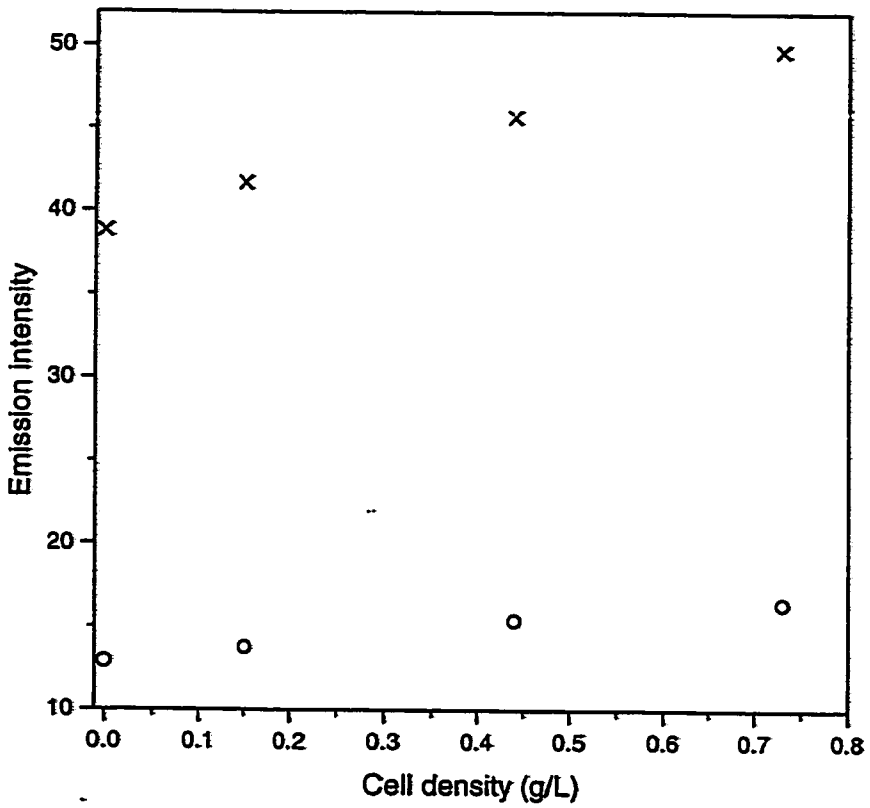

Figure 5.14 The effect of cell concentration on sensor response in the absence of filter membrane: (×) pH 4.4, (o) pH 6.7. Excitation wavelength: 415 nm; the emission was monitored at 612 nm.

In order to solve this background problem, a black microporous filter membrane was placed between the sensing film and the sample solution. A wire gauze was employed to keep the filter membrane in position (Figure 5.2). The membrane allows the passage of hydrogen ions into the sensing film but eliminates the scattered light from entering the detector. Figure 5.15 shows that the interference effect is substantially reduced after the addition of the black filter membrane.

In order to maintain culture purity, it is necessary to sterilize the apparatus before cultivation. Therefore, the sterilizability of the pH sensor is another important parameter to be considered before its application. The sensor placed inside the sealed quartz cuvette was steam-sterilized in an autoclave at 120°C for 20 minutes. Figure 5.16 shows that no significant change on the sensor response was observed after steam sterilizations. Calibration of the sensor was performed after sterilization by passing deaerated pH buffers through a microporous filter (0.45 μm pore size) into the cuvette containing the sterilized sensing film to avoid contamination.

After calibration of the sensor, on-line monitoring of fermentation was performed as described in the experimental section. Since the sensor response is affected by the oxygen concentration in the buffer solution, the fermentation was done in anaerobic condition so that the effect of dissolved oxygen concentration in the broth can be disregarded.

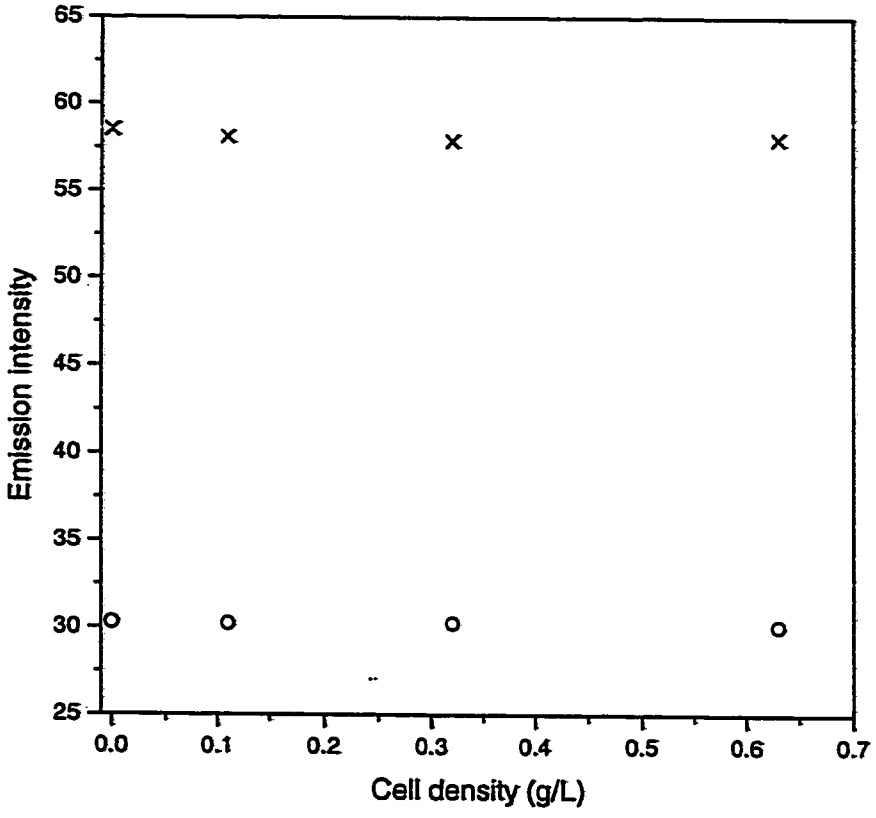

Figure 5.15 The effect of cell concentration on sensor response after addition of a black microporous filter membrane: (×) pH 4.0, (o) pH 6.1. Excitation wavelength: 415 nm; the emission was monitored at 612 nm.

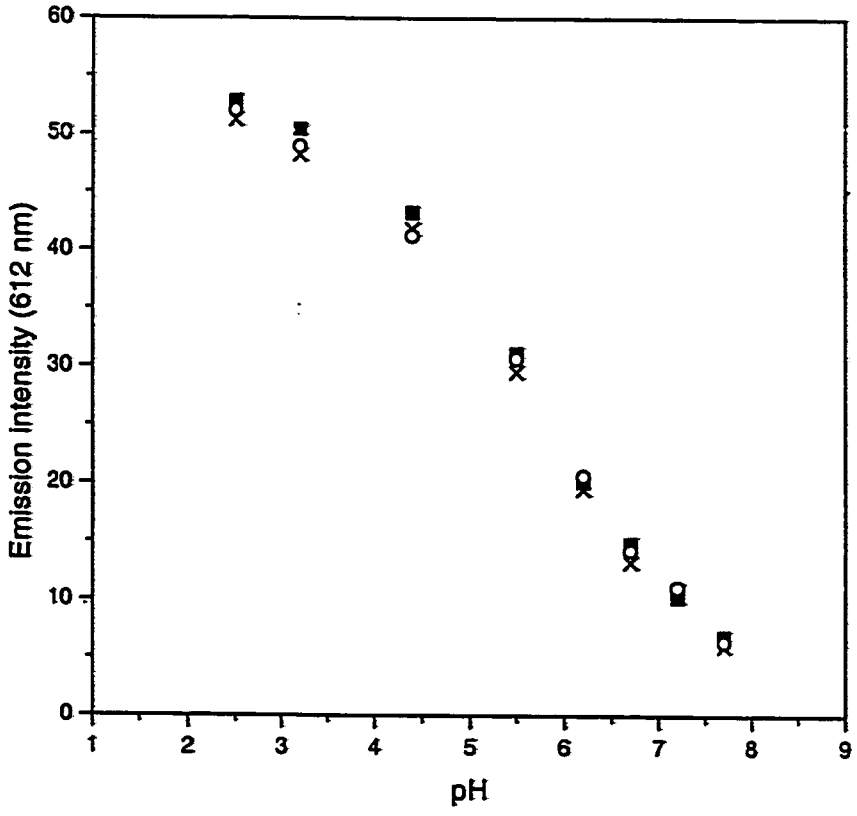

Figure 5.16 The sensor response before (■) and after 1st (×) and 2nd (o) steam sterilization. The excitation wavelength is 415 nm.

A comparison of the response from a conventional pH electrode with the optical pH sensor on the pH changes during fermentation was made. The results are shown in Figure 5.17. As the fermentation proceeds, the pH of the solution decreases gradually for about 15 h. After that period, the pH continuously increases and finally levels off. The initial fall and then rise in pH is consistent with the initial production of acidic products such as pyruvic acid followed by the conversion of pyruvic acid to neutral end-products such as acetoin and 2,3-butanediol by *Klebsiella pneumoniae* under anaerobic condition (Gottschalk, 1986). Our results showed that the response of the optical pH sensor correlated very well with the pH electrode with maximum disagreement of only 0.1 pH unit.

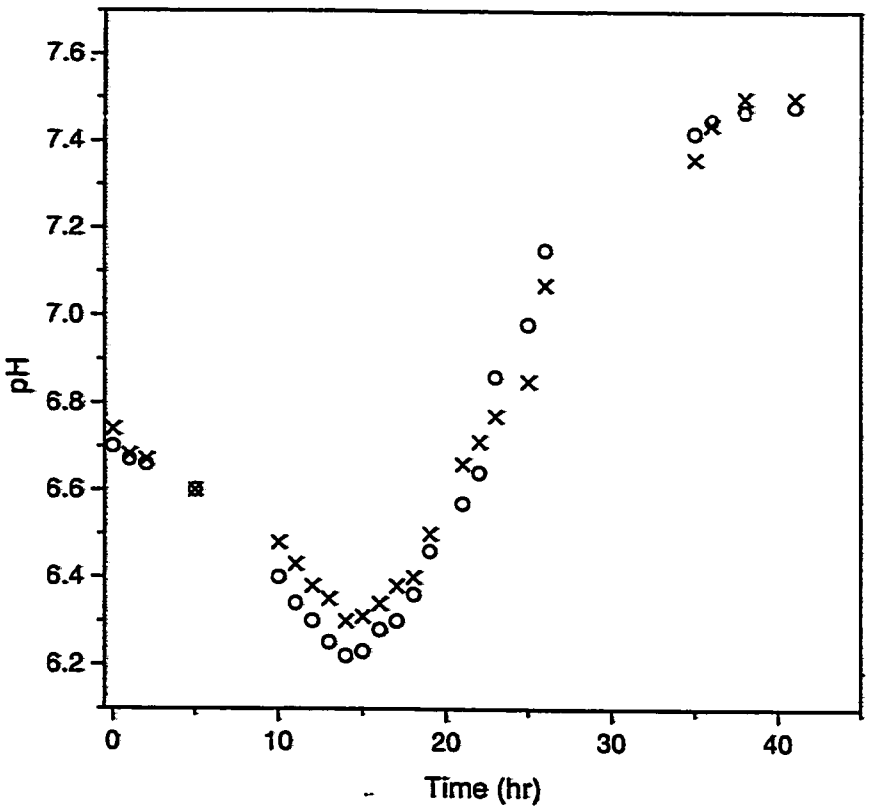

Figure 5.17 A comparison of the response from the pH optode (×) with a conventional pH electrode (o) during fermentation.

5.4 Concluding Remarks

We have demonstrated that the luminescent $[Ru(bpy)_2(dhphen)]^{2+}$ complex immobilized in Nafion film can be used as a luminescence-based pH sensor. This sensor exhibits advantages over many existing optical pH sensors including wider dynamic pH range (pH 1-8), ease of fabrication, good photostability and minimal interference from metal cations. The application of this pH optode to pH monitoring of fermentation by *Klebsiella pneumoniae* has been investigated. The interference from the medium can be eliminated by a black microporous filter membrane placed on top of the pH sensing film. The results obtained by the pH optode compared favorably with those measured by a conventional pH electrode with maximum disagreement of only 0.1 pH unit.

Chapter 6

Conclusions

There is a great demand on rapid and accurate toxicity methods for assessing the environmental impact of toxicants. Thus our ultimate goal is to develop a biosensor based on optical sensing of oxygen for toxicity monitoring. To achieve this, oxygen optode with desirable sensing properties must first be developed. We have demonstrated that an oxygen optode prepared by entrapping the $[Ru(Ph_2phen)_3^{2+}]$ adsorbed fumed silica in silicone rubber has superior sensing performance than that without fumed silica. The higher sensitivity (larger quenching ratio) of the sensing film is due to increased homogeneity of the film and stronger adsorption of oxygen in the support by the presence of high surface area hydrophilic fumed silica. In addition, the higher luminescence intensity and more linear Stern-Volmer calibration curve obtained from this optode make it suitable in the fabrication of an optical biosensor.

With the use of this oxygen optode, an optical scanning respirometer has been constructed to determine the toxicity of organic chemicals to activated sludge. The toxicity assessment is based on the inhibition of microbial respiration. In conjunction with optical fiber and other photo electronics, the rate of change in dissolved oxygen concentration (which is related to the degree of toxic effect) in the sample culture can be measured. IC_{50} values (concentration of a chemical that exhibits 50% respiration inhibition) of various substituted phenols, benzenes and alkanes were determined. Our results showed that the toxicity of phenolic chemical is higher than benzenes and alkanes. It is because phenolic compounds have stronger electronic interactions with cellular nucleophilies in the microorganism. Moreover, the reproducibility of this respirometer is comparable with other toxicity method such as ISO (B) and better than OECD method. On the other hand, the sensitivity of this method is dependent on the class of chemicals being tested. This respirometer is shown to be an effective

instrumentation for toxicity monitoring on activated sludge. In future studies, this respirometer can be extended to other biological applications such as yeast cell viability assay. Complementation in yeast is a newly developed method for identification of drug resistance genes in protozoan parasites, which facilitates the control of many diseases that are harmful to human. The IC_{50} estimation, conventionally done by the 96 well method, is necessary to identify drug sensitivity in different strains of yeast. The 96 well method is based on optical density measurement for growth of the yeast cells. It is subjected to interference from color or turbidity of the test sample and requires a rather long experimental time. Our respirometer based on measurement of oxygen consumption has the advantage of assaying a large number of samples in a short period of time.

In this study, QSARs (Quantitative Structure Activity Relationship) were also developed from the collected toxicity data on activated sludge. The value of QSARs lies in their ability to predict toxicity for untested compounds and to provide better insights on toxicity mechanisms. Multiple linear regression was used to correlate the toxicity with five different parameters including 1-octanol/water partition coefficient (log P), aqueous solubility (log S), molecular volume (V_i), molecular connectivity index (MCI) and combination of log P and ELUMO. The correlation results of log P and log S method are very similar. It is not unexpected as both parameters are related to hydrophobicity of the chemicals. They are quite successful to model substituted alkanes and benzenes, but not suitable for all chemicals together. Nevertheless, statistically significant equations can be obtained when eliminating phenolic chemicals in the correlation. The QSAR equations derived by molecular volume, molecular connectivity and combination of log P and ELUMO are most desirable as

they can cover all three classes of chemicals together. The molecular connectivity is simple to use while combination of log P and ELUMO provide better explanation on toxicity mechanism. The quality of the developed QSAR equations is further supported by the validation results. The ability of the models for predicting mixture toxicity has also been investigated. The use of MCI and log S are more accurate than other approaches in predicting mixture toxicity for all chemicals together and nonphenolic chemicals respectively. QSAR models covering as many chemical classes as possible are preferred for practical use. Further work is necessary to develop QSAR equations that can incorporate a larger range of chemicals such as amine, ester, ketone and acid.

The development of pH optode based on immobilization of luminescent metal organic complex $[Ru(bpy)_2(dhphen)]^{2+}$ (dhphen = 4,7-dihydroxy-1,10-phenanthroline) in Nafion has also been investigated in this project. The optode was found to display pH-dependent luminescent intensities. The emission intensity decreases gradually with increasing the pH of the solution from pH 1-8. The dye was stable inside the Nafion film over pH 1-9 and little leaching of dye was detected. Moreover, this optode has many desirable features including high sensitivity, good photostability and reproducibility and minimal interference from metal cations and common anions. We have also applied this pH optode to monitor the pH change in fermentation by *Klebsiella pneumoniae*. Our experimental results show that the responses of the optode are affected by the culture medium and cell concentration. These interference effects are substantially reduced after the addition of a black microporous filter membrane on top of the pH sensing film. For on-line pH monitoring of fermentation, the results obtained by the pH optode compared favorably with those measured by pH

electrode with maximum disagreement of only 0.1 pH unit. This system based on incorporation of pH-sensitive metal complex in polymer support as pH optode is relatively new, and hence has great potential to be developed. This pH optode is potentially useful for measuring pH in clinical and physiological studies in which no electrical connection to the human body is allowed.

References

Agayn, V. I. and Walt, D. R. "Fiber-optic sensor for continuous monitoring of fermentation pH". *Biotechnology*, Vol. 11, pp. 726-729 (1993).

Akers, K. S.; Sinks, G. D. and Schultz, T. W. "Structure-toxicity relationships for selected halogenated aliphatic chemicals". *Environmental Toxicology and Pharmacology*, Vol. 7, pp. 33-39 (1999).

Albery, W. J.; Hahn, C. E. W. and Brooks, W. N. "The polarographic measurement of halothane". *British Journal of Anaesthesia*, Vol. 53, pp. 447-454 (1981).

Anderson, K.; Koopman, B. and Bitton, G. "Evaluation of INT-dehydrogenase assay for heavy metal inhibition of activated sludge". *Water Research*, Vol. 22, pp. 349-353 (1988).

Bacci, M.; Baldini, F. and Bracci, S. "Spectroscopic behavior of acid-base indicators after immobilization on glass supports". *Applied Spectroscopy*, Vol. 45, pp. 1508-1515 (1991).

Bacci, M.; Baldini, F. and Scheggi, A. M. "Spectrophotometric investigations on immobilized acid-base indicators". *Analytica Chimica Acta*, Vol. 207, pp. 343-348 (1988).

Bacon, J. R. and Demas, J. N. "Determination of oxygen concentration by luminescence quenching of a polymer-immobilized transition metal complex". *Analytical Chemistry*, Vol. 59, pp. 2780-2785 (1987).

Badini, G. E.; Grattan, K. T. V. and Tseung, A. C. C. "Impregnation of a pH-sensitive dye into sol-gels for fibre optic chemical sensors". *Analyst*, Vol. 120, pp. 1025-1028 (1995).

Bates, M.; Feingold, A. and Gold, M. "The effects of anesthetics on an in-vivo oxygen electrode". *American Journal of Clinical Pathology*, Vol. 64, pp. 448-451 (1975).

Belsley, D. A.; Kuh, E. and Welsch, R. E., "Regression diagnostics: identifying influential data and sources of collinearity". Wiley, New York, 292pp (1980).

Bergman, I. "Rapid-response atmosphere oxygen monitor based on fluorescence quenching". *Nature*, Vol. 218, pp. 396 (1968).

Bitton, G. and Dutka, B. J. "*Toxicity Testing Using Microorganisms*". Vol. 1, CRC Press, Boca Raton, 265pp (1986).

Bláha, L., Damborsky, J. and Nemec, M. "QSAR for acute toxicity of saturated and unsaturated halogenated aliphatic compounds". *Chemosphere*, Vol. 36, pp. 1345-1365 (1998).

Blair, T. L.; Allen, J. R.; Daunert, S. and Bachas, L. G. "Potentiometric and fiber optic sensors for pH based on an electropolymerized cobalt porphyrin". *Analytical Chemistry*, Vol. 65, pp. 2155-2158 (1993).

Blum, D. J. W. "Chemical toxicity to environmental bacteria: quantitative structure activity relationships and interspecies correlations and comparisons" PhD thesis, Drexel University (1989).

Blum, D. J. W. and Speece, R. E. "A database of chemical toxicity to environmental bacteria and its use in interspecies comparisons and correlations". *Research Journal of Water Pollution Control Federation*, Vol. 63, pp. 198-207 (1991a).

Blum, D. J. W. and Speece, R. E. "Determining chemical toxicity to aquatic species". *Environmental Science and Technology*, Vol. 24, pp. 284-292 (1990).

Blum, D. J. W. and Speece, R. E. "Quantitative structure-activity relationships for chemical toxicity to environmental bacteria". *Ecotoxicology and Environmental Safety*, Vol. 22, pp. 198-224 (1991b).

Boisdè, G.; Blanc, F. and Perez, J. J. "Chemical measurements with optical fibers for process control". *Talanta*, Vol. 35, pp. 75-82 (1988).

Bolton, J. L.; Trush, M. A.; Penning, T. M.; Dryhurst, G. and Monks, T. J. "Role of quinones in toxicology". *Chemical Research in Toxicology*, Vol. 13, pp.135-160 (2000).

Broecker, B. and Zahn, R. "The performance of activated sludge plants compared with the results of various bacterial toxicity tests - a study with 3,5-dichlorophenol". *Water Research*, Vol. 12, pp. 165-172 (1977).

Brow, D.; Hitz, H. R. and Schäfer, L. "The assessment of the possible inhibitory effect of dye-stuffs on aerobic waste-water bacteria". Vol., 10, pp. 245-261 (1981).

Bulich, A. A. "Use of luminescent bacteria for determining toxicity in aquatic environments". In Markings, L. L. and Kimerle, R. A., eds., *Aquatic Toxicology*, American Society for Testing and Materials, Philadelphia, pp. 98-112 (1979).

Cab-O-Sil Untreated Fumed Silica Properties and Functions, Cabot Corporation, Illinois, (1993).

Cajina-Quezada, M. and Schultz, T. W. "Structure-toxicity relationships for selected weak acid respiratory uncouplers". *Aquatic Toxicology*, Vol. 17, pp. 239-252 (1990).

Camara, C., Moreno, M. C. and Orellana, G. "Chemical sensing with fiberoptic devices". In Wise, D. L. and Wingard, L. B. eds., *Biosensors with Fiberoptics*. Humana Press, Clifton, New Jersey, pp. 29-84 (1991).

Cardwell, T. J.; Cattrall, R. W.; Deady, L. W.; Dorkos, M. and O'Connell, G. R. "A fast response membrane-based pH indicator optode". *Talanta*, Vol. 40, pp. 765-768 (1993).

Cardwell, T. J.; Cattrall, R. W.; Deady, L. W.; Dorkos, M.; Kaye, A, J. and Papanikos, A. "Cellulose acetate-based pH indicator optodes". *Austrian Journal of Chemistry*, Vol. 48, pp. 1081-1087 (1995).

Carey, W. P. and Jorgensen, B. S. "Optical sensors for high acidities based on fluorescent polymers". *Applied Spectroscopy*. Vol. 45, pp. 834-838 (1991).

Cargill Thompson, A. M. W.; Smailes, M. C. C.; Jeffery, J. C. and Ward, M. D. "Ruthenium tris-(bipyridyl) complexes with pendant protonable and deprotonatable moieties: pH sensitivity of electronic spectral and luminescence properties". *Journal of Chemical Society, Dalton Transactions*, pp. 737-743 (1997).

Carraway, E. R.; Demas, J. N. and DeGraff, B. A. "Luminescence quenching mechanism for microheterogeneous systems". *Analytical Chemistry*, Vol. 63, pp. 332-336 (1991b).

Carraway, E. R.; Demas, J. N. and DeGraff, B. A. "Photophysics and oxygen quenching of transition-metal complexes on fumed silica". *Langmuir*, Vol. 7, pp. 2991-2998 (1991a).

Carraway, E. R.; Demas, J. N.; DeGraff, B. A. and Bacon, J. R. "Photophysics and photochemistry of oxygen sensors based on luminescent transition-metal complexes". *Analytical Chemistry*, Vol. 63, pp. 337-342 (1991c).

Clark, L. C. "Monitor and control of blood and tissue oxygen tensions". *Transactions American Society for Artificial Internal Organs*, Vol. 2, pp. 41-57 (1956).

Costa-Fernandez, J. M.; Diaz-Garcia, M. E. and Sanz-Medel, A. "Sol-gel immobilized room-temperature phosphorescent metal-chelate as luminescent oxygen sensing material". *Analytica Chimica Acta*, Vol. 360, pp. 17-26 (1998).

Cronin, M. T. D. and Dearden, J. C. "QSAR in toxicology. 1. Prediction of aquatic toxicity". *Quantitative Structure-Activity Relationship*, Vol. 14, pp. 1-7 (1995).

Davis, M. L. and Cornwell, D. A. *Introduction to environmental engineering*. 2nd ed., McGraw-Hill, New York, 822pp (1991).

Deardon, J. C.; Nicholson, R. M. " The prediction of biodegradability by the use of quantitative structure-activity relationships-correlation of biological oxygen-demand with atomic charge difference". *Pesticide Science*, Vol. 17, pp. 305-310 (1986).

Demas, J. N. and DeGraff, B. A. "Design and applications of highly luminescent transition metal complexes". *Analytical Chemistry*, Vol. 63, pp. 829A-837A (1991).

Demas, J. N.; DeGraff, B. A. and Coleman, P. B. "Oxygen sensors based on luminescence quenching". *Analytical Chemistry News & Features*, pp. 793A-800A (1999).

Demas, J. N.; DeGraff, B. A. and Xu, W. "Modeling of luminescence quenching-based sensors: comparison of multisite and nonlinear gas solubility models". *Analytical Chemistry*, Vol. 67, pp. 1377-1380 (1995).

Dewar, M. J. S.; Zoebisch, E. G.; Healy, E. F. and Stewart, J. J. P. "The development and use of quantum-mechanical molecular-models. 76. AM1- A new general-purpose quantum-mechanical molecular-model". *Journal of the American Chemical Society*, Vol. 107, pp. 3902-3909 (1985).

Draxler, S. and Lippitsch, M. E. "pH sensors using fluorescence decay time". *Sensors and Actuators B*, Vol. 29, pp. 199-203 (1995).

Draxler, S.; Lippitsch, M. E. "Optical pH sensors using fluorescence decay time". *Sensors and Actuators B*, Vol. 11, pp. 421-424 (1993).

Dutka, B. J.; Nyholm, N. and Petersen, J. "Comparison of several microbiological toxicity screening tests". *Water Research*, Vol. 17, pp. 1363-1368 (1983).

Ensafi, A. A. and Kazemzadeh, A. "Optical pH sensor based on chemical modification of polymer film". Vol. 63, pp. 381-388 (1999).

Evans, M. R.; Jordinson, G. M.; Rawson, D. M. and Rogerson, J. G. "Biosensors for the measurement of toxicity of wastewaters to activated sludge". *Pesticide Science*, Vol. 54, pp. 447-452 (1998).

Fuh, M. R. S.; Burgess, L. W.; Hirschfeld, T.; Christian, G. D. and Wang, F. "Single fiber optic fluorescence pH probe". *Analyst*, Vol. 112, pp.1159-1163 (1987).

Gabor, G.; Chadha, S. and Walt, D. R. "Sensitivity enhancement of fluorescent pH indicators using pH-dependent energy transfer". *Analytica Chimica Acta*, Vol. 313, pp. 131-137 (1995).

Ge, Z. F.; Brown, C. W.; Sun, L. F. and Yang, S. C. "Fiberoptic pH sensor-based on evanescent-wave absorption-spectroscopy". *Analytical Chemistry*, Vol. 65, pp. 2335-2338 (1993).

Giordano, P. J.; Bock, C. R. and Wrighton, M. S. "Excited state proton transfer of ruthenium(II) complexes of 4,7-dihydroxy-1,10-phenanthroline. Increased acidity in the excited state". *Journal of the American Chemical Society*, Vol. 100, pp. 6960-6965 (1978).

Gosh, M. M. and Zugger, P. D. "Toxic effect of mercury on the activated sludge process". *Journal of Water Pollution Control Federation*, Vol. 45, pp. 424-429 (1973).

Gottlieb, A.; Divers, S. and Hui, H. K. "In vivo applications of fiberoptic chemical sensors". In Wise, D. L. and Wingard, L. B. eds., *Biosensors with Fiberoptics*, Humana Press, Clifton, New Jersey, pp.325-366 (1991).

Gottschalk, G. "Bacterial fermenations". In Gottschalk, G. ed., *Bacterial Metabolism*, 2nd ed., Springer-Verlag, New York, pp.208-282 (1986).

Grant, S. A. and Glass, R. S. "A sol-gel based fiber optic sensor for local blood pH measurements". *Sensors and Actuators B*, Vol. 45, pp. 35-42 (1997).

Grigg, R. and Norbert, W. D. J. A. "Luminescent pH sensors based on di(2,2'-bipyridyl) (5,5'-diaminomethyl-2,2'-bipyridyl)-ruthenium(II) complexes". *Journal of Chemical Society, Chemical Communication*, pp. 1300-1302 (1992a).

Grigg, R. and Norbert, W. D. J. A. "The proton-controlled fluorescence of aminomethyltetraphenylporphyrin-tin(IV) derivatives". *Journal of Chemical Society, Chemical Communication*, pp. 1298-1230 (1992b).

Grigg, R.; Holmes, J. M.; Jones, S. K. and Norbert, W. D. J. A. "Luminescent pH sensors based on p-tert-butylcalix[4]arene-linked ruthenium(II) trisbipyridyl complexes". *Journal of Chemical Society, Chemical Communication*, pp. 185-187 (1994).

Grummt, U. W.; Pron, A.; Zagorska, M. and Lefrant, S. "Polyaniline based optical pH sensor". *Analytica Chimica Acta*, Vol. 357, pp. 253-259 (1997).

Gupta, B. D. and Sharma, S. "A long-range fiber optic pH sensor prepared by dye doped sol-gel immobilization technique". *Optics Communications*, Vol. 154, pp. 282-284 (1998).

Hall, E.; Sun, B.; Prakash, J. and Nirmalakhandan, N. "Toxicity of organic chemicals and their mixtures to activated sludge microorganisms". *Journal of Environmental Engineering*, Vol. 122, pp. 424-429 (1996).

Hansch, C., Leo, A. and Hoekman, D. "Exploring QSAR Hydrophobic, Electronic, and Steric Constants". American Chemical Society, Washington, 348pp (1995).

Hartmann, P. and Trettnak, W. "Effects of polymer matrices on calibration functions of luminescent oxygen sensors based on porphyrin ketone complexes". *Analytical Chemistry*, Vol. 68, pp. 2615-2620 (1996).

Hartmann, P; Leiner, M. J. P. and Lippitsch, M. E. "Luminescence quenching behavior of an oxygen sensor based on a Ru (II) complex dissolved in polystyrene". *Analytical Chemistry*, Vol. 67, pp. 88-93 (1995).

Hermens, J.; Busser, F.; Leeuwangh, P. and Musch, A. "Quantitative structure-activity relationships and mixture toxicity of organic chemicals in *Photobacterium phosphoreum*: The Microtox test.". *Ecotoxicology and Environmental Safety*, Vol. 9, pp. 17-25 (1985)

Hickey, J. P. and Passino-Reader, D. R. "Linear solvation energy relationships: rules of thumb for estimation of variable values". *Environmental Science and Technology*, Vol. 25, pp. 1753-1760 (1991).

Howard, P. H. and Meylan, W. M. "Handbook of Physical Properties of Organic Chemicals". Lewis Publishers, Boca Raton, 1585pp (1997).

International Standards Organization, *Test for Inhibition of Oxygen Consumption by Activated Sludge*, ISO Method 8192A (1986).

Jing, B.; Song, A.; Zhang, M. and Shen, T. "Luminescent pH sensors based on $Ru(bpy)_2L^{2+}$ where L are imidazo[f]1,10-phenanthrolines". *Chemistry Letters*, pp. 789-790 (1999).

Jones, T. P. and Porter, M. D. "Optical pH sensor based on the chemical modification of a porous polymer film". *Analytical Chemistry*, Vol. 60, pp. 404-406 (1988).

Jordan, D. M.; Walt, D. R. and Milanovich, F. P. "Physiological pH fiber-optic chemical sensor based on energy transfer". *Analytical Chemistry*, Vol. 59, pp. 437-439 (1987).

Junker, B. H.; Wang, D. I. C. and Hatton, T. A. "Fluorescence sensing of fermentation parameters using fiber optics". *Biotechnology and Bioengineering*, Vol. 32, pp. 55-63 (1988).

Kaiser, K. L. E. and Ribo, J. M. "*Photobacterium Phosphoreum* toxicity bioassay. II. Toxicity data compilation". *Toxicity Assessment*, Vol. 2, (1987).

Kamlet, M. J.; Doherty, R. M.; Veith, G. D.; Taft, R. W. and Abraham, M. H. "Solubility properties in polymers and biological media. 7. An analysis of toxicant properties that influence inhibition of bioluminescence *Photobacterium phosphoreum* (The Microtox Test)". *Environmental Science and Technology*, Vol. 20, pp. 690-695 (1986).

Kautsky, H.; Hirsch, A. and Davidshöfer, F. "Energie-Umwandlungen an Grenzflächen". *Berichte. Deutsche Chemische Gesellschaft*, Vol. 65, pp. 1762-1770 (1932).

Kavandi, J.; Callis, J.; Gouterman, M.; Khalil, G.; Wright, D.; Green, E.; Burns, D. and Mclachlan, B. "Luminescent barometry in wind tunnels". *Review of Scientific Instruments*, Vol. 61, pp. 3340-3347 (1990).

Khalili, G. E.; Gouterman, M. P. and Green, E. "Method of measuring oxygen concentration". *United States Patent*, 4 810 655, (1989).

Kier, L. B. and Hall, L. H. "Derivation and significance of valence molecular connectivity". *Journal of Pharmaceutical Sciences*. Vol. 70, pp. 583-589 (1981).

Kier, L. B. and Hall, L. H. "*Molecular Connectivity in Chemistry and Drug Research*". Academic Press, New York, 257pp (1976).

Kier, L. B. and Hall, L. H. "*Molecular Connectivity in Structure Activity Analysis*". Research Studies Press, Hertfordshire, 262pp (1986).

Kilroy, A. C. and Gary, N. F. "The toxicity of four organic solvents commonly used in the pharmaceutical industry to activated sludge". *Water Research*, Vol. 26, pp. 887-892 (1992).

King, E. F. and Dutka, B. J. "Respirometric techniques". In Dutka, B. J. and Bitton, G. eds., *Toxicity Testing Using Microorganisms*, Vol. 1, CRC Press, Boca Raton, pp. 75-112 (1986).

King, E. F. and Painter, H. A. "Inhibition of respiration of activated sludge: variability and reproducibility of results". *Toxicity Assessment*, Vol. 1, pp. 27-39 (1986).

Kirkbright, G. F.; Narayanaswamy, R. and Welti, N. A. "Fibre-optic pH probe based on the use of an immobilised colormetric indicator". *Analyst*, Vol. 109, pp. 1025-1028 (1984).

Kisaalita, W. S.; Slininger, P. J.; Bothast, R. J.; McCarthy, J. F. and Magin, R. L. "Application of fiber-optic fluorescence measurements to on-line pH monitoring of a *Pseudomonae* fermentation process". *Biotechnology Progress*, Vol. 7, pp. 564-569 (1991).

Klecka, G. M.; Landi, L. P. and Bodner, K. M. "Evaluation of the OECD activated sludge, respiration inhibition test". *Chemosphere*, Vol. 14, pp. 1239-1251 (1985).

Klimant, I. and Wolfbeis, O. S. "Oxygen-sensitive luminescent materials based on silicone-soluble ruthenium diimine complexes". *Analytical Chemistry*, Vol. 67, pp. 3160-3166 (1995).

Klimant, I.; Belser, P. and Wolfbeis, O. S. "Novel metal-organic ruthenium(II) diimine complexes for use as longwave excitable luminescent oxygen probes". *Talanta*, Vol. 41, pp. 985-991 (1994).

Kneas, K. A.; Xu, W.; Demas, J. N. and DeGraff, B. A. "Oxygen sensors based on luminescence quenching: interactions of tris(4,7-diphenyl-1,10-phenanthroline) ruthenium(II) chloride and pyrene with polymer supports". *Applied Spectroscopy*, Vol. 51, pp. 1346-1351 (1997).

Koch, R. "Molecular connectivity and acute toxicity of environmental pollutants". *Chemosphere*, Vol. 11, pp. 925-931 (1982).

Könemann, H. "Fish toxicity tests with mixtures of more than two chemicals; a proposal for a quantitative approach and experimental results". *Toxicology*, Vol. 19, pp. 229-238 (1981a).

Könemann, H. "Quantitative structure-activity relationships in fish toxicity studies part 1: relationship for 50 industrial pollutants". *Toxicology*, Vol. 19, pp. 209-221 (1981b).

Kong, Z.; Vanrolleghen, P. A. and Verstraete, W. "An activated sludge-based biosensor for rapid IC_{50} estimation and on-line toxicity monitoring". *Biosensors and Bioelectronics*, Vol. 8, pp. 49-58 (1993).

Koopman, B. and Bitton, G. "Toxicant screening in wastewaters". In Dutka, B. J. and Bitton, G. eds., *Toxicity Testing Using Microorganisms*, Vol. 2, CRC Press, Boca Raton, pp. 101-132 (1986).

Kosch, U.; Klimant, I. And Wolfbeis, O. S. "Long-lifetime based pH micro-optodes without oxygen interference". *Fresenius Journal of Analytical Chemistry*, Vol. 364, pp. 48-53 (1999).

Kosch, U.; Klimant, I.; Werner, T. and Wolfbeis, O. S. "Strategies to design pH optodes with luminescence decay times in the microsecond time regime". *Analytical Chemistry*, Vol. 70, pp. 3892-3897 (1998).

Kostov, Y. and Tzonkov S. "Membranes for optical pH sensors". *Analytica Chimica Acta*, Vol. 280, pp. 15-19 (1993).

Lai, Y. K. and Wong, K. Y. "The electrocatalytic oxidation of methanol by a ruthenium (V) oxo complex". Vol. 38, pp. 1015-1021 (1993).

Lakowicz, J. R.; Szmacinski, H. and Karakelle, M. "Optical sensing of pH and pCO_2 using phase-modulation fluorimetry and resonance energy transfer". *Analytica Chimica Acta*, Vol. 272, pp. 179-186 (1993).

Larson, R. J. and Schaeffer, S. L. "A rapid method for determining the toxicity of chemicals to activated sludge". *Water Research*, Vol. 16, pp. 675-680 (1982).

Lau, R. C. W; Choi, M. M. F. and Lu, J. "Alcohol sensing membrane based on immobilized ruthenium(II) complex in carboxylated PVC and surface covalently bonded alcohol oxidase". *Talanta*, Vol. 48, pp. 321-331 (1999).

Lee, J. E. and Saavedra, S. S. "Evanescent sensing in doped sol-gel glass films". *Analytica Chimica Acta*, Vol. 285, pp. 265-269 (1994).

Lee, W. W. S.; Wong, K. Y. and Li, X. M. "Luminescent dicyanoplatinum (II) complexes as sensors for the optical measurement of oxygen concentrations". *Analytical Chemistry*, Vol. 65, pp. 255-258 (1993a).

Lee, W. W. S.; Wong, K. Y.; Li, X. M.; Leung, Y. B.; Chan, C. S. and Chan, K. S. "Halogenated platinum porphyrins as sensing materials for luminescence-based oxygen sensors". *Journal of Material Chemistry*, Vol. 3, pp. 1031-1035 (1993b).

Leegwater, D. C. "QSAR-analysis of acute toxicity of industrial pollutants to the guppy using molecular connectivity indices". *Aquatic Toxicology*, Vol. 15, pp. 157-168 (1989).

Lehmann, H.; Schwotzer, G.' Czerney, P. and Mohr, G. J. "Fiber-optic pH meter using NIR dye". *Sensors and Actuators B*, Vol. 29, pp. 392-400 (1995).

Leiner, M. J. P. and Hartmann, P. "Theory and practice in optical pH sensing". *Sensors and Actuators B*, Vol. 11, pp. 281-289 (1993) and reference therein.

Leiner, M. J. P. and Wolfbeis, O. S. "Fiber optic pH sensors". In Wolfbeis, O. S. ed., *Fiber Optic Chemical Sensors and Biosensors*, Vol. I, CRC Press, Boca Raton, pp. 359-384 (1991).

Li, L. and Walt, D. R. "Dual-analyte fiber-optic sensor for the simultaneous and continuous measurement of glucose and oxygen". *Analytical Chemistry*, Vol. 67, pp. 3746-3752 (1995).

Li, X. and Rosenzweig, Z. "A fiber.optic sensor for rapid analysis of bilirubin in serum". *Analytica Chimica Acta*, Vol. 353, pp.263-273 (1997).

Li, X. M. and Wong, K.Y. "Luminescent platinum complex in solid films for optical sensing of oxygen". *Anaytical Chimica Acta*, Vol. 262, pp. 27-32 (1992)

Li, X. M.; Ruan, F. C. and Wong, K. Y. "Optical Characteristics of a ruthenium(II) complex immobilized in a silicone rubber film for oxygen measurement". *Analyst*, Vol. 118, pp. 289-292 (1993).

Li, X. M.; Ruan, F. C.; Ng, W. Y. and Wong, K. Y. "Scanning optical sensor for the measurement of dissolved oxygen and BOD". *Sensors and Actuators B*, Vol. 21, pp. 143-149 (1994).

Li, X.; Fortuney, A.; Guilbault, G. G. and Suleiman, A. A. "Determination of bilirubin by fiberoptic biosensor". *Analytical Letters*, Vol. 29, pp. 171-180 (1996).

Lin, C. T.; Böttcher, W.; Chou, M.; Creutz, C and Sutin, N. "Mechanism of the quenching of the emission of substituted polypyridineruhenium(II) complexes by iron(III), chromium(III), and Europium(III) ions". *Journal of the American Chemical Society*, Vol. 98, pp. 6536-6544 (1976).

Liu, D.; Thomson, K. and Kaiser, K. L. E. "Quantitative structure-toxicity relationship of halogenated phenols on bacteria". *Bulletin Environmental Contamination Toxicology*, Vol. 29, pp. 130-136 (1982).

Luehrs, D. C.; Hickey, J. P.; Nilsen, P. E.; Godbole, K. A. and Rogers, T. N. "Linear solvation energy relationship of the limiting partition coefficient of organic solutes between water and activated carbon". *Environmental Science and Technology*, Vol. 30, pp. 143-152 (1996).

Marazuela, M. D. and Moreno-Bondi, M. C. "Determination of choline-containing phospholipids in serum with a fiber-optic biosensor". *Analytica Chimica Actal*, Vol. 374, pp. 19-29 (1998).

Marazuela, M. D.; Cuesta, B.; Moreno-Bondi, M. C. and Quejido, A. "Free cholesterol fiber-optic biosensor for serum samples with simplex optimization". *Biosensors and Bioelectronics*, Vol. 12, pp. 233-240 (1997).

Marco, G. D.; Lanza, M.; Mamo, A.; Stefio, I.; Pietro, C. D.; Romeo, G. and Campagna, S. "Luminescent mononuclear and dinuclear iridium(III) cyclometalated complexes immobilized in a polymeric matrix as solid-state oxygen sensors". *Analytical Chemistry*, Vol. 70, pp. 5019-5023 (1998).

Marcos, S. D. and Wolfbeis, O, S, "Optical sensing of pH based on polypyrrole films". *Analytica Chimica Acta*, Vol. 334, pp. 149-153 (1996).

McFarland, J. W., "On the parabolic relationship between drug potency and hydrophobicity". *Journal of Medicinal Chemistry*, Vol. 13, pp. 1092-1196 (1970).

McNamara, K. P.; Li, X.; Stull, A. D. and Rosenzweig, Z. "Fiber-optic oxygen sensor based on the fluorescence quenching of tris (5-acrylamido, 1,10-phenanthroline) ruthenium chloride". *Analytica Chimica Acta*, Vol. 361, pp. 73-83 (1998).

Megharaj, M.; Pearson, H. W. and Venkateswarlu, K. "Toxicity of phenol and three nitrophenols towards growth and metabolic activities of *Nostoc linckia*, isolated from soil". *Archives of Environmental Contamination and Toxicology*, Vol. 21, pp. 578-584 (1991).

Meier, B.; Werner, T.; Klimant, I. and Wolfbeis, O. S. "Novel oxygen sensor material based on a ruthenium bipyridyl complex encapsulated in zeolite Y: dramatic differences in the efficiency of luminescence quenching by oxygen on going from surface-adsorbed to zeolite-encapsulated fluorophores". *Sensors and Actuators B*, Vol. 29, pp. 240-245 (1995).

Miller, M. T. and Karpishin, T. B. "Oxygen sensing by photoluminescence quenching of a heteroleptic copper (I) bis(phenanthroline) complex immobililzed in polystyrene". *Sensors and Actuators B*, Vol. 61, pp. 222-224 (1999).

Mills, A. "Optical oxygen sensors utilising the luminescence of platinum metals complexes". *Platinum Metals Review*, Vol. 41, pp. 115-127 (1997).

Mills, A. and Lepre, A. "Controlling the response characteristics of luminescent porphyrin plastic film sensors for oxygen". *Analytical Chemistry*, Vol. 69, pp.4653-4659 (1997).

Mills, A. and Thomas, M. "Effect of plasticizer viscosity on the sensitivity of an $[Ru(bpy)_3^{2+}(Ph_4B^-)_2]$-based optical oxygen sensor". *Analyst*, Vol. 123, pp. 1135-1140 (1998).

Mills, A. and Thomas, M. "Fluorescence-based thin plastic film ion-pair sensors for oxygen". *Analyst*, Vol. 122, pp. 63-68 (1997).

Mills, A. and Williams, F. C. "Chemical influences on the luminescence of ruthenium diimine complexes and its response to oxygen". *Thin Solid Films*, Vol. 306, pp. 163-170 (1997).

Mills, A; Lepre, A.; Theobald, B. R. C.; Slade, E. and Murrer, B. A. "Use of luminescent gold compounds in the design of thin-film oxygen sensors". *Analytical Chemistry*, Vol. 69, pp. 2842-2847 (1997).

Mimms, L. T.; McKnight, M. A. and Murray, M. W. "Spectrophotometic study of coverage and acid-base equilibrium of a chemically bonded base". *Analytica Chimica Acta*, Vol. 89, pp. 355-361 (1977).

Mohr, G. J. and Wolfbeis, O. S. "Optical sensors for a wide pH range based on azo dyes immobilized on a novel support". *Analytica Chimica Acta*, Vol. 292, pp. 41-48 (1994).

Montgomery, H. A. C. "The determination of biochemical oxygen demand by respirometric methods". *Water Research*, Vol. 1, pp. 631-662 (1967).

Moreno, M. C.; Jimenez, M.; Conde, C. P. and Cámara, C. "Analytical performance of an optical pH sensor for acid-base titration". *Analytia Chimica Acta*, Vol. 230, pp. 35-40 (1990).

Moreno, M. C.; Martinez, A.; Millan, P. and Camara, C. "Study of a pH sensitive optical fiber sensor based on the use of cresol red". *Journal of Molecular Structure*, Vol. 143, pp. 553-556 (1986).

Moreno-Bondi, M. C.; Wolfbeis, O. S.; Leiner, M. J. P. and Schaffan, B. P. H. "Oxygen optrode for use in a fiberoptic glucose biosensor". *Analytical Chemistry*, Vol. 62, pp. 2377-2380 (1990).

Munkholm, C.; Walt, D. R.; Milanovich, F. P. and Klainer, S. M. "Polymer modification of fiber optic chemical sensors as a method of enhancing fluorescence signal for pH measurement". *Analytical Chemistry*, Vol. 58, pp. 1427-1430 (1986).

Murtaza, Z; Chang, Q; Rao, G.; Lin, H. and Lakowicz, J. R. "Long-lifetime metal-ligand pH probe". *Analytical Biochemistry*, Vol. 247, pp. 216-222 (1997).

Nirmalakhandan, N. and Speece R. E. "Structure-activity relationships: Quantitative techniques for predicting the behavior of chemicals in the ecosystem". *Environmental Science and Technology*, Vol. 22, pp. 606-615 (1988).

Nirmalakhandan, N.; Arulgnanendran, V.; Mohsin, M.; Sun, B. and Cadena, F. "Toxicity of mixtures of organic chemicals to microorganisms". *Water Research*, Vol. 28, pp. 543-551 (1994a).

Nirmalakhandan, N.; Peace, J.; Egemen, E.; Mohsin, M.; Sun, B. and Hall, E. "Estimating toxicity of mixtures of organic chemicals to activated sludge using surrogate test cultures". *Water Science Technology*, Vol. 34, pp. 87-92 (1996).

Nirmalakhandan, N.; Sun, B.; Arulgnanendran, V. J.; Mohsin, M.; Wang, X. H.; Prakash, J. and Hall, N. "Analyzing and modeling toxicity of mixtures of organic chemicals to microorganisms". *Water Science and Technology*, Vol. 30, pp. 87-96 (1994b).

Offenbacher, H.; Wolfbeis, O. S. and Fürlinger, E. "Fluorescence optical sensors for continuous determination of near-neutral pH values". *Sensors and Actuators*, Vol. 9, pp. 73-84 (1986).

Okey, R. W: and Martis, M. C. "Molecular level studies on the origin of toxicity: identification of key variables and selection of descriptors". *Chemosphere*, Vol. 38, pp. 1419-1427 (1999).

Organization for Economic Cooperation and Development, Method 209, Activated sludge respiration inhibition test, adopted April 4, 1984. *OECD Guidelines for Testing of Chemicals*, Paris (1984).

Papkovsky, D. B; Yaropolov, A. I., Savitskii, A. P.; Olah, J.; Rumyantseva, V. D.; Mironov, A. F.; Troyanovskii, I. V. and Sadovskii, N. A. "Fiber-optic oxygen sensor based on phosphorescence quenching". *Biomedical Science*, Vol. 2, pp. 536-539 (1991).

Papkovsky, D. B. "Luminescent porphyrins as probes for optical (bio) sensors". *Sensors and Actuators B*, Vol. 11, pp. 293-300 (1993).

Papkovsky, D. B.; Olah, J.; Troyanovsky, I. V.; Sadovsky, N. A.; Rumyantseva, V. D.; Mironov, A. F.; Yaropolov, A. I. and Savitsky, A. P. "Phosphorescent polymer films for optical oxygen sensors". *Biosensors and Bioelectronics*, Vol. 7, pp. 199-206 (1992).

Papkovsky, D. B.; O'Riordan, T. C. and Guilbault, G. G. "An immunosensor based on the glucose oxidase label and optical oxygen detection". *Analytical Chemistry*, Vol. 71, pp. 1568-1573 (1999).

Papkovsky, D. B.; Ponomarev, G. V.; Trettnak, W. and O'Leary, P. "Phosphorescent complexes of porphyrin ketones: optical properties and application to oxygen sensing". *Analytical Chemistry*, Vol. 67, pp. 4112-4117 (1995).

Parker, J. W.; Laksin, O.; Yu, C.; Lau, M. L.; Klima, S.; Fisher, R.; Scott, I. and Atwater, B. W. "Fiber-optic sensors for pH and carbon dioxide using a self-referencing dye". *Analytical Chemistry*, Vol. 65, pp. 2329-2334 (1993).

Peterson, J. I.; Fitzgerald, R. V. and Buckhold, D. K. "Fiber-optic probe for in vivo measurement of oxygen partial pressure". *Analytical Chemistry*, Vol. 56, pp. 62-67 (1984).

Peterson, J. I.; Goldstein, S. R.; Fitzgerald, R. V. and Buckhold, D. K. "Fiber optic pH probe for physiological use". *Analytical Chemistry*, Vol. 52, pp. 864-869 (1980).

Pollak, M.; Pringsheim, P. and Terwoord, D. "A method of determining small quantities of oxygen". *The Journal of Chemical Physics*, Vol. 12, pp. 295-296 (1944).

Preininger, C.; Klimant, I and Wolfbeis, O. S. "Optical-fiber sensor for biological oxygen demand". *Analytical Chemistry*, Vol. 66, pp. 1841-1846 (1994).

Price, J. M.; Xu, W.; Demas, J. N. and DeGraff, B. A. "Polymer-supported pH sensors based on hydrophobically bound luminescent ruthenium(II) complexes". *Analytical Chemistry*, Vol. 70, pp. 265-270 (1998).

Pringsheim, E.; Terpetschnig, E. and Wolfbeis, O. S. " Optical sensing of pH using thin films of substituted polyanilines". *Analytica Chimica Acta*, Vol. 357, pp. 247-252 (1997).

Ravanel, P.; Taillandier, G. and Tissut, M. "Uncoupling properties of a chlorophenol series on *Acer* cell suspensions: a QSAR study". *Ecotoxicology and Environmental Safety*, Vol. 18, pp. 337-345 (1989).

Reteuna, C.; Vasseur, P. and Cabridenc, R. "Performances of three bacterial assays in toxicity assessment". *Hydrobiologia*, Vol. 188/189, pp. 149-153 (1989).

Rottman, C.; Ottolenghi, M.; Zusman, R.; Lev, O. Smith, M. Gong, G.; Kagan, M. L. and Avnir, D. "Doped sol-gel glasses as pH sensors". *Materials Letters*, Vol. 13, pp. 293-298 (1992).

Ruffolo, R.; Evans, C. E. B.; Liu, X. H.; Ni, Y.; Pang, Z. Park, P.; McWilliams, A. R.; Gu, X.; Lu, X.; Yekta, A.; Winnik, M. A. and Manners, I. "Phosphorescent oxygen sensors utilizing sulfur-nitrogen-phosphorus polymer matrixes: synthesis, characterization, and evaluation of poly(thionylphosphazene)-*b*-poly(tetrahydrofuran) block copolymers". *Analytical Chemistry*, Vol. 72, pp. 1894-1904 (2000).

Saari, L. A. and Seitz, W. R. "pH sensor based on immobilized fluoresceinamine". *Analytical Chemistry*, Vol. 54, pp. 821-823 (1982).

Saarikoski, J. and Viluksela, M. "Relation between physicochemical properties of phenols and their toxicity and accumulation in fish". *Ecotoxicology and Environmental Safety*, Vol. 6, pp. 501-512 (1982).

Sacksteder, L.; Demas, J. N. and DeGraff, B. A. "Design of oxygen sensors based on quenching of luminescent metal complexes: effect of ligand size on heterogeneity". *Analytical Chemistry*, Vol. 65, pp. 3480-3483 (1993).

Safavi, A. and Abdollahi, H. "Optical sensor for high pH values". *Analytica Chimica Acta*, Vol. 367, pp. 167-173 (1998).

Schultz, T. W "The use of the ionization constant (pK_a) in selecting models of toxicity in phenols". *Ecotoxicology and Environmental Safety*, Vol. 14, pp. 178-183 (1987).

Schultz, T. W and Cajina-Quezada, M. "Structure-activity relationships for mono alkylated or halogenated phenols". *Toxicology Letters*, Vol. 37, pp. 121-130 (1987).

Schultz, T. W. "Structure-toxicity relationships for benzenes evaluated with *Tetrahymena pyriformis*". *Chemical Research Toxicology*, Vol. 12, pp. 1262-1267 (1999).

Schultz, T. W. and Riggin, G. W. "Predictive correlations for the toxicity of alkyl- and halogen-substituted phenols". *Toxicology Letters*, Vol. 25, pp. 47-54 (1985).

Schultz, T. W.; Holocombe, G. W. and Phipps, G. L. "Relationships of quantitative structure-activity to comparative toxicity of selected phenols in the *Pimephales promelas* and *Tetrahymena pyriformis* test systems". *Ecotoxicology and Environmental Safety*, Vol. 12, pp. 146-153 (1986).

Schultz, T. W.; Wesley, S. K. and Baker, L. L. "Structure-activity relationships for di and tri alky substituted phenols". *Bulletin of Environmental Contamination and Toxicology*, Vol. 43, pp. 192-198 (1989).

Seitz, W. R. "Chemical Sensors based on fiber optics". *Analytical Chemistry*, Vol. 56, pp. 16A-34A (1984).

Shaw, G. "Quenching by oxygen diffusion of phosphorescence emission of aromatic molecules in polymethyl methacrylate". *Transactions. Faraday Society*, Vol. 63, pp. 2181-2189 (1967).

Shu, C. F. and Anson, F. C. "Dynamic consequences of ionic permselectivity -rapid ejection from nafion coatings of anions generated electrochemically from cationic precursors". *Journal of the American Chemical Society*, Vol. 112, pp.9227-9232 (1990).

Sixt, S.; Altschuh, J. and Brüggemann, R. "Quantitative structure-toxicity relationships for 80 chlorinated compounds using quantum chemical descriptors". *Chemosphere*, Vol. 30, pp. 2397-2414 (1995).

Song, A.; Parus, S. and Kopelman, R. "High-performance fiber optic pH microsensors for practical physiological measurements using a dual-emission sensitive dye". *Analytical Chemistry*, Vol. 69, pp. 863-867 (1997).

Sotomayor, M. D. P. T.; De Paoli, M. A. and de Oliveira, W. A. "Fiber-optic pH sensor based on poly(o-methoxyaniline)". *Analytica Chimica Acta*, Vol. 353, pp. 275-280 (1997).

Sullivan, B. P.; Salmon, D. J. and Meyer, T. J., "Mixed phosphine 2,2'-bipyridine complexes of ruthenium". *Inorganic Chemistry*, Vol. 17, pp. 3334-3341 (1978).

Sun, B.; Nirmalakhandan, N.; Hall, E.; Wang, X. H.; Prakash, J. and Maynes, R. "Estimating toxicity of organic chemicals to activated-sludge microorganism". *Journal of Environmental Engineering*, Vol. 120, pp.1459-1469 (1994).

Surgi, M.R. "Design and evaluation of a reversible fiber optic sensor for determination of oxygen" In Wise, D. L. ed., *Applied Biosensors*, Butterworths, Boston, pp. 249-290 (1989).

Szmacinski, H. and Lakowicz, J. R. "Optical measurements of pH using fluorescence lifetimes and phase-modulation fluorometry". *Analytical Chemistry*, Vol. 65, pp. 1668-1674 (1993).

Tang, N. H.; Blum, D. J. W. and Speece, R. E. "Comparison of serum bottle toxicity test with OECD method". *Journal of Environment Engineering*, Vol. 116, pp. 1076-1084 (1990).

Tang, N. H.; Blum, D. J. W.; Nirmalakhandan, N. and Speece and R. E. "QSAR parameters for toxicity of organic chemicals to *Nitrobacter*". *Journal of Environmental Engineering*, Vol. 118, pp. 17-37 (1992).

Trettnak, W. and Wolfbeis, O. S. "A fiberoptic cholesterol biosensor with an oxygen optrode as the transducer". *Analytical Biochemistry*, Vol. 184, pp. 124-127 (1990).

Trettnak, W.; Leiner, M. J. P. and Wolfbeis, O. S. "Optical Sensors: Part 34. Fibre optic glucose biosensor with an oxygen optrode as the transducer". *Analyst*, Vol. 113, pp. 1519-1523 (1988).

Trevizo, C. and Nirmalakhandan, N. "Prediction of microbial toxicity of industrial organic chemicals". *Water Science Technology*, Vol. 39, pp. 63-69 (1999).

Veith, G. D. and Broderius, S. J. "Structure toxicity relationships for industrial chemicals causing type (II) narcosis syndrome". In Kaiser, K. L. E. ed., *QSAR in Environmental Toxicology- II*, Reidel D., pp. 385-391 (1987).

Veith, G. D. and Mekenyan, O. G. "A QSAR approach for estimating the aquatic toxicity of soft electrophilies [QSAR for soft electrophiles]". *Quantitative Structure-Activity Relationship*, Vol. 12, pp. 349-356 (1993).

Veith, G. D.; DeFoe, D. and Knuth M. "Structure-activity relationships for screening organic chemicals for potential ecotoxicity effects". *Drug Metabolism Reviews*, Vol. 15, pp. 1295-1303 (1985).

Warne, M. A.; Osborn, D.; Lindon, J. C. and Nicholson, J. K. "Quantitative structure-toxicity relationships for halogenated substituted-benzenes to *Vibrio fischeri*, using atom-based semi-empirical molecular-orbital descriptors". *Chemosphere*, Vol. 38, pp. 3357-3382 (1999).

Watkins A. N.; Wenner, B. R.; Jordan, J. D.; Xu, W.; Demas, J. N. and Bright, F. V. "Portable, low-cost, solid-state luminescence-based O_2 sensor". *Applied Spectroscopy*, Vol. 52, pp. 750-754 (1998).

Weast, R.C. ed., *CRC Handbook of Chemistry and Physics*, 66th ed., CRC Press: Boca Raton, 1985, D-145.

Whitaker, J. E.; Haugland, R. P. and Prendergast, F. G. "Spectral and photophysical studies of benzo[c]xanthene dyes: dual emission pH sensors". *Analytical Biochemistry*, Vol. 194, pp. 330-344 (1991).

Wolfbeis, O. S. "Biomedical applications of fiber optic chemical sensors". In Wolfbeis, O. S. ed., *Fiber Optic Chemical Sensors and Biosensors*, Vol. 2, CRC Press, Boca Raton, pp.267-313 (1991).

Wolfbeis, O. S. "Fiber-optic sensors in bioprocess control". In Twork, J. V. and Yacynych, A. M. eds., *Sensors in Bioprocess Control*, Marcel Dekker, New York, pp. 95-125 (1990).

Wolfbeis, O. S. "Oxygen sensors". In Wolfbeis, O. S. ed., *Fiber Optic Chemical Sensors and Biosensors*, Vol. 2, CRC Press, Boca Raton, pp. 19-53 (1991).

Wolfbeis, O. S. and Posch, H. E. "Optical sensors. 20. A fiber optic ethanol biosensor". *Fresenius Zeitschrift Fur Analytische Chemie*, Vol. 332, pp. 255-257 (1988).

Wolfbeis, O. S.; Posch, H. E. and Kroneis, H. W. "Fiber optical fluorosensor for determination of halothane and/or oxygen". *Analytical Chemistry*, Vol. 57, pp. 2556-2561 (1985).

Wolfbeis, O. S.; Weis, L. J.; Leiner, M. J. P. and Zieger, W. E. "Fiber-optic fluorosensor for oxygen and carbon dioxide". *Analytical Chemistry*, Vol. 60, pp. 2028-2030 (1988).

Wolfbeis, O. S.; Leiner, M. J. P. and Posch, H. E. "A new sensing material for optical oxygen measurement, with the indicator embedded in an aqueous phase". *Mikrochim Acta*, Vol. 3, pp. 359-366 (1986).

Wong, K. Y.; Zhang, M. Q.; Li, X. M. and Lo, W. H. "A luminescence-based scanning respirometer for heavy metal toxicity monitoring". *Biosensors and Bioelectronics*, Vol. 12, pp. 125-133 (1997).

Wu, X.; Choi, M. M. F. and Xiao, D. "A glucose biosensor with enzyme-entrapped sol-gel and an oxygen-sensitive optode membrane". *Analyst*, Vol. 125, pp. 157-162 (2000).

Wyatt, W. A.; Poirier, G. E.; Bright, F. V. and Hieftje, G. M. "Fluorescence spectra and lifetimes of several fluorophores immobilized on nonionic resins for use in fiber-optic sensors". *Analytical Chemistry*, Vol. 59, pp. 572-576 (1987).

Xu, S. and Nirmalakhandan, N. "Use of QSAR models in predicting joint effects in multi-component mixtures of orangic chemicals". *Water Research*, Vol. 32, pp. 2391-2399 (1998).

Xu, W.; Kneas, K. A.; Demas, J. N. and DeGraff, B. A. "Oxygen sensors based on luminescence quenching of metal complexes: osmium complexes suitable for laser diode excitation". *Analytical Chemistry*, Vol. 68, pp. 2605-2609 (1996).

Xu, W.; McDonough III, R. C.; Langsdorf, B.; Demas, J. N. and DeGraff, B. A. "Oxygen sensors based on luminescence quenching: interactions of metal complexes with the polymer supports". *Analytical Chemistry*, Vol. 66, pp. 4133-4141 (1994).

Yeager H. L. "Transport properties of perfluorosulfonate polymer membranes" In Eisenberg A. and Yeager H.L. eds., *Perfluorinated Ionomer Membranes*, ACS Symposium Series 180, American Chemical Society, Washington D.C., pp. 41-63 (1982).

Yoshioka, Y.; Nagase, H.; Ose, Y. and Sato, T. "Evaluation of the test method 'activated sludge, respiration inhibition test' proposed by the OECD". *Ecotoxicology and Environmental Safety*, Vol. 12, pp. 206-212 (1986).

Zen, J. M. and Patonay, G. "Near-infrared fluorescence probe for pH determination". *Analytical Chemistry*, Vol. 63, pp. 2934-2938 (1991).

Zhao, Y.; Richman, A.; Storey, C.; Radford, N. B. and Pantano, P. "In situ fiber-optic oxygen consumption measurements from a working mouse heart". *Analytical Chemistry*, Vol. 71, pp. 3887-3893 (1999).

Zhujun, Z. and Seitz, W. R. "A fluorescence sensor for quantifying pH in the range from 6.5 to 8.5". *Analytica Chimica Acta*, Vol. 160, pp. 47-55 (1984).

Zhujun, Z.; Zhang, Y.; Wangbai, M.; Russell, R.; Shakhsher, Z. M.; Grant, C. L.; Seitz, W. R. and Sundberg, D. C. "Poly(vinyl alcohol) as a substrate for indicator immobilization for fiber-optic chemical sensors". *Analytical Chemistry*, Vol. 61, pp. 202-205 (1989).

List of Publications

Journal Articles

1. Chan, C. M.; Fung, C. S.; Wong, K. Y. and Lo, W. "Evaluation of a luminescent ruthenium complex immobilized inside Nafion as pH sensors". *Analyst*, Vol. 123, pp. 1843-1847 (1998).

2. Chan, C. M.; Lo, W.; Wong, K. Y. and Chung, W. F. "Monitoring the toxicity of phenolic chemicals to activated sludge using a novel optical scanning respirometer". *Chemosphere*, Vol. 39, pp.1421-1432 (1999).

3. Chan, C. M.; Chan, M. E.; Zhang, M.; Lo, W. and Wong, K. Y. "The performance of oxygen sensing films with ruthenium-adsorbed fumed silica dispersed in silicone rubber". *Analyst*, Vol. 124, pp. 691-694 (1999).

4. Chan, C. M.; Lo, W. and Wong, K. Y. "Application of a luminescence-based pH optrode to monitoring of fermentation by *Klebsiella pneumoniae*". *Biosensors and Bioelectronics*, Vol. 15, pp. 7-11 (2000).

Conferences Presentations

1. Chan, C. M.; Wong, K. Y. and Lo, W. H. "Toxicity monitoring using a novel optical scanning respirometer. *Abstracts of Fourth Symposium on Chemistry Postgraduate Research in Hong Kong,* Hong Kong Baptist University, April 19, 1997, paper A-19.

2. Chan, C. M; Lo, W. H.; Wong, K. Y. and Chung W. F. "Development of luminescence-based sensor for toxicity monitoring". *Abstracts of 215th American Chemical Society National Meeting*, Dallas, Texas, March 29-April 2, 1998, paper ANYL-047.

3. Chan, C. M.; Wong, K. Y. and Lo, W. H. "Development of pH sensor based on a luminescent ruthenium complex": *Abstracts of Fifth Symposium on Chemistry Postgraduate Research in Hong Kong,* The Hong Kong Polytechnic University, 25 April 1998, paper A-15.

4. Chan, C. M.; Chan, M. Y.; Zhang, M.; Lo, W. and Wong, K. Y. "The performance of oxygen sensing films with ruthenium-adsorbed fumed silica dispersed in silicone rubber". *Abstracts of Sixth Symposium on Chemistry Postgraduate Research in Hong Kong,* City University of Hong Kong, 24 April 1999, paper AE-24.

5. Chan, C. M.; Lo, W. H. and Wong, K. Y. "Application of a luminescence-based pH optode to monitoring of fermentation by *Klebsiella pneumoniae*". *Abstracts of the Seventh Symposium on Chemistry Postgraduate Research in Hong Kong.* Hong Kong University of Science and Technology, 29 April 2000, paper A-29.

Appendix

Algorithm for Calculation of Molecular Connectivity Index

The hydrogen suppressed molecular skeleton is first written down. Each atom is designated by a cardinal number which is the total number of adjacent atoms for simple index (δ value) or the total number of adjacent bonded atoms plus all pi and lone pair electrons for valence index (δ^v value). For example, the oxygen atom in an alcohol, ROH, the δ value is 1 while δ^v is 5. The molecular skeleton is then dissected into constituent atoms or bonds according to the order of index. Using the Randic algorithm, a value for each atom or bond is computed: $(\delta_i)^{-0.5}$ for zero order index, $(\delta_i\delta_j)^{-0.5}$ for first order index, $(\delta_i\delta_j\delta_k)^{-0.5}$ for second order index. The molecular index is the simple sum of these atom or bond values over the entire molecule.

Sample calculation of connectivity index:

1. <u>1,2-dichloropropane</u> – ^1X

a. δ assignment

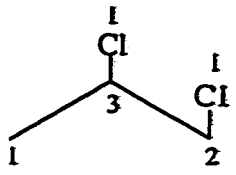

b. first bond order dissection

$(1\times3)^{-0.5}$, $(3\times1)^{-0.5}$, $(3\times2)^{-0.5}$, $(2\times1)^{-0.5}$

c. summation of bond terms

$^1X = 0.577 + 0.577 + 0.408 + 0.707 = 2.27$

2. <u>2-chlorophenol</u> – $^2X^v$

a. δ assignment

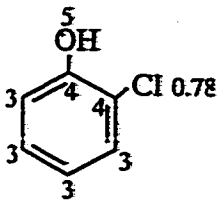

b. second order dissertation

$2(4\times4\times3)^{-0.5} + 2(4\times3\times3)^{-0.5} + 2(3\times3\times3)^{-0.5} + (5\times4\times4)^{-0.5} + (5\times4\times3)^{-0.5} + (0.78\times4\times4)^{-0.5} + (0.78\times4\times3)^{-0.5}$

c. summation of bond terms

$^2X^v = 1.85$